SEISMOLOGY AND TECTONICS OF THE NORTH AMERICAN PLATE IN THE ARCTIC: NORTHEAST SIBERIA AND ALASKA

By

David Bruce Cook

A DISSERTATION

Submitted to
Michigan State University
in partial fulfillment of the requirements
for the degree of

DOCTOR OF PHILOSOPHY

Department of Geological Sciences

1988

Thr

have bee

of the N

the west

boundary

methods

investiga

Th

affinity

converge

consiste

In

mechan

northwe

Pacific

eastern

North

current

In

its adja

Americ

ABSTRACT

SEISMOLOGY AND TECTONICS OF THE NORTH AMERICAN PLATE IN THE ARCTIC: NORTHEAST SIBERIA AND ALASKA

By

David Bruce Cook

Through the use of geological and geophysical methods, new conclusions have been reached regarding the tectonic setting and history of three regions of the North American plate within the Arctic. The settings of these regions, the western Bering Sea margin, interior Alaska and the North American plate boundary in northeast Siberia, are independently examined using seismological methods or tectonostratigraphic terrane analysis. The results of each investigation are summarized as follows:

The western Bering Sea margin is composed of five terranes of oceanic affinity which were accreted during a period of Cretaceous to Miocene convergence. Presently, extension is taking place in the western Bering Sea, consistent with results from the remainder of the Bering Sea region.

In northern and western Alaska, however, intraplate earthquake focal mechanism solutions indicate three distinct regions of stress orientation. A northwest-southeast horizontal stress in much of interior alaska is created by Pacific plate subduction at the Aleutian trench. Stresses in northern and eastern Alaska are northeast-southwest, similar to the mid-continent region of North American. The Yukon-Koyukuk province and the Bering Sea are currently undergoing extension.

Interplate earthquake focal mechanism solutions in northeast Siberia and its adjacent seas are used to delineate the position and character of the North American plate boundary in Siberia. The onshore continuation of the Arctic

mid-ocean
as a comp
caused by
close to th
complete
arc-arc jun
Okhotsk pl

mid-ocean ridge does not represent a continental rift, and is instead expressed as a compressional zone within the Cherskii Mountains. This transition is caused by the uniqueness of this boundary where the pole of rotation lies very close to the plate boundary, causing an abrupt transition in faulting style. A complete data set extends the Arctic mid-ocean ridge to the Aleutian-Kuril arc-arc junction best fits a three plate system, with an independent Sea of Okhotsk plate.

To Grandpa Cook,
who defined persistence and pride . . . .

ACKNOWLEDGEMENTS

When the completion of a challenge so engrossing becomes a reality, everyone with whom I shared even a brief time must be thanked, for you all somehow helped me through the past eight years.

Naming names is especially difficult, but what better place to start than at the beginning: John McGuire and Uncle Ken, you are the ones who introduced me to and gave me access to Geology - thanks for putting me on the right track!

A strong influence was Kaz, who grabbed me as a Junior and forced me to make decisions which were rarely easy but invaluable as lessons. As an advisor, no one else will make you work so hard; yet Kaz plays more than an advisor's role, and for that he gets my sincere appreciation. I also thank the rest of my committee, John Wilband, Mike Velbel, Bill Cambray and Larry Ruff, who seemed to make the bad times worse, yet definitely made the result all the better.

There are many other people within the department who deserve tremendous thanks for their influence and friendship: Stoney, my "anchor man," Tom Vogel, who taught me to disprove before ever proving, and four people whose assistance is irreplaceable: Loretta, the "woman in black" (don't we still have a date on the pool table?); Cathy (who forced me to face reality and volleyballs when I often ought not have); Mona, who can always bring a smile to her face and add a little cheer to the day; and fellow cave dweller and THE Dungeon Master, Diane.

There were so many other friends who shared good times and various emotions during all this. Thanks to all of you, especially Jim (my computer mentor), Bruce (who'll go down in belch history), Tim, Soo Meen, Cindy, Don, Jim, Tim, Frank, Amy, Ben, Bob, Bill, Jim, Mike, Beth, John, Dana, Ken, Deb, Paul, Paige and Scott for a few thoughts on science, and alot of thoughts of other things. Thanks to Chris S. for friendship and philosophy on a starry Texas night with California wine. Mitch was a great lab assistant, but is an even greater friend. Special thanks to Erin, who often was my verbal punching bag, yet still gave me a couch to sleep on when the nights got too long. Thanks also to the staff at Eureka Elementary School, for encouraging and helping both Shellon and myself.

Many people had a part in the scientific cooperation necessary to complete this project. I thank Boris Baranov and L. Parfenov (whose verbal and written input occasionally changed arm-waving into fact), and Chris "Curly" Wolf (friend and consultant in hardware, software, volleyball and a few million other things). Computer software was provided by Seth Stein (Surface wave analysis), Glenn Kroeger (Body-wave synthetics) and John Wilband ("XY" and others). Thanks also goes to Chuck DeMets, and the NUVEL group, for data prior to publication. For a wide variety of reasons, thanks also goes to Norm Sleep, Dave Stone, Art Grantz, Dave Scholl, Chuck Estabrook, Doug Christensen, Bill Harbert, G. Leonard Johnson, Fumiko Tajima, Hiroo Kanamori and Jack Sweeny.

I am
with fund
to proces
area).
Geologica
Fellowshi
University
also prov
Research
grant no.

Of
student c
my own
sat throu
humor a
believed
we've bee
with alot,

Fina
shant forg

I am extremely grateful to Amoco Production Company, which provided me with funding for purchase of satellite imagery as well as the facilities in which to process the images (thereby gracing me with the first "sights" of my field area). Assistantships and support were provided by the Department of Geological Sciences, Michigan State University, and by a Continuing Doctoral Fellowship awarded by the College of Natural Science, Michigan State University. Further support was provided by Dr. Ted "Tornado" Fujita (who also provided wit). This research was funded, in part, by Office of Naval Research contract no. N00014-83-K-0693 and by National Science Foundation grant no. 87-21119.

Of course, my family was more than supportive throughout my whole student career. Mom and Dad taught me responsibility early, and let me make my own mistakes and successes - I love you for that. The rest of the family sat through many a one-sided conversation and provided encouragement and humor as necessary. First in my life, although she may not have always believed it, was Shellon, who probably spent less time with me the two years we've been married than she had before we were together. SSC, you've put up with alot, and you are to be congratulated long before myself.

Finally, Dr. Zapp was a lifesaver more than once - thanks. Oh, and I shant forget Lobachevsky, who showed me the light. . . . .

TABLE OF CONTENTS

S

I

I

(

CHAPT
PRESEN
NO

LIST OF TABLES

LIST OF FIGURES

The N

the Arctic

particularly

the genera

inaccessibil

These two

geological

The goal

geology an

of the Arct

A lo

spans the

Terranes

the Berin

publicatio

investigat

all geolo

Therefore

descriptio

research

and west

INTRODUCTION TO RESEARCH

The North American plate occupies a major portion of the globe north of the Arctic circle. However, the exact location and nature of its boundaries, particularly within the Soviet Union, is poorly known. This is due, in part, to the general remoteness of the Arctic region as well as to the complete inaccessibility to regions of northeastern Siberia, USSR to western scientists. These two factors combined have prevented any major accumulation of reliable geological or geophysical data over an area of millions of square kilometers. The goal of this dissertation is to examine, to whatever extent is possible, the geology and tectonics of the North American plate in two neighboring regions of the Arctic: Alaska and northeast Siberia.

A logical place to begin is within the Bering Sea. This body of water spans the gap between the two continental regions in question. Chapter One, Terranes of the Western Bering Sea Margin: Constraints on the Evolution of the Bering Sea, incorporates a previously underutilized data source, Soviet publications, with relatively recent LANDSAT imagery data. Commonly, Soviet investigators will not recognize plate tectonic theory, and would rather explain all geological observations in terms of "vertical tectonics" and "oceanization." Therefore, Soviet publications were important more for their data and descriptions than for their interpretations. Completion of this phase of the research laid a good groundwork from which to expand both east (into Alaska) and west (into Siberia). More importantly, I became exposed to the intricacies, however u

with an are

Alask

great deal

Intraplate

fundamen

regions.

the data

limitation

such as

magnitud

M_b 4.5

events.

short-pe

surface-

exceede

In

based c

means

mechar

consist

limitat

Even

are fo

T

Chapt

however unpleasant and frustrating, of working with Soviet literature dealing with an area of complete physical inaccessibility.

Alaska, relatively less remote and less difficult to access, provides a great deal more background than its neighbor to the west. In Chapter Two, Intraplate Seismicity of Alaska: Implications for Regional Stresses, the fundamentals of seismological investigations were developed for the Arctic regions. Since a great deal of data is available from Alaska, the reliability of the data could be more easily verified. This, in turn, outlined potential limitations of further seismological investigations in areas of lower data density, such as northeast Siberia. The intraplate seismicity of Alaska is not of great magnitude. In fact, nearly all events are less than M_b 6.0, and many are in the M_b 4.5 - 5.0 range. There are inherent difficulties in working with such small events. Signal-to-noise ratios are small, data are often constrained to short-period waveforms, and the limits of advanced numerical techniques (e.g., surface-wave analysis and body-wave modelling) are often strained if not exceeded.

In light of such constraints, it is important to note that the conclusions based on seismological investigations of Alaska and northeast Siberia are by no means definitive or unique. In fact, the interpretation of any one focal mechanism solution may give an ambiguous conclusion at best. However, the consistency observed among many mechanisms, despite their individual limitations, is where the strength of this type of investigation is expressed. Even more encouraging is the realization that many of the numerical methods are found to work down to magnitudes of 5.5 and often as low as 5.0.

The final application, having laid the foundation and tested it, is in Chapters Three and Four. The seismicity of the North American plate boundary in northeast Siberia had been poorly defined. The determination of epicentral distribution and source parameters was necessary in order to identify the present-day kinematics of the plate boundary. Chapter Three, Seismicity and Focal Mechanisms of the North American-Eurasian Plate Boundary in Siberia, examines the seismicity in detail, arriving at conclusions regarding the seismic character along sub-segments of the plate boundary in northeast Siberia and the Laptev Sea. Chapter Four, Present-Day Plate Interactions in Northeast Asia: North American, Eurasian and Okhotsk Plates, utilizes the results of Chapter Three and of previous studies in order to examine the present nature of the North American plate boundary in northeast Siberia. Interestingly enough, the plate boundary ends where Chapter One began - in the western Bering Sea.

CHAPTER ONE

TERRANES OF THE WESTERN BERING SEA MARGIN: CONSTRAINTS ON THE EVOLUTION OF THE BERING SEA

INTRODUCTION

The western margin of the Bering Sea consists of an amalgamation of tectonostratigraphic terranes (Jones et al., 1977) which form present-day Kamchatka Peninsula and Koryakia (Koryak Highlands). Along this margin, subduction, rifting, and volcanism (island arc, Andean-type and intraplate) have each been active for some time period since the Cretaceous. The complexities of this varied tectonic history are preserved within the terranes bounding the western Bering Sea. This paper delineates the terranes of the Koryak-Kamchatka system which have accreted since Cretaceous time, and uses characteristics of these terranes as an aid in constraining the tectonic evolution of the Bering Sea region.

Koryakia is composed of several terranes with oceanic affinities which lie between the Okhotsk-Chukotsk volcanic belt and the Bering Sea (Figure 1-1). The oceanic terranes' basement ages and times of accretion young in a seaward direction. Northwest of the Okhotsk-Chukotsk volcanic belt, terranes with continental affinities (e.g., Omolon and Prikolymsk; Fujita and Newberry, 1983) predominate. To the south is Kamchatka Peninsula, which is composed of ten terranes having oceanic affinity that have accreted since Mesozoic time (Watson, 1985; Watson and Fujita, 1985). Numerous volcanic arcs, presumed to have developed through interactions of the Farallon, Izanagi, Kula and Pacific plates, are preserved within the Kamchatka terranes.

The terranes of the western Bering Sea margin provide new insights on the evolution of the Bering Sea region. Many investigators have examined the general terrane makeup within northeast Siberia, but not at sufficiently fine scale to constrain the regions Cenozoic evolution. Within Koryakia, Churkin and Trexler (1981), Churkin (1983), Fujita and Newberry (1983) and Natal'in

Figure 1-1: Regional geography of the Bering Sea Region. The Ohkotsk - Chukotsk volcanic belt is shown in the shaded area. Arrows represent present-day Pacific convergence direction of Engebretson, et al., 1985. Basins and canyons abbreviated as follows: NT- Norton Basin; NV - Navarin Basin; PC - Pribilof Canyon; SG - St. George Basin; ZC - Zemchug Canyon.

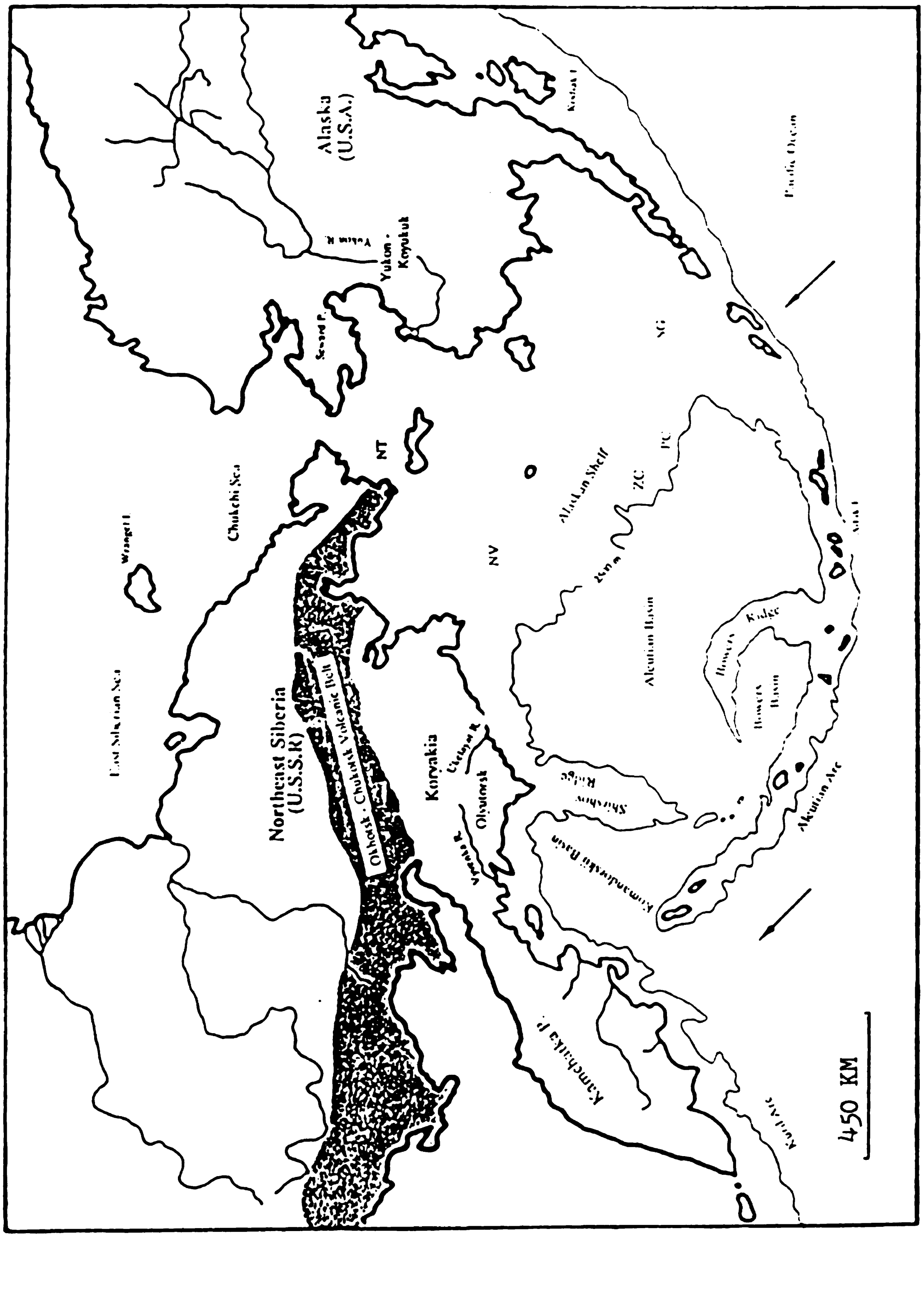

Alaska (U.S.A.)
Northeast Siberia (U.S.S.R)
Okhotsk - Chukotsk Volcanic Belt
Koryakia
Chukchi Sea
Yukon - Koyukuk
NT
NV
ZC
PC
SG
Aleutian Basin
Bowers Ridge
Bowers Basin
Aleutian Arc
Olyutorsk
450 KM

Figure 1-1

and Parfenov (1983) have all identified the accretion of "Olyutorsk" (Figure 1-1) in the Cenozoic. Kazimirov (1985) considered Olyutorsk to be a volcanic and siliceous-sediment filled depression, fault bounded to the north. Only very recently did Koltypin and Kononov (1986) identify several discrete terranes in Olyutorsk which accreted independently during Cenozoic time. I shall use "Olyutorsk" to represent a subregion of Koryakia rather than a distinct terrane, and define it as the area between the Ukelayat and Vyvenka river basins to the north and the Bering Sea to the south (Figure 1-1).

Since the area of interest is not accessible to western scientists, I have used two primary methods of investigation: published literature (both in Russian and in translation), and satellite image interpretation. Satellite imagery at scales of 1:1,000,000 (mosaics) and 1:250,000 (LANDSAT Multi-Spectral Scanner (MSS)) enabled me to identify structural trends and surface morphologies useful in terrane identification and characterization. These two primary data sources were supplemented by Soviet geologic maps. I recognize that there are limitations in this method of terrane analysis, such as non-uniform data distribution and inability to verify some of the information. However, for a region which is so remote and inaccessible, such an approach can provide useful and otherwise unobtainable information on the geologic make-up and evolution.

BERING SEA SETTING

The Bering Sea is separated from the Pacific basin by the Aleutian island arc, and is bounded to the northeast by the Alaskan shelf (Beringian margin). Within the Bering Sea there are three major basins (Aleutian, Bowers and Komandorskii), each of which apparently have distinct tectonic histories. There are also two prominant undersea rises, the Shirshov and Bowers ridges (Figure 1-1).

Determining the genesis and present geologic character of these features is crucial for developing a model of the Bering Sea's evolution. Below, I summarize present knowledge regarding these features, which I combine with terrane data from the western Bering Sea to develop a model for the evolution of the Bering Sea region.

Beringian Margin

A series of northwest trending basins line the outer margin of the Alaskan shelf. These basins, originally thought to have formed during the Paleogene, now appear to have been more active in the Miocene (Harbert et al., 1987). The oldest sediments identified from the Cost wells within the Navarin, Norton and St. George basins are Eocene (Turner et al., 1984). However, these Eocene sediments form a thin, discontinuous layer in most of the basins, and the dominant sediment thickness is of Miocene age. Thus, the basins appear to have developed around Eocene time, with renewed or increased subsidence during Miocene time.

Miocene to present extension is also suggested further inland by basaltic volcanism in the Yukon-Koyukuk province of Alaska (Nakamura et al., 1980) and by the occurance of extensional earthquakes (Sykes and Sbar, 1974; Liu and Kanamori, 1979) . Additionally, extensional features, discussed below, are also present in the Komandorskii basin to the west. Therefore, extension is taking place on a regional scale in the Bering Sea and along many of its margins.

Aleutian Basin

The Aleutian basin is the largest of the three major Bering Sea basins, and has been intensely investigated by a number of workers (e.g., Scholl et al., 1975; Marlow et al., 1982; Cooper et al., 1976a). These investigations have shown the basin to be underlain by "normal" oceanic crust (Scholl et al., 1975) with a depth to Moho of about 16 km (Cooper et al., 1977; Bogdonov and Neprochnov, 1984), about 4 km deeper than under the Pacific plate. Kienle (1971) found that the free-air gravity anomaly within the Aleutian Basin was approximately zero, and concluded that the basin was in isostatic equilibrium. Magnetic anomalies trending nearly north-south have been identified within the basin by Cooper et al. (1976a), who identified them as M1 to M13 (117-132 Ma). More recent work in conjunction with GLORIA has supported the existence of these anomalies (Cochrane et al., 1987), although age modelling has not yet been completed.

The sediment layer within the Aleutian basin is quite thick, ranging from 4 to 9 (Scholl et al., 1975) or 11 km (Bogdanov and Neprochnov, 1984). The oldest of these sediments are probably Cretaceous to Tertiary in age (Scholl et al., 1975). Heat flow within the basin is not unusual, ranging from 41 to 75 milliwatts per meter squared (mW/m^2) (Ben-Avraham and Cooper, 1981) and averaging 62 mW/m^2.

The history of the Aleutian basin has been debated by many authors (e.g., Scholl et al., 1975; Cooper et al., 1976b; Marlow et al., 1982; Ben-Avraham and Cooper, 1981). A critical point is the age of the underlying crust. It has been suggested that the crust is a trapped remanent of either the Kula plate (e.g., Scholl et al., 1975; Ben-Avraham and Cooper, 1981) or Izanagi plate (Rea and Dixon, 1983). If the Cretaceous age reported by Cooper et al. (1976a) is correct, the trapping hypothesis is plausible. If, however, the crust is younger, a different evolution must be explored. In any case, there is no good evidence for a spreading center within the basin, seemingly eliminating the possibility of *in situ* formation.

Bowers Basin and Ridge

Located in the south-central Bering Sea, adjacent to the Aleutian arc, are the Bowers basin and ridge. Bowers basin is poorly studied relative to the other major basins of the Bering Sea.

Bowers ridge stands more than 2.0 km above the surrounding sea floor (Cooper et al., 1981), and may be a remnant volcanic arc (Kienle, 1971; Ben-Avraham and Cooper, 1981). Seismic reflection and refraction data (Ludwig et al., 1971a; Scholl et al., 1975; Cooper et al., 1981), gravity surveys (Kienle, 1971) and magnetic profiles (Kienle, 1971; Cooper et al., 1976a, 1981) suggest that westward directed subduction occurred under the eastern flank of the ridge. Sediments of at least early Tertiary age are found within summit basins of the ridge (Scholl et al., 1975).

Bowers ridge extends from the Aleutian ridge in an arcuate shape, convex northeastwardly, then narrows and plunges westward into a channel separating it from the southern tip of the Shirshov ridge. Within this channel, the continuation of the structure is expressed as a small ridge with a slight southward convexity. Data from GLORIA surveys (Cochrane et al., 1987) indicates there is a basement continuity between the two structures, although Rabinowitz (1974) argues from seismic profiling that they are separate structures.

Bowers basin may be intermediate between the Aleutian and Komandorskii basins. There is a small variation (-30 to +30 mGals) of the free-air anomaly within the basin, and magnetic signatures, if present, are weak. Cooper et al. (1976a) suggest that any magnetic anomalies may have been effectively demagnetized by the thermal influence of Pacific subduction under the Aleutian arc. Sediment thickness within Bowers basin is slightly less than in the Aleutian basin (Scholl et al., 1975), although depth to basement appears to be the same.

Aleutian Arc

The southern boundary of the Bering Sea is formed by the Aleutian island arc, which extends westward from Alaska Peninsula to Kamchatka Peninsula. The total distance along the strike of the arc is more than 2000 km, and Pacific plate convergence ranges from nearly orthogonal in the east to parallel in the west, along the Komandorskii Islands. Structural trends and geochemical similarities indicate that Cape Kamchatka (Figure 1-2) may actually be an accreted fragment of the westernmost Aleutian arc (Watson and Fujita, 1985; Zinkevich et al., 1987).

The arc is thought to have formed at least 50 m.y. ago (Eocene), based upon ages obtained from the Finger Bay volcanics on Adak Island. Since these are the oldest exposed rocks, an even older initiation of arc formation is plausible. Cretaceous sediments found within the Aleutian basin to the north (Scholl et al., 1975) may also suggest an earlier, Cretaceous, formation of the Aleutian arc (Scholl et al., 1983). A cessation of volcanism and associated uplift and erosion along the ridge beginning at 15 Ma is indicated by the high erosional rates and broadly deformed rocks of that time (Marlow et al., 1973). This volcanic quiescence, which continued until approximately 3 Ma, was suggested by Anderson (1970) to be the result of plutonic emplacement along the length of the arc. An equally speculative hypothesis is that such broad uplift and deformation may have accompanied the subduction of the extinct Pacific-Kula ridge (DeLong et al., 1978), a small segment of which is still preserved south of the central Aleutians (Moore et al., 1987). Since 3 Ma, new stratovolcanos have formed north of the previous volcanic centers, lying unconformably above the erosional remnants of the earlier volcanic arc (Scholl et al., 1975).

The genesis of the Aleutian arc has been debated by many investigators who seem to disagree on the latitude of its initiation. Some favor a southern formation of the arc, with subsequent northward migration as part of a megaterrane which was emplaced along southern Alaska and northeast Siberia (Moore et al., 1983). Others argue that the arc has formed nearly *in situ* (Harbert, 1987), possibly along an old transform fault on the Izanagi plate (Woods and Davies, 1977). Recent paleomagnetic data (Harbert, 1987), tend to support the *in situ* formation hypothesis.

Shirshov Ridge

Shirshov Ridge is a highly asymmetric feature which separates the Aleutian basin on the east from the Komandorskii basin on the west. It rises some 1 to 2 km above the surrounding basins, and is a bathymetric (Scholl et al., 1975), gravimetric (Ben-Avraham and Cooper, 1981) and magnetic (Cooper et al., 1976c) offshore extension of the Olyutorsk Peninsula (Figure 1-2). The eastern margin of the ridge slopes gradually into the Aleutian basin; some of the uppermost overlying sedimentary cover continues undisrupted from the ridge to the Aleutian basin (Savostin et al., 1986). Some sedimentary layers to the east of the ridge are folded (Ludwig et al., 1971b). The western flank of Shirshov ridge drops steeply into the Komandorskii basin. This is due to a large number of faults which dissect and downthrow the ridge's western margin into the Komandorskii basin. Savostin et al. (1986) report that these are listric normal faults. Some of the sedimentary cover on the Shirshov ridge is thicker

Figure 1-

Figure 1-2: Detailed geography of the western Bering Sea region. "DSDP 191" is the 1972 Deep Sea Drilling Project site 191. Note Pacific convergence (arrow; Engebretson et al., 1985) is nearly parallel to western Aleutian trench strike.

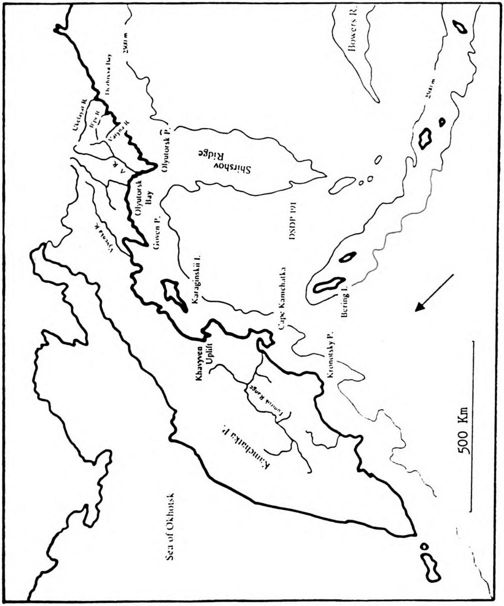
Sea of Okhotsk
Shirshov Ridge
Olyutorsk P.
Olyutorsk Bay
Karaginskii I.
DSDP 191
Cape Kamchatka
Kronotsky P.
Bering I.
Bowers R.
500 Km

Figure 1-2

(up to a
basin (B
sediment
thinner d

Ext
reported
extensive
caution
Neproch
chipped
similar
al. (198
allochth

Pe
sample
Using a
analyse
basalts
classifi
therefo
less r
(Mach
differe
not ch
subali
Olyut

(up to a maximum of 2 km; Neprochnov et al., 1985) than in the Komandorskii basin (Bogdanov and Neprochnov, 1984). There is, however, variation of the sediment thicknesses within the summit basins of Shirshov ridge, with generally thinner deposits on the western flank (Ludwig et al., 1971b).

Extensive dredging has been conducted on Shirshov ridge, recovering reportedly basement samples and overlying sediments. However, due to extensive glaciation, the potential for ice rafted debris necessitates extreme caution in using these rocks for dating or characterization of their source. Neprochnov et al. (1985) and Peyve and Yurkova (1987) describe "freshly chipped" basement recoveries which range from gabbro to low-titanium basalts, similar to those found onshore in the Olyutorsk Peninsula. Neprochnov et al. (1985) also discarded many samples which they suspected to be allochthonous.

Peyve and Yurkova (1987) presented a detailed analysis of the dredge samples, and assigned a Cretaceous age to the basalts of Shirshov ridge. Using a variety of major and minor element (e.g., Ti, Al, Na, K, Cr, Ni, Zr, Y) analyses, Peyve and Yurkova (1987) attempted to assign a tectonic setting to basalts of both Shirshov ridge and Olyutorsk range. Many of their classifications were based upon highly mobile elements (e.g., Sr and K), therefore, I ignored results based upon these elements. However, when using less mobile elements (e.g., Cr and Ti), basalts of the Olyutorsk range (Machevna complex) clearly clustered along Peyve and Yurkova's (1987) basalt differentiation trend of Pacific island arcs. Shirshov ridge dredge samples did not cluster as tightly, but ranged from the island arc differentiation trend to a subalkalic trend similar to ocean island basalts. A second group of basalts from Olyutorsk Peninsula (Olyutorka complex) were classified as "transitional" (Peyve and Yurkova, 1987), due to their variation from the island arc differentiation trend to an ocean island basalt trend.

A multitude of origins have been proposed for Shirshov ridge, including a hot spot trace (Ben-Avraham and Cooper, 1981), a spreading ridge (Kienle, 1971; Neprochnov et al., 1985), a remnant arc (Karig, 1972), an ophiolitic "pile" (Peyve and Yurkova, 1987) and a remnant continent (Nur and Ben-Avraham, 1972). Whatever its origin, basalt geochemical similarities (Peyve and Yurkova, 1987) and geophysical signatures (Ben-Avraham and Cooper, 1981; Cooper et al., 1976c) between onshore East Olyutorsk terrane and Shirshov ridge strongly support the interpretation of Shirshov ridge as an offshore continuation of the East Olyutorsk terrane.

There is an apparent basement structural correlation, first noted by Ludwig et al. (1971b), between Bowers and Shirshov ridges. GLORIA data (Cochrane et al., 1987) show that the northern end of Bowers ridge plunges downward and curves westward toward the southern tip of Shirshov ridge. This apparent topographic connection is further supported by a continuous magnetic anomaly, identified by Cooper et al. (1976a), which extends along the crest of both Bowers and Shirshov ridges as well as along the correlative basement axis. This suggests that the two ridges may have had a common genesis, and were separated at some later period of their evolution. Rabinowitz (1974) used seismic reflection data to identify two basement peaks separated by less than 10 km and, therefore, suggested differing structural origins for the Bowers and Shirshov ridges. However, the southern extent of Shirshov ridge, as noted by Rabinowitz (1974), has dual peaks, and may continue into the basement in the same manner.

Komandorskii Basin

The Komandorskii basin extends westward from Shirshov ridge to the continental margin of Kamchatka Peninsula. Its southern and northern boundaries are the Aleutian arc and Koryakia, respectively. The basin is apparently floored by oceanic crust (Ludwig et al., 1971b; Creager and Scholl, 1973), exhibits high heat flow (85 to 210 mW/m^2; Rabinowitz and Cooper, 1977; Bogdanov and Neprochnov, 1984), and has a thin (1 to 2 km) sedimentary cover of Miocene and younger age (Scholl et. al., 1975). Weak magnetic anomalies (generally less than 200 gammas; Cooper et al., 1976a) are found within the basin, paralleling north-south trending basement ridges of 0.5 to 1.0 km amplitudes (Cooper et al., 1976a). The depth to basement in the Komandorskii basin is apparently shallow (4-5 km), contrasting with greater depths (greater than 7 km) in both the Aleutian and Bowers basins (Cooper et al., 1976a).

Data obtained from the Komandorskii basin since 1982 has drastically changed the view of its evolution. New structural data obtained by a Soviet expedition (29th cruise of the R/V Dmitrii Mendeleyev; Savostin et. al., 1986) have shown "systematic extensional features" which converge in the southeast corner of the basin. Seliverstov (1987) presents seismic profiles showing volcanic edifices north of Bering Island within the Komandorskii basin; down-dropped graben structures and fumaroles are also present (Bogdanov, 1986). Furthermore, redating of the original DSDP basement basalts (DSDP Site 191) has shown them to be Miocene (approximately 9.2 Ma), rather than the originally reported Oligocene (29 Ma) age (D. Scholl, pers. comm.). These data all point to the existence of Miocene to present rifts within the Komandorskii basin. These rifts, north of Bering Island and in southeastern Komandorskii

Basin, trend nearly due north and are semi-orthogonal to the Pacific convergence direction.

WESTERN BERING SEA TERRANES

Koryakia's Cretaceous development is described by Natal'in and Parfenov (1983) as a Andean-type margin. Fujita and Newberry (1983) identified the Koryak terrane, a forearc basin sequence composed of coarse clastics, tuffs and sediments derived from the Okhotsk-Chukotsk volcanic belt (Fujita and Newberry, 1983; Natal'in and Parfenov, 1983). These rocks are the continentward abutment against which the terranes of Olyutorsk have been accreted.

Olyutorsk has commonly been considered a single oceanic terrane which accreted in the Cenozoic (e.g., Churkin and Trexler, 1981; Fujita and Newberry, 1983) along a thrust boundary preserved in the Ukelayat and Vyvenka River basins. Extrapolation of this terrane south into Kamchatka has often been proposed (Natal'in and Parfenov, 1983; Koltypin and Kononov, 1986), but not explicitly proven. Here I identify a number of smaller terranes that compose Olyutorsk (Figure 1-3), and present new evidence for their correlation to terranes in Kamchatka (Figure 1-4) as identified by Watson (1985) and Watson and Fujita (1985).

Ukelayat-Central Kamchatka Terrane

The Ukelayat-Central Kamchatka (UCK) terrane extends from southern Kamchatka northward through Kamchatka and western Karaginskii Island, then northeast and east through Olyutorsk. The eastern boundary of this terrane is defined by large thrust faults along its entire length. These thrusts dip 30^{o} to 40^{o} east-southeast in Kamchatka (Tsikunov and Petrov, 1973) and 15^{o} to 40^{o}

Figure 1-3: 1:1,000,000 satellite mosaic of the Olyutorsk region. Boundaries of terranes composing Olyutorsk are shown by dotted lines. OP - Olyutorsk Peninsula; GP - Goven Peninsula; A - Apuka Mountains; P - Pakhachinsk Plateau.


Ukelayat R.
Il'pi R.
Vatyna R.
A
OP
Apuka R.
P
Pakhacha R.
Vyvenka R.
GP

Figure 1-3

Fig

Figure 1-4: Map of terranes identified by this study. Dashed lines are inferred boundaries.

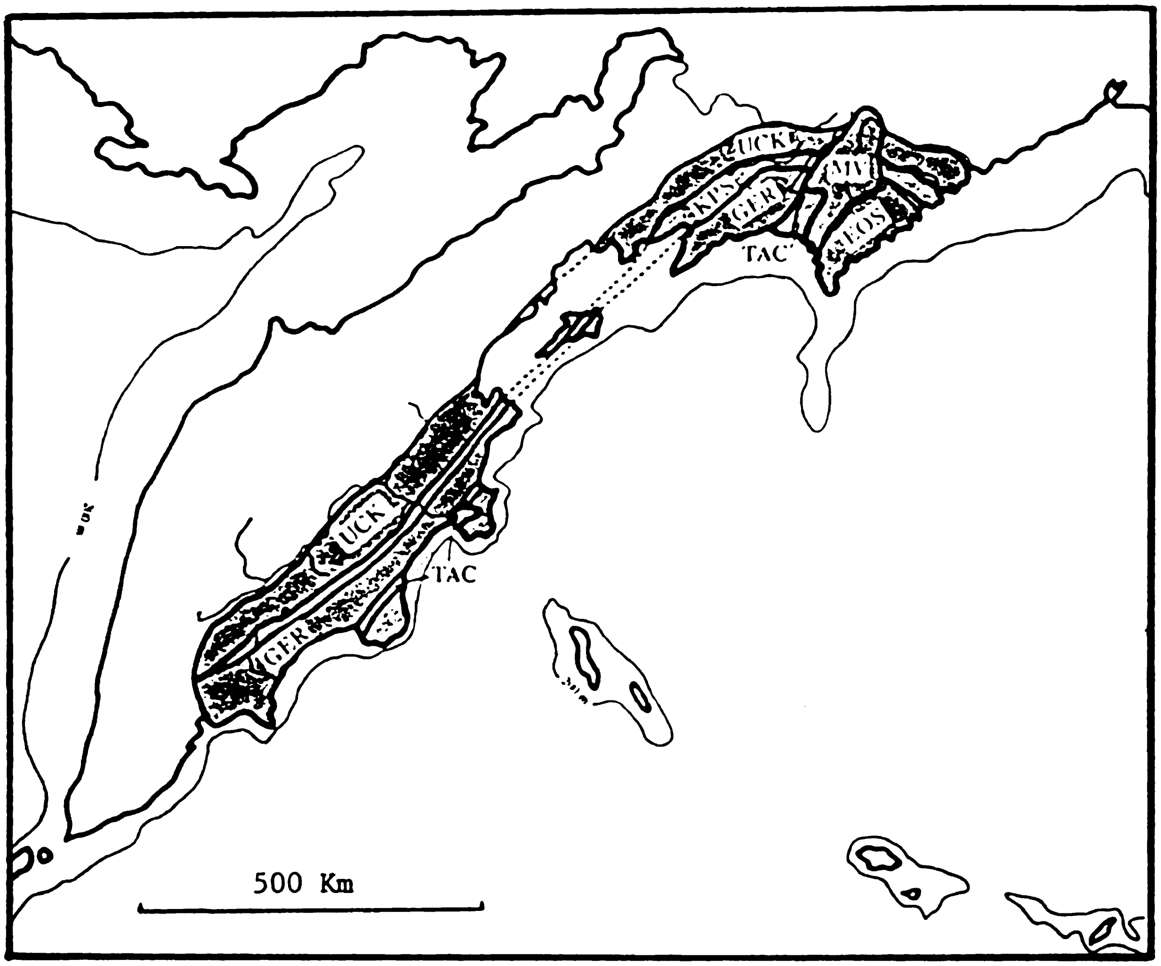

Figure 1-4

(Aleksandrov et al., 1980) or possibly 75° (Koltypin and Kononov, 1986) southeast in Olyutorsk.

In Kamchatka, a small basement exposure is found in the Khavyven uplift. The uplift consists of metamorphic greenschists and microquartzites containing mafic and ultramafic intrusives (Gnibidenko and Marakhanov, 1973; Shul'diner et al., 1979). These basement rocks are likely to be of Cretaceous or Jurassic age (Watson and Fujita, 1985). On western Karaginskii Island, Dolmatov et al. (1969) identify a Cretaceous basal layer of mafic green tuffs and "cherty cement" which may correlate to the Khavyven exposure in Kamchatka. No basement is identified in Olyutorsk, and in general, basement rocks are not well exposed, and are interpreted to lie under the extent of the terrane in Kamchatka based on geophysical data (Utnasin et al., 1975; Rivosh, 1964).

Andesites, basalts, tuffs, conglomerates and sandstones of unknown age lie unconformably upon the basement rocks in Kamchatka (Figure 1-5b). Eocene (?) to Oligocene rocks of the Kelmenskaya suite contain tuffs and sandy clastic rocks (Watson, 1985; Watson and Fujita, 1985). Finally, the Miocene and Late Miocene to Pliocene Yelovsk and Kavran suites consist of tuffaceous sandstones, siltstones and tuffs with occasional interbedded conglomerates (Watson, 1985).

In Olyutorsk, Koltypin and Kononov (1986) identify a Cretaceous (Santonian to Danian) flyschoid formation as the oldest rocks in that region of the UCK terrane. No details are given as to the lithologies which compose this formation. Paleocene to Eocene rocks consist of a molasse complex (Koltypin and Kononov, 1986), including silts, shales and fine sands. Above these lie Eocene to Oligocene clastics, volcanics and tuffs.

Paleo
cont
secti
inter
but
sand
Kar

on
this
eas
(Co
of
ter
roc
sou
in
Gr
Ki
(C
te
ei
co
in
A

Serova et al. (1975) detail the lithology and micropaleontology of the Paleogene to Miocene on Karaginskii Island. The Eocene is reported to contain volcanic ash tuffs with interbedded sandstones and siltstones. This section is overlain conformably by an Oligocene sandstone unit with intermittent interbedded sandstone and siltstone. The Miocene is thin (350 m), but contains predominant tuffs of basic composition with interbedded sandstones and siltstones. The benthic foraminifera found in these sections on Karaginskii Island are also noted extensively in much of Koryakia.

The compositions of post-Cretaceous rocks in Kamchatka, Olyurtorsk and on Karaginskii Island are similar (Figure 1-5b). This similarity indicates that this is one terrane extending from southern Kamchatka to Dezhneva Bay in eastern Olyutorsk. A continuous magnetic anomaly of greater than 500 gammas (Cooper et. al., 1976c) along the terrane's length also support the identification of UCK as a single terrane. Basement rocks, where exposed, suggest that the terrane is oceanic; overlying volcanics, marine and non-marine sedimentary rocks are consistent with this interpretation, but suggest a nearby terrigenous source as well. The basement of the UCK terrane most likely began formation in the Jurassic or Early Cretaceous (Watson and Fujita, 1985). In Kamchatka, Gnibidenko and Marakhanov (1973) obtained K-Ar dates of 92-122 Ma within the Khavyven basement sequence. This age is probably a metamorphic date (Gnibidenko and Marakhanov, 1973), and may represent the time of this terrane's accretion. Watson (1985) suggested the terrane may have represented either normal oceanic crust or a back-arc basin. The data presented here, when considered in light of constraints imposed by adjacent seaward terranes, support interpretation of the terrane as an obducted fragment of normal oceanic crust. A sedimentary sequence (Cretaceous to Paleogene Sediments terrane) and an

Figu

Figure 1-5a: Lithologic symbols used in the stratigraphic columns in Figures 5b-5g.

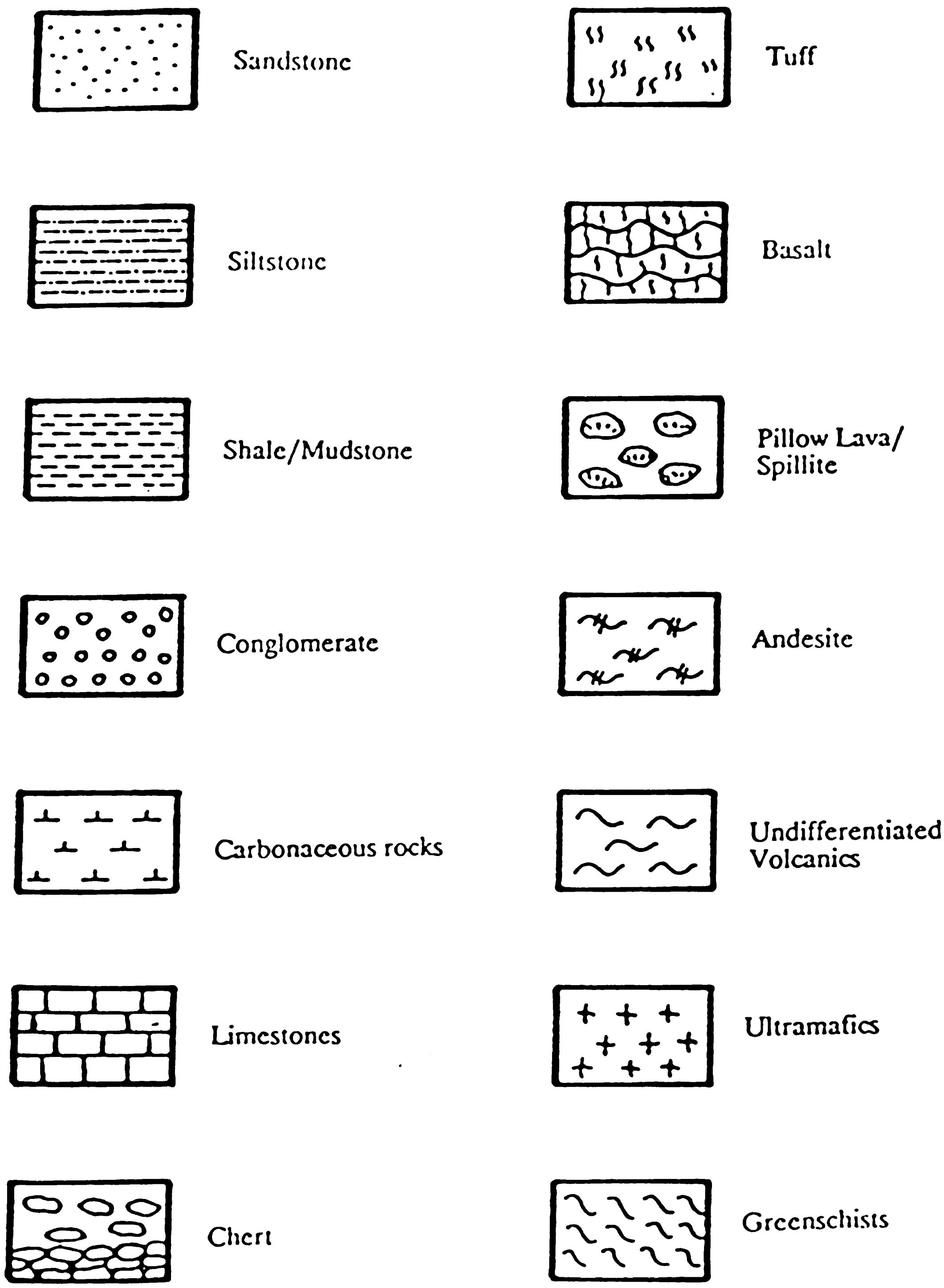
Sandstone
Tuff
Siltstone
Basalt
Shale/Mudstone
Pillow Lava/
Spillite
Conglomerate
Andesite
Carbonaceous rocks
Undifferentiated
Volcanics
Limestones
Ultramafics
Chert
Greenschists

Figure 1-5a

Fig

Figure 1-5b: Stratigraphic columns for the Ukelayat-Central Kamchatka terrane. Columns are summaries for each region. Suite names beside each column are given in full below.
Kamchatka: Kv - Kavron; Yl - Yelovsk; Kl - Kelmenskaya

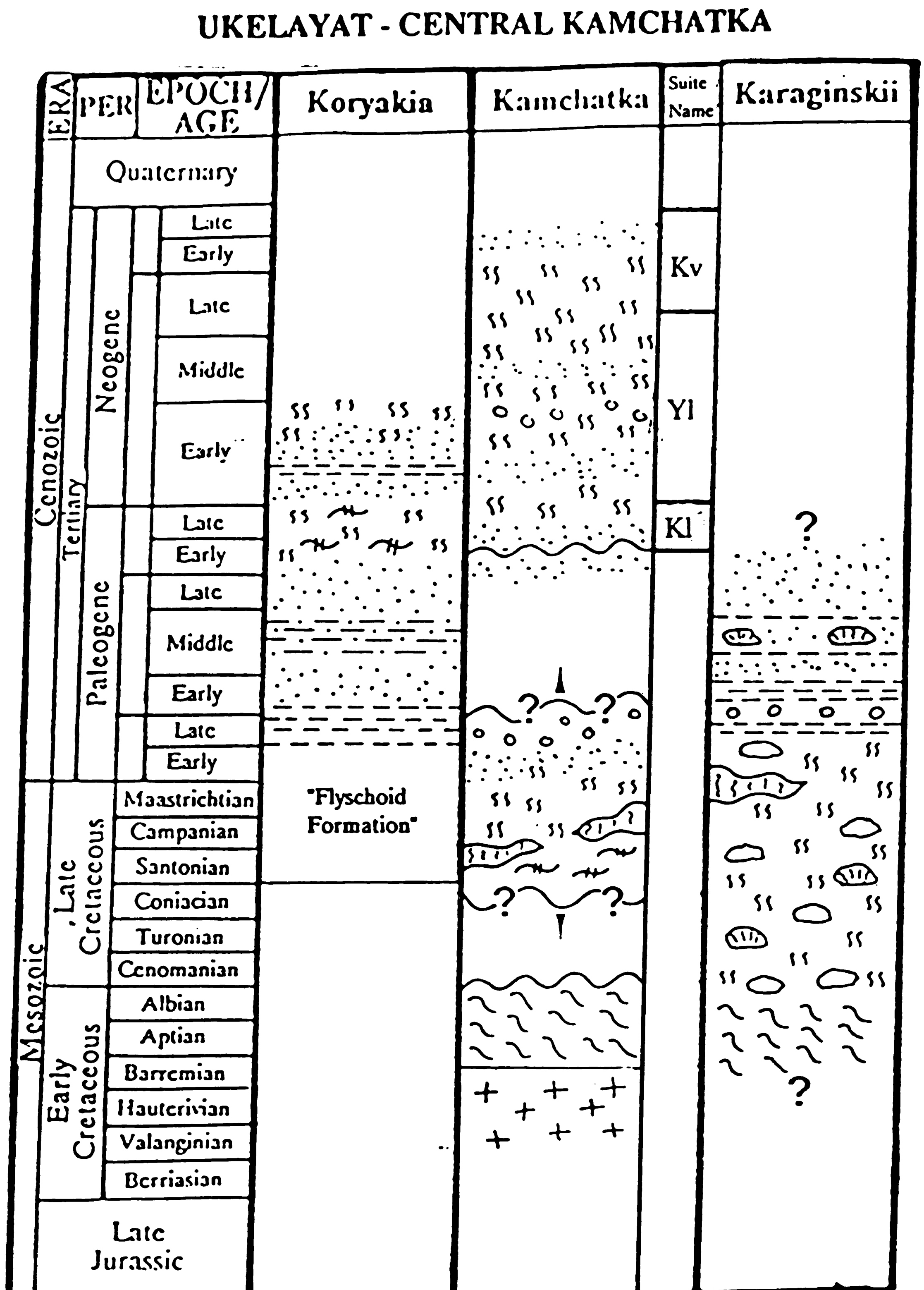

UKELAYAT - CENTRAL KAMCHATKA
ERA
PER
EPOCH/AGE
Koryakia
Kamchatka
Suite Name
Karaginskii
Quaternary
Cenozoic
Tertiary
Neogene
Paleogene
Late
Early
Middle
Mesozoic
Late Cretaceous
Early Cretaceous
Maastrichtian
Campanian
Santonian
Coniacian
Turonian
Cenomanian
Albian
Aptian
Barremian
Hauterivian
Valanginian
Berriasian
Late Jurassic
"Flyschoid Formation"
Kv
Yl
Kl

Figure 1-5b

Figure

Figure 1-5c: Stratigraphic columns for the Cretaceous - Paleogene Sediments terrane. Columns are summaries for each region. Suite names beside each column are given in full below.
Koryakia: Al - Aluga; Vl - Val'en; Ml - Mil'gernay; Tv - Tavensk; Ay - Ayaon
Kamchatka: Dr - Drozdovsk; Kp - Khapitsk

Mesozoic	Cenozoic	ERA

CRETACEOUS - PALEOGENE SEDIMENTS

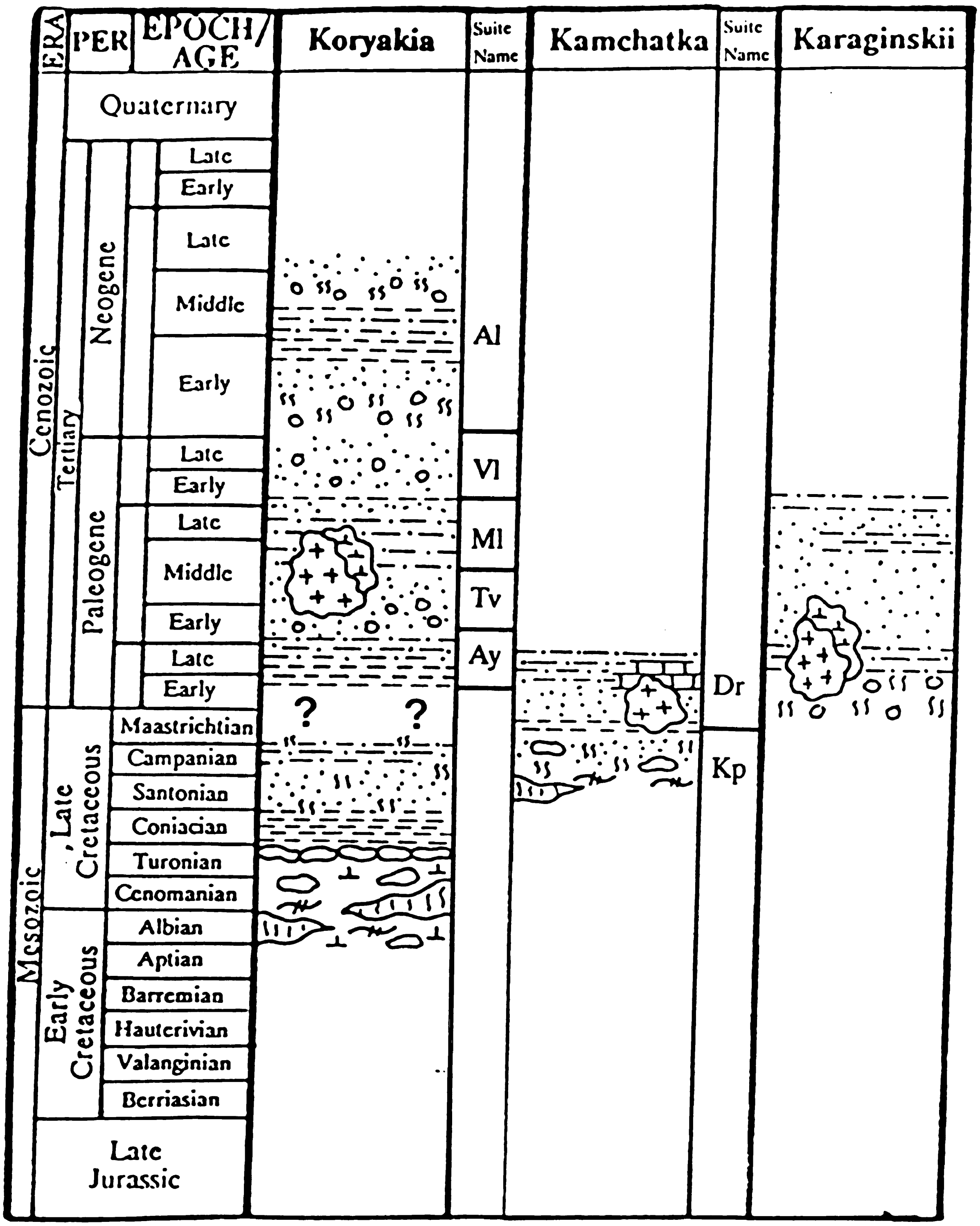

Figure 1-5c

Figure 1-5d: Stratigraphic columns for the Goven - Eastern Ranges terrane. Columns are summaries for each region. Suite names beside each column are given in full below.
Koryakia: Al - Aluga; Gv - Goven; Lv - Lavrov; Py - Pylga
Kamchatka: Os - Osipov; Ch - Chazhmin; St - Stanislavsk; Bs - Bushuyka

GOVEN - EASTERN RANGES

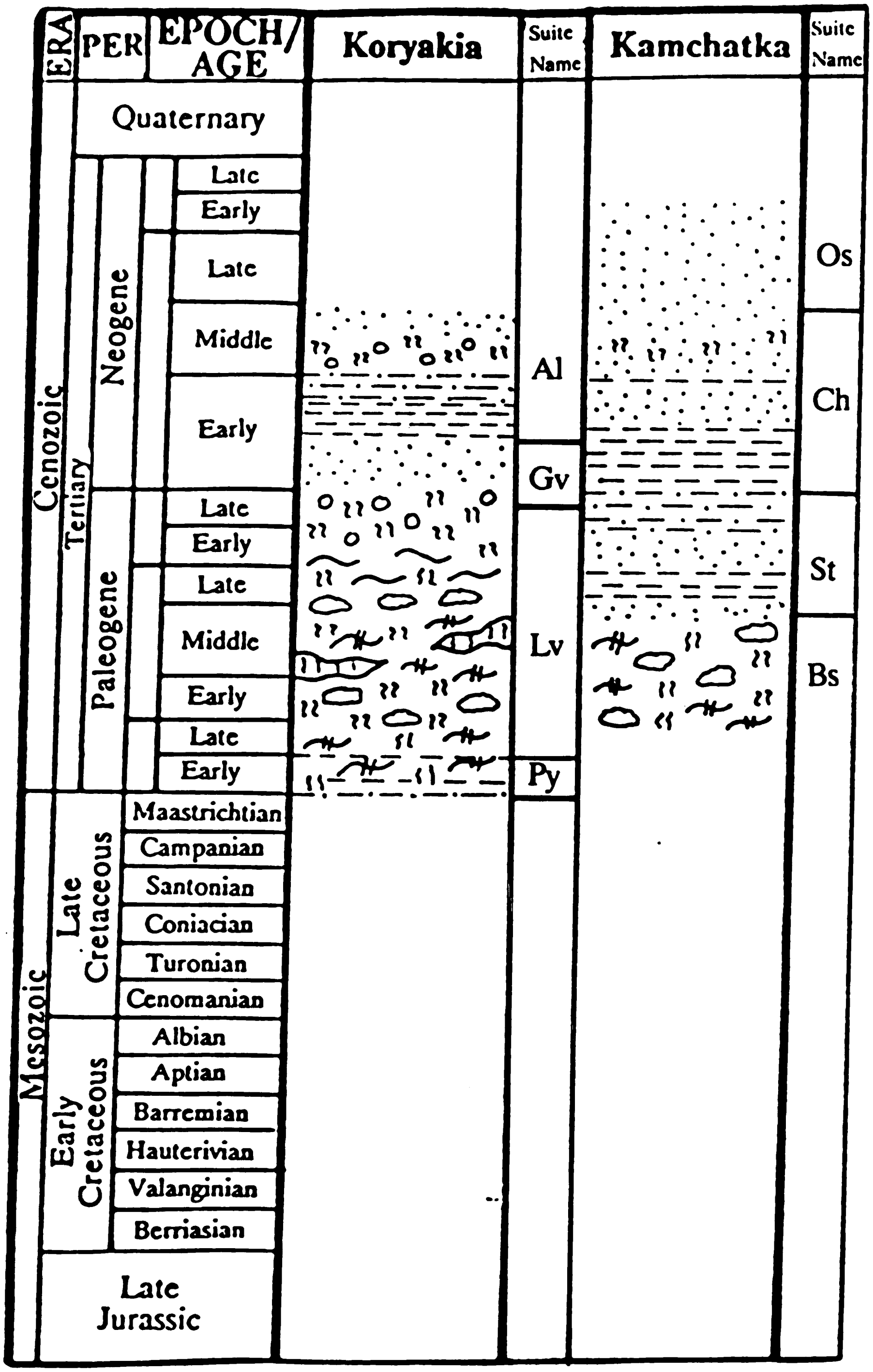

Figure 1-5d

Figure 1-5e: Stratigraphic columns for the Tertiary Accretionary Complex terrane. Columns are summaries for each region. Suite names beside each column are given in full below.
Koryakia: Al - Aluga
Kamchatka: Ts - Tyushevka series; Ch - Chazhmin; Bg - Bogachevka

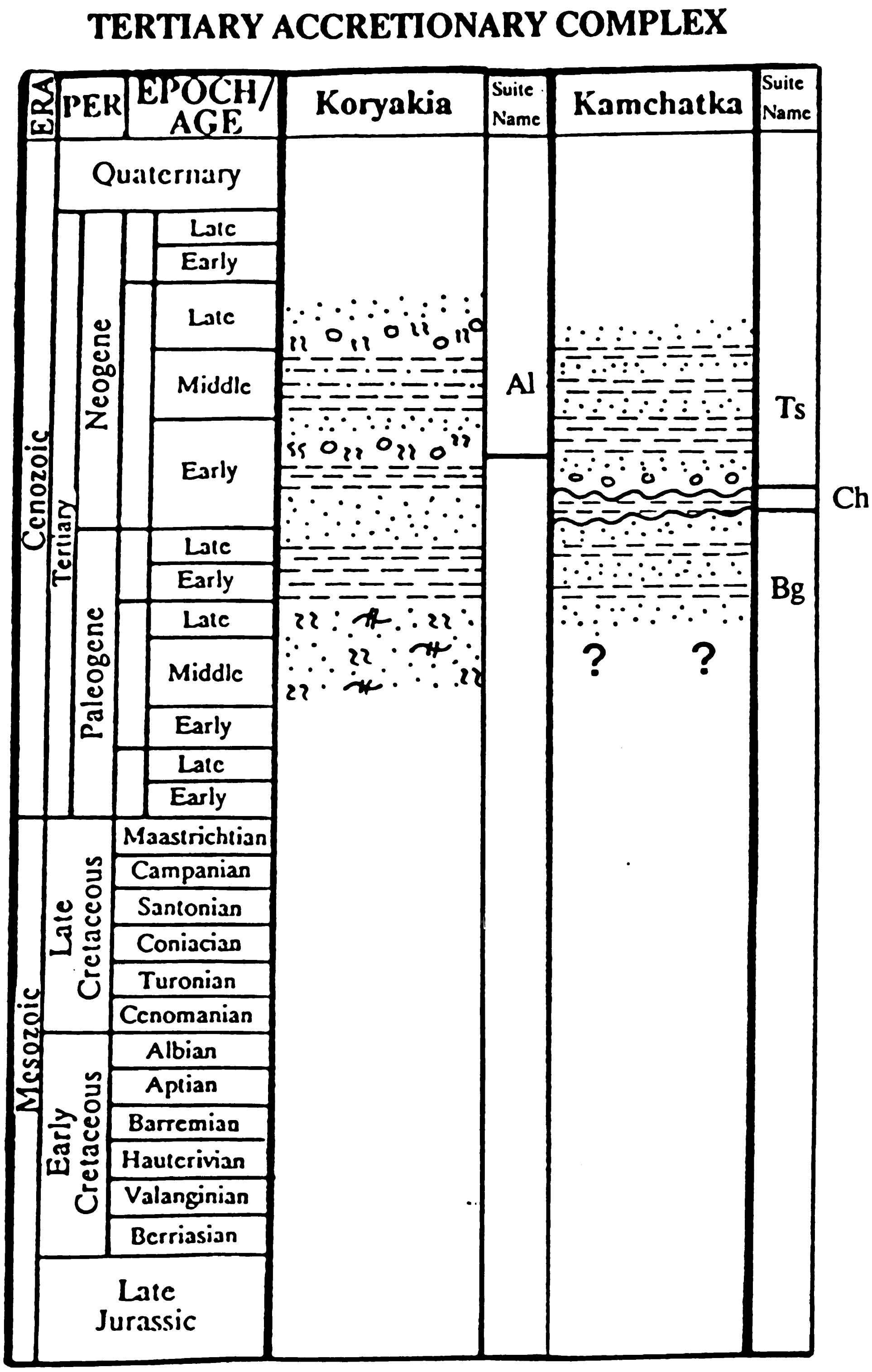

TERTIARY ACCRETIONARY COMPLEX
ERA
PER
EPOCH/ AGE
Koryakia
Suite Name
Kamchatka
Suite Name
Quaternary
Cenozoic
Tertiary
Neogene
Paleogene
Late
Early
Late
Middle
Early
Late
Early
Late
Middle
Early
Late
Early
Mesozoic
Late Cretaceous
Maastrichtian
Campanian
Santonian
Coniacian
Turonian
Cenomanian
Early Cretaceous
Albian
Aptian
Barremian
Hauterivian
Valanginian
Berriasian
Late Jurassic
Al
Ts
Ch
Bg
? ?

Figure 1-5e

Figure 1-5f: Stratigraphic column for the East Olyutorsk - Shirshov terrane.
Suite names beside each column are given in full below.
Koryakia: Al - Aluga

EAST OLYUTORSK - SHIRSHOV

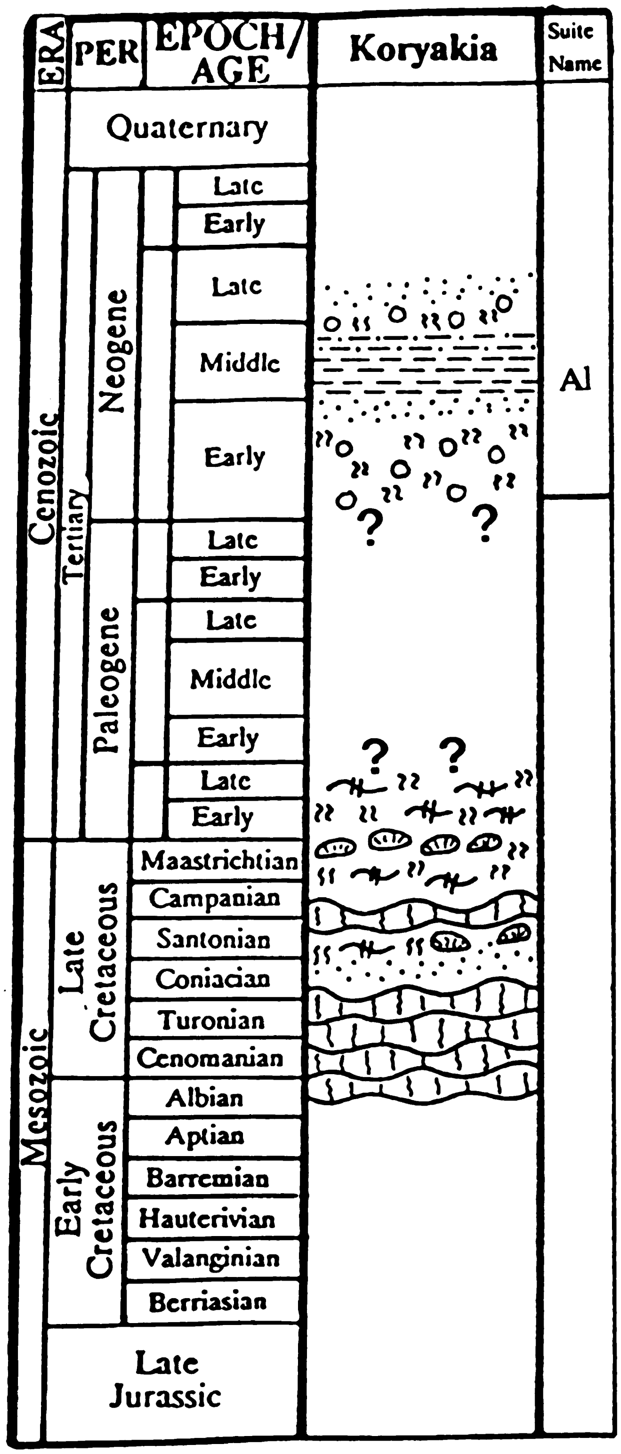

Figure 1-5f

Figure 1-5g: Stratigraphic column for the Miocene volcanics.

MIOCENE VOLCANICS

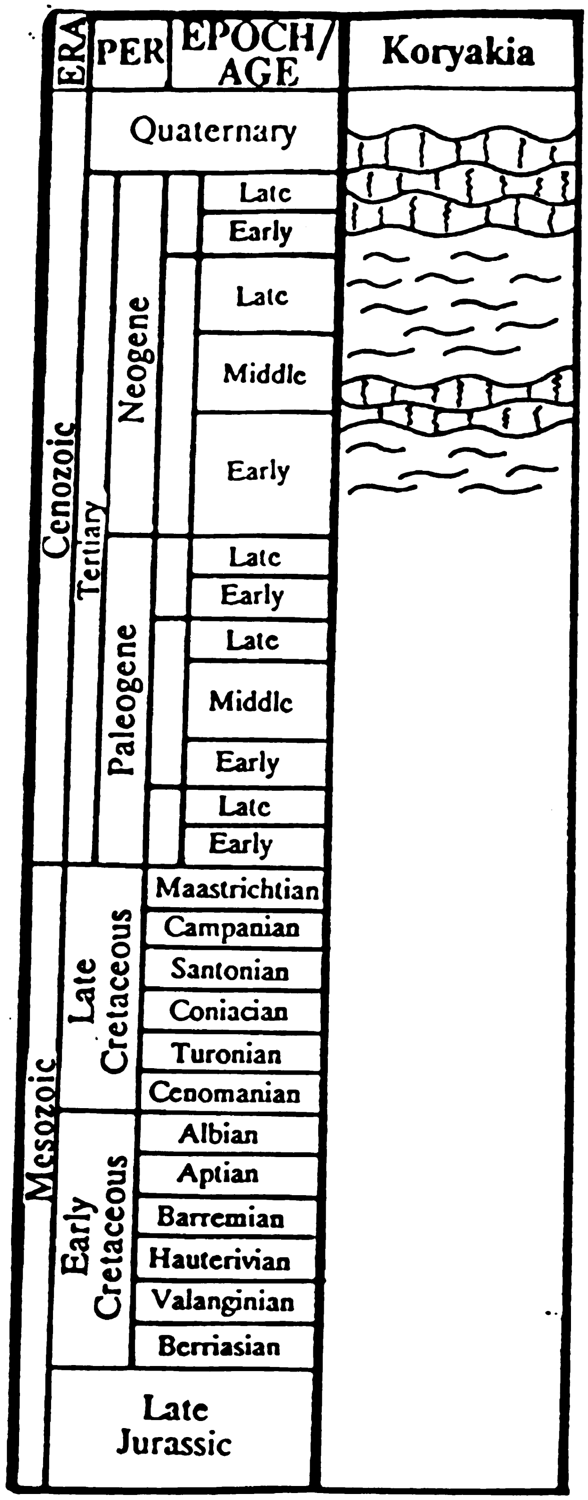

Figure 1-5g

island arc complex (Goven-Eastern Ranges terrane) are found southeast of the UCK terrane.

Cretaceous to Paleogene Sediments Terrane

A narrow Cretaceous to Paleogene sedimentary (KPS) terrane which contains numerous allochthonous ultramafic and gabbroic rocks is thrust over the UCK terrane. The KPS terrane ranges from 20 to 60 km in width, and extends from central Kamchatka (Tumrok Range) northward through central Karaginskii Island and into Olyutorsk where it follows the basin of the Vyvenka River to the northeast (Figure 1-6). The KPS terrane is overlain for a small distance by younger volcanics, and is then identified further east between the Il'pi and Vatyna river valleys in easternmost Olyutorsk (Figure 1-4). Yermakov and Mishin (1974) traced the units laterally from eastern Olyutorsk to the Kamchatka isthmus based on mineralogic consistencies within the rocks. In Kamchatka, Watson (1985) included these sediments and ultramafics within the Eastern Ranges terrane. However, faults bound these sediments, and considering the lithologic correlations to Olyutorsk and Karaginskii Island, it is suggested that the Kamchatka KPS deposits should be considered separate from the Eastern Ranges.

In Olyutorsk, the oldest rocks of the KPS terrane are Albian to Cenomanian basalts and andesites, with occasional lenses of carbonates and cherts (Bogdanov et al., 1982). Above these volcanics are 1 to 1.5 km of tuffs, cherts and fine clastic rocks which microfossil data suggest are Cenomanian to Maastrichtian in age (Bogdanov et al., 1982). The contact between these rocks and the overlying Ayaon suite (Yermakov and Mishin, 1974) is not described.

Figure 1-6: 1:250,000 LANDSAT image close-up showing the linear deformation of the KPS terrane. MV denotes a small Miocene volcanic pile.

Figure 1-6

The thickest (up to 8 km) Paleogene section of the KPS terrane is found in Olyutorsk, where Yermakov and Mishin (1974) have divided the complex into four suites (Figure 1-5c), consisting primarily of sandstones, siltstones, and argillites, with lesser amounts of conglomerates, tuffs, tuffaceous sandstones and cherty-argillaceous rocks. These suites, the Ayaon, Tavensk, Mil'gernay and Val'en, are summarized below.

The Ayaon suite is composed of fine-grained clastics. They are dark grey in color, and contain a matrix of organic compounds and silt-sized grains. Common grain types include quartz, plagioclase and volcanic fragments with basic composition. A lesser amount of poorly sorted sandstone is also found within the suite. The sandstone is composed of quartz, plagioclase, extrusive volcanic rock fragments (acidic, intermediate and basic), chert and other fine-grained material.

The overlying Tavensk suite contains coarser grained sediments including sandstones, gravellites and conglomerates. The sandstones are poorly sorted, and are made up of extrusive volcanic clasts, chert, quartz, plagioclase and silt. Rare thin beds of fine-grained clastics are similar to the rocks of the Ayaon suite.

Parallel or cross-bedded, occasionally massive, fine- to medium-grained sandstones and siltstones dominate the Mil'gernay suite. Matrix is minimal within the rocks, constituting less than 10% of the total make-up. Grains are usually quartz, plagioclase, acid volcanics, lesser basic and intermediate rocks, chert and shaley rock fragments. The siltstones of the Mal'gernay suite are sometimes microstratified, distinguishing them from siltstones of the Ayaon or Tavensk suites.

The Val'en suite is also composed of coarse-grained rocks: sandstones, gravellites and conglomerates. The sandstones are poorly sorted with quartz, plagioclase, acid volcanic fragments (rarely basic or intermediate), chert and fine-grained clastic rock fragments. No data are given on the coarser sedimentary rocks.

Several investigators (e.g., Dundo et. al., 1982; Fujita and Newberry, 1983; Palandzhjan, 1986; Koltypin and Kononov, 1986) have identified ultramafic ophiolite blocks (e.g., Vatyna, Vyvenka) within the sediments of the KPS terrane in Olyutorsk. These blocks sometimes have associated pillow structures, siliceous and/or carbonaceous rocks (Aleksandrov et. al., 1980), and are older than the sediments of the KPS terrane (Alekseyev, 1979).

Bogdanov et al. (1982) identify an east-dipping thrust fault running north-south through Karaginskii Island which separates the KPS terrane from the UCK terrane. On the eastern (upthrown) side of the thrust, Bogdanov et al. (1982) identify volcanic and siliceous rocks and abundant ultramafic exposures. Within this same central region, Serova et al. (1975) describe north-south trending Paleogene tuffs, tuff-breccias, siltstones and interbedded siltstones and sandstones. Dolmatov et al. (1969) and Dundo et al. (1982) further describe Late Cretaceous mafic and ultramafic blocks among the Cretaceous to Paleocene deposits on the island.

The Khapitsk suite in Kamchatka (Watson, 1985) is equivalent to the Cretaceous units of the KPS terrane identified in Olyutorsk. Watson (1985) included these rocks within the Eastern Ranges terrane of Kamchatka Peninsula. However, the Khapitsk suite has a differing lithology and is apparently fault bounded. The suite includes layers of tuffs, tuffaceous clastics and cherts among andesitic and basaltic volcanics (Shapiro, 1981), and

oc
Li
le
re
al
ca
ag

as
is
th
F
to
pr
se

la
ro
1
b
su
(l
li

th
P

occasional exposures of ultramafic rocks (e.g., Tumrok Range; Watson, 1985). Limestone blocks are often found in association with these ultramafics. This led Rotman et al. (1973) to suggest the ultramafics and associated rocks may represent a subduction zone melange complex. The Drozdovsk suite contains alternating deposits of sandstones and argillites, with occasional tuffaceous or calcareous horizons. Benthic foraminifera suggest a Danian to Early Paleocene age for the suite (Serova et al., 1970).

The ultramafics (e.g. Vatyna, Karaginskii, Tumrok) complexes can be used as a marker for lateral correlation of the KPS terrane. Additionally, correlation is aided through identification of extensive surficial expressions of folding of the sediments observed on LANDSAT and mosaic imagery (Figure 1-3 and 1-6). Finally, aeromagnetic values (Cooper et. al. 1976c) consistently range from 100 to 300 gammas over the KPS terrane. Within the faulted boundaries, the presence of ultramfic blocks, decrease in magnetic intensity and distinct sedimentologic lithologies characterize the KPS terrane.

Faulting and folding are found internally throughout the terrane, although lateral slip seems to dominate in Kamchatka (Watson, 1985). Deformation of the rocks is extensive in Olyutorsk (Aleksandrov et al., 1980; Mitrofanov et al., 1980), and fold wavelengths of 1 to 8 km are observed in the Vyvenka River basin (Figure 1-6). Filatova and Yegorov (1983) note that field evidence suggests maximum shortening within this complex occurred in eastern Olyutorsk (between the Il'pi and Vatyna rivers), indicating that plate motion was most likely perpendicular to the northern margin during emplacement.

The KPS terrane is thrust over the UCK terrane to the west. The age of the sediments and thrust faults ties very well with the timing (Cretaceous - Paleogene boundary) of compression and major thrusting in southern Koryakia

(Harbert et al., 1987; Kazimirov, 1985), as well as in Kamchatka (Watson and Fujita, 1985). Subduction, back-arc and oceanic settings must be considered as possible sources for the KPS terrane sediments. The sediments must have originally lain stratigraphically above the UCK terrane, and were then thrust over the UCK terrane during obduction. Therefore, I suggest these were accretionary wedge sediments which were lying upon the UCK terrane. This presents a simple solution to their present structural position and is consistent with the observed lithologies.

Although not examined in this investigation, Yermakov (1975) and Yermakov and Suprunenko (1975) propose that this terrane extends along the Alaskan Shelf, through Zemchug and Pribilof canyons, southeastward to Shumagin and Kodiak islands. If this is the case, the accretion of the Goven-Eastern Ranges (GER) terrane may be synchronous with the docking of the Peninsular terrane along southern Alaska and the Beringian margin.

Goven-Eastern Ranges Terrane

Watson (1985) identified the Eastern Ranges terrane in Kamchatka, and suggested that it represented an island arc complex. Here I show that lithologic and geophysical correlations are consistent with a northward extension of the terrane from Kamchatka into Olyutorsk, and that the data support Watson's (1985) interpretation.

Within Olyutorsk, the terrane extends eastward from the Goven Peninsula to the Pakhachinskii Plateau and Range, where it is buried beneath younger volcanics (Figure 1-3). I therefore have named the entire terrane Goven-Eastern Ranges (GER). The terrane is thrust upon the KPS terrane to the west, and an accretionary complex underthrusts the terrane to the east (Figure 1-4). If lateral succession is consistent in the western Bering Sea,

(
r
a
F
a

a
th
an
la
Py

sil
Ge
Th
Pe
dis
ons

then it is likely the terrane also is found on eastern Karaginskii Island. The only data which could be obtained describe eastern Karaginskii Island as a "flysch complex" (Bogdanov et al., 1982), and no specific lithologic or age data are known.

In Olyutorsk, the Paleocene to Miocene rocks of the GER terrane consist of the Pylga, Lavrov, Goven and Kylan suites (Figure 1-5d). The Pylga suite is found near the coastline of Olyutorsk Bay and extends from the southern tip of Goven Peninsula to the Apuka River in the east. The suite consists mostly of marine sediments, including argillites, siltstones, sandy shales, tuffs and andesites (Pichugina et al., 1974b). The Pylga suite has been dated as Early Paleocene based on planktonic foraminifera (Pichugina et al., 1974b), and is approximately 2000 meters thick.

Above the Early Paleocene Pylga are later Paleogene suites, the Lavrov and Goven. The Lavrov suite consists of volcanic and/or cherty rocks, while the overlying Goven suite is dominated by clastic rocks: sandstones, siltstones and argillites (Pichugina et al., 1974a). The distinct lithologic change and a lack of fossils in the Lavrov and Goven suites distinguish them from the older Pylga suite.

The Early to Middle Miocene Aluga series, primarily sandstones and siltstones, has an extensive distribution and consistent facies over Il'pinski, Goven and Olyutorsk Peninsulas, thereby suggesting it is an overlap succession. The thickness of the Aluga series varies greatly, from 1200 m in the Il'pi Peninsula to 10000 m in the Apuka Range region (Pichugina et al., 1974a). This distribution pattern and the age of the sediments correlates quite well with the onset of Miocene volcanism in central Olyutorsk. The uplift associated with the volcanism may, therefore, represent the source of the sediments composing the Aluga series.

Descriptions of correlative lithologies in Kamchatka are given by Watson (1985). Watson (1985) and Watson and Fujita (1985) identify underlying Cretaceous volcanic rocks, the Vetlovsk suite, in Kamchatka which have not been described in Olyutorsk. It is possible that similar rocks in Olyutorsk are overlain by the extensive Miocene basalts which border the northeastern margin of the terrane or are concealed under the continental shelf west of the Komandorskii Basin.

Overlying the Vetlovsk suite with "minor unconformity" (Watson, 1985) are the Bushuyka and Stanislavsk suites. The Bushuyka suite is composed of andesitic tuffs and cherts. Again, as seen in the Pylga and Lavrov suites in Olyutorsk, a distinct lithologic change marks the horizon between the Vetlovsk and Bushuyka suites in Kamchatka. Conformably overlying the Bushuyka suite is the Stanislavsk suite, consisting of sandstones and siltstones (Shapiro and Seliverstov, 1975), and lacking any paleontological remains.

Finally in Kamchatka, a sequence of fine clastics composing the Chazhmin suite is found overlying the Stanislavsk suite. This unit has been assigned an Early Miocene age by Watson (1985). A thick (greater than 2000 m) overlap succession of clastic sediments (the Osipov suite) lies unconformably on the Chazhmin suite in Kamchatka; the Chazmin and Osipov are suggested to be analogs of the Aluga suite in Olyutorsk.

Thus, there exists a one-to-one correlation between the rocks comprising the Goven terrane in Olyutorsk and those of the Eastern Ranges of Kamchatka and, therefore, a single Goven-Eastern Ranges terrane is proposed. The volcanic and clastic-siliceous sedimentary rocks of the GER terrane are very similar

Therefor

represen

tuffs (W

young v

diversity

period of

Tertiary

A l

Tertiary (

east (Fig

southeast

Kamchatk

the shelf

continuati

lithologies

Olyutorsk

abruptly b

The

and argill

in Kamch

overlap s

unit of t

Kamchatk

It is

just befor

similar to the arc facies which today comprise the Aleutian Island arc. Therefore, by analogy, it seems reasonable to suggest that the GER terrane represents an accreted island arc complex. Basement ultramafics, basalts and tuffs (Watson and Fujita, 1985) found in Kamchatka, and possibly buried by young volcanics in Olyutorsk, support the conclusion. The thickness and diversity of sediments may indicate a lengthy evolution with at least one period of volcanic quiescence and erosion.

Tertiary Accretionary Complex Terrane

A large northwest dipping thrust fault separates the GER terrane from a Tertiary (Eocene (?) to Miocene) accretionary complex (TAC) to located to the east (Figure 1-4). The TAC is identified as a narrow (less than 50 km) band southeast of the GER terrane and west of Kronotsky Peninsula and Cape Kamchatka. The gravimetrically identified East Kamchatka synclinorium along the shelf east of Karaginskii Island (Shapiro, 1976) may be the offshore continuation of the TAC, connecting the Kamchatka rocks with similar lithologies along the easternmost margin of the Govena Peninsula. Within Olyutorsk, the TAC extends a short distance northeast and and is terminated abruptly by overlying Miocene volcanics.

The TAC consists almost entirely of siltstones, sandstones, tuffs, cherts and argillites (Shapiro and Seliverstov, 1975; Koltypin and Kononov, 1986), both in Kamchatka and Koryakia (Figure 1-5e). The Miocene Aluga suite is an overlap succession composed of sandstones and siltstones, and is the youngest unit of the TAC in Olyutorsk. Watson (1985) identified this terrane in Kamchatka as the East Kamchatka basin.

It is important to note that the Aleutian island arc came into existence just before or during the formation and emplacement of the TAC terrane.

The

imp

mus

one

geor

enti

conv

com

subd

subd

been

plate

Paci

possi

impo

Cape

basin

East

(here

River

regio

strati

domi

Olyut

discus

Therefore, the extension of this terrane from central Kamchatka into Koryakia implies that westward subduction along the entire Kamchatka-Koryak margin must have continued until at least early Miocene. In order to accomplish this, one of two geometries must have existed during this time. In the first geometry, a unitary fragment of oceanic crust would be present along the entire western Bering Sea margin. This fragment would have had uniform convergence and rate relative to this boundary until such time as it was completely subducted. In the second geometry, two separate plates would be subducting along the Koryak-Kamchatka boundary: one north of the Aleutian subduction zone and one to the south. The northern convergence could have been due to the relative compression between the Eurasian and North American plates (Harbert et al., 1987). The southern zone would have been related to Pacific subduction along the eastern margin of Kamchatka. It is not presently possible to distinguish between these two models. The solution, however, has important implications for the accretion mechanisms of Kronotsky Peninsula and Cape Kamchatka of Kamchatka, as well as for the evolution of the Komandorskii basin and east Kamchatka synclinorium of Shapiro (1976).

East Olyutorsk-Shirshov Terrane

The lithologic information in the easternmost extent of Olyutorsk (hereafter refered to as "East Olyutorsk," extending south from the Vatyna River to Olyutorsk Peninsula; Figure 1-2 and 1-4) is less detailed than in other regions of Olyutorsk. However, East Olyutorsk appears to have a less complex stratigraphy, with Cretaceous to Paleocene basic to intermediate volcanics dominating. Here I will primarily discuss the onshore extent of the East Olyutorsk - Shirshov (EOS) terrane; the details of the Shirshov Ridge were discussed earlier in the paper.

Fou

Yurkova

basic vol

of the E

are very

along t

therefore

The Gyt

tholeiites

terrane.

complexe

The

Olyutork

basalts (

similar t

extensive

sediment

Maastric

Th

Peninsul

separati

and Ko

tectonic

group to

west-dipp

band of s

Four volcanic complexes are identified in East Olyutorsk by Peyve and Yurkova (1987): Machevna, Gytgynskii, Nichakvayam and Olyutorka. All are basic volcanics of Cretaceous age. The Machevna complex comprises the bulk of the EOS terrane. These low-potassium basalts often occur as pillows, and are very similar to basalts dredged from the Shirshov Ridge. These basalts fall along the island-arc basalt differentiation trend of the Ti-Cr plot, and therefore, Peyve and Yurkova (1987) identify them as island-arc volcanics. The Gytgynskii and Nichakvayam complexes are small exposures of low-silica tholeiites located at the extreme north and west boundaries of the EOS terrane. There have been no basalts similar to the Gytgynskii or Nichakvayam complexes yet recovered from dredgings along the Shirshov Ridge.

The very southern tip of Olyutorsk Peninsula is composed of the Olyutorka complex, which is composed of transitional low-silica, high-titaniaum basalts (Peyve and Yurkova, 1987). It is these rocks which are chemically similar the sub-alkalic basalts dredged from the Shirshov Ridge. There are extensive formations of andesite-basalt tuffs, as well as volcanic and siliceous sediments, associated with the onshore volcanics, which range from Santonian to Maastrichtian in age (Koltypin and Kononov, 1986).

Thrust faults are found in easternmost Olyutorsk and on Olyutorsk Peninsula in the south, however, a major thrust bounds the EOS terrane, separating it from the KPS terrane on the north (Palandzhjan, 1986; Koltypin and Kononov, 1986). The thrust fault on Olyutorsk Peninsula defines a tectonic contact between the Olyutorka complex volcanics and the Machevna group to the north. Along the eastern margin of the EOS terrane there is a west-dipping fault where the Machevna group has been thrust over a narrow band of silty schists (Koltypin and Kononov, 1986). The western boundary of the terrane, which is truncated along the Apuka River valley (Figure 1-2 and 1-4), is most likely buried beneath the Miocene volcanics of the Pakhachinskii plateau and Apuka Mountains (Figure 1-3).

I consider the Shirshov Ridge to be an offshore continuation of East Olyutorsk for the following reasons: 1) topographic continuity (Scholl et al., 1975); 2) continuous gravity and magnetic signature (Ben-Avraham and Cooper, 1981; Cooper et al., 1976c); 3) dredge samples from the Shirshov Ridge are mineralogically similar to those on the southern portion of the Olyutorsk Peninsula (Neprochnov et al., 1985); 4) major and trace element chemistries of dredge rocks from Shirshov Ridge are similar to onshore chemistries in East Olyutorsk (Peyve and Yurkova, 1987); and 5) ages of the Shirshov volcanics and overlying sediments suggest common ages of genesis for both the Shirshov and East Olyutorsk rocks (Bogdanov and Neprochnov, 1984).

The presence of andesite and basalt volcanics and their directly associated tuffs and sediments strengthen Peyve and Yurkova's (1987) interpretation of the East Olyutorsk region as a remnant island arc. The geochemical similarity to other island arcs and presence of pillow basalts seem to provide conclusive evidence for this classification. Shirshov ridge has been interpreted by many (e.g., Scholl et al., 1975; Dickinson, 1978; Ben-Avraham and Cooper, 1981) to be a volcanic arc, which is consistent with the onshore conclusions.

Stratigraphic succession of the Aluga series across the EOS and GER terranes suggest that they were joined by Middle Miocene time (Figure 1-5f). Whether the accretion of the GER and EOS terranes to Olyutorsk was independent or if they had become a super-terrane, with the TAC pinched between them, before colliding with Kamchatka-Olyutorsk is uncertain, and is unlikely to be determined due to the obstruction of their spatial contact by a sequence of Miocene volcanics.

Miocene Volcanics

Laterally extensive Miocene volcanics cover south-central Olyutorsk from the central coastline of Olyutorsk Bay on the south to the Vyvenka and Ukelayat river basins on the north (Figure 1-4). To the east the volcanics terminate sharply along the Apuka and Achayvayam river valleys, while to the west the volcanics make an irregular boundary with the underlying GER and TAC terranes.

These volcanics are predominantly tholeiitic and alkaline basalts (Dundo et al., 1982; Bogdanov and Neprochnov, 1984). Although no major or trace element geochemical data are available, the volcanics are visible on satellite imagery (Figure 1-3), and can be seen as laterally extensive and lobate flows. Such charateristics are consistent with the expected behavior of relatively low viscosity basalts (Fink, 1987).

The stratigraphically lowest volcanics (Figure 1-5g) are sometimes described as intermediate volcanics (Bogdanov and Neprochnov, 1984), while the overlying flows are similar to plateau basalts. This may reflect source chamber inversions during the eruption process (Smith, 1979) or early contamination (of the intermediate volcanics) by the country rock. It is interesting to note that the Miocene age of these volcanics is very similar to other extensional indicators in the Bering Sea, including the age of rifting in the Komandorskii basin to the south.

EVOLUTION

Based upon the character of the terranes identified in Kamchatka and Koryakia (Figures 1-4 and 1-5), in addition to the geological and geophysical data available on the Bering Sea, a Cretaceous to present evolution for the Bering Sea region is proposed (Figure 1-7). I realize this evolution is, in part, similar to reconstructions done by the many others (e.g., Scholl et al., 1975; Marlow and Cooper, 1980; Marlow et al., 1982) who have investigated the Bering Sea region. The uniqueness of this model lies in the timing and tectonic settings which I derive from the western Bering Sea margin terranes and in the Neogene events of the western Bering Sea. In this model, I assume that a simple four plate system (Farallon, Izanagi, Kula and Pacific) has been involved since Early Cretaceous. Plate motion and convergence data have been taken from Engebretson et al. (1987) and Harbert et al. (in press).

Early Cretaceous

In the Early Cretaceous, the Farallon plate interacted with the northern Pacific basin margins, with the Farallon-Izanagi spreading ridge located to the south. The Farallon plate converged with Koryakia in a northerly direction, at a rate of 37 to 111 km/my (Harbert et al., in press). The Farallon-Izanagi ridge was rotating in a clockwise direction, and formed a northward migrating triple junction along the Eurasian coast.

Watson (1985) suggested that the triple junction formed by the intersection of the Farallon-Izanagi spreading center with the Eurasian coast migrated northward through Kamchatka between 115 Ma and 100 Ma. This is based on the lack of Albian to Turonian volcanic rocks in Kamchatka, and Albian to "middle Cretaceous" clastic sediments, possibly related to uplift as the ridge was subducted, found in the Omgon and Kvakhon terranes of Kamchatka

Figure 1-7: Tectonic evolution of the western Bering Sea since Early Cretaceous time. Schematic cross-sections for the time period are shown through Paleogene time. A)Early Cretaceous B) Late Cretaceous C) Paleogene D) Neogene to Present, including a generalized present-day cross-section approximately east-west through Olyutorsk derived from this study and a cross-section through Kamchatka at the latitude of Kronotsky Peninsula, modified from Watson (1985).

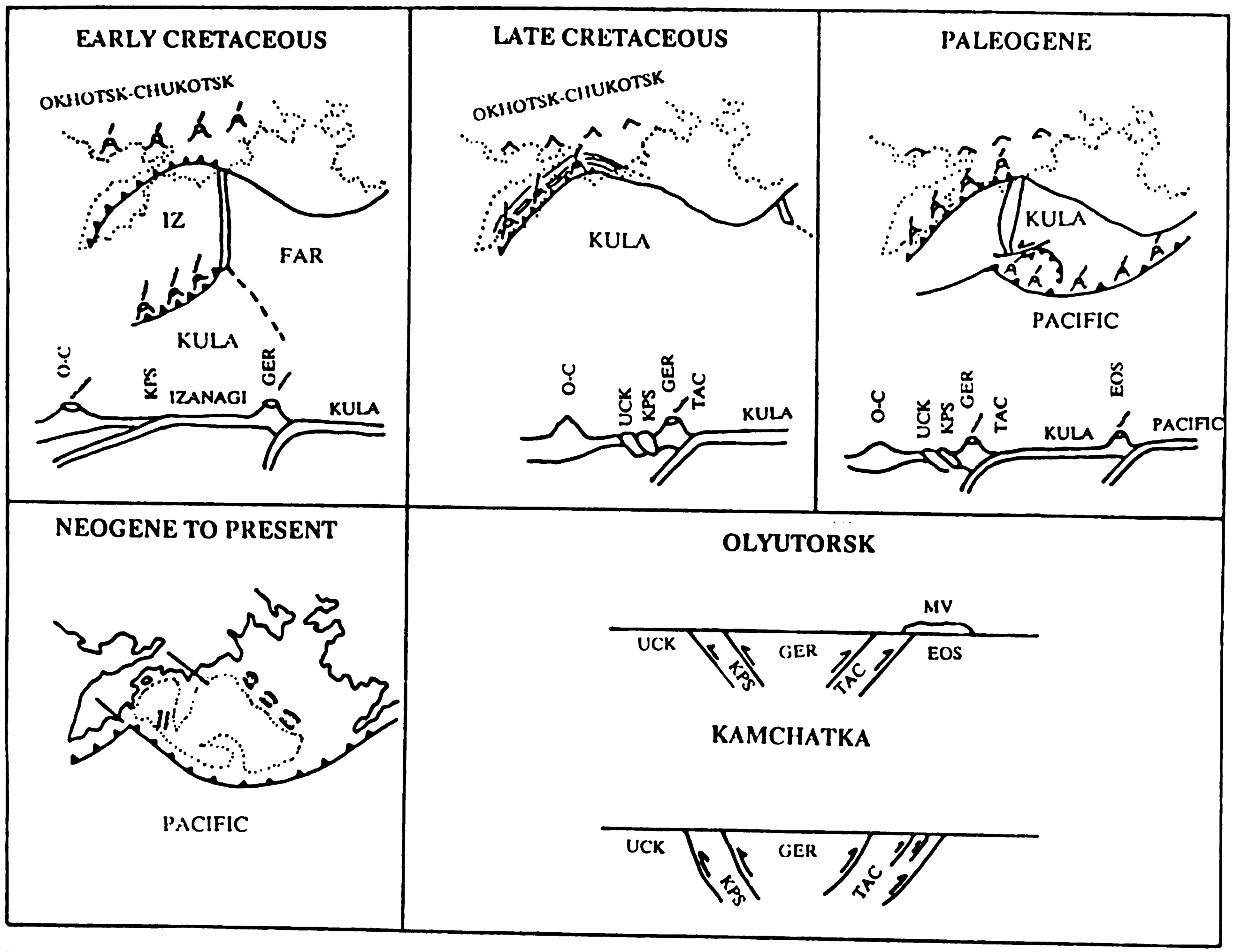
EARLY CRETACEOUS
OKHOTSK-CHUKOTSK
IZ
FAR
KULA
O-C
KPS
IZANAGI
GER
KULA
LATE CRETACEOUS
OKHOTSK-CHUKOTSK
KULA
O-C
UCK
KPS
GER
TAC
KULA
PALEOGENE
KULA
PACIFIC
O-C
UCK
KPS
GER
TAC
KULA
EOS
PACIFIC
NEOGENE TO PRESENT
PACIFIC
OLYUTORSK
MV
UCK
KPS
GER
TAC
EOS
KAMCHATKA
UCK
KPS
GER
TAC

Figure 1-7

(Watson and Fujita, 1985). In addition, from 115 to 100 Ma the convergence rate between the Farallon plate and Koryakia was uncharacteristically slow (approximately 10 km/my; Harbert et al., in press), and may have resulted from subduction of a thermally buoyant ridge.

Synchronous with the passing of the triple junction was the formation of the Okhotsk-Chukotsk volcanic belt within northeast Siberia. There was a wide arc-trench gap associated with the Okhotsk-Chukotsk arc resulting from the shallow angle of subduction (Fujita and Newberry, 1983) of the Izanagi plate. This is, however, consistent with what may be expected since the convergence rate of the Izanagi plate was very rapid (192 to 222 km/my; Harbert et al., in press) compared to the Farallon plate convergence.

Late Cretaceous

As the Izanagi plate subducted beneath the Koryakia-Kamchatka margin, the Kula plate was located to the south, and was subducting under the Goven - Eastern Ranges island arc (Figure 1-7a). At the end of Cretaceous or beginning of the Paleogene, a fragment of the Izanagi plate (UCK terrane) and accretionary wedge sediments (KPS terrane) were obducted onto the Koryakia margin as the Goven-Eastern Ranges island arc (GER terrane) collided with the zone of Izanagi subduction (Figure 1-7b). Subduction of the Izanagi plate ceased, and the Kula plate continued subduction under the Goven-Eastern Ranges arc, becoming the new Olyutorsk-Kamchatka margin. The timing of this event is based upon the age of the youngest marine sediments found in the KPS terrane. It is also possible that the cessation of volcanism in the Okhotsk-Chukotsk arc correlates with end of the Izanagi plate's rapid convergence and the comparitively slower (157 km/my) northwesterly convergence of the Kula plate along the Koryakia-Kamchatka margin.

Paleogene

Although collision of the Goven-Eastern Ranges island arc occurred by Early Paleogene, sediments as young as Miocene are found within the TAC terrane, which represents the frontal accretionary wedge of the Goven-Eastern Ranges island arc. This suggests that westward subduction continued under the Goven-Eastern Ranges arc until Miocene time. However, during the Paleocene to Miocene formation of the Tertiary accretionary complex, the Aleutian island arc also developed, trapping the fragment of oceanic crust which now floors the Aleutian basin (Cooper et al., 1976a). In order for subduction to continue until Miocene along the Olyutorsk-Kamchatka margin, as indicated by the extent of the TAC terrane, either 1) A small subducting fragment of Kula (?) plate must have remained to the west of the Bering Sea and the Pacific plate, or, 2) synchronous westward subduction of two different plates (Pacific and North America (?)) occurred north and south of the Aleutian subduction zone, or, 3) back-arc spreading was inititated in the area of the Komandorskii Basin. As of yet, there is no evidence conclusively supporting any model. However, the westward translation and accretion of the Cape Kamchatka terrane (Watson, 1985) in Eocene to Oligocene time (Watson and Fujita, 1985) is consistent with continued westward convergence under the Goven-Eastern Ranges arc at least through Paleogene time.

The East Olyutorsk-Shirshov arc, which had initiated its formation in the Senonian, became inactive during the Paleogene, possibly after being trapped on the Kula plate fragment north of the Aleutian arc. However, convergence continued between the floor of the Bering Sea and the Olyutorsk margin from 60 to at least 40 my ago, thereby causing the East Olyutorsk-Shirshov arc to impinge upon the eastern Olyutorsk margin. Oceanic crust to the west of the

East Olyutorsk-Shirshov island arc was subducted along the TAC terrane locus, which may correlate offshore to the "East Kamchatka synclinorium" (Shapiro, 1976) extending northward from Cape Kamchatka to the east of Karaginskii Island toward Goven Peninsula. Shortening also continued to be taken up along the eastern Kamchatka margin. The western convergence of the paleo-Komandorskii basin and the Komandorskii Islands also brought Cape Kamchatka into its present position during Eocene to Oligocene (Watson and Fujita, 1985). This was the final step in bringing the pre-Miocene features of the Bering Sea to their present positions, and was nearly the end of the compressional period within the Bering Sea.

An apparent basement correlation between the Shirshov and Bowers ridge (Cooper et al., 1976a) presents the interesting possibility that Bowers ridge was also part of the East Olyutorsk-Shirshov island arc system. If this was the case, southern Bowers ridge may have impinged upon the Aleutian island arc and separated from the Shirshov ridge along a left-lateral strike-slip fault (Kienle, 1971) which is now preserved in the basement rocks between Shirshov and Bowers ridges. Shortening along Bowers ridge was accomodated by renewed subduction under its eastern and northern flanks, while the Shirshov ridge remained tectonically inactive. Miocene rifting in the Komandorskii basin and related normal faulting (Savostin et al., 1986) has also structurally broadened Shirshov ridge, as first noted by Ludwig et al. (1971a). Thus differing Paleogene to Neogene evolutions of the Shirshov and Bowers ridges can explain the discrepencies in their observed geophysical (gravity, magnetic and seismic) character (Ludwig et al., 1971b; Kienle, 1971; Rabinowitz, 1974).

Neogene to Present

The emplacement of the EOS terrane brought the major structural features into their present positions within the Bering Sea region. This emplacement was also followed closely by the end of compression, and the transition by mid-Miocene to large scale extension in the whole Bering Sea region. Evidence for extension is found in the Komandorskii basin, where rift volcanism is presently taking place and 9 Ma basalts have been recovered at DSDP site 191, in central Olyutorsk, where there is extensive Miocene basaltic volcanism, in the Beringian margin basins, which have large thicknesses of Miocene sediments, and in Alaska's Yukon-Koyukuk province, where extensional earthquake mechanisms have been determined. This geologic evidence is in contrast to the Neogene compression between North America and Siberia predicted by the models of Pitman and Talwani (1972), Vink (1984) or Engebretson and Wallace (1984).

Within the Komandorskii basin, the present rifting, and the possibility of related onshore activity in Olyutorsk, can now explain the high heat flow values and shallow depth to basement (relative to the Aleutian basin) noted earlier. Seliverstov (1987) presents seismic profiles across a volcanic edifice within a 20 km wide graben structure which may be associated with the modern rift north of Bering Island (Bogdanov, 1986). The rift runs near the DSDP site 191 drill hole, and is shown by Savostin et al. (1986) to be offset by transforms which may also intersect the Shirshov ridge.

Miocene volcanism is also found in central Olyutorsk (Bogdanov and Neprochnov, 1984; Koltypin and Kononov, 1986), where it covers portions of the EOS, TAC, KPS and GER terranes. The volcanics are basic in composition, and appear as laterally extensive flows in the region of the Apuka Mountains and Pachachinsk Plateau. Whether there is a direct correlation between volcanism in the Komandorskii basin and central Olyutorsk is unclear at present.

The Beringian margin basins are thought to have originated in Eocene time based upon the oldest sediments flooring the basins. However, Miocene sediments have substantial thicknesses, and represent a renewed or increased extensional period at the Beringian Margin. The basins do not exhibit typical spreading structure, and are inconsistent with models of back-arc extension which require spreading perpendicular to convergence direction (Jurdy, 1979), and may instead be the response of a pre-existing weakness to extensional back-arc forces. This may be similar to extensional back-arc features oriented parallel to relative convergence noted by Karig et al. (1978) in the Mariana trough.

In the Yukon-Koyukuk province of Alaska, extensional focal mechanisms of earthquakes have been determined by numerous investigators (e.g. Liu and Kanamori, 1979; Biswas et al., 1986; Estabrook, 1985; and Chapter 2, this thesis). Thus it appears that the extension observed in the western Bering Sea and the Beringian margin extends even farther eastward to interior Alaska. The consistent extensional earthquakes of western Alaska are enigmatic when viewed in terms of Alaskan tectonics. A regional extensional episode, however, could best explain such events. Lockhart (1984), in his study of the Seward Peninsula concluded that the extension observed in Seward Peninsula is not caused by localized rifting, but by a regional extension. Such a conclusion is consistent with observations over the whole Bering Sea region.

CONCLUSIONS

The western Bering Sea margin is composed of five terranes of oceanic affinities which have accreted since Cretaceous time. Of the five, two represent island arcs (GER and EOS), two are packages of marine sediments (KPS and TAC) and one is a fragment of oceanic crust. Since Miocene time, volcanism has covered much of the exposure of these terranes in Olyutorsk, where extensional basaltic eruptions are observed, and in Kamchatka where island-arc type volcanics predominate.

The geology of these terranes preserves information which better constrains the Cretaceous and Cenozoic evolution of the Bering Sea. Obducted oceanic crust and sediments, possibly remnents of the Izanagi plate, have been identified in northern Olyutorsk. Evidence within the GER (island arc) and TAC (accretionary wedge) terranes indicates subduction continued along the Kamchatka-Olyutorsk margin until Miocene time. Miocene volcanism stitches Olyutorsk together with another Cretaceous island arc (EOS terrane) which collided with the margin pre-Miocene. The Bowers Ridge may also be a remnant of this island arc, offset from the Shirshov Ridge along a left-lateral fault. Some of the terranes preserved in the western Bering Sea may also continue under the Beringian Margin and/or be preserved in southern Alaska and its margins.

LIST OF REFERENCES

LIST OF REFERENCES

Aleksandrov, A. A., N. A. Bogdanov, S. A. Palandzhyan and V. D. Chekhovich, Tectonics of the northern part of the Olyutorsk zone of the Koryak Highlands, Geotectonics, 14, 241-248, 1980.

Alekseyev, E. S., Fundamental features of the evolution and structure of the southern part of the Koryak Highlands, Geotectonics, 13, 57-64, 1979.

Anderson, R. E., Tectonic overview of the Aleutian-Bering Sea region, Am. Assoc. Petrol. Geol., 2467, 1970

Ben-Avraham, Z. and A. K. Cooper, Early evolution of the Bering Sea by collision of oceanic rises and North Pacific subduction zones, Geol. Soc. Am. Bull., 92, 485-495, 1981.

Biswas, N. N., K. Aki, H. Pulpan and G. Tytgat, Characteristics of regional stresses in Alaska and neighboring areas, Geophys. Res. Lett., 13, 177-180, 1986.

Bogdanov, N. A., Geologic evolution of the Bering Sea Komandorsky Deep Basin (abstract), Am. Assoc. Petrol. Geol., 70, p. 914, 1986.

Bogdanov, N. A. and Yu. P. Neprochnov, Geology of the Bering Sea deep basins, in, Origin and History of Marginal and Inland Seas, Proceedings of the 27th International Geological Congress, 23, 1-17, 1984.

Bogdanov, N. A., V. D. Chekhovich, A. N. Sukhov and V. S. Vishnevskaya, Tectonics of the Olyutor zone, in, Yu. M. Pushcharovsky and S. M. Tilman (eds.), Notes on the Tectonics of the Koryak Upland, Nauka, Moscow, 189-217, 1982.

Bogdanov, I. A., Vishnevskaya, V. S., and Sukhov, A. N., Upper Cretaceous deposits of the Shirshov Ridge, Bering Sea, Doklady ESS, 273, 81-84, 1983.

Churkin, M., Tectonostratigraphic terranes of Alaska-Chukotka, in Accretion Tectonics in the Circum-Pacific Regions, edited by M. Hashimoto and S. Uyeda, p. 37-42, TERRAPUB, Tokyo, 1983.

Churkin, M. Jr. and J. H. Trexler, Continental plates and accreted oceanic terranes in the Arctic, in, A. E. M. Narin, M. Churkin, Jr. and F. G. Stehli (eds.), The Ocean Basins and Margins, v. 5, Plenum Press, 1-20, 1981.

Cook, D. B., Seismology and Tectonics of the North American Plate in the Arctic: Northeast Siberia and Alaska, PhD Dissertation, Michigan State University, E. Lansing, pp., 1988.

Cooper, A. K., M. S. Marlow and D. W. Scholl, Mesozoic magnetic lineations in the Bering Sea marginal basin, J. Geophys. Res., 81, 1916-1934, 1976a.

Cooper, A. K., D. W. Scholl and M. S. Marlow, Plate tectonic model for the evolution of the eastern Bering Sea, Geol. Soc. Am. Bull., 87, 1119-1126, 1976b.

Cooper, A. K., K. Bailey, J. Howell, M. S. Marlow and D. W. Scholl, Preliminary residual magnetic map of the Bering Sea Basin and Kamchatka Peninsula, U. S. Geological Survey Misc. Field Studies Map MF 715m, 1:250,000, 1976c.

Cooper, A. K, M. S. Marlow and D. W. Scholl, The Bering Sea - A multifarious marginal basin, in, M. Talwani and W. C. Pitman III (eds.), Island Arcs, Deep Sea Trenches and Back-Arc Basins, American Geophysical Union, 437-450, 1977.

Cooper, A. K., M. S. Marlow and Z. Ben-Avraham, Multichannel seismic evidence bering on the origin of Bowers Ridge, Bering Sea, Geol. Soc. Am. Bull., 92, 474-484, 1981.

DeLong, S. E., P. J. Fox and F. W. McDowell, Subduction of the Kula ridge at the Aleutian trench, Geol. Soc. Am. Bull., 89, 83-95, 1978.

Dickinson, W. R., Plate tectonic evolution of north Pacific rim, J. Phys. Earth, 26, S1-S19, 1978.

Dolmatov, B. K., S. A. Mel'nikova and Yu. M. Stefanov, The Mesozoic of Karaginskiy Island, Eastern Kamchatka, Doklady AN SSSR, Ser. Geologia, 187, 63-65, 1969.

Dundo, O. P. and B. Kh. Egiazarov (eds.), Geological Map of the Bering Sea Area, 1:2,500,000, 4 sheets, Ministry of Geology of the USSR, 1982.

Engebretson, D. C., A. Cox and R. G. Gordon, Relative motions between oceanic and continental plates in the Pacifci basin, Geol Soc. Am. Spec. Pap. 206, 59 pp., 1985.

Estabrook, C. H., Seismotectonics of northern Alaska, M. S. Thesis, 139 pp., University of Alaska, Fairbanks.

Fink, J. and J. Zimbelman, Using morphologic indicators to assess lava flow rheology: Royal Gardens basalt flows, Kilauea Volcano, Hawaii (abstract), Int. Union of Geodesy and Geophys., XIX General Assembly, v. 2, p. 417, 1987.

Fujita, K. and J. T. Newberry, Accretionary terranes and tectonic evolution of northeast Siberia, in Accretion Tectonics in the Circum-Pacific Regions, edited by M. Hashimoto and S. Uyeda, p. 43-57, TERRAPUB, Tokyo, 1983.

Gaynanov, A. G., Kosminskaya, I. P., and Stroyev, P. A., Geophysical studies of the deep structure of the Bering Sea, Izvestiya Earth Physics, 8, 461-465, 1968.

Gnibidenko, G. S., Tectonics of the floor of the Bering Sea: Geotectonics, 7, 237-243, 1973.

Gnibidenko, H. S. and V. I. Marakhanov, Structure of the east Kamchatka anticlinorium, Academy of Sciences of the U.S.S.R., Doklady, Earth Science Section, 210, 74-77, 1973.

Harbert, W. New paleomagnetic data from the Aleutian Islands: Implications for terrane migration and deposition of the Zodiac fan, Tectonics, 6, 585-602, 1987.

Harbert, W., L. S. Frei, A. Cox and D. C. Engebretson, Relative motions between Eurasia and North America in the Bering Sea region, Tectonophysics, 134, 239-261, 1987.

Harbert, W., L. Frei, R. Jarrard, S. Halgedahl and D. Engebretson, Paleomagnetic and plate tectonic constraints on the evolution of the Alaskan-Eastern Siberian Arctic, Geol. Soc. Am., Decade of North American Geology, chapter 34, vol. 23, in press.

Jones, D. L., N. J. Silberling and J. Hillhouse, Wrangellia-a displaced terrane in northwestern North America, Can. J. Earth Sci., 14, 2565-2577, 1977.

Jurdy, D. M., Relative plate motions and the formation of marginal basins, J. Geophys. Res., 84, 6796-6802, 1979.

Karig, D. E., Remnant arcs, Geol. Soc. Am. Bull., 83, 1057-1068, 1972.

Karig, D. E., R. N. Anderson and L. D. Bibee, Charactersitics of back arc spreading in the Mariana trough, J. Geophys. Res., 83, 1213-1226, 1978.

Kienle, J., Gravity and magnetic measurements over Bowers Ridge and Shirshov Ridge, Bering Sea, J. Geophys. Res., 76, 7138-7153, 1971.

Koltypin, A. V. and M. V. Kononov, Istoria formirovania yuzhno-Koryakski pozdnemelovi - Paleogenovi ostrovni dug, Izdatel'stvo Moskovskovo Universiteta, Otdel Geologicheskii (in Russian), 61, 25-38, 1986.

Liu, H. L. and H. Kanamori, Determination of source parameters of mid-plate earthquakes from the waveforms of body waves, Bull. Seis. Soc. Am., 70, 1989-2004, 1980.

Lockhart, A. B., A gravity survey of the central Seward Peninsula, Alaska (abstract), Geol. Soc. Am. Abstr. Prog., Cordilleran Section, 16, 319, 1984.

Ludwig, W. J., S. Murauchi, N. Den, M. Ewing, H. Hotta, R. E. Houtz, T. Yoshii, T. Asanuma, K. Hagiwara, T. Sato and S. Ando, Structure of the Bowers Ridge, Bering Sea, J. Geophy. Res., 76, 6350-6366, 1971a.

Ludwig, W. J., R. E. Houtz and M. Ewing, Sediment distribution in the Bering Sea: Bowers Ridge, Sirshov Ridge and enclosed basins, J. Geophy. Res., 76, 6367-6375, 1971b.

Marlow, M. S. and A. K. Cooper, Mesozoic and Cenozoic structural trends beneath the southern Bering Sea shelf, Am. Assoc. Petr. Geol., 64, 2139-2155, 1980.

Marlow, M. S. and A. K. Cooper, Wandering Terranes in Southern Alaska: The Aleutia Microplate and Implications for the Bering Sea, J. Geophy. Res., 88, 3439-3446, 1983.

Marlow, M. S., D. W. Scholl, E. C. Buffington and T. R. Alpha, Tectonic history of the central Aleutian arc, Geol. Soc. Am. Bull., 84, 1555-1574, 1973.

Marlow, M. S., A. K. Cooper, D. W. Scholl and H. McLean, Ancient plate boundaries in the Bering Sea region, London Geol. Soc. Spec. Publ. 10, 201-211, 1982.

Mitrofanov, N. P., A. M. Podol'skiy, N. Y. Kostin, M. A. Talalay and S. D. Sheludchenko, The Koryak volcanic-plutonic complex, Intern. Geol. Rev., 22, 1335-1345, 1980.

Moore, J. C., T. Byrne, P. W. Plumley, M. Reid, H. Gibbons and R. S. Coe, Paleogene evolution of the Kodiak Islands, Alaska: Consequences of ridge-trench interaction in a more southerly latitude, Tectonics, 2, 265-293, 1983.

Moore, G. W., Plate-tectonics Map of the Circum-Pacific Region, Amer. Assoc. Petrol. Geol., 14 p., 1 sheet, scale 1:20,000,000, 1982.

Nakamura, K., G. Plafker, K. H. Jacob and J. N. Davies, A tectonic stress trajectory map of Alaska using information from volcanoes and faults, Bull. Earthquake Res. Inst., 55, 89-100, 1980.

Natal'in, B. A. and L. M. Parfenov, Accretional and eugeosynclinal folded systems of the northwest Pacific rim, in Accretion Tectonics in the Circum-Pacific Regions, edited by M. Hashimoto and S. Uyeda, p. 59-68, TERRAPUB, Tokyo, 1983.

Neprochnov, Y. P., Sedov, V. V., Merklin, L. R., and Rudnik, G. B., New data on structure of the Shirshov Ridge, Bering Sea, Doklady ESS, 277, 114-118, 1984.

Neprochnov, Y. P., Sedov, V. V., Merklin, L. P., Zinkevich, V. P., Levchenko, O. V., Baranov, B. V., and Rudnik, G. B., Tectonics of the Shirshov Ridge, Bering Sea, Geotectonics, 19(3), 194-207, 1985.

Nur, A. and Z. Ben-Avraham, Speculations on mountain building and the lost Pacifica continent, J. Phys. Earth, 26 (suppl.), S21-S37, 1978.

Palandzhjan, S. A., Ophiolite belts int he Koryak Upland, northeast Asia, Tectonophysics, 127, 341-360, 1986.

Peyve, A. A. and R. M. Yurkova, Basalts of the Sirshov Ridge, Bering Sea, Transactions (Doklady) of the USSR Academy of Sciences, Earth Science Section, 285, 72-75, 1987.

Pichugina, G. K., L. V. Kryshtofivich and B. Kh. Yegiazarov, Stratigraphic scheme of the Paleogene and Miocene deposits of the northwestern part of the Olyutorskii-Kamchatskii folded system, in Stratigraphy and Lithology of the Cretaceous, Paleogene and Neogene Deposits of the Koryak-Anadyr' District, edited by V. N. Vereshchagin (in Russian), p. 42-47, NIIGA, Leningrad, USSR, 1974a.

Pichugina, G. K., B. V. Yermakov and O. K. Bazhenova, New data on the stratigraphy of the southern part of the Koryak Highlands, in Stratigraphy and Lithology of the Cretaceous, Paleogene and Neogene Deposits of the Koryak-Anadyr' District, edited by V. N. Vereshchagin (in Russian), p. 48-52, NIIGA, Leningrad, USSR, 1974b.

Pitman, W. C., III and M. Talwani, Sea-floor spreading in the North Atlantic, Geol. Soc. Am. Bull, 83, 619-649, 1972.

Rabinowitz, P. D., Seismic profiling between Bowers Ridge and Shirshov Ridge in the Bering Sea, J. Geophys. Res., 79, 4977-4979, 1974.

Rabinowitz, P. D. and A. Cooper, Structure and sediment distribution in the western Bering Sea, Marine Geology, 24, 309-320, 1977.

Rea, D. K. and J. M. Dixon, Late Cretaceous and Paleogene tectonic evolution of the North Pacific Ocean, Earth Planet. Sci. Lett., 65, 145-166, 1983.

Rivosh, L. A., Some geophysical data bearing on deep structure of the Central Kamchatka trough, Inter. Geol. Rev., 6, 2009-2014, 1964.

Rotman, V. K., B. A. Markovskiy and M. I. Khotina, The Kamchatka ultrabasic province, Int. Geology Rev., 15, 1015-1024, 1973.

Rzhevskiy, N. N., and Shimarayev, V. N., Fundamental features of the geologic structure of the western part of the Bering Sea: Int. Geol. Rev., 22(1), 84-88, 1980.

Savostin, L. A., B. V. Baranov, T. Z. Grigoryan and L. R. Merklin, Tectonics and origin of the western Bering Sea, Transactions (Doklady) of the USSR Academy of Sciences, Earth Science Section, 286, 88-91, 1986.

Scholl, D. W. and J. S. Creager, Geologic synthesis of Leg 19 (DSDP) Results: Far north Pacific and Aleutian Ridge, and Bering Sea, in, J. S. Creager, D. W. Scholl et al., Initial Reports of the Deep Sea Drilling Project, 19, Washington, 897-913.

Scholl, D. W., E. C. Buffington and M. S. Marlow, Plate tectonics and the structural evolution of the Aleutian-Bering Sea region, in, R. B. Forbes (ed.), Contributions to the geology of the Bering Sea Basin and Adjacent Regions, Geol. Soc. Am Spec. Pap. 151, 1-32, 1975.

Scholl, D. W., T. L. Vallier and A. J. Stevenson, Arc, forearc and trench sedimentation and tectonics, Amlia corridor of the Aleutian Ridge, in, J. S. Watkins and C. L. Drake (eds.), Studies in Continental Margin Geology, American Association of Petroleum Geologists Memoir 34, 413-439, 1983.

Seliverstov, N. I., Seismoakusticheski Issledovania Perekhodnikh zon, Academia Nauk SSSR, Moskva, (in Russian), 112 pp., 1987.

Serova, M. Ya., G. P. Borzunova and M. N. Shapiro, The Paleogene in the southern part of the Karagin Island (Eastern Kamchatka), Izvestia AN SSSR, Ser. Geologia, 11, 73-83, 1975.

Shapiro, M. I., Northeastern continuation of the East Kamchatka synclinorium, Geotectonics, 10, 76-78, 1976.

Shapiro, M. N. and V. A. Seliverstov, Morphology and age of folded structures in eastern Kamchatka at the latitude of the Kronotsky Peninsula, Geotectonics, 9, 240-244, 1975.

Shul'diner, V. I., S. V. Vysotskiy and A. I. Kanchuk, The crystalline basement of Kamchatka: structure and evolution, Geotectonics, 13, 136-145, 1979.

Silant'yev, S. A., Baranov, B. V., and Kolesov, G. M., Geochemistry and petrology of the Shirshov Ridge amphibolites, Bering Sea, Geochemistry International, 23(5), 64-75, 1985.

Smith, R. L., Ash-flow tuffs, in, C. E. Chapin and W. E. Elston (eds.), Ash-flow Tuffs, Geol. Soc. Am., Special Paper 180, 5-27, 1979.

Sykes, L. R. and M. L. Sbar, Focal mechanism solutions of intrplate earthquakes and stresses in the lithosphere, in, L. Kristjansson (ed.), Geodynamics of Iceland and the North Atlantic Area, D. Reidel, p. 207-224, 1974.

Tsikunov, A. G. and V. S. Petrov, Overthrust in Vostochnyy Khrebet (Eastern Range) Kamchatka, Int. Geol. Rev., 15, 208-212, 1973.

Turner, R. F., C. M. McCarthy, C. D. Comer, J. A. Larrson, J. g. Bolm, T. O. Flett and A. J. Adams, Geological and operational summary St. George Basin COST No. 2 well, U. S. Geological Survey Open File Report, 84-18, 1984.

Utnasin, V. K., A. I. Abdurakhimov, G. I. Anosov, S. T. Balesta, Y. A. Budyanskiy, Y. K. Markhinin and V. I. Fedorenko, Deep structure of Klyuchevoskoy group of volcanoes and problem of magmatic hearths, Int. Geol. Rev., 17, 791-806, 1975.

Vink, G. E., A hotspot model for Iceland and the Voring Plateau, J. Geophys. Res., 89, 9949-9959, 1984.

Wallace, W. K. and D. C. Engebretson, Relationships between plate motions and Late Cretaceous to Paleogene magmatism in southwestern Alaska, Tectonics, 3, 295-315, 1984.

Watson, B. F., The tectonic evolution of Kamchatka Peninsula, USSR, M.S. Thesis, Michigan State University, E. Lansing, 1985.

Watson, B. F. and K. Fujita, Tectonic evolution of Kamchatka and the Sea of Okhotsk and implications for the Pacific Basin, in Tectonostratigraphic Terranes of the Circum-Pacific Region, edited by D. G. Howell, p. 333-348, Circum-Pacific Council for Energy and Mineral Resources, Houston, Texas, 1985.

Woods, M. T. and G. F. Davies, Late Cretaceous genesis of the Kula plate, Earth. Planet. Sci. Lett., 58, 161-166, 1982.

Yermakov, B. V., Ukelayatsko-Shumagin flysch depression in Koryakia and south Alaska, Soviet Geology and Geophysics, 16, 31-34, 1975.

Yermakov, B. V. and V. F. Mishin, Lithologic criteria for subdividing the clastic flyschoid complex in the southern part of the Koryak Highlands, in Stratigraphy and Lithology of the Cretaceous, Paleogene and Neogene Deposits of the Koryak-Anadyr' District, edited by V. N. Vereshchagin (in Russian), p. 75-78, NIIGA, Leningrad, USSR, 1974.

Yermakov, B. V. and I. O. Suprunenko, Structure and conditions of development of Upper Cretaceous and Miocene flysch of Koryak-Kamchatka, Int. Geol. Rev., 18, 1139-1148, 1976.

Yurkova, R. M., Peyve, A. A., Zinkevich, V. P., and Cherkashin, V. I., Amphibolites of the Shirshov Ridge, Bering Sea, Int. Geol. Rev., 27, 1051-1068, 1985.

Zinkevich, V. P., A. D. Kazimirov, A. A. Peyve and G. M. Churakov, New data on the structure of the Cape Kamchatskiy Peninsula, eastern Kamchatka, Transactions (Doklady) of the USSR Academy of Sciences, Earth Science Section, 285, 89-92, 1985.

CHAPTER TWO

INTRAPLATE SEISMICITY OF ALASKA: IMPLICATIONS FOR REGIONAL STRESSES

INTRODUCTION

Alaska is characterized by a gradient of seismicity which decreases from south to north. This undoubtedly arises partially from the decreasing effect of Pacific subduction away from the Aleutian trench (Figure 2-1). Realizing Alaska is tectonically and geologically complex, and due to the rapid northward decrease in seismicity, any extrapolation of a coherent stress pattern beyond the vicinity of the Aleutian Arc may at first seem unwarranted. However, as has been shown in earlier studies (e.g., Gedney and Berg, 1969; Gedney, 1970; Nakamura et al., 1980), consistent regional stress trends are observed south of the Brooks Range. The manifestation of these stresses in structural, volcanic, gravimetric and seismic indicators presents the opportunity to evaluate sources of stress.

The various methods utilized in evaluating lithospheric stresses commonly compliment each other. Early analyses of stresses often were limited to a single method (e.g., first motion studies (Scheidegger, 1964)) which could create a systematic bias in the interpretation. However, massive compilations and analyses, such as those done by M. L. Zoback (Zoback and Zoback, 1980; Zoback et al., 1984, 1986) suggest that consistent stresses are indicated by differing methods, and that these stresses often encompass vast regions (e.g., the mid-continent, Zoback et al., 1986).

This investigation presents new source parameters for 11 earthquakes north of 64°N in Alaska. These data are combined with borehole elongation orientations and focal mechanism solutions in northern Alaska and northwest Canada in order to define the stress regimes within Alaska. The results modify the studies of Nakamura et al. (1980) and Biswas et al. (1986). The

Figure 2-1: Regional geography of Alaska and surrounding areas. Faults are from Grantz (1966) and Brogan et al. (1975). BI - Barter Island; H - Huslia; B-K - Bendeleben-Kigluaik Mountains; R - Rampart; SC - Stevens Creek; F - Fairbanks

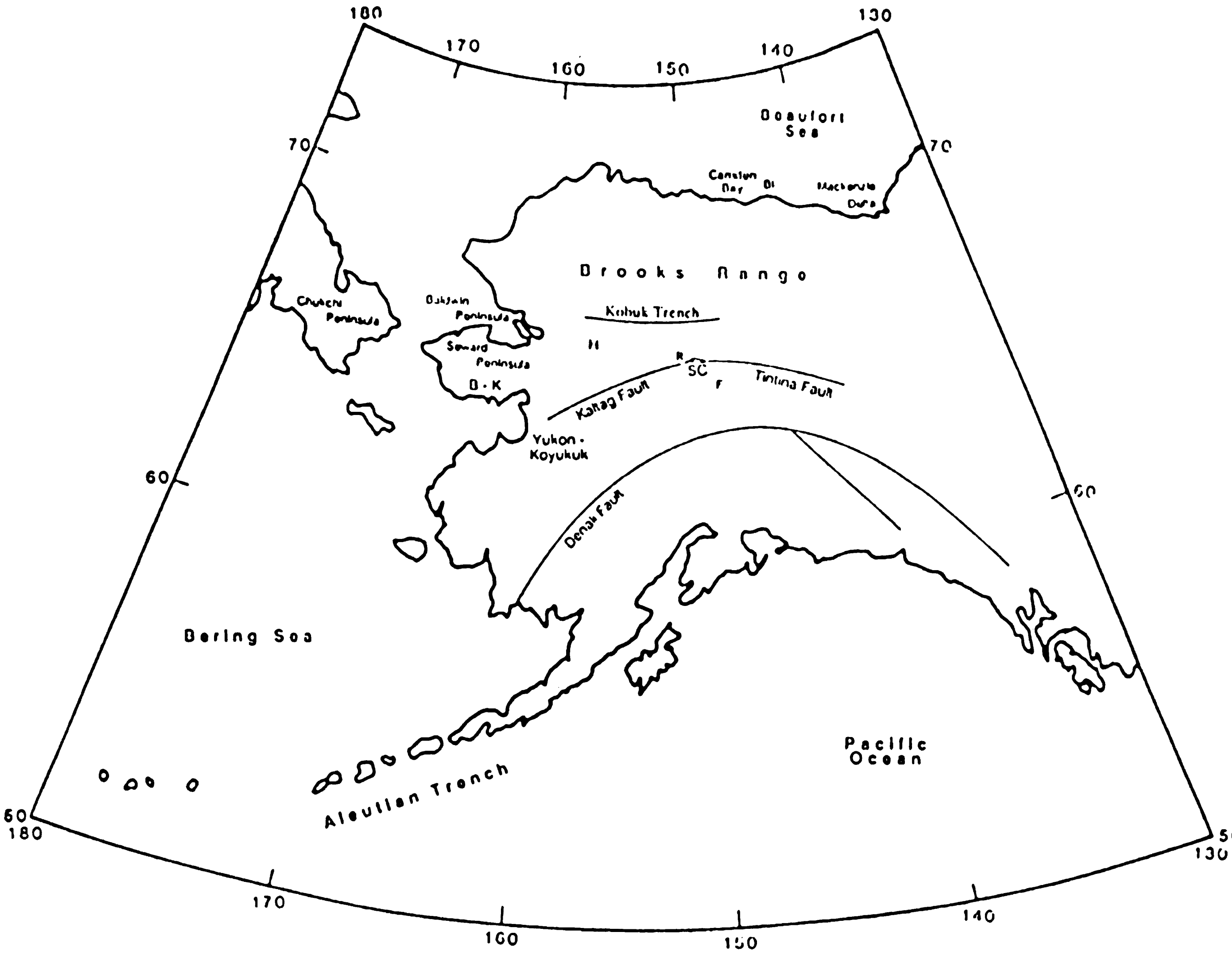
Beaufort Sea
Camden Bay
Mackenzie Delta
Brooks Range
Kobuk Trench
Chukchi Peninsula
Seward Peninsula
Kaltag Fault
SC
Tintina Fault
Yukon - Koyukuk
Denali Fault
Bering Sea
Aleutian Trench
Pacific Ocean
180
170
160
150
140
130
70
60
50

Figure 2-1

gross delineation of stresses are, however, in good agreement with even the earliest Alaskan stress studies (e.g., Gedney and Berg, 1969).

NEW FOCAL MECHANISMS

New source parameters were obtained for eleven earthquakes of magnitude 4.2 to 6.0 (Table 2-1). For three events (nos. 1, 4, 9), focal mechanisms have been presented by other investigators prior to this study, and are modified in this study in light of new or re-evaluated data. Source parameters were obtained through the use of P-wave first motions, surface wave analysis, aftershock studies and body-wave modelling. Brief explanations of these methods are given, followed by discussions of each of the 11 earthquakes to be used as indicators of the stress regimes within Alaska.

Methods

Four methods have been used to constrain source parameters: P-wave first motions, surface wave analysis, master event relocations, and synthetic seismogram (long and short period) computations. Due to the small size of the events (Mb 4.2 to 6.3) studied, the signal to noise ratio is often poor. Therefore, independent confirmation of results using different techniques is essential.

First motions were read from World Wide Standardized Seismograph Network (WWSSN) and Canadian network seismograms. This was supplemented by first motions reported in the International Seismological Center (ISC) Bulletin and the International Seismological Summary (ISS). Long and short period data are used in all cases.

Rayleigh waves are analyzed for some post-1964 events, which are recorded on standardized instruments. Those Rayleigh waves with periods

Figure 2-2: Synthetic seismograms for the October 29, 1968, Rampart mainshock. STF is the source-time function, given as rise, run and fall times, in seconds. Crustal structure parameters include P-wave velocity (α, km/s), S-wave velocity (β, km/s), density (ρ, gm/cm^3) and thickness (T, km).

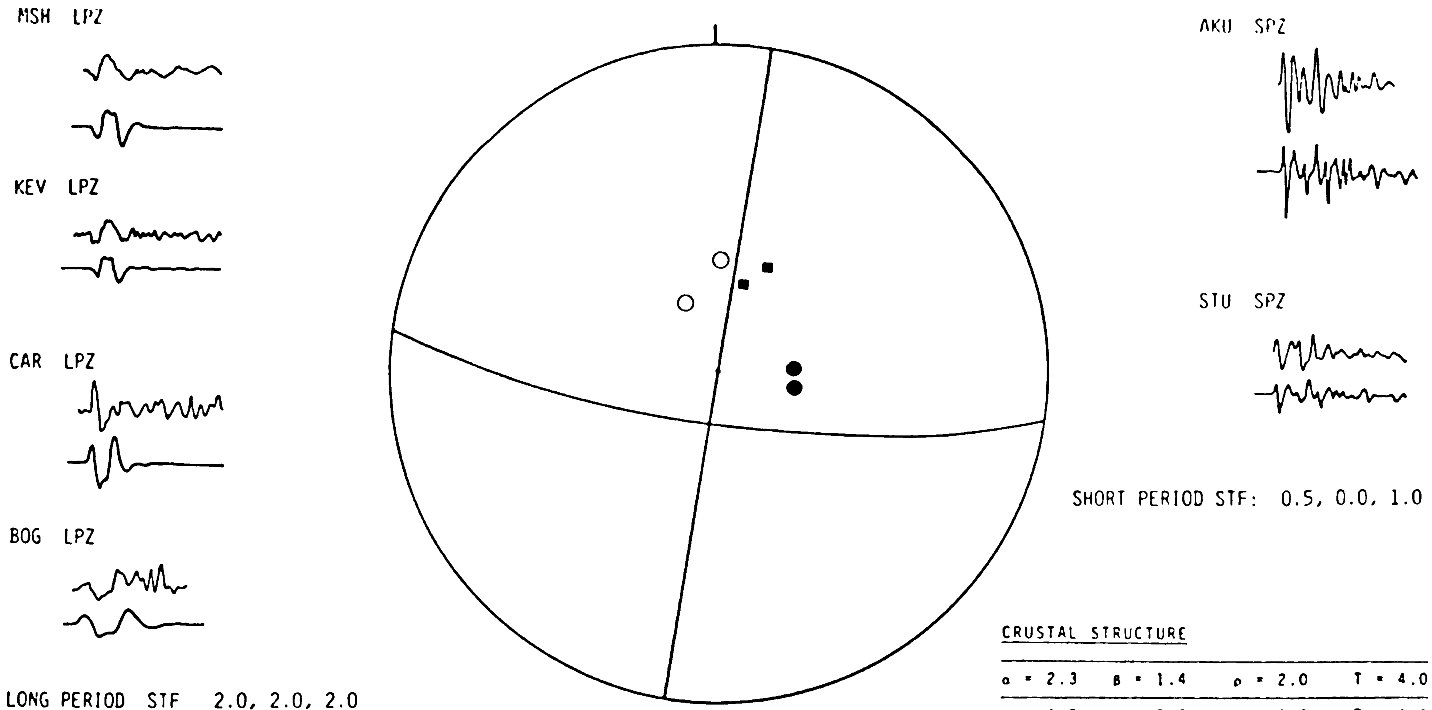

CRUSTAL STRUCTURE

α = 2.3	β = 1.4	ρ = 2.0	T = 4.0
α = 4.9	β = 2.9	ρ = 3.2	T = 6.5
α = 6.3	β = 3.8	ρ = 3.4	∞

68-OCT-29 SYNTHETICS DEPTH = 14 KM.

Figure 2-2

between 20 and 100 seconds were used. The amplitude spectra were computed and equalized to a common station magnification of 1500 and 90 degrees. To differentiate between signal and incoherent noise at individual stations, spectral amplitudes were plotted against frequency and examined. The final plot of spectral amplitude vs. station azimuth is then generated for several frequency windows. The resultant radiation pattern is then compared to the theoretical radiation pattern generated from the fault strike, dip, and slip angle.

Master Event relocations are used to identify the fault plane accurately. The largest ("master") event of a sequence of earthquakes is assumed to be best located and have the most representative travel time residuals. By assuming that the travel paths of the master event and its aftershocks are similar (valid over a small focal area), the master event residuals are used as corrections for travel-times of smaller events for matching source-receiver pairs. This yields better relative locations by effectively removing the effects of lateral inhomogeneities in the earth.

Synthetic seismograms are computed for long and short period body waves using the method of Kroeger (1987). These further constrain the focal mechanism and focal depth. Detailed crustal structure is not important in calculating long period synthetic seismograms since the period of the waveform is long relative to the thicknesses of layers within the crust. This treatment is not appropriate, however, for short period synthetics. Good constraints on composition, density, seismic velocity, and thickness are important (Seno and Kroeger, 1983). These better constrained parameters are, therefore, used in all synthetic seismogram calculations. The crustal constraints are obtained from the works of previous authors and are noted in the discussions.

Earthquake Parameters

Event one is the October 29, 1968, Mb=6.0 earthquake referred to as the Rampart event. Gedney (1970) arrived at a strike-slip solution, with the P-axis trending NW-SE (Figure 2-2). Rayleigh wave radiation patterns generated for various periods between 25 and 60 seconds produce a four-lobed pattern (Figure 2-3) which fits well with the theoretical pattern based on Gedney's (1970) solution. To better constrain the fault plane, a Master Event relocation of the 140 associated aftershocks was also done. Although the majority of ISC reported aftershock epicenters trended NNE-SSW relative to the mainshock, a disturbing E-W trend was observed with two of the larger (Mb > 4.2) aftershocks. Following the relocation, however, these two shocks took on an approximately 005^{o} trend relative to the mainshock, as did the smaller aftershocks (Figure 2-4). This trend matches well with the N08E striking nodal plane in the focal mechanism, and this nodal plane is taken as the fault plane. The relocated aftershock trend is also sub-parallel to the Minook Creek valley and a northward trending segment of the adjoining Yukon River. Master event relocation therefore supports Gedney's (1970) conclusion that the Minook Creek valley is as the surface expression of the fault. Focal mechanisms were constrained for two aftershocks (events 2 and 3, magnitude 4.6 and 4.4 respectively) using P-wave first motions. Both of these solutions are very similar to the mainshock (Figure 2-5), with nearly north-south trending nodal planes chosen as the fault planes.

Both long- and short-period synthetic seismograms were computed to constrain the depth of the Rampart mainshock (no. 1). Excellent matches are obtained using the listed fault parameters. Crustal structure, from Jones et al. (1981), source-time-functions, and resulting seismograms are shown in

Figure 2-3: Rayleigh wave radiation pattern for the October 29, 1968 Rampart earthquake. Stippled pattern is the theoretical radiation pattern for the solution given in Table 2-1.

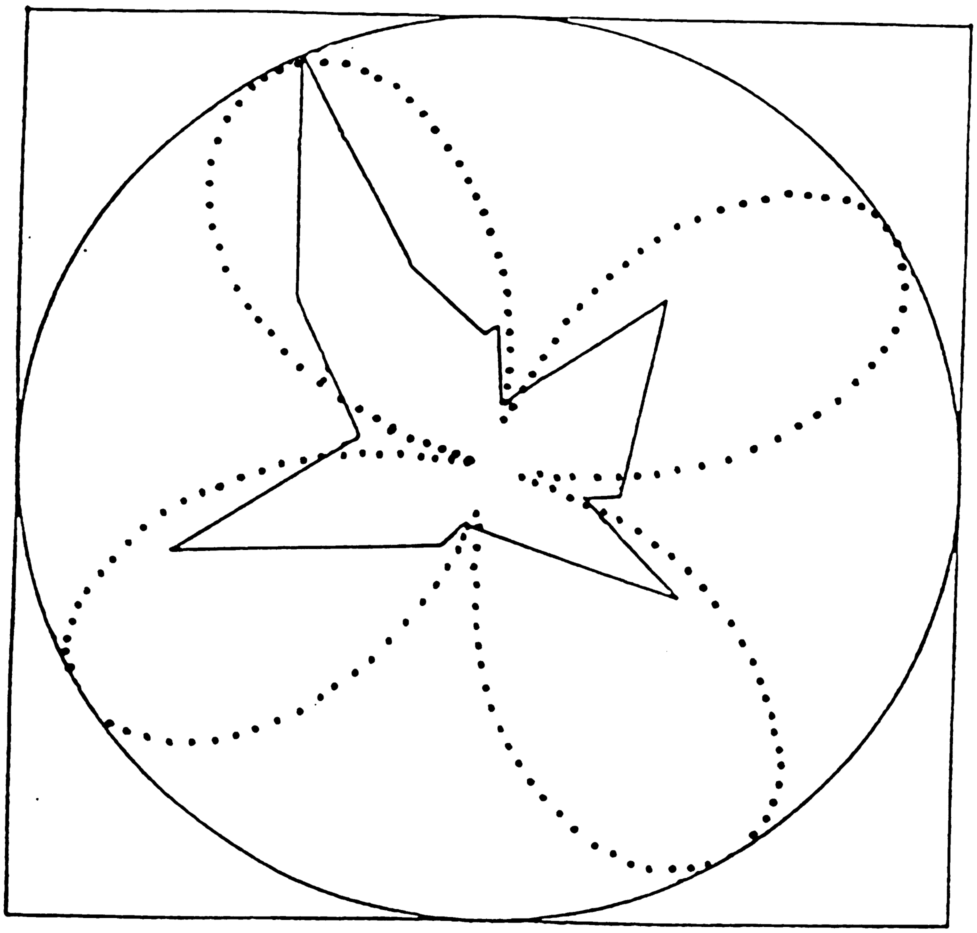

29 OCTOBER 1968
PERIOD = 60 SECONDS

Figure 2-3

Figure 2-4: Master event relocation of the October 29, 1968 Rampart mainshock and 140 aftershocks. Note the north-south realignment of the four largest aftershocks (small stars) after relocation.

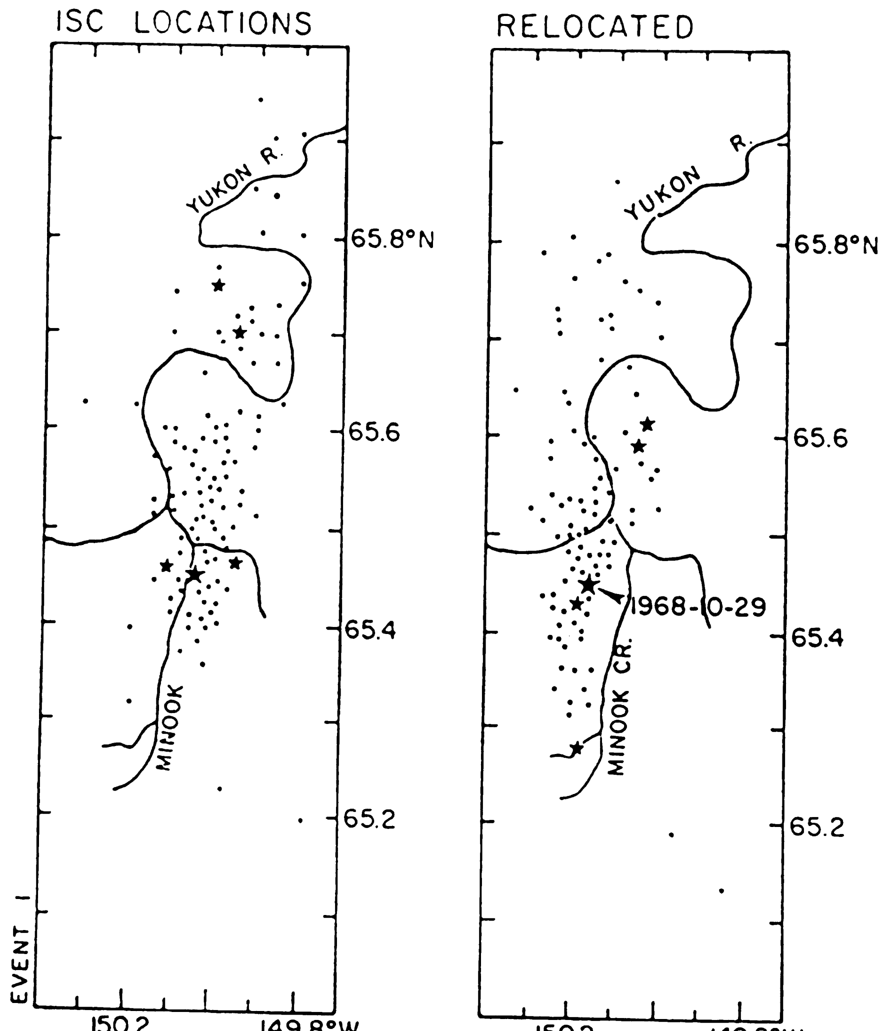
ISC LOCATIONS
RELOCATED
YUKON R.
MINOOK
MINOOK CR.
1968-10-29
65.8°N
65.6
65.4
65.2
150.2
149.8°W
EVENT 1

Figure 2-4

Figure 2-5: P-wave focal mechanisms for two Rampart aftershocks. Small circles are ISC reported compressions (filled) and dilatations (open). Large circles are compressions (filled) and dilatations (open) read from WWSSN and Canadian network seismograms. P indicates the position of the compressional stress axis.

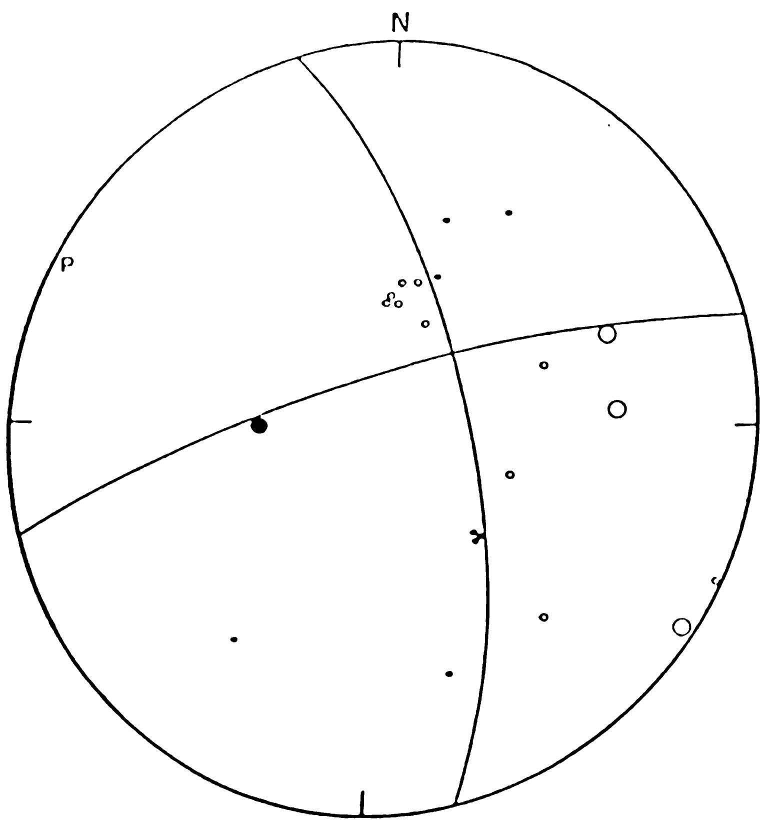

31 OCTOBER 1968

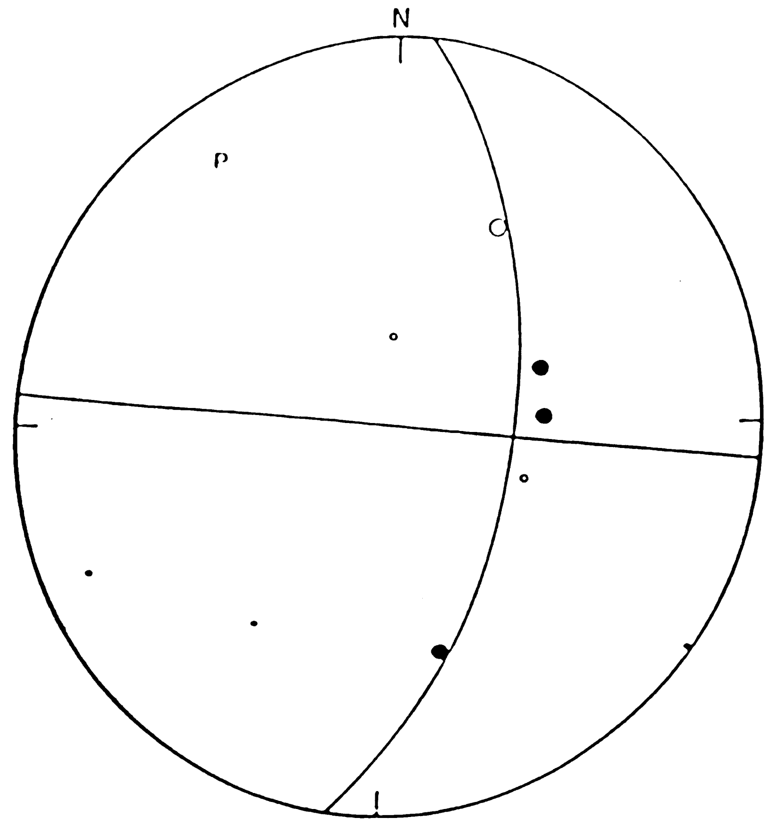

03 NOVEMBER 1968

Figure 2-5

Table 2-1: Earthquake parameters for north, central and western Alaska.

LA.TT - Latitude in degrees north

LON.GT - Longitude in degrees west

M.AG - Magnitude: M_b unless noted as ^{L} (Local magnitude) or ^{S} (Surface wave magnitude)

PLANEx - Orientation of the nodal plane, using the convention of Aki and Richards (1980) (Dip down to the right of strike).

REFS - References, as follows:

A40:	Adkins, 1940
B62:	Balakina, 1962
D60:	Davis, 1960
DZ85:	Dziewonski et al., 1985
E85:	Estabrook, 1985
G85:	Gedney, 1985
H79:	Hasegawa et al., 1979
J68:	Jordan et al., 1968
LK80:	Liu and Kanamori, 1980
LW74:	Leblanc and Wetmiller, 1974
R62:	Ritsema, 1962
S61:	Schaffner, 1961
S64:	Stevens, 1964
SS74:	Sykes and Sbar, 1974

Table 2-1: EARTHQUAKE PARAMETERS FOR NORTH, CENTRAL AND WESTERN ALASKA

ID	YRMODY	HRMNSE.C	LA.TT	LON.GT	M.AG	DEPTH	PLANE1	PLANE2	P-AXIS	T-AXIS	B-AXIS	REFS
1	681029	221616.5	65.46	150.07	6.0	14.	008/90	098/82	321/06	052/06	188/82	
2	681031	002545.7	65.74	149.94	4.6		346/70	252/80	300/06	208/20	045/68	
3	681103	073739.4	65.74	149.86	4.4		004/64	094/90	324/17	222/17	094/64	
4	850309	140804.6	66.3	149.8	5.8	7.	016/74	108/90	334/12	241/10	108/74	E85
		140804.3	66.2	150.0	5.9		210/86	120/85	345/01	075/06	250/84	NEIC
		140807.2	66.53	149.94			211/79	305/71	166/22	258/06	002/67	D285
5a	661220	002628.5	66.82	148.1	4.8		058/80	148/80	013/15	104/00	194/76	
b	661220	005753.8	66.79	148.4	4.9							
6	810712	012756.4	67.71	161.20	5.2		106/85	196/87	331/01	062/08	231/84	
7	660826	101932	66.71	162.7	5.0		280/84	190/80	146/12	055/03	311/79	
8	641213	003326.9	64.88	165.57	5.3	17.	263/57	014/60	233/47	139/02	047/44	
9	580407	153040	66.03	156.59	7.3		226/36	058/53	352/79	143/09	234/05	R62
10	730411	051218.1	64.61	160.04	4.2		014/36	250/70	199/55	319/19	059/28	
11	680122	234430.4	70.3	144.4	4.7	<10	281/85	016/54	231/29	334/19	094/53	
J1	670621	180449.5	64.8	147.4	5.4		315/63	216/75	171/30	267/08	011/58	J68
J2	679621	181302.9	64.8	147.4	5.6		275/84	181/48	146/32	041/23	283/47	J68
G1	811230	134726.8	64.5	147.9	4.2^L		295/90	025/82	340/06	250/06	115/82	G85
G2	840823	204151.0	64.5	147.9	4.1^L		100/83	007/77	323/14	231/05	127/75	G85
A1	370722	170928	64.55	147.20	7.3		034/67	131/77	354/27	261/07	158/62	A40
E1	721128	133537.4	65.7	145.5	5.0^S		015/78	112/70	331/22	064/05	166/66	E85
E6	750309	141941.9	65.9	149.7	4.6^L		008/64	102/82	328/25	232/12	116/62	E85
E7	850214	050402.2	66.3	149.8	5.4		034/90	303/90	168/00	258/00	VERT	E85
E9	801006	145735.4	66.8	155.0	4.6		250/76	340/81	114/02	206/18	027/76	E85
E11	Composite		66.3	157.0			086/08	358/90	312/06	043/05	178/82	E85
E19	750331	125303.5	69.9	142.3	3.8		060/80	158/60	015/30	113/10	223/58	E85
H1	750614	205026.9	72.0	132.3	5.1		135/73	036/59	358/34	250/63	160/54	H79
LW1	720726	184621.7	66.5	136.0	4.8		328/86	236/64	196/21	099/14	337/64	LW74
SS5	651005	001715.1	65.4	134.0	5.2	8.	044/52	272/50	336/01	250/63	067/26	SS74
SS6	650416	232218.6	64.69	160.23	5.8	12.	137/25	305/66	206/69	027/22	307/04	SS74 LK80

Figure 2-2. A best fit between observed and computed waveforms is found for a focal depth of 14 km. Of particular interest is the fit obtained with the short period synthetics. Good matches for a full 40 seconds of record are observed for AKU and STU (Figure 2-6). A well constrained crustal structure is an important factor in obtaining this match. Seno and Kroeger (1983) also found that good short period synthetics could be computed with good crustal constraint at the source.

Event 4 is a 1985 earthquake located very near the 1968 Rampart series. A centroid moment tensor solution has been determined by Dziewonski et al. (1985), and P-wave solutions have been presented by Estabrook (1985) and also in the ISC bulletin (March, 1985) by the National Earthquake Information Center (NEIC) (Table 2-1; Figure 2-7). A series of 22 aftershocks, which occurred within two months after the mainshock and ranged in magnitude from 3.4 to 5.1 (Estabrook, 1985), fall along a trend of 040 degrees. This trend is very similar to the trends of nodal planes determined by NEIC (030^{o}) and Dziewonski et al. (1985) (031^{o}), although somewhat discordant with Estabrook (1985) (016^{o}). Estabrook (1985) does state that the northerly trending nodal plane is likely to represent the fault plane due to parallelism with the active Dall Mountain fault and other seismic trends in the vicinity. Cross sections through the hypocentral region (Figure 2-8; Estabrook, 1985) indicate a steep northwest dip of the fault plane. Estabrook's (1985) solution indicates a southeast dipping plane, and thus, the mainshock focal mechanism solutions of the NEIC and Dziewonski (1985) fit the aftershock data better. Brogan et al. (1975) suggest that the Dall Mountain fault has a normal faulting component, down to the west. This further supports nodal planes chosen by the NEIC and

Figure 2-6: Short-period synthetic seismograms calculated at various depths for the station AKU, using the given solution (Table 2-1) of the October 29, 1968 Rampart event.

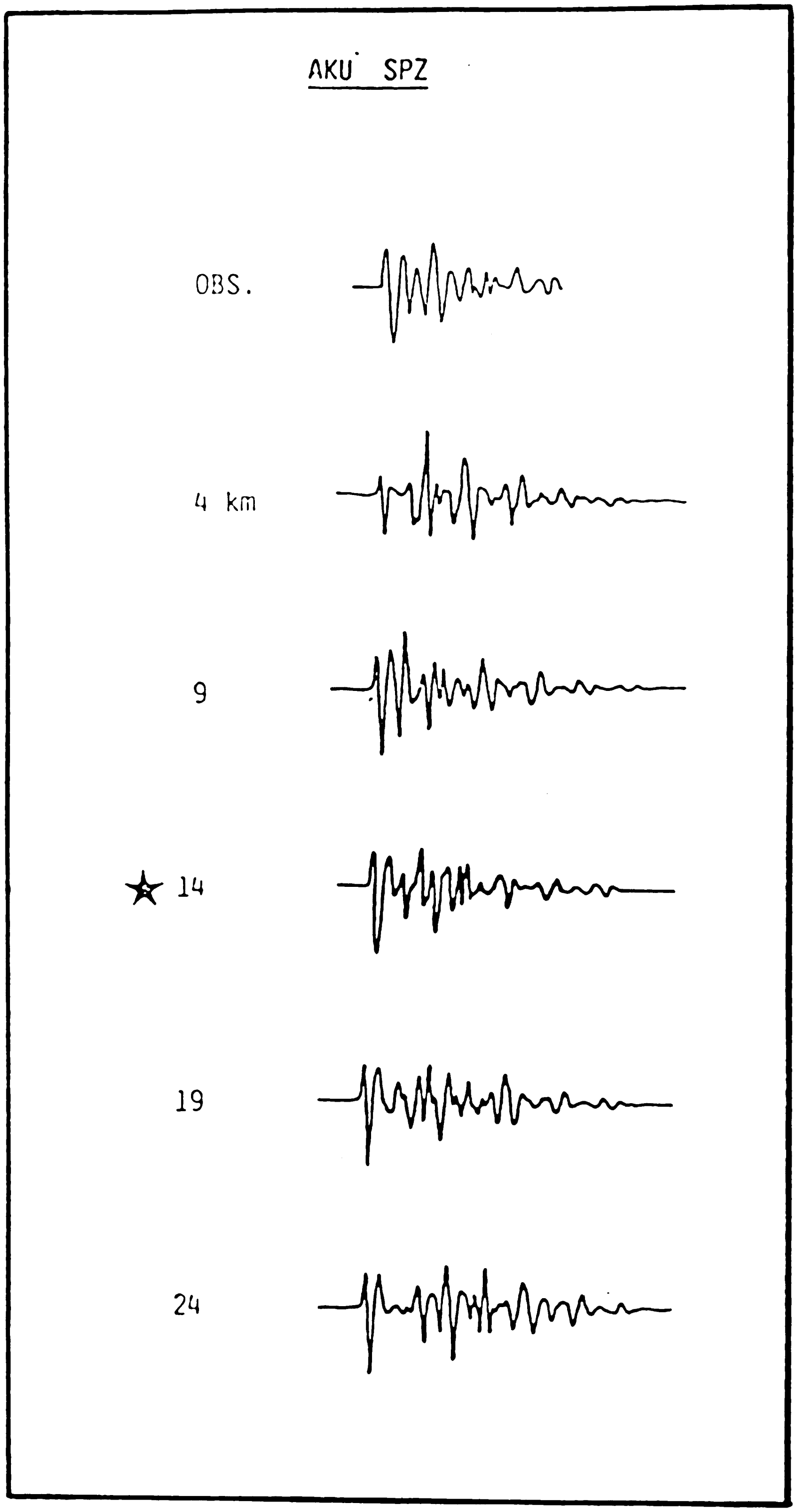

Figure 2-6

Figu

Figure 2-7: Focal mechanism solutions for the March 9, 1985 earthquake (#4, Table 2-1). All solutions indicate left-lateral strike-slip along the north-northeast to northeast trending probable fault plane.

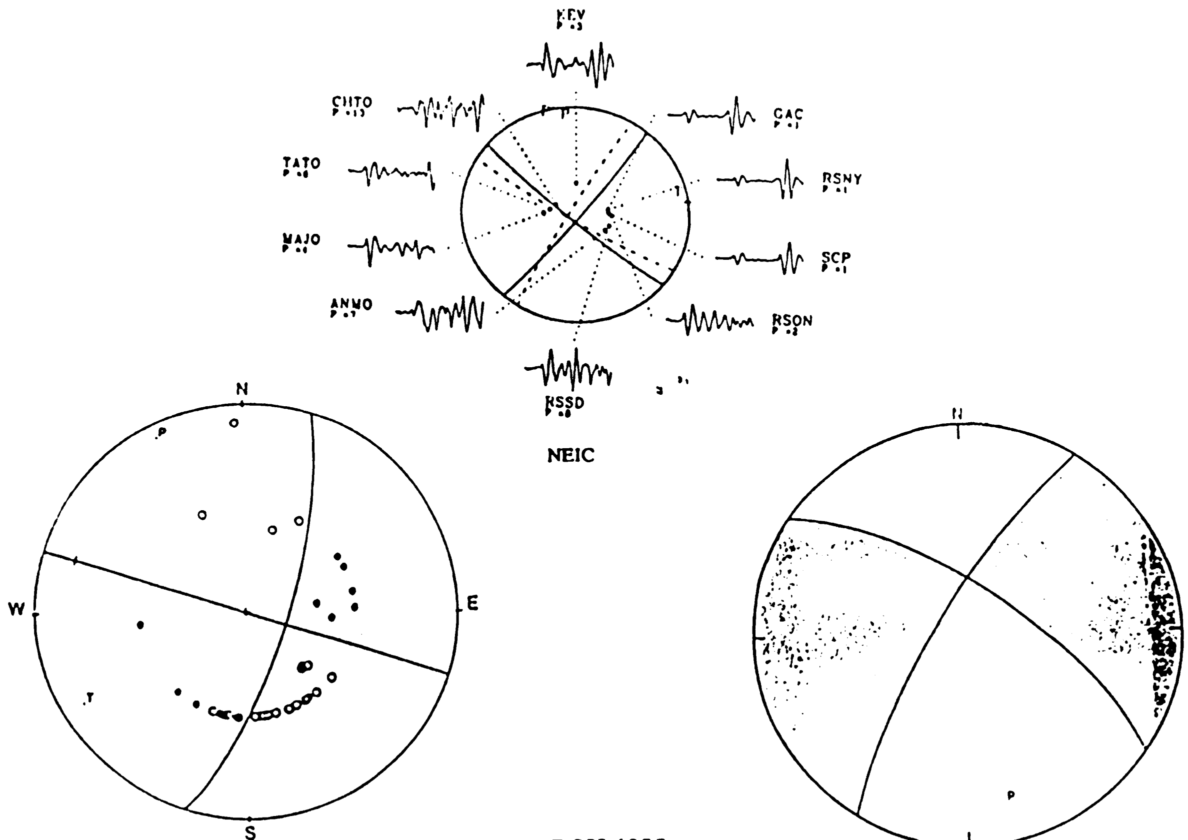

NEIC

Estabrook et al., 1985

Dziewonski et al., 1985

9 MARCH 1985

Figure 2-7

Figure 2-8: Cross sections from Estabrook (1985) for the March 9, 1985, earthquake and aftershocks. The A-A' section suggests a northeast trending fault plane with a steep northwest dip.

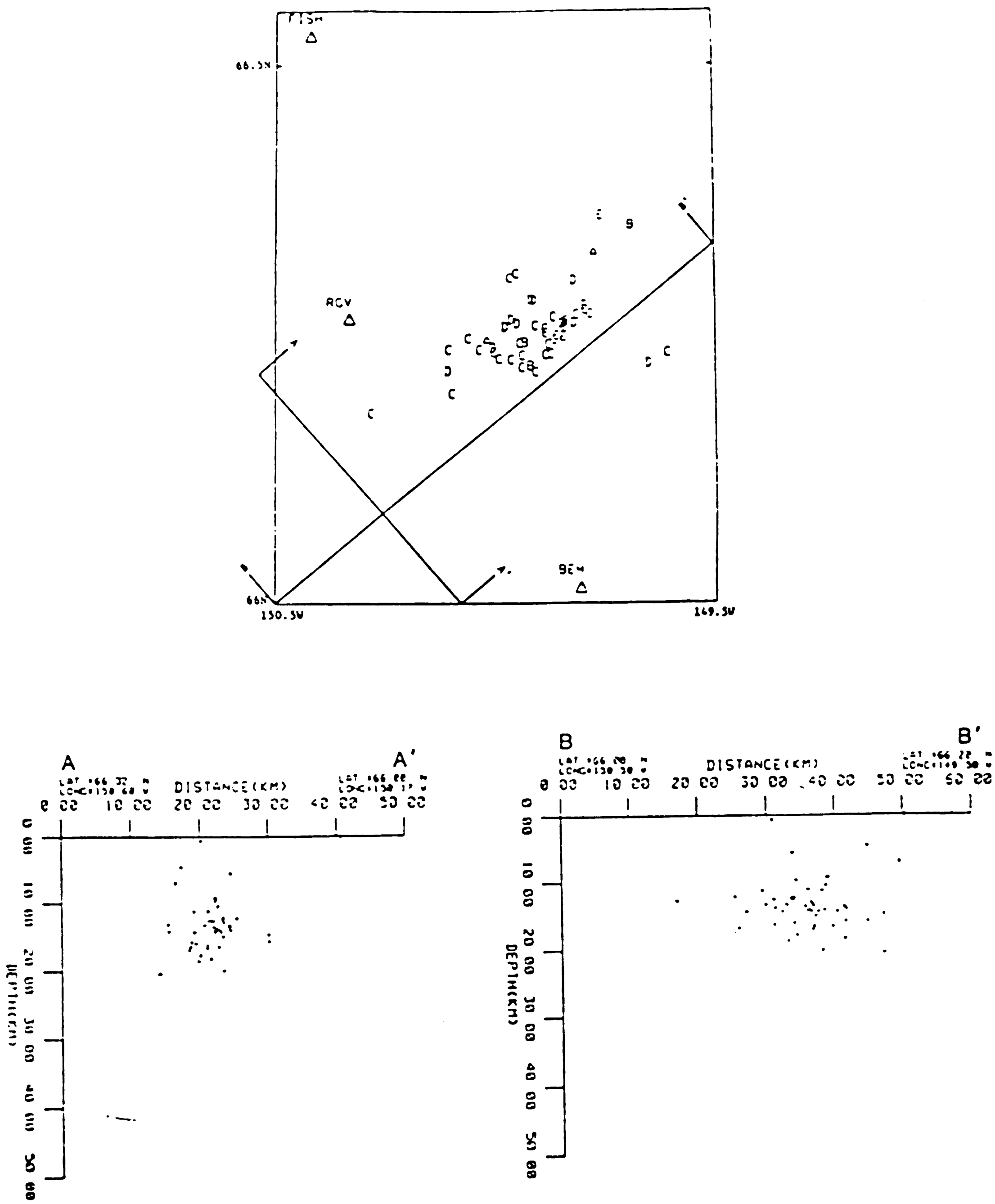

Figure 2-8

Dziewonski (1985), although all three solutions indicate left-lateral slip along the north to northeast trending plane.

Events 5a and b were an earthquake doublet known as the Caro series which occurred approximately 200 km NNE of the Rampart (nos. 1, 2 and 3) events. The pair, occurring on December 20, 1966, are separated by 31 minutes and are of magnitudes 4.8 and 4.9, respectively. Only the focal mechanism for the second event (Figure 2-9) is well constrained due to the lack of good P-wave first motions recorded for the first event. A remarkable similarity between long period waveforms, however, leads Coley (1983) to believe that both of the events are of the same mechanism. The first 60 seconds of long period waveform recorded at COL, shown in Figure 2-9, exemplifies these similarities.

Geologic mapping in this area by Beikman (1980) shows a predominance of N55E trending faults. This is consistent with the N60E striking nodal plane constrained for this event, which is therefore taken as the fault plane.

An Mb=5.2 earthquake (no. 6) occurred in the western Brooks Range on July 12, 1981. This event appears to have occurred along a nearly east-west striking right-lateral strike-slip fault. Reading WWSSN seismograms permitted a solution to be obtained despite ISC reported first motions being inconsistent within the focal sphere. Additionally, an observed lack of Rayleigh wave energy with high amplitude Love waves at TUC and ISC reported long- and short-period dilitations at BJI helped to constrain the east-west trending nodal plane (Figure 2-10).

Master Event relocation of aftershocks for this event shows dramatic results. The ISC reported epicenters of 14 aftershocks show no linear trends. Following relocation, however, an approximate 110 degree trend is identified

Figure 2-9: P-wave focal mechanism for the second (00h 57m 53s) December 20, 1966 earthquake (#5b). Long-period waveforms at College Station (COL) are shown for both events. The remarkable similarity lead Coley (1983) to suggest the two events had similar focal mechanisms.

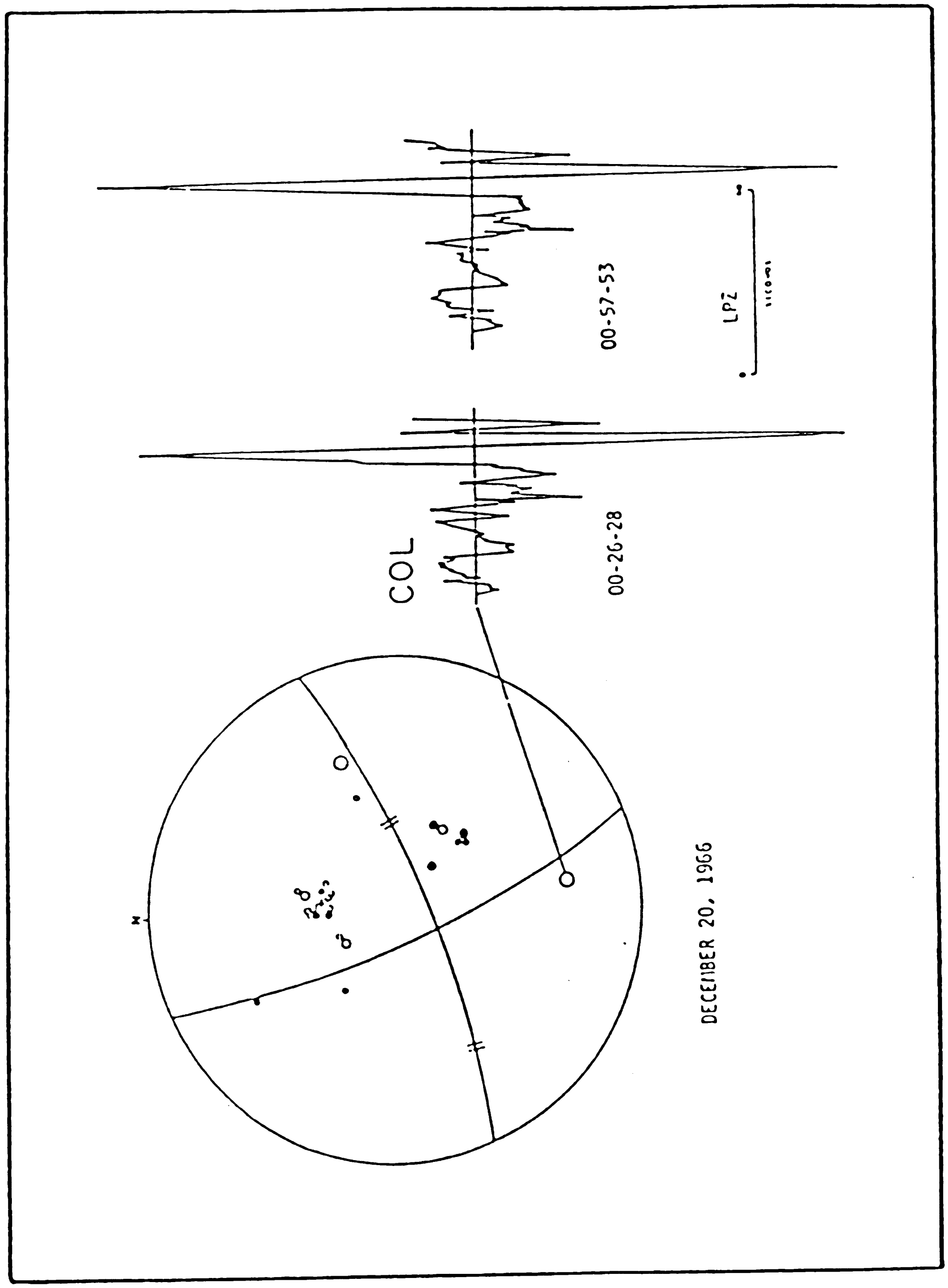

Figure 2-9

Figure 2-10: P-wave mechanism for the 1981 Kobuk Trough earthquake (#6). The large open square indicates a reported long- and short-period dilatation at BJI. The small star is a nodal pick at TUC based on a large Love/Rayleigh wave ratio. Other conventions are as in Figure 2-5.

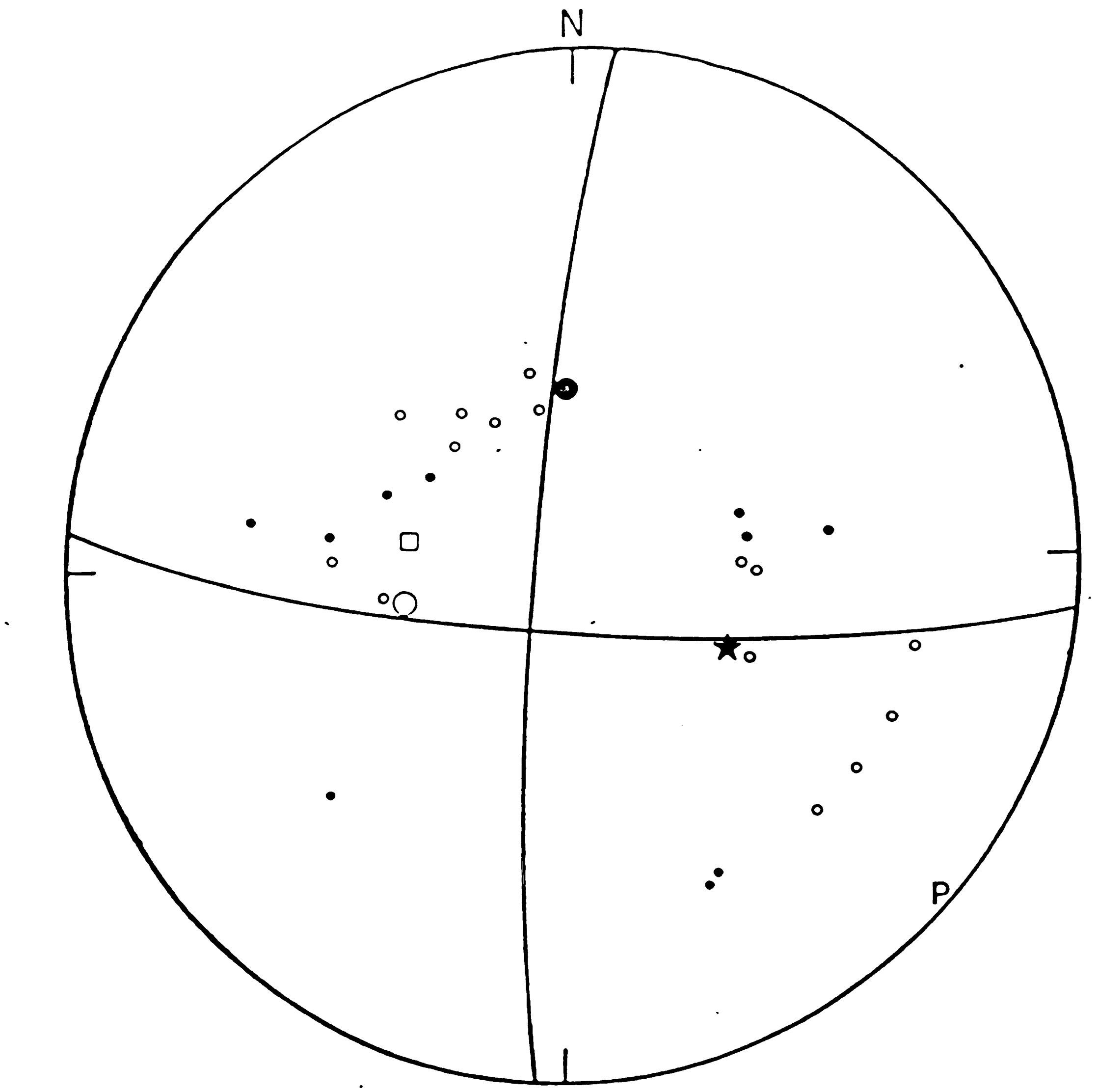

12 JULY 1981

Figure 2-10

(Figure 2-11). This trend is very consistent with the 106 degree striking nodal plane, which is chosen to be the fault plane for this earthquake. The right lateral strike-slip motion is also consistent with the observations of Oldow (pers. comm.), who has mapped a number of Recent strike-slip faults within the Brooks Range.

A centroid moment tensor solution for the July 12, 1981, earthquake by Dziewonski et al. (1988) presents a best double couple solution with nodal planes oriented 247o/73^o and 154^o/79^o. This solution is in poor agreement with aftershock distribution (Figure 2-11) and geologic data which identifies the Kobuk trough as a nearly east-west trending fault (Brogan et al., 1975). Hinzen (1986) has shown that many moment tensor solutions differ from P-wave and surface wave solutions. Moment tensors represent a mean solution for the entire rupture process, whereas P-waves are indicative of conditions at rupture initiation. Therefore, the discrepancy of the moment tensor solution may be due to a change in slip direction or fault geometry (e.g., curved fault planes) after initial rupture.

An earthquake on Baldwin Peninsula in 1966 (no. 7) is the westernmost strike-slip solution found in northern Alaska. Focal mechanism constraint using P-wave first motions is fairly good, and allows only slight variation of the nodal planes (Figure 2-12).

The relative motion of this event (no. 7) is similar to other events (nos. E9, E11 and 6) in the western Brooks range, and may represent right-lateral motion on a western extension of the fault-controlled Kobuk trough (Grantz, 1966; Brogan et al., 1975). There is a normal faulting component to the focal mechanism, which may be induced by the vertical stresses in Seward Peninsula (Lockhart, 1984) just south of Baldwin Peninsula.

Figure 2-11: Master event relocation for the aftershock sequence of the 1981 Kobuk Trough earthquake. ISC reported epicentral positions relocate to an approximate N70W trend, very close to the N74W trending nodal plane.

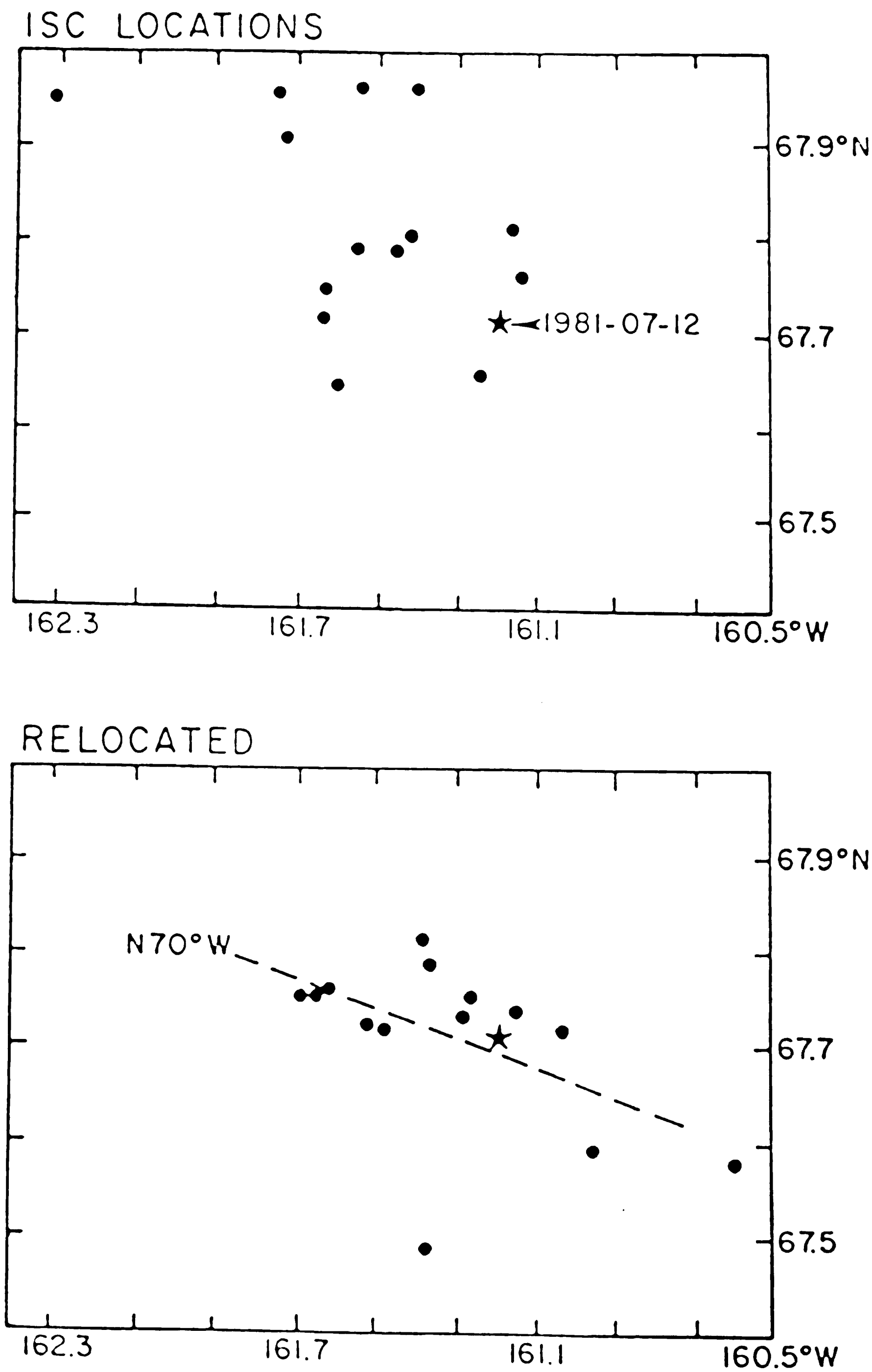
ISC LOCATIONS
1981-07-12
67.9°N
67.7
67.5
162.3
161.7
161.1
160.5°W
RELOCATED
N70°W
67.9°N
67.7
67.5
162.3
161.7
161.1
160.5°W

Figure 2-11

Figure 2-12: P-wave mechanism for the August 26, 1966 Baldwin Peninsula earthquake. Conventions are as in Figure 2-5.

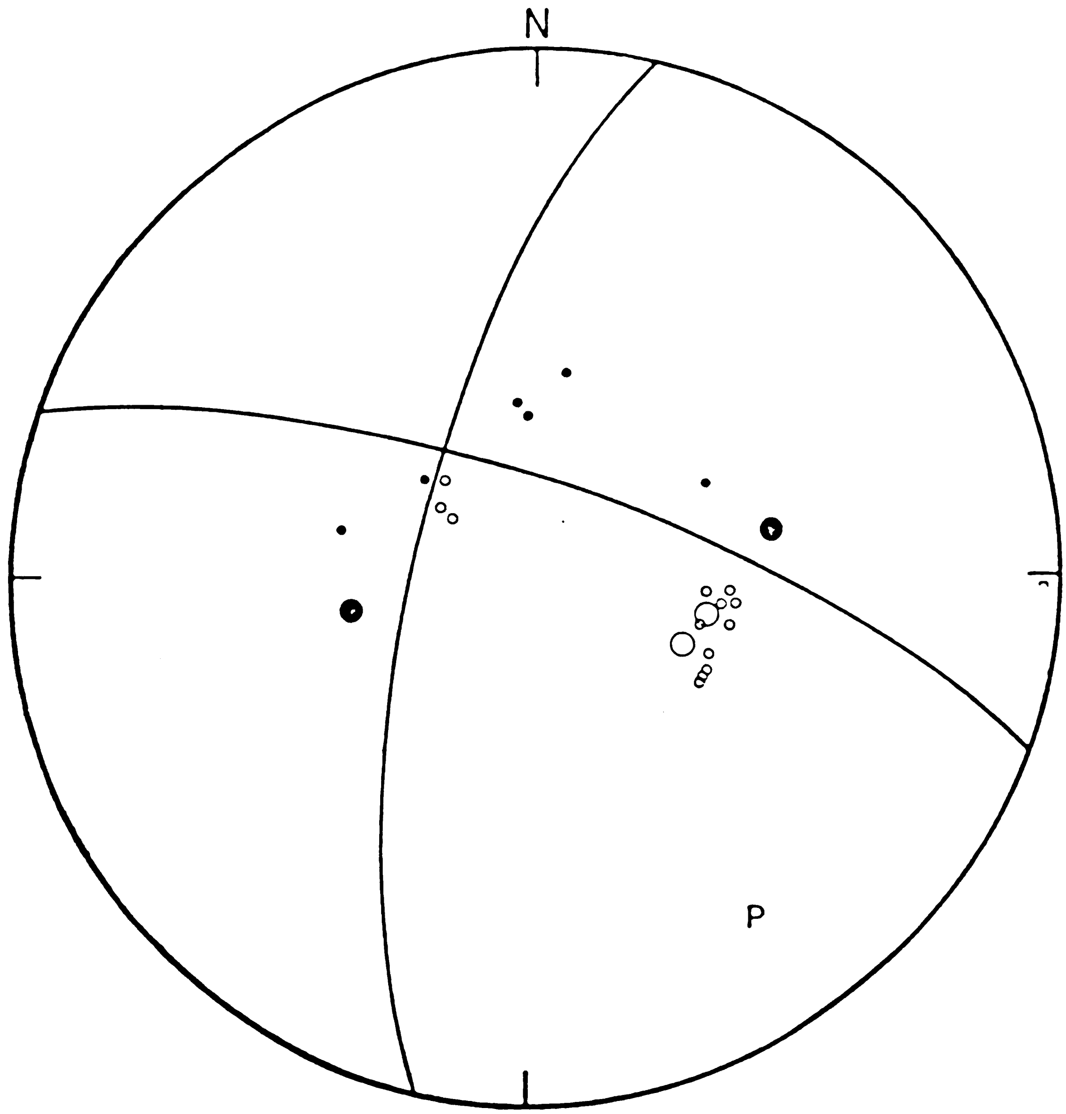

26 AUGUST 1966

Figure 2-12

norr

mot

for

(Fig

is p

syst

198

epic

exce

ther

desc

allu

mor

196

occu

mag

6.5

Scha

vari

prop

P-wa

obta

how

The December 13, 1964, Mb=5.3 Seward Peninsula event (no. 8) has a normal dip-slip mechanism which is very well constrained by P-wave first motions (Figure 2-13). Short period body-wave synthetic seismograms computed for a good azimuthal distribution of stations indicated a best fit depth of 17 km (Figure 2-13), and are consistent with the P-wave focal mechanism.

This earthquake occurred in the Bendeleben-Kigluiak Mountain Ranges, and is probably located on the nearly east-west striking Kigluiak normal fault system within these mountains (Hudson and Plafker, 1978; Nakamura et al., 1980). Hudson and Plafker (1978) map the Kigluiak fault in the vicinity of the epicenter as an ENE striking, northward dipping plane (Figure 2-14), which is in excellent agreement with one nodal plane (strike/dip = $263^{o}/57^{o}$), which is thereby presumed to represent the fault plane. Hudson and Plafker (1978) describe modern offset along the Kigluiak fault, including "abruptly separated alluvium," and scarps which juxtapose bedrock along unconsolidated deposits and moraines, which is consistent with its interpretation as the active fault of this 1964 earthquake.

Event 9 is the largest earthquake of an extensive series of earthquakes to occur in 1958. This event, often referred to as the Huslia earthquake, had a magnitude of 7.3, and was followed by many aftershocks, including a magnitude 6.5 on April 13, 1958. The event has been investigated by many (e.g., Schaffner, 1961; Balakina, 1962; Ritsema, 1962; Stevens, 1964), resulting in a variety of focal mechanism solutions. Coley (1983) modified the solution proposed by Ritsema (1962), which was a proposed single-couple based on P-wave first motions and S-wave polarization angles (Figure 2-15), in order to obtain a more consistent fit with the S-wave data. Coley's (1983) solution, however, has non-orthogonal nodal planes. The solution presented here (Table

Figure 2-13: P-wave first motions and short-period synthetic seismograms for the December 13, 1964, Seward Peninsula earthquake (#8). Conventions are as in Figures 2-2 and 2-5.

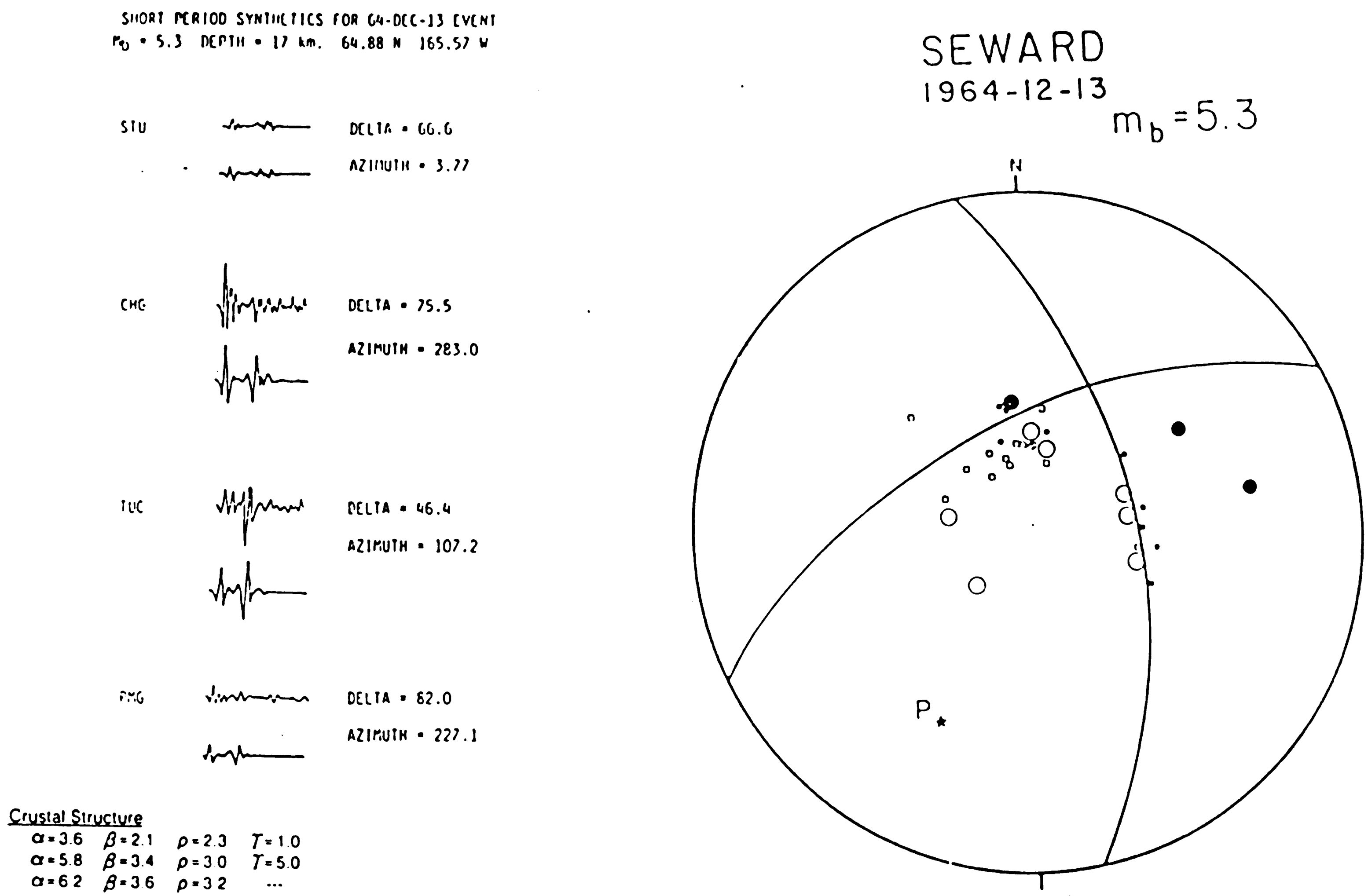
SHORT PERIOD SYNTHETICS FOR 64-DEC-13 EVENT
M_b = 5.3 DEPTH = 17 km. 64.88 N 165.57 W
STU
DELTA = 66.6
AZIMUTH = 3.77
CHG
DELTA = 75.5
AZIMUTH = 283.0
TUC
DELTA = 46.4
AZIMUTH = 107.2
DELTA = 82.0
AZIMUTH = 227.1
Crustal Structure
α=3.6 β=2.1 ρ=2.3 T=1.0
α=5.8 β=3.4 ρ=3.0 T=5.0
α=6.2 β=3.6 ρ=3.2 ...
SEWARD
1964-12-13
m_b=5.3
N
P

Figure 2-13

Figure 2-14: Map of the Kigluaik-Bendeleben fault system from Hudson and Plafker (1978). The star represents the epicenter of the December 13, 1964 earthquake.

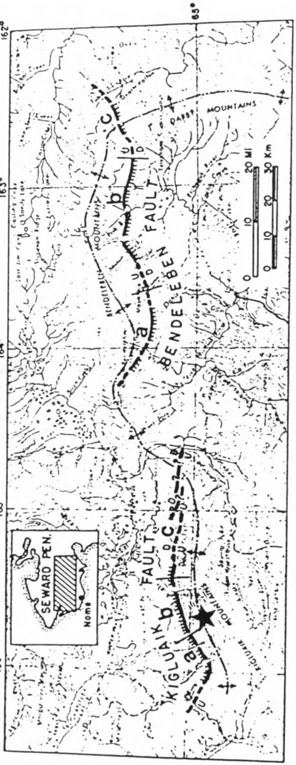
162°
163°
164°
165°
166°
65°
BENDELEBEN FAULT
KIGLUAIK FAULT
DARBY MOUNTAINS
BENDELEBEN MOUNTAINS
KIGLUAIK MOUNTAINS
SEWARD PEN.
Nome
20 MI
30 Km

Figure 2-14

Figure 2-15: Shear-wave polarizations and focal mechanism of Ritsema (1962) for the April 7, 1958, Huslia earthquake (#9). Dashed line shows the fit of the preferred solution (Figure 2-16) to the P-wave and S-wave data.

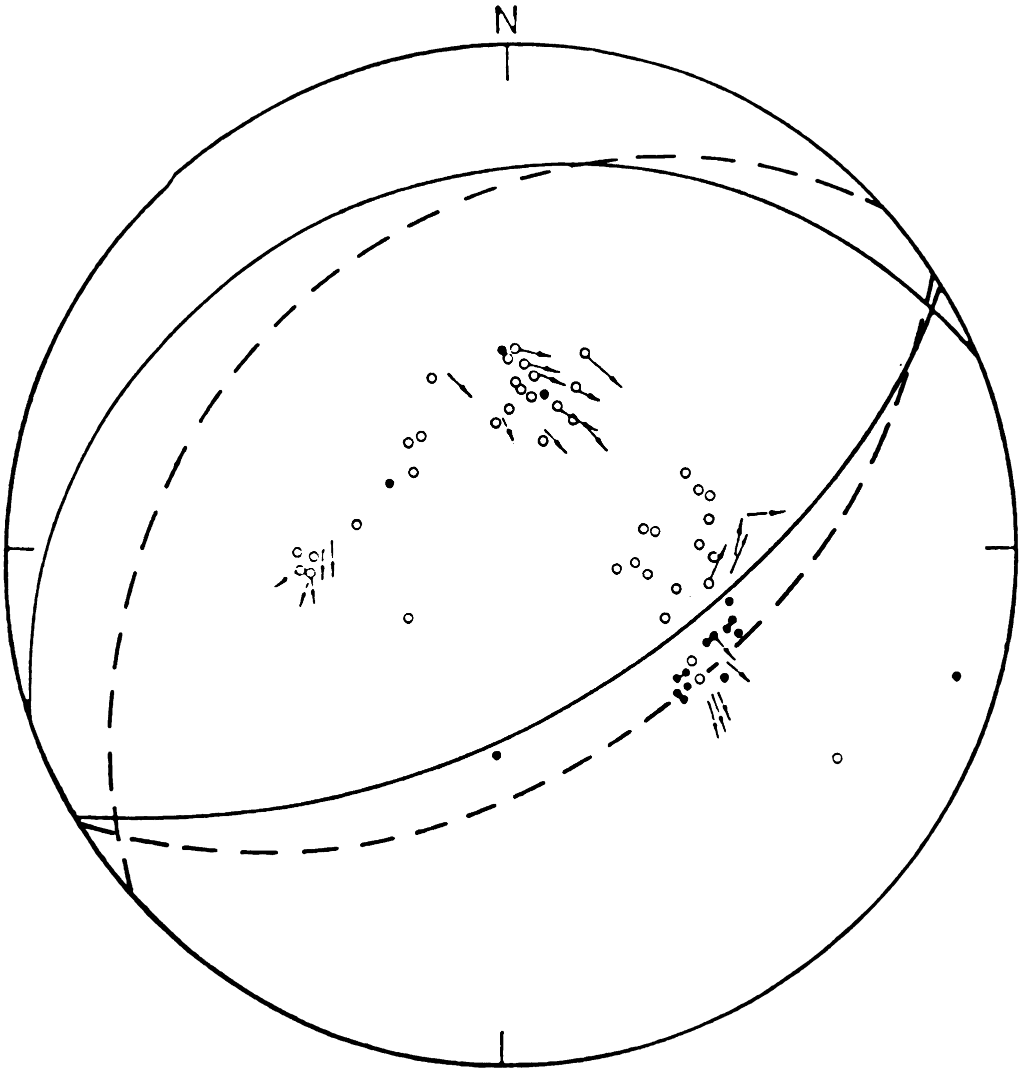

07 APRIL 1958
RITSEMA SOLUTION

Figure 2-15

2-1; Figure 2-16) is a slight modification of Ritsema's (1962) and Coley's (1983), and has been chosen to best fit all the data and to maintain orthogonality of the nodal planes.

Event 10 was a small (M_b=4.2) event which occurred at almost exactly the same epicenter as a 1965 magnitude 5.8 earthquake (Sykes and Sbar, 1974; no. SS6) east of Seward Peninsula. Despite the small size of the event, a moderately well constrained focal mechanism was determined by reading P-wave first motions and using ISC reported first motions (Figure 2-17). The solution is dominantly normal faulting, with a steeply dipping nodal plane trending 070^{o}, and a less well constrained gently dipping plane trending 014^{o}. The east-west trending plane is constrained mainly by ISC reported first motions. The nodal planes are nearly orthogonal to Sykes and Sbar's (1974) solution for the nearby 1965 event, but the north-trending nodal plane parallels the dominant fault trend (Bickel and Patton, 1957) in the epicentral region. Furthermore, the mechanism is consistent with other earthquake solutions, including the 1965 event, which indicate extension in western Alaska.

The January 22, 1968, Barter Island earthquake (Mb=4.7; no. 11) was located about 2 km offshore of northeastern Alaska, at the northern end of the Canning Displacement Zone (CDZ) of Grantz and May (1982). First motions indicate this event has a strike-slip solution with a large normal faulting component (Figure 2-18). Rayleigh waves were analyzed to further constrain the focal mechanism obtained from first motions. Although data in the southwest quadrant are sparse, a fair match is found between the observed radiation pattern and the theoretical pattern generated from the focal mechanism (Figure 2-18). A node is present in the radiation pattern, and is not inconsistent with what is expected from the dip slip mechanism shown.

Figure 2-16: Focal mechanism of the Huslia earthquake derived from orthogonalizing the nodal planes of Coley (1983), whose solution was based upon the best fit of P-wave first motions and Ritsema's (1962) S-wave polarizations.

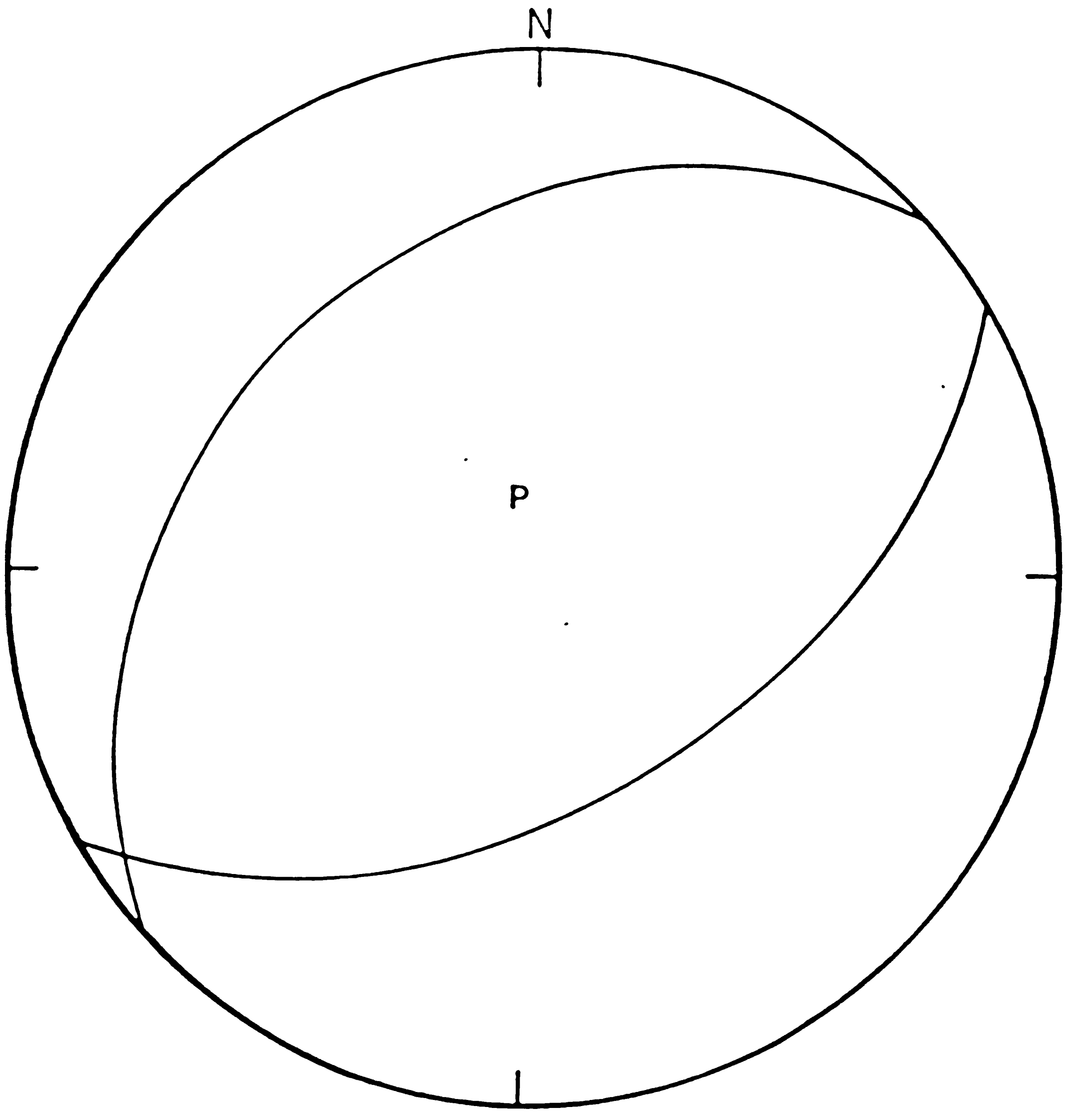

07 APRIL 1958
THIS STUDY

Figure 2-16

Figure 2-17: P-wave first motions for the $M_b=4.2$, April 11, 1973 event (#10) east of the Seward Peninsula. Conventions are as in Figure 2-5.

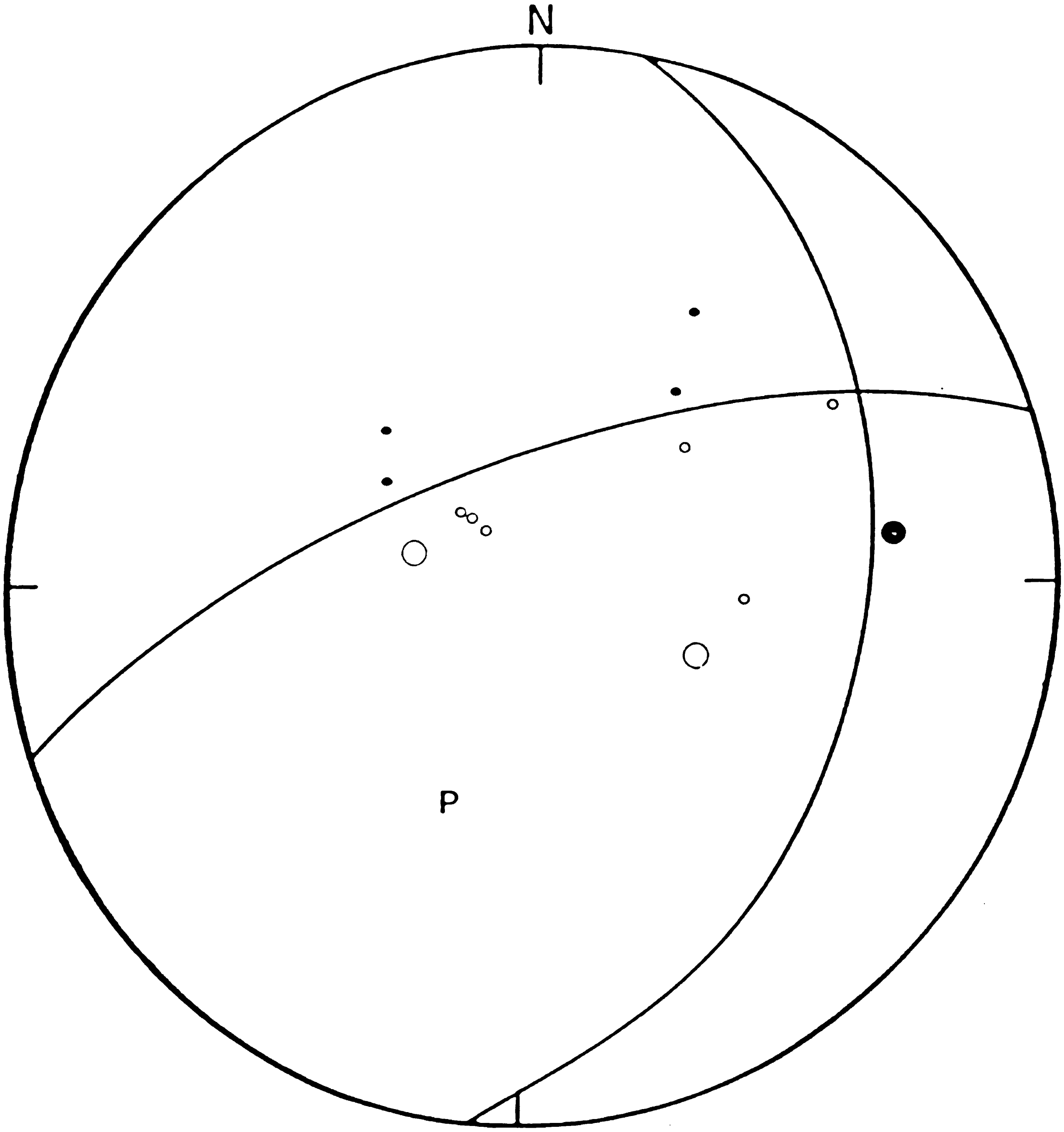

11 APRIL 1973

Figure 2-17

Figure 2-18: P-wave first motion plot and Rayleigh wave radiation pattern for the January 22, 1968, Barter Island earthquake (#11). Conventions are as in Figure 2-5.

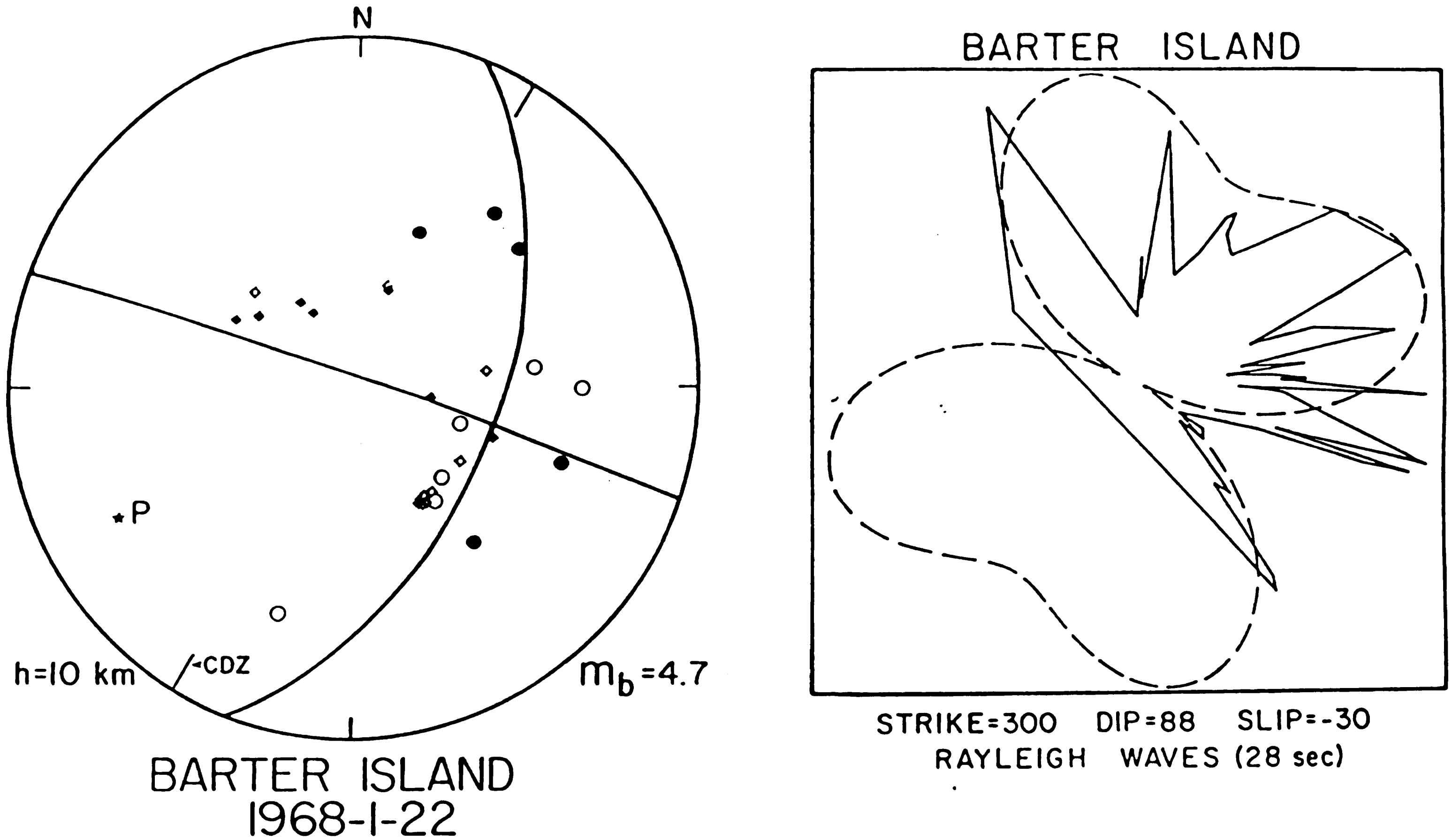
N
h=10 km
CDZ
P
m_b=4.7
BARTER ISLAND
1968-1-22
BARTER ISLAND
STRIKE=300 DIP=88 SLIP=-30
RAYLEIGH WAVES (28 sec)

Figure 2-18

The small magnitude of this event prevented a good distribution of body waves which could be used for synthetic seismogram computation. Seismograms calculated at two stations, using either of the proposed solutions, do match with observed records when placed at very shallow (<5 km) focal depths (Figure 2-19). Crustal structure is taken from Grantz and May (1982).

Reflection seismic lines from the R/V S.P. Lee show approximately east-west striking, steeply dipping normal faults (Grantz and May, 1982; Figure 2-20). This corresponds with the 095^{o} striking nodal plane of the mechanism, which is therefore taken as the fault plane for this event. Grantz et al. (1987) describe west-northwest trending normal faults and listric growth faults which drop the northern wall down along the continental slope. Thrusting, if active, occurs only on low-angle detachment faults, which do not match the dip of the fault plane in the solution. Quaternary deposits are offset by as much as 10 meters, consistent with recent activity on the faults. The sense of strike-slip motion on this event is opposite that which is expected if it were due to stresses/strains along the CDZ.

Biswas et al. (1986) proposed a nearly pure strike-slip solution for the Barter Island earthquake, with nodal planes of $050^{o}/60^{o}$ and $315^{o}/80^{o}$. Such a solution is inconsistent with P-wave first motions read from seismograms (specifically at MBC, CMC, DUG and FSJ), with the nodal azimuths on the Rayleigh wave radiation pattern, and with the trends of any of the faults identified in the Barter Island or Camden Bay region. Due to these inconsistencies, the solution of Biswas et al. (1986) is not considered in this study.

Figure 2-19: Synthetic seismogram at State College, Pennsylvania, calculated for the Barter Island earthquake focal mechanism solutions of Biswas et al. (1986) and from this study. Fits for either mechanism can only be obtained when a very shallow (< 5 km) depth is used.

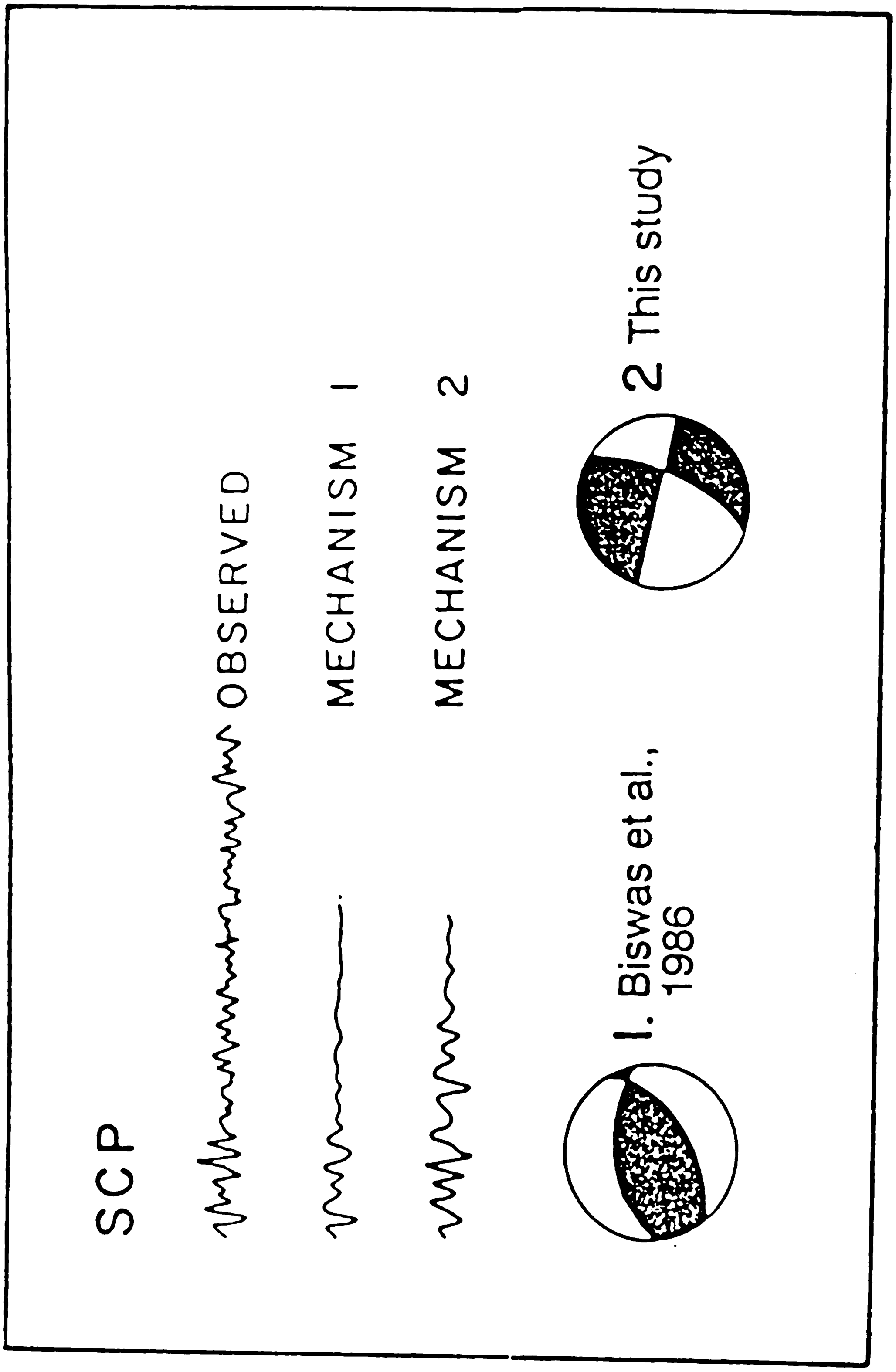
SCP
OBSERVED
MECHANISM 1
MECHANISM 2
1. Biswas et al.,
1986
2 This study

Figure 2-19

Figure 2-20: Map and seismic section in the vicinity of the 1968 Barter Island earthquake. The motion along the north-south nodal plane is opposite that of the Canning Displacement Zone. The east-west nodal plane parallels the strike of the steeply dipping normal faults in the seismic section, and is most likey the fault plane.

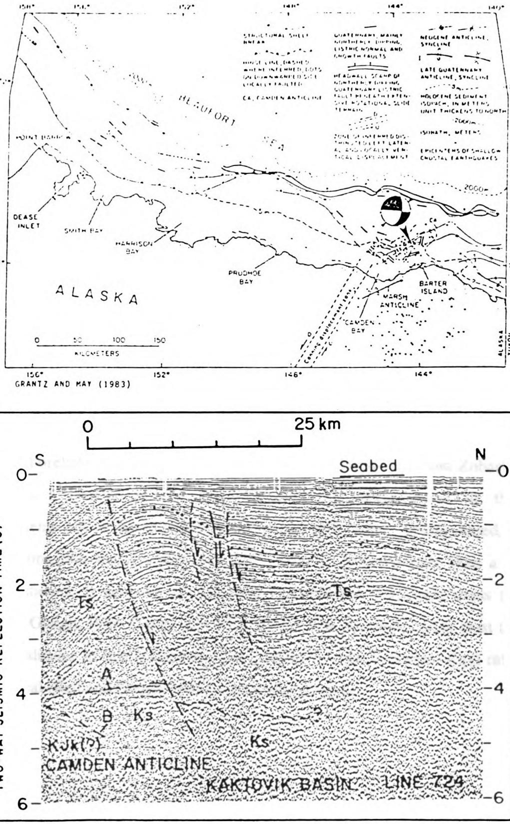
BEAUFORT
SEA
POINT BARROW
DEASE INLET
SMITH BAY
HARRISON BAY
PRUDHOE BAY
ALASKA
BARTER ISLAND
MARSH ANTICLINE
CAMDEN BAY
CA
2000m
ALASKA YUKON
0 50 100 150
KILOMETERS
156° 152° 146° 144°
70° 70°
GRANTZ AND MAY (1983)
0 25 km
S N
Seabed
TWO-WAY SEISMIC-REFLECTION TIME (S)
0 2 4 6
Ts
Ts
A
B
Ks
Ks
KJk(?)
CAMDEN ANTICLINE
KAKTOVIK BASIN
LINE 724

Figure 2-20

STRESS INDICATORS

In addition to the earthquake source parameters presented above, I have included parameters of 16 earthquakes from other sources and 9 borehole elongation stress determinations from northwestern Canada (Table 2-1 and 2-2; Figure 2-21).

The earthquakes, ranging in magnitude from 3.8 to 7.3, have well constrained nodal plane orientations. The solutions represent compressive maximum horizontal stress if one of the two following criteria for the principal stress axes' dips are met:

$$P, T < 30^{o} \text{ (Strike slip faulting)}$$
$$\text{or}$$
$$T > 30^{o} > P \text{ (Thrust faulting)}$$

where P is the principal compressive stress and T is the principal tensile stress. If the principal stress axes' dips meet the criteria

$$P > 30 > T \text{ (Normal faulting)}$$

then the maximum compressive stress is considered vertical.

The borehole elongation data (Table 2-2) are summarized from Zoback et al. (1984). Details of the theory behind the interpretation of these measurements can be found in Bell and Gough (1979, 1981). Briefly stated, the axis of elongation found within well drill holes, at depths greater than a few hundred meters, is assumed to represent the minimum horizontal stress (S_h) (Bell and Gough, 1979; Gough and Bell, 1981). The maximum stress must then be perpendicular to this orientation, and is thought to be horizontal (S_H) rather than vertical (Bell and Gough, 1981) in northwest Canada.

Table 2: WELL ELONGATION PRINCIPLE COMPRESSIVE STRESS DATA FROM NORTHWEST CANADA

Latitude	Longitude	Azi	Ref#
66.000 N	132.500 W	354	CN61
66.200 N	134.000 W	349	CN62
66.400 N	134.700 W	354	CN63
65.800 N	135.200 W	038	CN64
66.600 N	138.400 W	040	CN65
65.800 N	140.300 W	000	CN66
66.400 N	140.200 W	345	CN67
68.100 N	135.000 W	062	CN68
68.400 N	135.500 W	056	CN69

MEAN AZI OF ALL DATA = 17.556

Data from: Zoback et al., 1984.

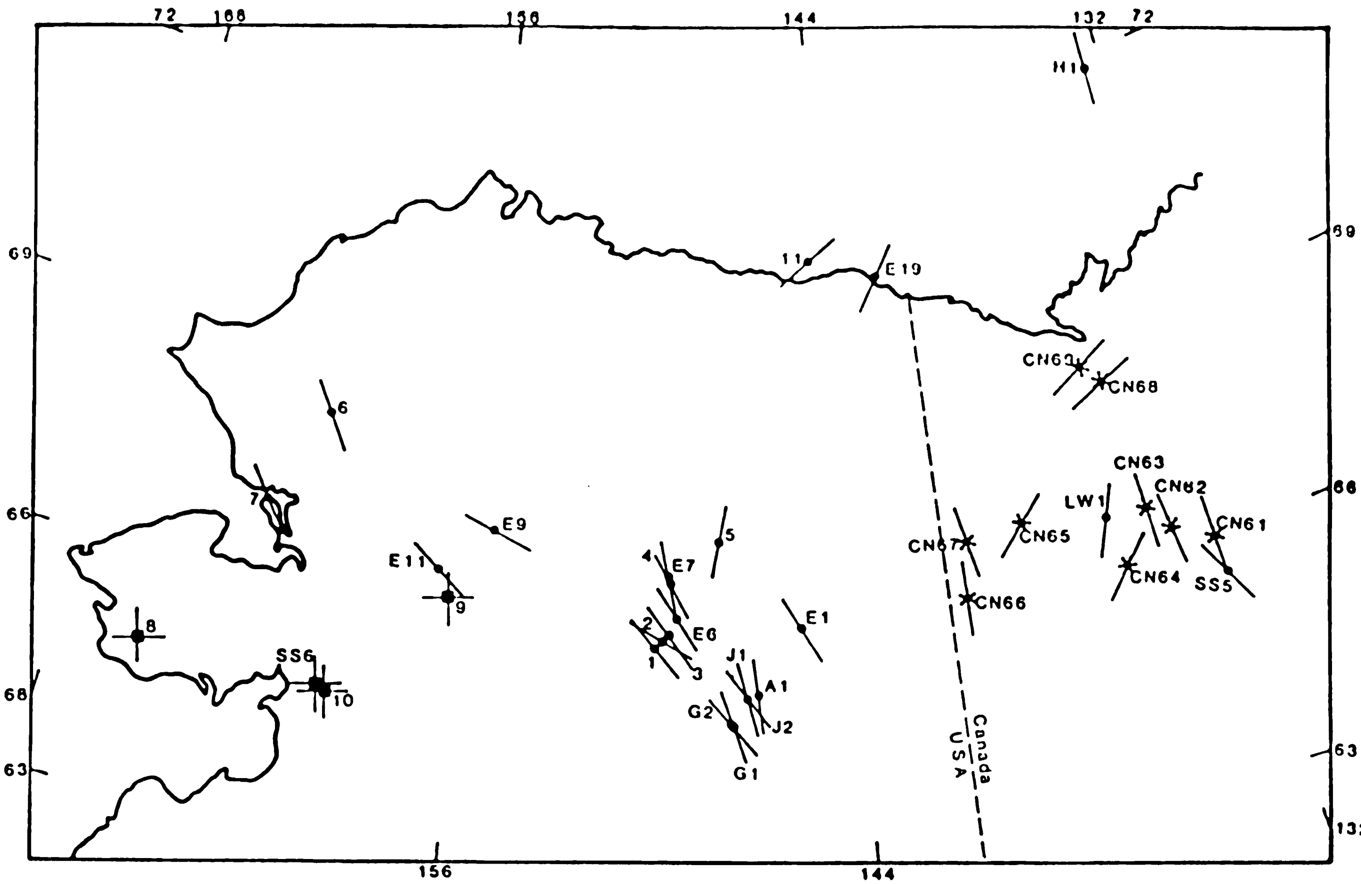

Figure 2-21: Plot of the principle compressive stress orientations in Alaska and northwest Canada, north of 64^{O}N. Data point labels correspond to references in Tables 2-1 and 2-2. Data points which are circles indicate horizontal compressive stresses from earthquake focal mechanisms, squares are vertical compressive stresses from earthquake focal mechanisms, and stars are borehole elongation maximum horizontal compressive stresses.

STRESS REGIMES

Compression due to Pacific subduction and related back-arc extension represent two principal tectonic sources which would probably be incorporated into any hypothesis regarding the distribution of stresses within south-central Alaska. Conclusions of previous investigations have indicated these sources are indeed affecting the regional stress (e.g., Nakamura et al. (1980), Gedney (1970), Biswas et al. (1986)). Further north and east, however, Pacific induced stresses should decrease, and other sources, such as ridge push from the Arctic mid-ocean ridge or continental margin sediment loading may influence the regional stress (Hasegawa et al., 1979). Local stresses or structural geometries could be responsible for small variations in the overall stress pattern within Alaska and northwest Canada.

The data presented here delineate distinct regions of compression and extension associated with the subduction of the Pacific plate. Stress orientations in northeast Alaska indicate that stresses identified east of the Canadian Rockies and in the Mackenzie delta region (Gough et al., 1983) may also continue north and west of the Davidson mountains to at least Camden Bay. Thus, three separate regional stress regimes, central Alaska, western Alaska and northern Alaska, are identified (Figure 2-22).

Central Alaska

Source parameters for 17 earthquakes (nos. 1, 2, 3, 4, 5, 6, 7, G1, G2, J1, J2, A1, E1, E6, E7, E9, AND E11) are used to define the central Alaska stress regime (Figure 2-22). All the earthquakes occurred north of 64^{o}N and south of 68^{o}N. The westernmost of these earthquakes (nos. 6 and 7) occur at the western end of the Kobuk Valley, northeast of Seward Peninsula.

Figure 2-22: Proposed distribution of stresses in Alaska and surrounding areas. Hatchured region is under northwest-southeast horizontal compression associated with Pacific subduction. Northern Alaska and the Beaufort Sea is undergoing north-northeast to northeast horizontal compression, and western Alaska and the Bering Sea are undergoing extension. Long dashed boundary is the compression to extension transition proposed by Nakamura et al. (1980). Short dashed line is the transition as proposed by Biswas et al. (1986). SPB is the stress province boundary of Gough et al. (1983).

Of the 17 events, 16 have near horizontal P-axis orientations with a northwest-southeast (284^{o}-354^{o}) trend (Table 2-1). This indicates that the compressive stresses generated by the subduction of the Pacific plate are reflected in earthquakes for hundreds of kilometers not only north and northeast of the Aleutian trench, but also into the southwestern Brooks Range. Compressive horizontal stress directions (Table 2-1) are in good agreement with the stress trajectories proposed for the Fairbanks and Rampart areas (Gedney, 1970; Nakamura et al., 1980; Biswas et al., 1986), but horizontal compression extends further north and west than Nakamura et al.'s (1980) proposed boundary marking the transition from compression to extension. Biswas et al. (1986) redefine the transition boundary to extend north to the Arctic coast, but maintain extension in the western Brooks Range where earthquakes (nos. 6, 7, E9, E11; see also Gedney and Marshall, 1981) indicate NW-SE directed compression. Therefore, results of this study indicate the Brooks Range must be included within the compressional regime (Figure 2-22).

An interesting consistency should be noted within the central Alaska region. There is a slight, yet systematic variation of P-axis orientations between earthquakes in the Fairbanks region (nos. A1, J1, J2, G1, G2) and those in the Rampart region (nos. 1, 2, 3, 4, E6, E7). Focal mechanisms of earthquakes in the Fairbanks region, which lie south of the Kaltag-Stevens Creek-Tintina fault system, have a more north-northwest P-axis trend (mean orientation = 339^{o}, range of 323^{o} to 354^{o}) than the Rampart region solutions (mean P-axis orientation = 326^{o}, range 300^{o} to 348^{o}) north of the Kaltag-Stevens Creek-Tintina fault system. Furthermore, four of the five events (J1, J2, G1, G2) in the Fairbanks region are part of earthquake pairs which occurred at the same epicentral locations. For each pair, the second event (J2 and G2) has a more west-northwest P-axis trend similar to that north of the Kaltag-Stevens Creek-Tintina fault system. Gedney (1970) has shown that the strain north of the Kaltag-Stevens Creek-Tintina fault system is significantly less than south of the system. Thus, it appears that in regions of less strain (e.g., north of the Kaltag-Stevens Creek-Tintina fault (Gedney, 1970)) or in areas where strain has been released (after the first of an earthquake pair) the P-axes orient in a more northwest to west-northwest direction.

Western Alaska

Northwest of the Kaltag fault, normal faulting earthquakes (nos. 8, 9, 10, SS6) indicate extension is the active tectonic process. This region, which is nearly 1000 km from the Aleutian trench axis, includes Seward Peninsula and the northern Yukon-Koyukuk province. Uyeda and Kanamori (1979) identified two stress regimes associated with the Aleutian subduction zone. The first, near the volcanic arc, is compressional. Further from the arc, however, tension is indicated, despite the Bering sea being an "inactive" (Uyeda and Kanamori, 1979) back-arc region.

There is additional evidence of recent extension within the western Alaska - Bering Sea region. Hudson and Plafker (1978) identified major normal faults (Kigluaik and Bendeleben) in southern Seward Peninsula (Figure 2-14). A December, 1964, magnitude 5.3 earthquake (no. 8) most likely occurred on the Kiguaik fault. The east - west trending, north dipping nodal plane matches very well with the mapped character of the Kigluaik fault (Hudson and Plafker, 1978). Quaternary basaltic volcanism has also been noted in Seward Peninsula and northern Yukon - Koyukuk province (Hopkins et al., 1971; Hudson, 1977; Beikman, 1980). Finally, Lockhart (1984) used gravity anomalies to propose extension in the Seward Peninsula, and suggested such stresses must exist on a regional scale.

Nakamura et al. (1980) and Biswas et al. (1986) both included western Alaska, with Seward Peninsula, northern Yukon-Koyukuk province and the western Brooks Range, in the extensional regimes of their Alaskan stress models. As discussed earlier, data from this investigation suggest that the western Brooks Range, at least north of the Kobuk Trench, supports horizontal compressive stresses and is therefore not part of the western Alaska extensional region (Figure 2-22). The distribution of Tertiary to Quaternary basalts in the Yukon-Koyukuk province and Seward Peninsula, but not within the western Brooks Range (Stone and Wallace, 1987), supports the placement of a northern boundary on the extensional region. It is possible that the compression is preferentially transmitted along the Brooks Range due to a more homogenous basement and/or lithospheric differences from Seward Peninsula and Yukon-Koyukuk province. However, data do indicate that Seward Peninsula and northern Yukon-Koyukuk province are undergoing extension as concluded by Nakamura et al. (1980) and Biwas et al. (1986). The extension is related to regional back-arc stresses (Lockhart, 1984), which are acting over the entire Bering Sea region (Chapter 1).

Northern Alaska

The stresses south of the Brooks Range have been determined by numerous investigations using a variety of methods (e.g., Gedney, 1970; Nakamura et al., 1980; Biswas et al., 1986; this study). Although each of these investigations may differ in detail, the general Pacific compression (central Alaska) and back-arc extension (western Alaska) models seem to apply in every case. North of the Brooks Range, however, the determination of the stress regime(s) has been hampered by the sparse availability of data.

Examination of two moderate earthquakes (#11, this study; #E19, Estabrook, 1985) located offshore northern Alaska near Camden Bay indicates stress orientations similar to those derived from borehole elongations in northwest Canada. Both earthquakes are predominantly strike-slip, and have a northeast trending, moderately (29^{o} to 30^{o}) dipping principal compressive stress orientation. This orientation is similar to stresses derived from drill hole elongations located in the Yukon and Northwest Territories (Table 2-2; Figure 2-21) as well as to that of the 1985 Nahanni earthquake in the Northwest Territories (Wetmiller et al., 1988; Dziewonski et al., 1986).

The orientation of principal horizontal stress in northeast Alaska differs from that predicted by ridge push forces (compression approximately north-south) or loading of the continental margin (extension approximately north-south). It is likely that the stresses in northern Alaska are more complex than within the Mid-Continent region, and cannot be ascribed solely to sediment loading or ridge push forces. The solutions of the two southern Beaufort Sea earthquakes have fault planes, with normal faulting components, parallel to the continental margin, although the tensional axes are not perpendicular to the margin. It may be suggested that tensional sediment loading stresses are nearly equal to compressive ridge push stresses perpendicular to the margin. These two opposing stresses may in effect cancel one another, allowing yet another source to be reflected in the observed stress orientations.

Gough et al. (1983) identified a "stress province boundary" which separated the Mid-Continent stress (NE-SW) regime from an Alaskan stress

(NW-SE) regime (Figure 2-22). This extended the Mid-Continent stress orientation (NE-SW) northwest to the Mackenzie Delta region, with the Rocky Mountain front approximating the position of the stress province boundary. The two Beaufort Sea earthquakes (nos. 11 and E19) also exhibit the Mid-Continent stress orientation. I therefore suggest that the stresses within southern Beaufort Sea may be similar to those presently operating in the Yukon and Northwest Territories of Canada, and that this stress regime is separated from Alaskan stresses (Gough et al., 1983) by a line which runs along the Davidson Mountains to the northern Brooks Range.

CONCLUSIONS

This study has improved upon earlier evaluations of Alaskan stresses by evaluating earthquake source parameters and borehole elongations in Alaska and northwestern Canada. Previous studies within Alaska by means of seismicity (e.g., Gedney, 1970; Biswas et al., 1986), volcanic alignments (Nakamura et al., 1980) and theoretical modelling (e.g., Richardson et al., 1979) have extrapolated stresses over large areas void of data. Additional data presented in this investigation have filled portions of the void and allowed a more detailed outline of the stress regimes to be obtained. Compressive stresses derived from the subduction of the Pacific plate at the Aleutian trench radiate north and northeast into central Alaska. The compressive stresses may also be preferentially transmitted westward along the Brooks Range, thus explaining continued strike-slip faulting as far west as Kotzebue Sound. Therefore, extension cannot be generalized throughout western Alaska, as had been done previously (Nakamura et al., 1980; Biswas et al., 1986).

Western Alaska, south of approximately 66^{o}N, is undergoing extension related to back-arc stresses. The extension is manifested not only in the seismicity, which is dominated by normal faulting earthquakes, but also in the geology (Hudson and Plafker, 1978) and the gravimetric signature (Lochhart, 1984). Lockhart's (1984) conclusion that the back-arc stresses must be of regional extent is supported by investigations elsewhere in the Bering Sea (Chapter 1; Savostin et al., 1986).

The Mid-Continent stress regime (Zoback et al., 1986) appears to extend into the Beaufort Sea. Thus, the stress province boundary identified by Gough et al. (1983) extends beyond northwest Canada into northern Alaska. This boundary separates the Mid-Continent stresses from Pacific induced stresses along the entire length of the Rocky Mountains, and may continue along the northeastern Brooks Range as well. If northern Alaska is influenced by multiple sources of stress, including ridge push and continental margin extension, these opposing stresses appear to cancel one another.

LIST OF REFERENCES

LIST OF REFERENCES

Agnew, J. D., 1980. Seismicity of the Central Alaska Ranges, Alaska: 1904-1978, M.A. Thesis, 88 pp., Univ. of Alaska, Fairbanks.

Balakina, L. M., 1962. General regularities in the direction of the principal stresses effective in the earthquake foci of the seismic belt of the Pacific Ocean, Iz. AN SSSR Ser. Geof., 1471-1483 (Eng. Trans.).

Beikman, H. M., 1980. Geologic Map of Alaska, U. S. Geol. Survey, 1:2,500,000, 2 sheets.

Bell, J. S. and D. I. Gough, 1979. Northeast-southwest compressive stress in Alberta: Evidence from oil wells, Earth Planet. Sci. Let., 45, 475-482.

Bell, J. S. and D. I. Gough, 1981. Intraplate stress orientations from Alberta oil-wells, in, R. J. O'Connell and W. S. Fyfe, eds., Evolution of the Earth, Am. Geophy. Union Geodynamics Series, 5, 96-104.

Bhattacharya, B. and N. N. Biswas, 1979. Implications of N. Pacific plate tectonics in central Alaska: Focal mechanisms of earthquakes, Tectonophysics, 53, 99-130.

Bickel, R. S. and W. W. Patton, Jr., 1957. Preliminary geologic map of the Nulato and Kateel Rivers area, Alaska, U. S. Geol. Survey Misc. Geol. Inv. Map I-249, scale 1:125,000.

Biswas, N. N. and K. Aki, 1984. Maximum horizontal stress trajectories in Alaska from seismicity studies (abs.), Earthquake Notes, Seis. Soc. Am., 55, p. 23.

Biswas, N. N., K. Aki, H. Pulpan and G. Tytgat, 1986. Characteristics of regional stresses in Alaska and neighboring areas, Geophysical Research Letters, 13, 177-180.

Biswas, N. N., L. Gedney and J. Agnew, 1980. Seismicity of western Alaska, Bull. Seis. Soc. Am., 70, 873-884.

Biswas, N. N., J. Pujol, G. Tytgat and K. Dean, 1986. Synthesis of seismicity studies for western Alaska, Tectonophysics, 131, 369-392.

Brogan, G. E., L. S. Cluff, M. K. Korringa and D. B. Slemmons, 1975. Active faults of Alaska, Tectonophysics, 29, 73-85.

Churkin, M., Jr., H. L. Foster and R. M. Chapman, 1982. Terranes and suture zones in east central Alaska, J. Geophys. Res., 87B, 3718-3730.

Churkin, M., Jr., and J. H. Trexler Jr., 1981. Continental plates and accreted oceanic terranes in the Arctic, in A. E. M. Narin, M. Churkin Jr. and F. G. Stehli, The Ocean Basins and Margins, v. 5, 672 pp., Plenum Publishing Corp.

Coley, M. J., 1983. Intraplate Seismicity in Central Alaska and Chukotka, M.S. Thesis, 97 pp., Michigan State University, E. Lansing.

Dziewonski, A. M., J. E. Franzen and J. H. Woodhouse, 1985. Centroid moment tensor solutions for January-March 1985, Phys. Earth and Planet. Int., 40, 249-258.

Dziewonski, A. M., J. E. Franzen and J. H. Woodhouse, 1986. Centroid moment tensor solutions for October-December 1985, Phys. Earth and Planet. Int., 43, 185-195.

Dziewonski, A. M., G. Ekstrom, J. E. Franzen and J. H. Woodhouse, 1988. Global seismicity of 1981: centroid-moment tensor solutions for 542 earthquakes, Phys. Earth Planet. Int., 50, 155-182.

Estabrook, C. H., 1985. Seismotectonics of Northern Alaska, M. S. Thesis, 139 pp., University of Alaska, Fairbanks.

Fujita, K., D. B. Cook and M. J. Coley, 1983. Tectonics of the western Beaufort and Chukchi seas, EOS, 64, p. 163.

Gedney, L., 1970. Tectonic stresses in S. Alaska in relationship to regional seismicity and the new global tectonics, Bull. Seis. Soc. Am., 60, 1789-1802.

Gedney, L., 1985. Stress trajectories across the northeast Alaska Range, Bull. Seis. Soc. Am., 75, 1125-1134.

Gedney, L. and E. Berg, 1969a. Some characteristics of the tectonic stress pattern in Alaska, Geophys. J. Royal Ast. Soc., 17, 293-304.

Gedney, L. and E. Berg, 1969b. The Fairbanks earthquakes of June 21, 1967; aftershock distribution, focal mechanisms, and crustal parameters, Bulletin of the Seismological Society of America, 59, 73-100.

Gedney, L., S. Estes and N. Biswas, 1980. Earthquake migration in the Fairbanks, Alaska seismic zone, Bulletin of the Seismological Society of America, 70, 223-241.

Gedney, L. D., S. A. Estes, N. N. Biswas and D. L. Marshall, 1982. A note on further activity in the Fairbanks, Alaska, seismic zone, Bulletin of the Seismological Society of America, 72, 1415-1417.

Gedney, L. and D. Marshall, 1981. A rare earthquake sequence in the Kobuk Trough, northwestern Alaska, Bull. Seis. Soc. Am., 71, 1587-1592.

Gough, D. I. and J. S. Bell, 1981. Stress orientations from oil well fractures in Alberta and Texas, Can. J. Earth Sci., 18, 638-645.

Gough, D. I., C. K. Fordjor and J. S. Bell, 1983. A stress province boundary and tractions on the North American plate, Nature, 305, 619-621.

Grantz, A., 1966. Strike-slip faults in Alaska, U.S. Geol. Sur. Prof. Paper 267, 82 pp.

Grantz, A. and S. May, 1982. Rifting history and structural development of the Continental margin north of Alaska, in, J. S. Watkins and C. L. Drake,eds., Studies in Continental Margin Geology, Am. Assoc. Pet. Geol., 77-100.

Hasegawa, H. S., C. W. Chou and P. W. Basham, 1979. Seismotectonics of the Beaufort Sea, Canadian Journal of Earth Science, 16, 816-830.

Hinzen, K-G., 1986. Comparison of fault-plane solutions and moment tensors, J. of Geophysics, 59, 112-118.

Hopkins, D. M., J. O. Mathews, J. A. Wolfe and M. L. Silberman, 1971. A Pliocene flora and insect fauna from the Bering Strait region, Paleogeography, Paleoclimatology, Paleoecology, 9, 211-231.

Hubbard, R. J., 1988. Age and significance of sequence boundaries on Jurassic and early Cretaceous rifted continental margins, The American Association of Petroleum Geologists Bulletin, 72, 49-72.

Hudson, T., 1977. Geologic map of Seward Penninsula, Alaska, U.S. Geol. Survey Map 77-796A.

Hudson, T. and G. Plafker, 1978. Kigluaik and Bendeleben faults, Seward Peninsula, U. S. Geol. Survey Circular 772-B, B47-B50.

Jones, D. L., N. J. Silberling, H. C. Berg and G. Plafker, 1981. Map showing tectonostratigraphic terrains of Alaska, columnar sections, and summary description of terrains, U.S. Geol. Sur. Open File Report 81-792, 20p. with maps.

Jordan, J. N., G. J. Dunphy and S. T. Harding, 1968. The Fairbanks, Alaska, earthquakes of June 21, 1967, Preliminary Engineering Seismological Report, 60 pp.

Kroeger, G. C., 1987. Synthesis and Analysis of Teleseismic Body Wave Seismograms, PhD Dissertation, Stanford University, Palo Alto, CA, 135 pp.

Liu, H. L., and H. Kanamori, 1980. Determination of source parameters of mid-plate earthquakes from the waveforms of body waves, Bull. Seis. Soc. Amer., 70, 1989-2004.

Lockhart, A. B., 1984. A gravity survey of the central Seward Peninsula, Alaska (Abstract), Geol. Soc. Am. Cordill. Sect., 16, 319.

Nakamura, K., K. H. Jacob and J. N. Davies, 1977. Volcanoes as possible indicators of tectonic stress orientation - Aleutians and Alaska, Pageoph, 115, 87-112.

Nakamura, K., G. Plafker, K. H. Jacob and J. N. Davies, 1980. A tectonic stress trajectory map of Alaska using information from volcanoes and faults, Bull. Earthquake Res. Inst., 55, 89-100.

Packer, D. R., G. E. Brogan and D. B. Stone, 1975. New data on plate tectonics of Alaska, Tectonophysics, 29, 87-102.

Patton, W. W., 1973. Reconnaissance geology of the northern Yukon-Koyukuk Province, Alaska, U.S. Geol. Sur. Prof. Paper 774-A, 17 pp.

Patton, W. A., I. L. Tailleur, W. P. Brosge and M. A. Lamphere, 1977. Preliminary report on the ophiolites of northern and western Alaska, in, R. G. Coleman and W. P. Irwin, eds., North American Ophiolites, State of Oregon Dept. of Geology and Mineral Industries, p. 51-57.

Richardson, R. M., S. C. Solomon and N. H. Sleep, 1979. Tectonic stress in the plates, Rev. of Geophys. and Space Phys., 17, 981-1019.

Ritsema, A. R., 1962. P and S amplitudes of two earthquakes of the single force couple type, Bull. Seis. Soc. Amer., 52, 723-746.

Savostin, L. A., B. V. Baranov, T. Z. Grigoryan and L. R. Merklin, Tectonics and origin of the western Bering Sea, Transactions (Doklady) of the USSR Academy of Sciences, Earth Science Section, 286, 88-91, 1986.

Schaffner, H. J., 1961. Tabillen Kinematischen Erdhebenherdparameters, Pub. Inst. Agnew, Geophysik, Freiberg.

Scheidegger, A. E., 1964. The tectonic stress and tectonic motion direction in Europe and western Asia as calculated from earthquake fault plane solutions, Bull. Seis. Soc. Am., 54, 1519-1528.

Seno, T., and G. C. Kroeger, 1983. A reexamination of earthquakes previously thought to have occurred within the slab between the trench axis and double seismic zone, northern Honshu Arc, J. Phys. Earth, 31, 195-216.

Scholz, C. H., M. Barazangi and M. L. Sbar, 1971. Late Cenozoic evolution of the Great Basin, western United States, as an ensialic inter-arc basin, Geol. Soc. Am. Bull., 82, 2979-2990.

Stevens, A. E., 1964. Earthquake mechanism determination by S-wave data, Bull. Seis. Soc. Amer., 54, 457-474.

Sykes, L. R., and M. L. Sbar, 1974. Focal mechanism solutions of intraplate earthquakes and stresses in the lithosphere, Geodynamics of Iceland and the north Atlantic area, D. Reidel Publishing, Holland, 323 pp.

Stone, D. B. and W. K. Wallace, 1987. A Geological framework of Alaska, Episodes, 10, 283-28.

Uyeda, S., and H. Kanamori, 1979. Back-arc opening and the mode of subduction, J. Geophys. Res., 84, 1049-1061.

VanWormer, J. D., J. Davies and L. Gedney, 1974. Seismicity and plate tectonics in south central Alaska, Bull. Seismol. Soc. Amer., 64, 1467-1475.

Wetmiller, R. J., R. B. Horner, H. S. Hasegawa, R. G. North, M. Lamontagne, D. H. Weichert and S. G. Evans, 1988. An analysis of the 1985 Nahanni earthquakes, Bull. Seis. Soc. Am., 78, 590-616.

Zoback, M. L. and M. Zoback, 1980. State of stress in the conterminous United States, J. Geophys. Res., 85, 6113-6156.

Zoback, M., S. P. Nishenko, R. M. Richardson, H. S. Hasegawa, M. D. Zoback, 1986. Mid-plate stress, deformation, and seismicity, in, Vogt, P. R. and Tucholke, B. E., eds., The Geology of North America, vol. M, The Western North Atlantic Region, Geological Society of America, 297-312.

Zoback, M., M. D. Zoback and M. E. Schiltzl, 1984. Index of stress data for the North American and parts of the Pacific Plate, U.S. Geol. Sur. Prof. Paper 84-157, 62 pp.

CHAPTER THREE

SEISMICITY AND FOCAL MECHANISMS OF THE NORTH AMERICAN - EURASIAN PLATE BOUNDARY IN SIBERIA

INTRODUCTION

The seismicity of the North American plate boundary in the Arctic and Siberia has been the subject of only limited study due to the scarcity of large (m_b > 6.0) earthquakes. The majority of Arctic earthquakes occur on the Arctic mid-ocean ridge, separating the North American and Eurasian plates (Fujita et al., in press). This narrow (< 50 km wide) linear trend is potentially the longest such trend of the mid-ocean ridge system (Sykes, 1965), and bisects the Eurasian basin and enters Siberia at the continental slope of the Laptev Sea (Figure 3-1). Within northeast Siberia, the seismicity becomes spatially diffuse, extending as a broad trend from the Lena River delta to the southern Cherskii Mountains where there is a bifurcation of epicenters to the south and east (Figure 3-2).

Since the installation of the World Wide Standardized Seismograph Network (WWSSN) only two earthquakes (April 19, 1962 and August 25, 1964) of magnitude greater 6.0 have occurred in this region. Source parameters for the 1964 event, and a select few other earthquakes, have been determined by various western investigators (e.g., Sykes, 1967; Chapman and Solomon, 1976; Jemsek et al., 1986). Soviet investigations (Lazareva and Misharina, 1965; Savostin and Karasik, 1981; Savsotin et al., 1983; Koz'min, 1984) also have been sparse, and appear to utilize International Seismological Center (ISC) Bulletin and Bureau Central International De Seismologie (BCIS) reported first motions and/or data from the Soviet northeast Siberian local network. Results of these studies are frequently inconsistent with each other, as well as with western studies, for both large and intermediate size events.

Several investigators (e.g., Chapman and Solomon, 1976; Savostin and Karasik, 1981) have utilized this restricted set of focal mechanism solutions in

Figure 3-1: Regional geographic map of northeast Siberia showing key features of interest. B-T denotes the location of Balagan-Tas volcano and EP denotes the El'ginskii Plateau. The position of the star indicates the Aleutian-Kurile arc-arc junction.

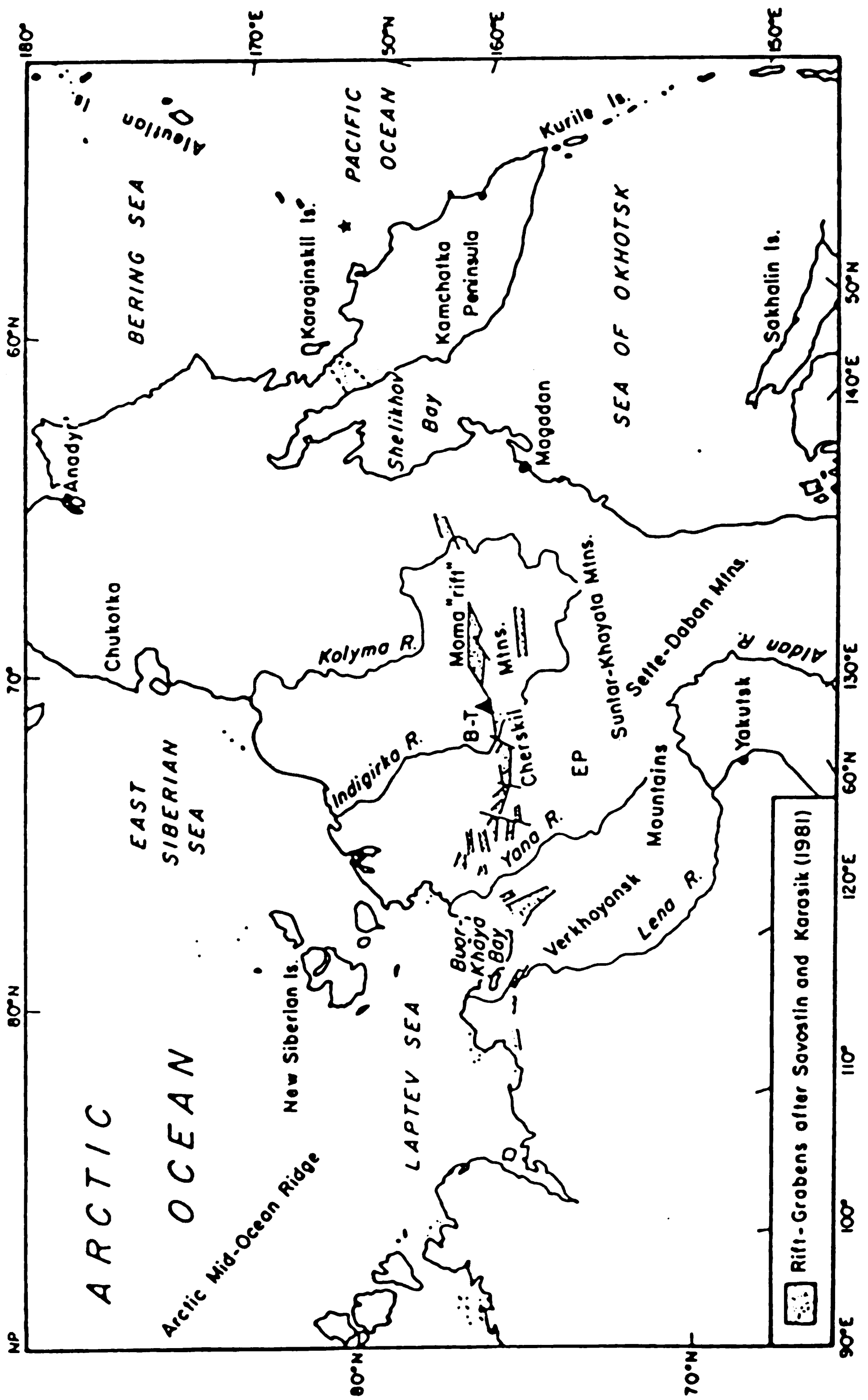

ARCTIC OCEAN
Arctic Mid-Ocean Ridge
New Siberian Is.
LAPTEV SEA
EAST SIBERIAN SEA
BERING SEA
Aleutian Is.
Karaginskii Is.
PACIFIC OCEAN
Kamchatka Peninsula
Kurile Is.
SEA OF OKHOTSK
Sakhalin Is.
Shelikhov Bay
Magadan
Anadyr
Chukotka
Kolyma R.
Moma "rift"
Mtns.
Indigirka R.
B-T
Cherskii
EP
Suntar-Khayata Mtns.
Sette-Daban Mtns.
Aldan R.
Yakutsk
Yana R.
Verkhoyansk Mountains
Lena R.
Buor-Khaya Bay
Rift-Grabens after Savostin and Karasik (1981)
NP
180°
170°E
160°E
150°E
150°N
50°N
60°N
70°
80°N
70°N
140°E
130°E
120°E
110°
100°
90°E

Figure 3-1

Figure 3-2: Shallow and intermediate (h < 100 km) teleseismic seismicity of northeast Siberia and adjacent Arctic mid-ocean ridge. Epicenters are from the ISC only. Large dots with stars are events used in this study. Open stars are events used from McMullen (1985). The shaded region along the Kurile and Aleutian arc denotes numerous events.

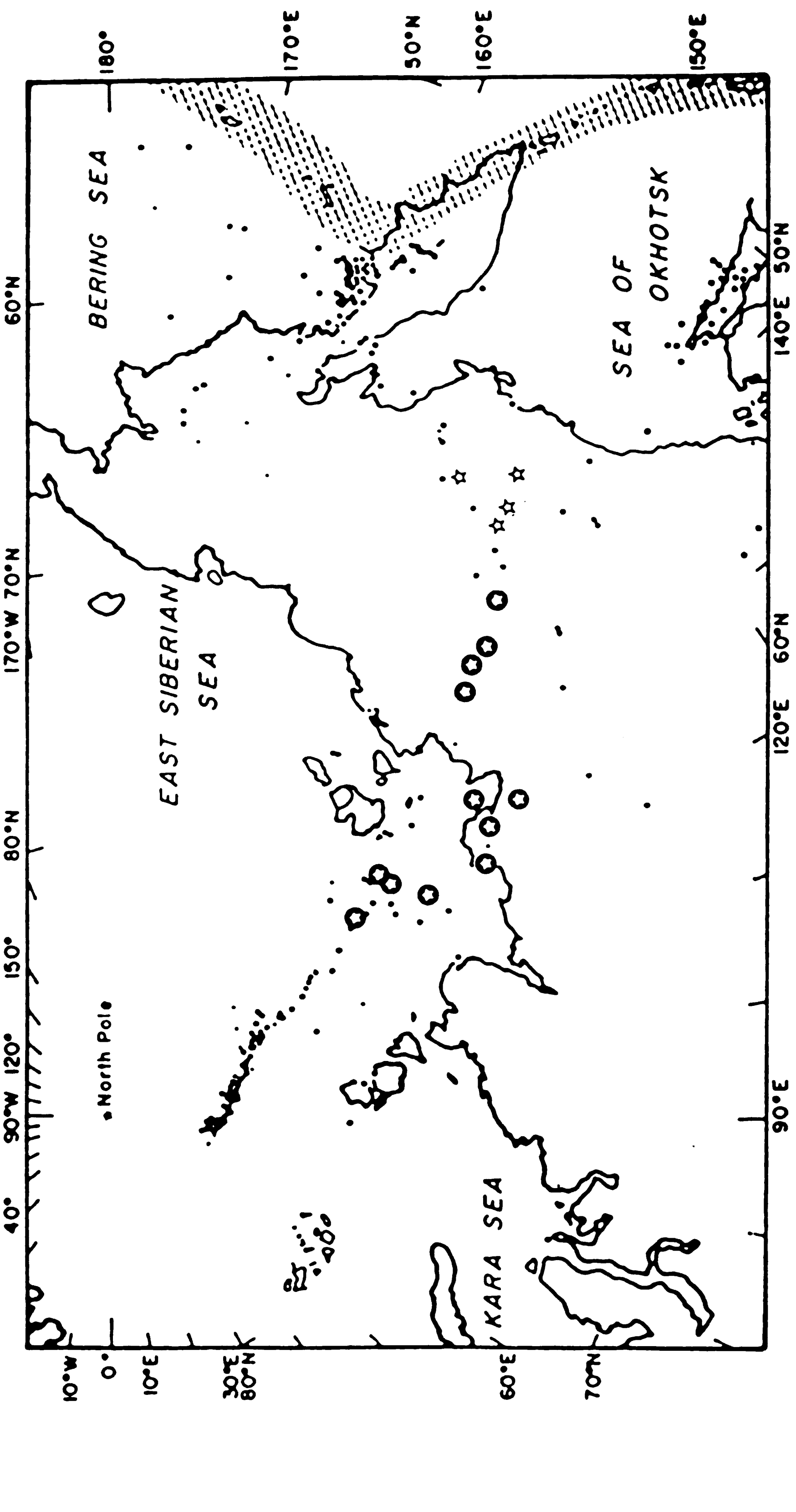
BERING SEA
SEA OF OKHOTSK
EAST SIBERIAN SEA
KARA SEA
North Pole
180°
170°E
50°N
160°E
150°E
60°N
70°N
170°W
80°N
150°
120°
90°W
40°
10°W
0°
10°E
30°E
60°E
70°E
140°E
120°E
90°E

Figure 3-2

an attempt to define the kinematics of the North American plate within northeast Siberia. Others (e.g., Morgan, 1972; Minster et al., 1974; Minster and Jordan, 1978 and DeMets et al., in press) have used data exclusive of northeastern Siberia to define the North American - Eurasian pole of rotation. However, the proximity of the pole of rotation to the physical plate boundary (DeMets et al., in press) and the potential existence of a Sea of Okhotsk plate (Savostin and Karasik, 1981; McMullen, 1985; Seno, 1985) could negatively affect the results of such broad studies.

This investigation attempts to better define the seismicity associated with the North American plate boundary in northeast Siberia through the determination of source parameters for the intermediate size ($4.5 < m_b < 6.0$) earthquakes. The result increases the data set available for investigation of the North American plate boundary the Arctic and Siberia, may sheds new light on the reliability of data from regions which are relatively inaccessible.

TECTONIC SETTING

The exact position of the North American plate boundary in northeast Siberia has long been debated by numerous workers (e.g., Chapman and Solomon, 1976; Zonenshain et al., 1978; Savostin and Karasik, 1981). Despite its presently undefined position, there is basic agreement upon the general trend between the Arctic ocean and the southern Cherskii Mountains. The setting of this area includes extremely rugged topography contrasted by large depressions with thick accumulations of sediments.

To the north, the Arctic mid-ocean ridge enters the continental shelf of northeast Siberia in the central Laptev Sea (Figure 3-1). The Laptev Sea is thought to be floored by grabens as old as Eocene (Savostin and Karasik, 1981). It is bounded to the east by the New Siberian Islands and to the southwest by the Lena River delta. The sea's southernmost extent is Bour Khaya Bay.

South and southeast from Bour Khaya Bay extends a series of depressions (Savostin and Karasik, 1981) bounded by prominent features such as the Cherskii Mountains and Moma Range (Figure 3-1). The general trend of the depressions and *en echelon* uplifts within the Cherskii Mountains is northwest - southeast. The depressions are bounded by normal faults, and are often cut by faults described as strike-slip or transform (Zonenshain et al., 1978), although they rarely are traced beyond the depression walls (Savostin and Karasik, 1981). If the depressions are structurally assymetric as Grachev (1973) notes within the Moma Rift, these transverse faults may be better described as transfer faults (Lister et al., 1986) rather than transform faults. L. Parfenov (pers. comm., 1986) reports that thrust and strike-slip faulting is now active within these depressions.

Sediments within the depressions range from Eocene (?) in the Laptev Sea, Oligocene in the Lena River delta region, Oligocene to Miocene in the northernmost Cherskii Mountains, and Pliocene in the southern regions of the Cherskii Mountains. The deposits are described only as sands and unconsolidated cobbles (Savostin and Karasik, 1981). Large (> 5 km) alluvial fans on the borders of the depressions are observable on LANDSAT imagery, as are a few small volcanic cones.

Numerous authors have suggested that the series of southeast trending depressions are the continental continuation of the Arctic mid-ocean ridge (e.g., Grachev et al., 1970; Churkin, 1972; Chapman and Solomon, 1976; Savostin and Karasik, 1981; Grachev, 1982). This conclusion is based on high heat flow, basaltic volcanism and relative subsidence (Argunov and Gavrikov, 1960; Naymark, 1976; Savostin and Karasik, 1981) found throughout the system. However, as early as the 1960's, investigators were finding evidence of compression and uplift (Lazareva and Misharina, 1965; Rezanov and Kochetkov, 1962) which may contradict the interpretation of the Cherskii - Moma system as an active rift, although the uplift could be associated with thermal doming.

SEISMICITY

The Arctic mid-ocean ridge is reflected in a very narrow, linear band of seismicity as it crosses the Arctic basin. However, the linearity ends as the ridge impinges upon the continental shelf at the Laptev Sea. Southward from this point, the epicenters become quite dispersed, extending from the New Siberian Islands west to the Lena River delta. Upon entering continental Siberia, there is a local decrease in seismicity, and then increased seismicity follows the general southeast trend of the Cherskii Mountains in a diffuse, 400 km wide band.

A first-order observation of this epicentral trend camouflages some more important points. When the epicentral distribution is examined as a function of magnitude it becomes quite evident that the larger ($M_b > 4.5$) events form a linear band along the western margin of the northern Cherskii Mountains (Figure 3-2). This immediately questions the location accuracy of the smaller earthquakes which are often detected only by Soviet local networks, since larger events are recorded and located by a multitude of global stations. A study by Fujita et al. (1987) examined the seismicity in northeast Siberia and concluded there was a bias of epicentral location as a function of spatial and temporal local station distribution. Their results also suggested that many epicenters in northeast Siberia were located using P-wave polarizations at a single station of the Soviet northeast seismograph network. This method creates annular rings (Figure 3-3) around stations because the critical refracted arrival of very close events artificially locates the epicenter at a minimum radius of 90 km (assuming a 33 km thick crust with velocity = 6 km/s and an upper mantle velocity = 7.5 km/s). Additionally, temporal gaps in seismicity developed as stations opened and closed. Therefore, the diffuse distribution of smaller earthquakes may be due, in part, to location capabilities. The trend of the larger (M_b > 4.5) events is more representative of the actual interplate epicentral distribution in the northern Cherskii Mountains and Laptev Sea.

FOCAL MECHANISM SOLUTIONS

From the interplate earthquakes in the Laptev Sea and northern Cherskii Mountains, twelve events large enough for study (magnitude 5.0-6.2) have been identified (Table 3-1). These were chosen from epicentral data available in the International Seismological Summary (ISS), the International Seismological Center (ISC) Bulletin, the Preliminary Determination of Epicenters (PDE) and Zemletryaseniya v SSSR (USSR Academy of Sciences earthquake annual). Seven new focal mechanism solutions are presented (Table 3-1), and solutions for the other five events are from other sources. Alternative mechanisms are presented for some of the moment tensor solutions since inconsistencies were observed between these solutions and mechanisms obtained through studies based on P-wave first motions (Appendix 3A).

The methods used to determine mechanisms for earthquakes in this study are detailed in Chapter 2. To summarize, the general approach includes first motion studies using data read from the WWSSN and Canadian Seismograph

Figure 3-3: Distribution of seismicity reported in the Seismologicheskii Bulleten for the year 1976. Size of cross is linear with increasing event size. Filled and open circles are locations of Soviet seismograph stations. From Fujita et al. (1987).

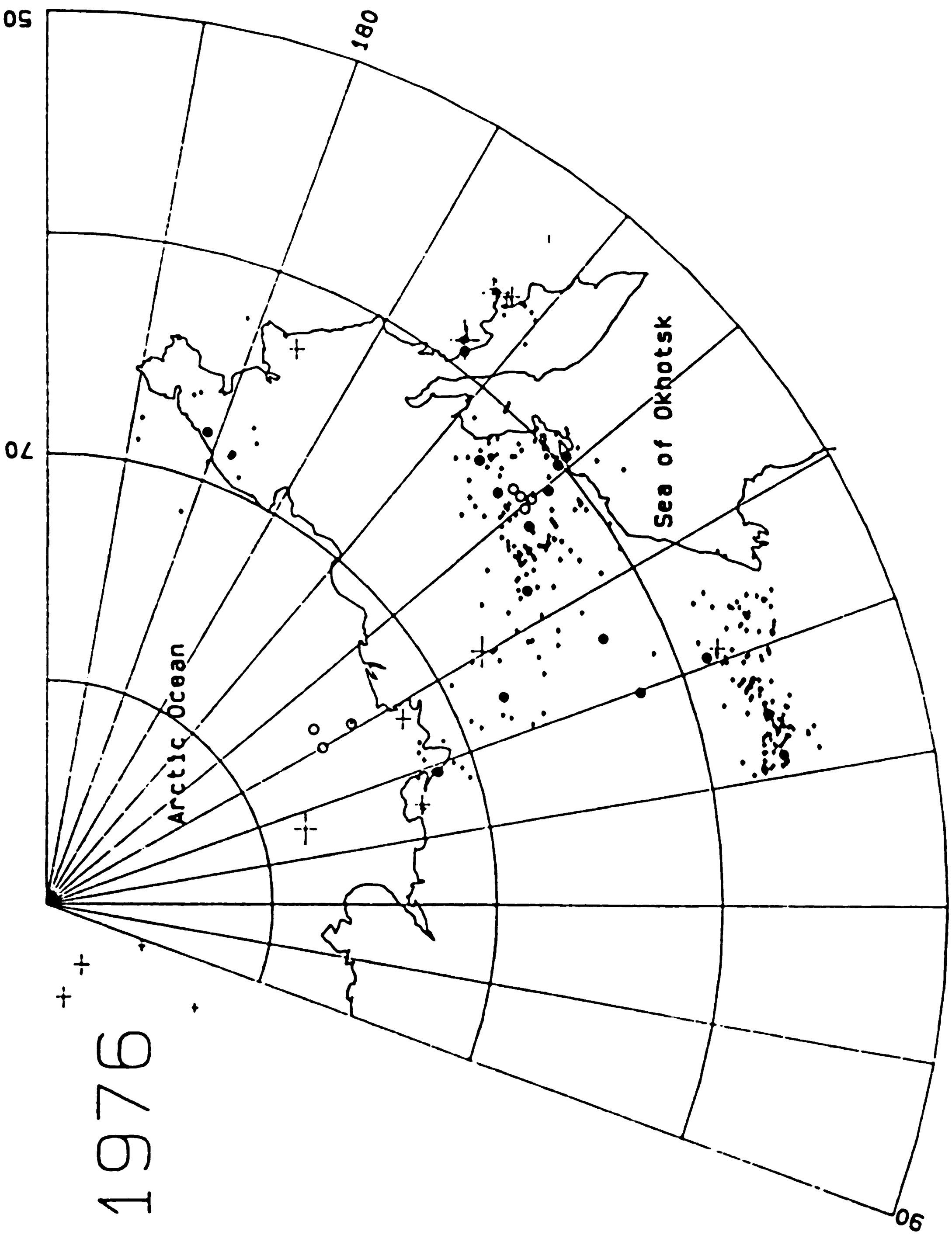

Figure 3-3

Table 3-1: FOCAL MECHANISMS AND SLIP VECTORS

Nr	Date	Lat N	Long E	h	m_b	Plane1	Plane2	Az	S
01	1964 08 25	78.15	126.65	05	6.2	338/54	184/58	068	2
						346/48	164/42	075	1
						338/34	184/58	068	3
						176/67	033/36	121	C
02	1960 12 03	76.64	131.24	28	5	070/60	175/65	086	4
						167/72	347/18	*	C
03	1969 04 07	76.55	130.86	11	5.4	314/48	157/45	067	1
						020/70	120/65	030	C
						016/40	160/50	070	3
						300/64	152/30	057	5
						011/38	268/80	178	6
						330/60	195/60	061	7
04	1983 06 10	75.53	122.75	25	5.4	144/72	029/39	118	1
						142/59	008/40	108	8
						150/70	034/40	060	C
05	1964 07 21	72.10	130.10	12	5.4	170/45	326/50	056	C
06	1980 02 01	73.06	122.59	22	5.4	168/50	274/71	005	C
	Alternate					011/75	274/72	005	C
07	1963 05 20	72.20	126.25	10	5.0	174/60	270/80	000	C
	Alternate					012/80	282/90	010	C
08	1975 08 12	70.76	127.12	16	5.1	164/72	286/30	018	C
	Alternate					167/70	067/70	159	C
09	1962 04 19	69.80	138.98	17	6.2	170/40	350/50	*	C
10	1984 11 22	68.53	140.88	26	5.4	087/75	341/45	066	9
						058/90	328/84	058	C
11	1976 01 21	67.70	140.00	18	5.0	090/45	338/70	068	C
						106/34	348/72	078	3
						088/58	180/87	091	6
12	1968 09 09	66.17	142.13	06	5.0	241/74	146/62	054	C
						284/68	174/50	084	3
						274/69	162/47	071	6

Plane 1 is the presumed fault plane
h: Focal depth
Az: Azimuth of the horizontal projection of the slip vector.
* Denotes azimuth indeterminate due to poor nodal plane constraint
S: Reference-
C This study
1 Jemsek et al., 1986
2 Sykes, 1967
3 Savostin and Karasik, 1981
4 Lazareva and Misharina, 1965
5 Chapman and Solomon, 1976
6 Koz'min, 1984
7 Conant, 1972
8 Dziewonski et al., 1983
9 Dziewonski et al., 1985

Network, and supplemented with ISC Bulletin (or ISS or Seismologicheskii Bulleten, Akademiya Nauk SSSR) reports. For this study, some seismograms from the Soviet seismograph network were also available and were used in both first motion analysis and body-wave modelling. Whenever possible, synthetic seismograms and Rayleigh wave radiation patterns were computed in order to better constrain source mechanism and focal depth.

One additional method used in the northern Cherskii Mountains was interpretation of LANDSAT multi-spectral scanner imagery. Surface mapping of the region using this data allowed the delineation of recent and past fault trends and precipitated the choice of fault plane when fault traces were identified in close proximity to epicenters.

Focal mechanism solutions from this chapter will be used in Chapter 4, in conjunction with solutions from McMullen (1985) and other investigators, to constrain the present-day plate geometry and pole(s) of rotation of the North American plate in northeast Siberia.

Laptev Sea

Four earthquakes (Table 3-1, nos. 1-4) span the transition zone between the Arctic mid-ocean ridge seismicity and the more dispersive pattern found on the continental shelf. Of these, the northernmost event (no. 1) occurs within the linear band of earthquakes bisecting the Eurasian Basin. Of the other three events, two (nos. 2 and 3) are on the extrapolation of the Arctic mid-ocean ridge into the continental shelf. The third event (no. 4) occurred southwest of the other shelf events, well off any linear extrapolation of the ridge axis.

The August 25, 1964 earthquake is one of the largest to occur in the oceanic part of the Arctic. Several investigators have presented solutions for this event, including a body-wave inversion by Jemsek et al. (1986) which indicates nearly pure normal faulting (Figure 3-4). The P-wave first motion distribution, which cannot constrain any eastward dipping plane, does not fit the west dipping nodal plane of the Jemsek et al. (1986) solution (Figure 3-4). Other solutions by Sykes (1967) and Savostin and Karasik (1981) have a more steeply west-dipping nodal plane which better fits the P-wave first motion data.

Body-wave modelling of the 1964 event proved to be unsuccessful using published solutions. P-waves from six stations were modelled using a focal mechanism constrained using first motions picked from seismograms, including Moscow, and supplemented with ISC Bulletin data (Figure 3-4). Fair matches were obtained using a simple trapezoidal source-time function and a focal depth of 13 km. A better match may be possible using a more complex source-time function as suggested by Jemsek et al. (1986).

Sykes (1967) and Solomon and Julian (1974) have noted that P-wave solutions of ridge crest events may have non-orthogonal nodal planes due to erroneous take-off angles resulting from lateral variability of the upper mantle structure beneath the ridge. Sykes' (1967) solution for the August, 1964, earthquake has nodal planes separated by 73^{o}, citing anomalous upper mantle structure below the rift as a cause of distorted raypaths. Since the velocity profile of this thermal regime is poorly known, it is not possible to correct for the anomalous take-off angle. Althoug there is a better fit of the P-wave data, the solution of Sykes (1967) cannot be preferred until new take-off angles can be calculated.

Lazareva and Misharina (1965) present a solution for a magnitude 5 earthquake (December 3, 1960; no. 2) located further into the shelf of the Laptev Sea. The solution, which is evidently constrained by using P-wave first motions from the ISS and BCIS, is presented by Lazareva and Misharina (1965)

Figure 3-4: Solutions and synthetics for the August 25, 1964 event. Filled circles are compressions, open circles are dilatations. Large circles are first motions picked from seismograms. Small circles are ISC Bulletin reported first motions. Lower hemisphere projection. Synthetics are for the solution presented in this study.

— — — Sykes, 1967

—·— Jemsek et al., 1986

——— This study

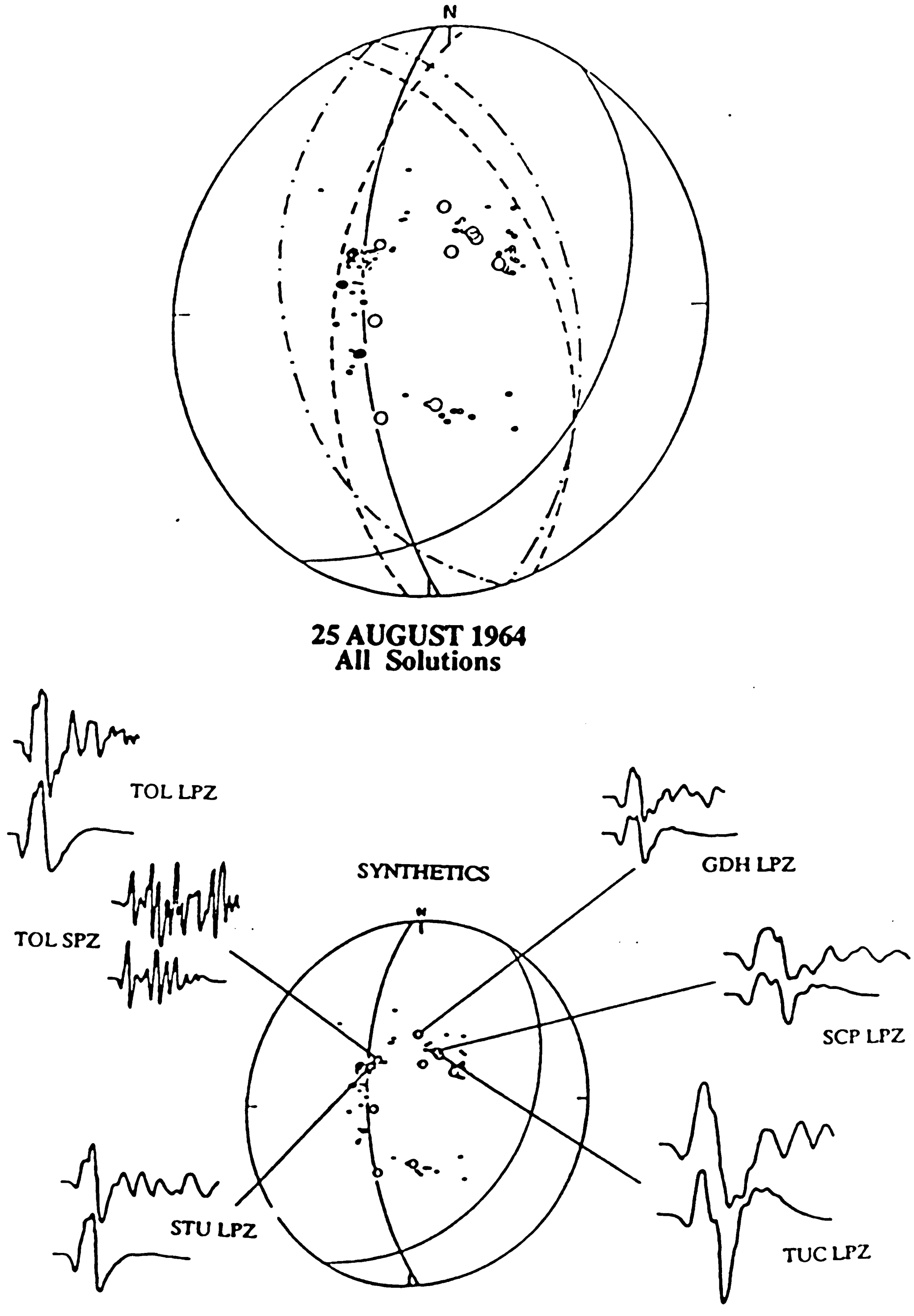
N
25 AUGUST 1964
All Solutions
TOL LPZ
SYNTHETICS
GDH LPZ
TOL SPZ
SCP LPZ
STU LPZ
TUC LPZ

Figure 3-4

with non-orthogonal nodal planes (Figure 3-5), as in the case of Sykes' (1967) solution for the August, 1964, earthquake discussed above. Lazareva and Misharina's (1965) solution has a large strike-slip component which is apparently an attempt to fit a compression reported at Matsishiro (MAT) (Figure 3-5). However, the residual at MAT is 5 minutes, suggesting an incorrect phase has been choosen as the initial P-wave. I present an alternative normal faulting solution, although the data are insufficient to constrain the east-dipping nodal plane. The better constrained strike of the west-dipping plane, presumed to be the fault plane, parallels the trend of the Arctic mid-ocean ridge.

Event 3 occurred on April 7, 1969, and has been studied by numerous workers (e. g., Conant, 1972; Chapman and Solomon, 1976; Savostin and Karasik, 1981; Koz'min, 1984; Jemsek et al., 1986). The solutions range from strike-slip to normal faulting. A body-wave inversion is presented in Jemsek et al. (1986), who note that the solution is extremely uncertain due to waveform complexity and poor station distribution. Like the August, 1964, event, the body-wave inversion does not fit the P-wave first motion data (Figure 3-6).

Short- and long-period body wave synthetic seismograms were calculated at three WWSSN stations, limited to the western quadrants, using a best fit P-wave source mechanism (Figure 3-7). There is a good fit, particularly in the short-period waveforms, suggesting that the P-wave solution and focal depth (12 km) are plausible models for the initial rupture. However, the poor azimuthal distribution of the stations prevent tight control on the slip. The decreasing fit of long-period records, and the differing body-wave inversion solution, may indicate a complex rupture process.

Figure 3-5: Solutions for the December 3, 1960, event on the Arctic mid-ocean ridge. Data are from the ISS and BCIS. Double triangle represents conflicting polarities reported in ISS and BCIS. Small "M" denotes position of MAT, which reported a compression with a residual of 5 minutes.
— — — Lazareva and Misharina, 1965
——— This study

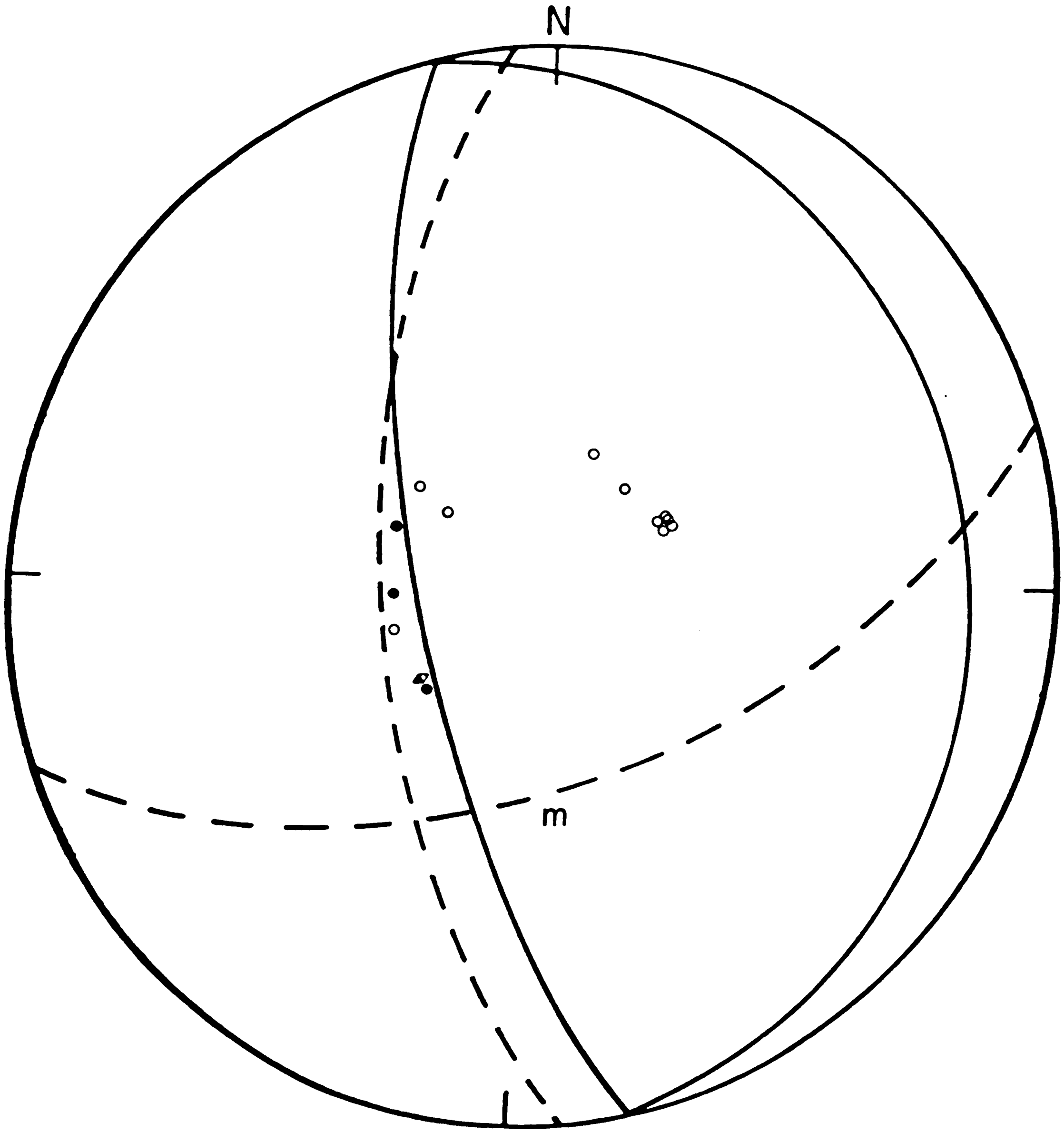

3 DECEMBER 1960
All Solutions

Figure 3-5

Figure 3-6: Solutions for the April 7, 1969, event. Data are the same on each plot. Conventions as in Figure 3-4.

- • • • • Conant, 1972
- — — Chapman and Solomon, 1976
- • — • — Jemsek et al., 1986
- — · · — Savostin and Karasik, 1981
- - - - - Koz'min, 1984
- ——— This study

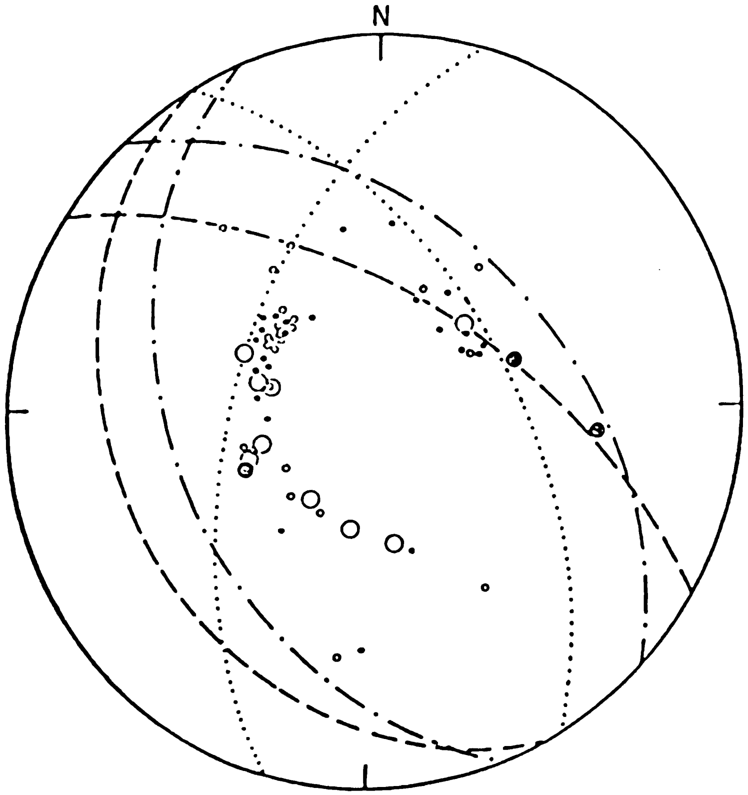

7 APRIL 1969
Conant, 1972
Chapman and Solomon, 1976
Jemsok et al., 1986

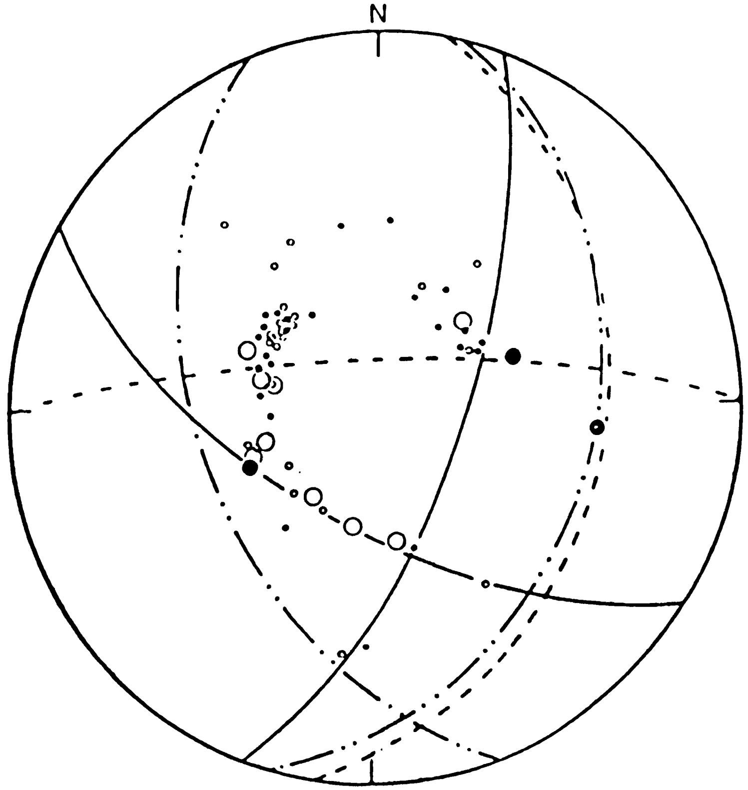

7 APRIL 1969
Savostin and Karasik, 1981
Koz'min, 1984
This study

Figure 3-6

Figure 3-7: Synthetics for the April 7, 1969, event.

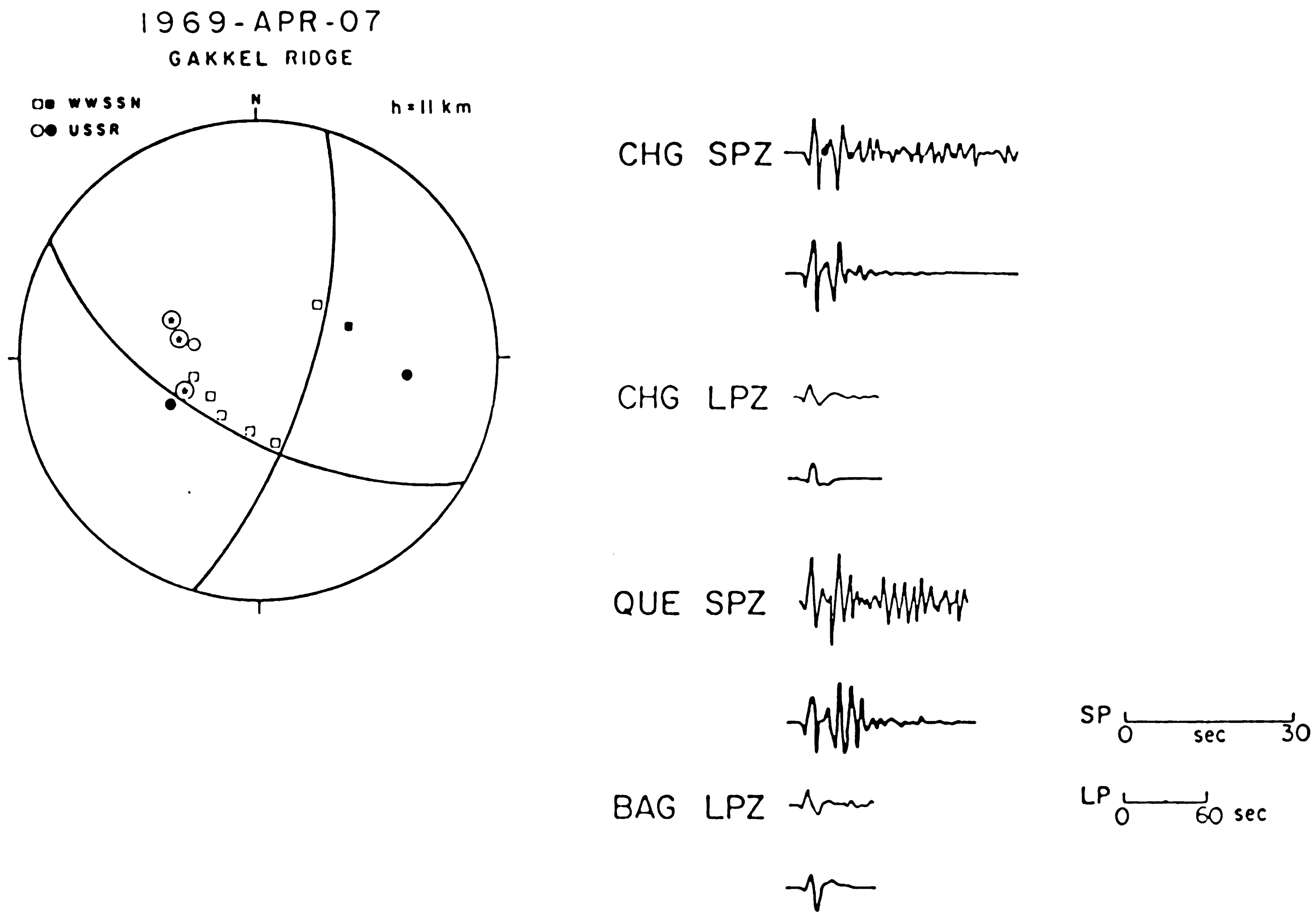

1969-APR-07
GAKKEL RIDGE
WWSSN
USSR
N
h=11 km
CHG SPZ
CHG LPZ
QUE SPZ
BAG LPZ
SP 0 sec 30
LP 0 60 sec

Figure 3-7

Synthetic seismograms were also calculated at four Soviet stations for which records were available. The Soviet stations do not operate a standardized instrument, and therefore, the instrument response of each station varied. All the instruments are quasi-broadband, and response curves and galvanometer periods were available (Prilozhenie k Seismologicheskomu Bulletenu). The resulting waveform matches (Figure 3-8; note time increases right to left) were very encouraging. In every case, the general waveform shape was similar; only the wavelength seemed to vary. This may be due to use of an incorrect instrument response in the calculation, since Soviet station equipment changes may not have been reported immediately, or because of pooly calibrated equipment. The general agreement, however, is consistent with the WWSSN synthetics and suggest the P-wave mechanism in Table 3-1 is a well constrained solution.

The last of the outer shelf events included in this study occurred on June 10, 1983. Centroid moment tensor and body-wave inversion solutions (Dziewonski et al., 1983; Jemsek et al., 1986) both suggest normal faulting with a significant strike-slip component, very simiilar to the P-wave solution of the April, 1969, earthquake. The focal depths of 12 km and 22 km (Dziewonski et al., 1983 and Jemsek et al., 1986, respectively) differ dramatically. Jemsek attributes the difference to the data used, noting that WWSSN data are not low-pass filtered as are the Global Digital Seismograph Network (GDSN) data used by Dziewonski et al. (1983). Jemsek et al. (1986) therefore conclude that the WWSSN data are better at resolving "small" events. Only P-wave first motion data reported in the ISC Bulletin and Seismological Bulletin of the USSR are used to constrain the mechanism presented in this study (Table 3-1). These

P-wave data are better fit to the moment tensor solutions of Dziewonski et al. (1983) and Jemsek et al. (1986) than had been observed for events 1 and 3.

Lena River Delta

Earthquakes around the Lena River Delta are characterized by a decrease in magnitude relative to those on the shelf to the north. I have examined three earthquakes (nos. 6, 7 and 8) on the southern extent of Lena River delta (Figure 3-2), and one (no. 5) to the east in Bour Khaya Bay. The epicentral trend of the three earthquakes on the delta follow the hinge line of the Siberian platform (Andreev, 1983), suggesting there may be some structural control on their occurrence.

On July 21, 1964, a magnitude 5.4 earthquake (no. 5) occurred in Bour Khaya Bay at the southern extent of Laptev Sea shelf seismicity. Although the event lies on a linear extrapolation of the Arctic mid-ocean ridge axis, epicenters to the north are distributed in a broad pattern extending from the New Siberian Islands to west of the Lena River delta. Kogan (1974) determined the upper crustal structure in the Bour Khaya Bay area using seismic refraction data. Through these studies Kogan (1974) delineated a low velocity zone which continued to approximately 20 km depth and which is flanked by "normal" continental crust and shelf sediments. The identification of this low velocity zone beneath the projection of the ridge axis is consistent with Sykes' (1967) and Lazareva and Misharina's (1965) use of non-orthogonal nodal planes on other Laptev Sea shelf events (nos. 1 and 2).

A number of P-wave first motions were read from WWSSN and Canadian Network seismograms in an attempt to constrain the nodal planes. All of these were dilitational, however, as were 70 percent of the ISC and BCIS reported first motions (Figure 3-10). The data was consistent with a normal

Figure 3-8: Synthetics for the April 7, 1969, event calculated for Soviet seismograph stations.

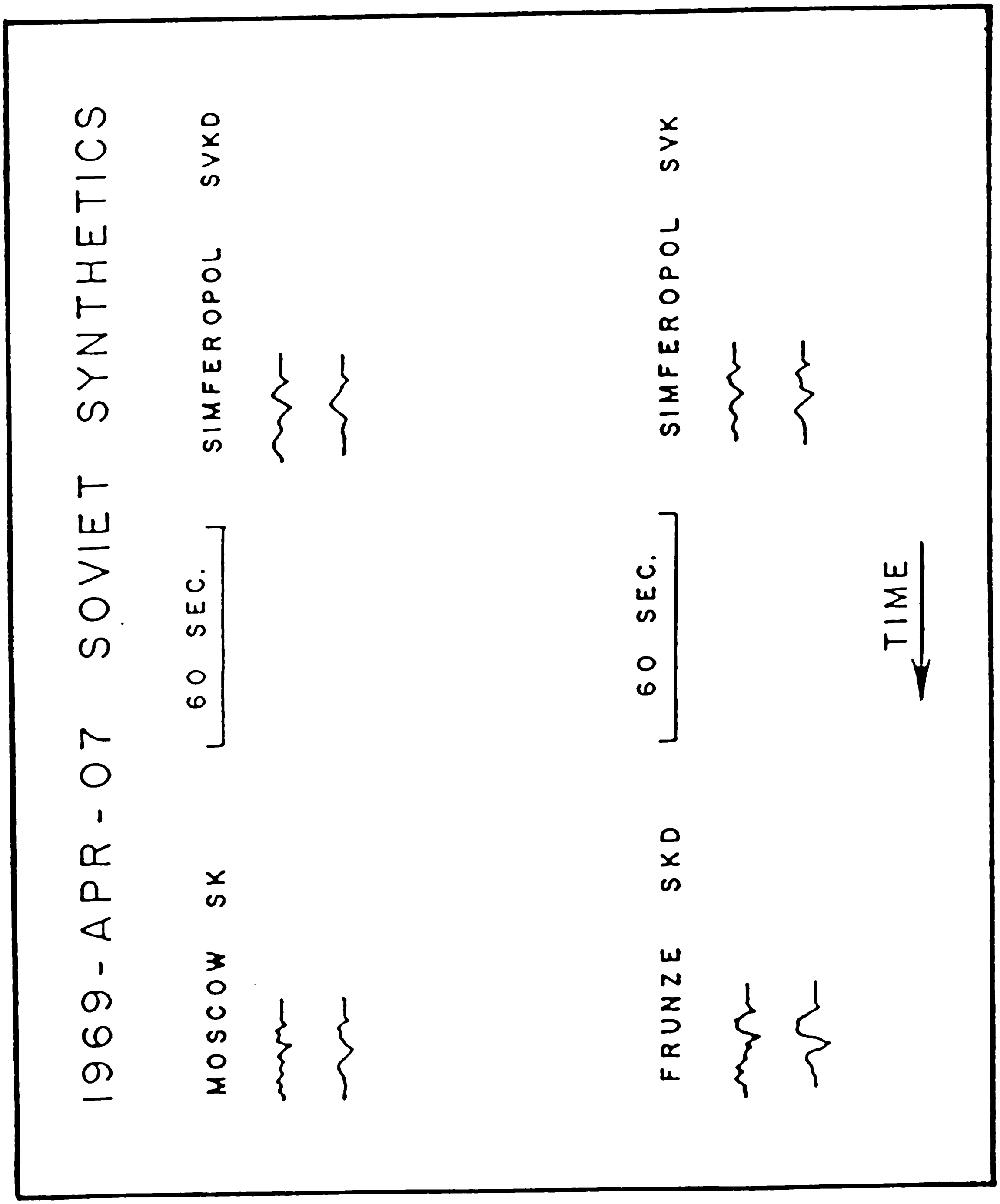
1969-APR-07 SOVIET SYNTHETICS
MOSCOW SK
60 SEC.
SIMFEROPOL SVKD
FRUNZE SKD
60 SEC.
SIMFEROPOL SVK
TIME

Figure 3-8

Figure 3-9: Solutions for the June 10, 1983, event. Data are from the Seismologicheskii Bulleten SSSR and the ISC Bulletin. Conventions as in Figure 3-4.

· — · — Dziewonski et al., 1983

— — — Jemsek et al., 1986

——— This study

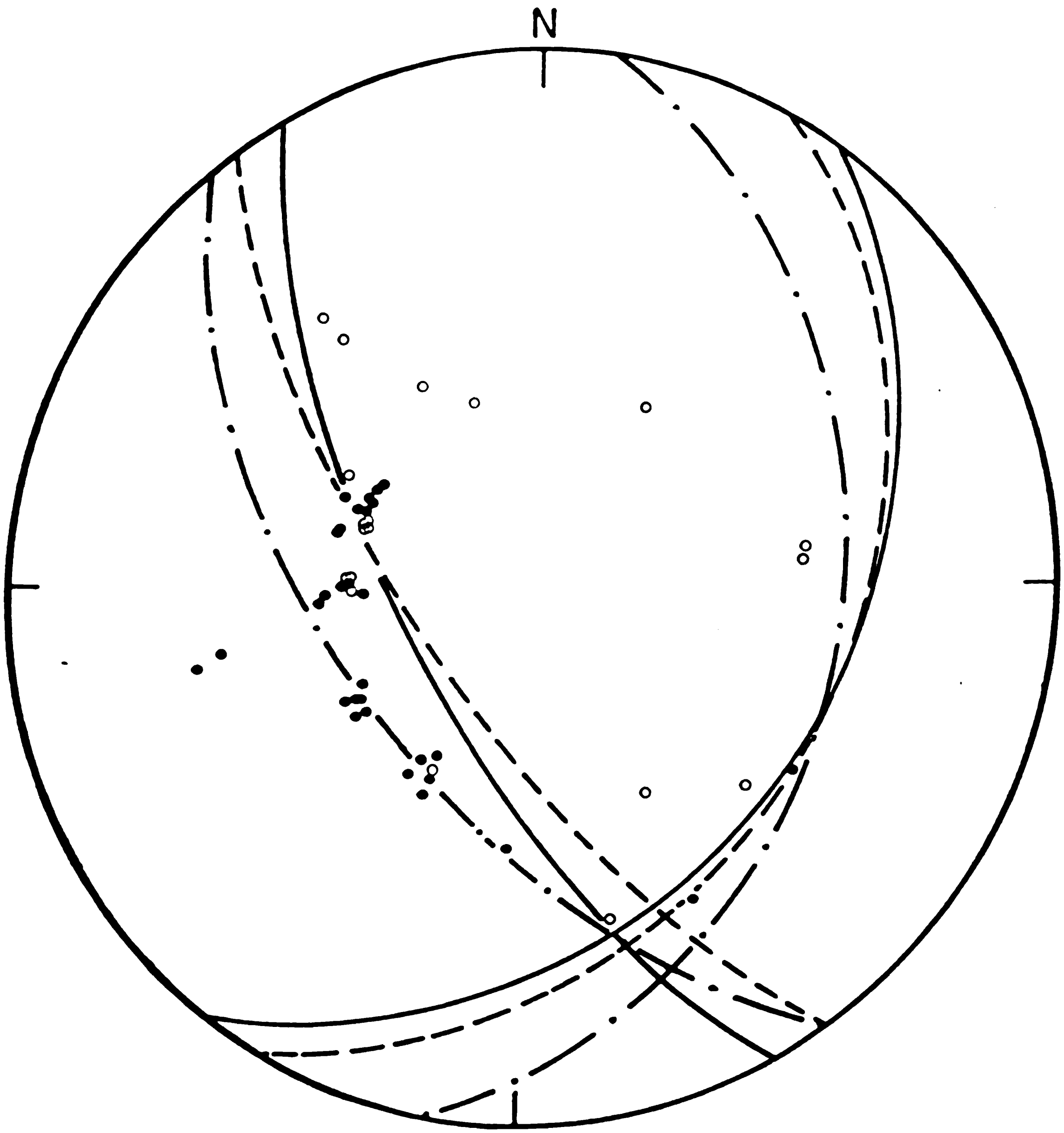

10 JUNE 1983
All Solutions

Figure 3-9

fault, although nodal plane orientations were completely unconstrained. However, the Rayleigh wave radiation pattern was quite good and indicated a nearly pure normal faulting mechanism with north-northwest striking nodal planes (Figure 3-10).

Using the crustal model of Kogan (1974), short-period synthetic seismograms were computed at six stations distributed in all but the southeast quadrant of the focal sphere. The match between the synthetic and observed seismograms are very good through the first 15 to 20 seconds of waveform (Figure 3-11). The depth is constrained at 12 km. Since the P-wave and Raleigh wave data did not constrain the amount of slip for the mechanism, variations of the preferred solution were calculated using a variety of slip directions. As shown in Figure 3-12, the variations drastically affect the match of the synthetic waveform, suggesting the preferred solution is quite robust.

Earthquakes in 1980, 1963 and 1975 (nos. 6, 7 and 8, respectively) occurred along the hinge line of the Siberian platform south of the Lena River delta. Due to the smaller magnitudes of events 7 and 8 (M_b 5.0 and 5.1, respectively), only P-wave first motion studies could be conducted. The February 1, 1980, event (no. 6) had magnitudes of 5.4 (M_b) and 5.3 (M_s) and was conducive to Rayleigh wave analysis as well. The lack of a second tightly constrained nodal plane seems to make the solutions for earthquakes 6 through 8 non-unique. For events 6 and 7, only the east striking nodal plane is constrained; the north striking nodal plane could dip either east or west (Figure 3-13 and 3-14). Examination of the Rayleigh wave radiation pattern for event 6 (Figure 3-13) suggests a west dipping nodal plane would be the preferred solution. Event 8 (August, 1975) differs in that the north striking nodal plane is relatively well constrained, and the second nodal plane may dip north, east

Figure 3-10: P-wave solution and Rayleigh wave radiation pattern for the July 21, 1964, earthquake in Bour Khaya Bay. Squares are data points used in Rayleigh wave analysis. Solid line on Rayleigh wave pattern corresponds to theoretical radiation based on the P-wave solution. First motion conventions as in Figure 3-4.

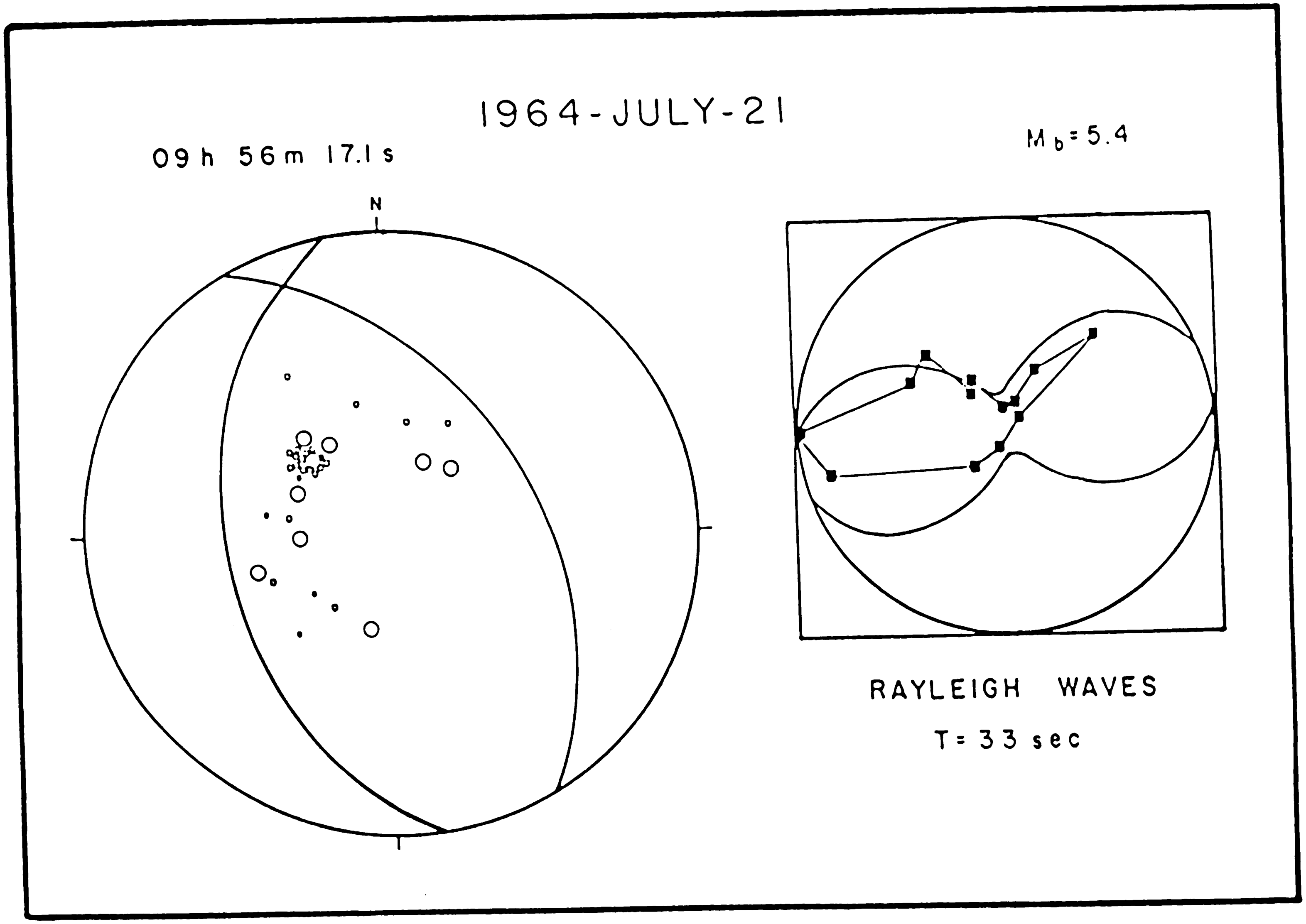

Figure 3-10

Figure 3-11: Synthetics for the July 21, 1964, event.

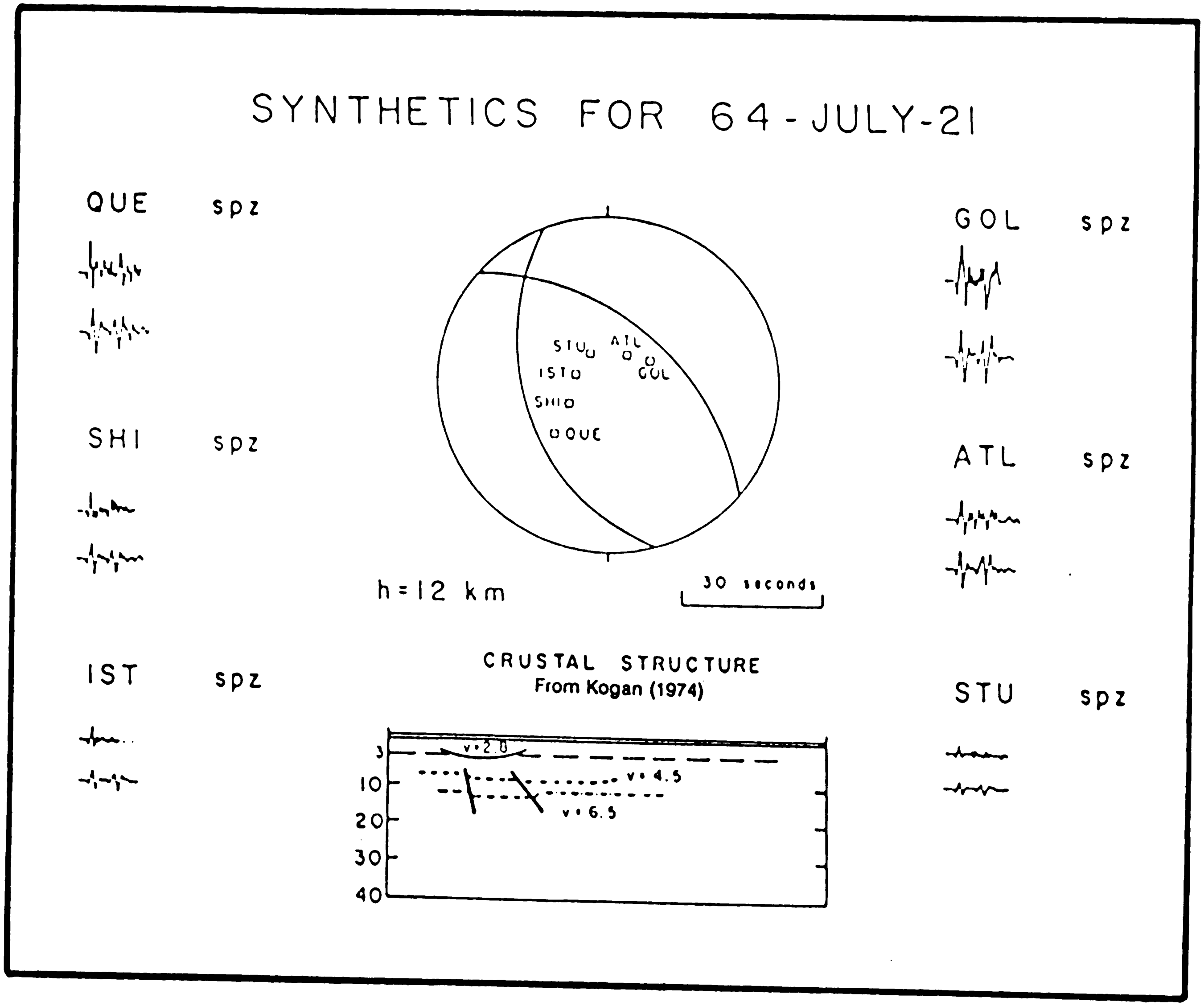
SYNTHETICS FOR 64-JULY-21
QUE spz
SHI spz
IST spz
GOL spz
ATL spz
STU spz
STU
ATL
IST
GOL
SHI
QUE
h=12 km
30 seconds
CRUSTAL STRUCTURE
From Kogan (1974)
v=2.8
v=4.5
v=6.5
3
10
20
30
40

Figure 3-11

Figure 3-12: Waveform dependence on focal mechanism solution. Small variations of the focal mechanism produced pronounced change in waveform character.

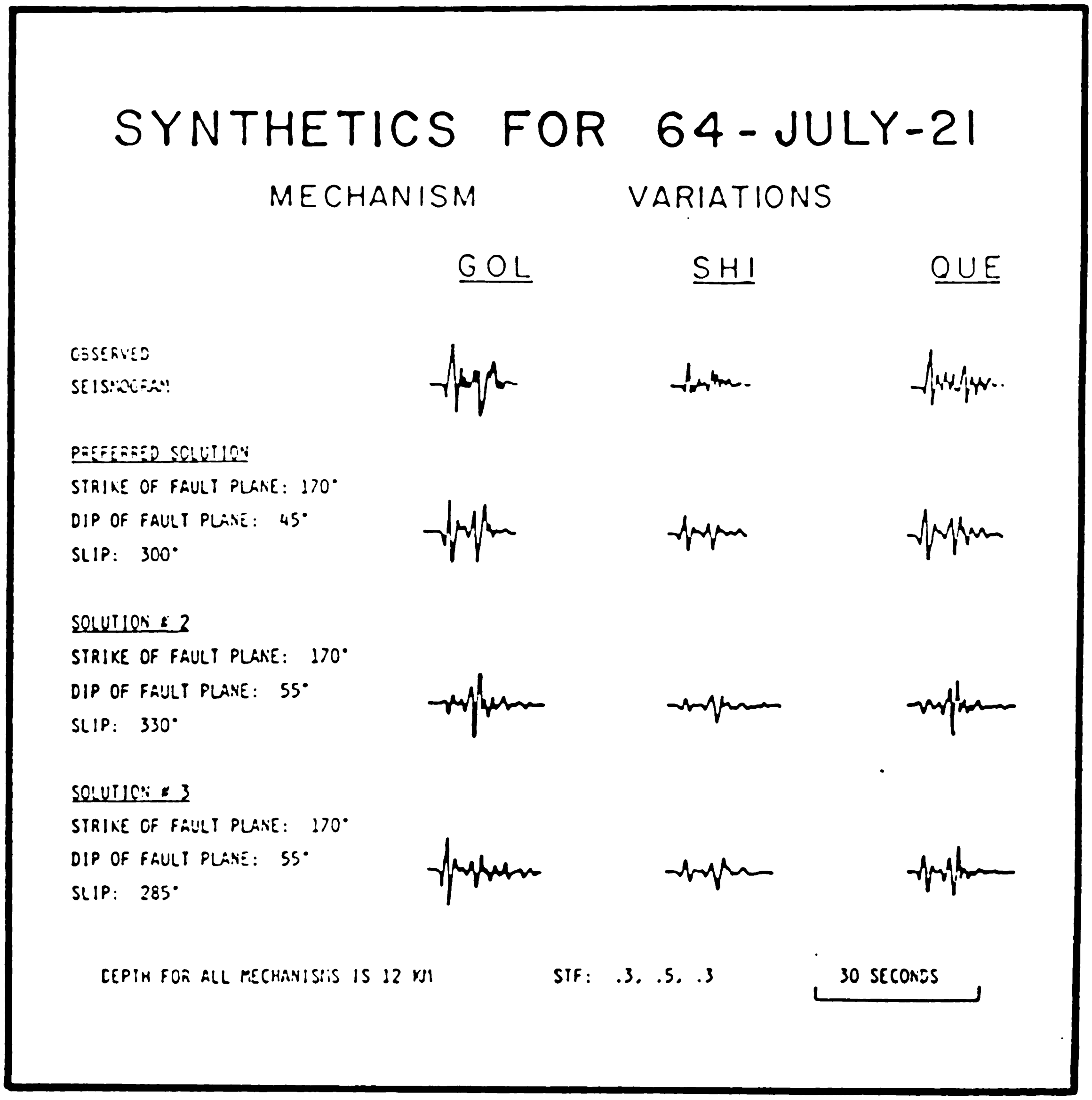
SYNTHETICS FOR 64-JULY-21
MECHANISM VARIATIONS
GOL
SHI
QUE
OBSERVED SEISMOGRAM
PREFERRED SOLUTION
STRIKE OF FAULT PLANE: 170°
DIP OF FAULT PLANE: 45°
SLIP: 300°
SOLUTION # 2
STRIKE OF FAULT PLANE: 170°
DIP OF FAULT PLANE: 55°
SLIP: 330°
SOLUTION # 3
STRIKE OF FAULT PLANE: 170°
DIP OF FAULT PLANE: 55°
SLIP: 285°
DEPTH FOR ALL MECHANISMS IS 12 KM
STF: .3, .5, .3
30 SECONDS

Figure 3-12

Figure 3-13: P-wave solution and Rayleigh wave radiation pattern for the February 1, 1980, earthquake south of the Lena River delta. Dashed line represents alternative solution for the P-wave mechanism. Conventions as in Figure 3-4 and Figure 3-10.

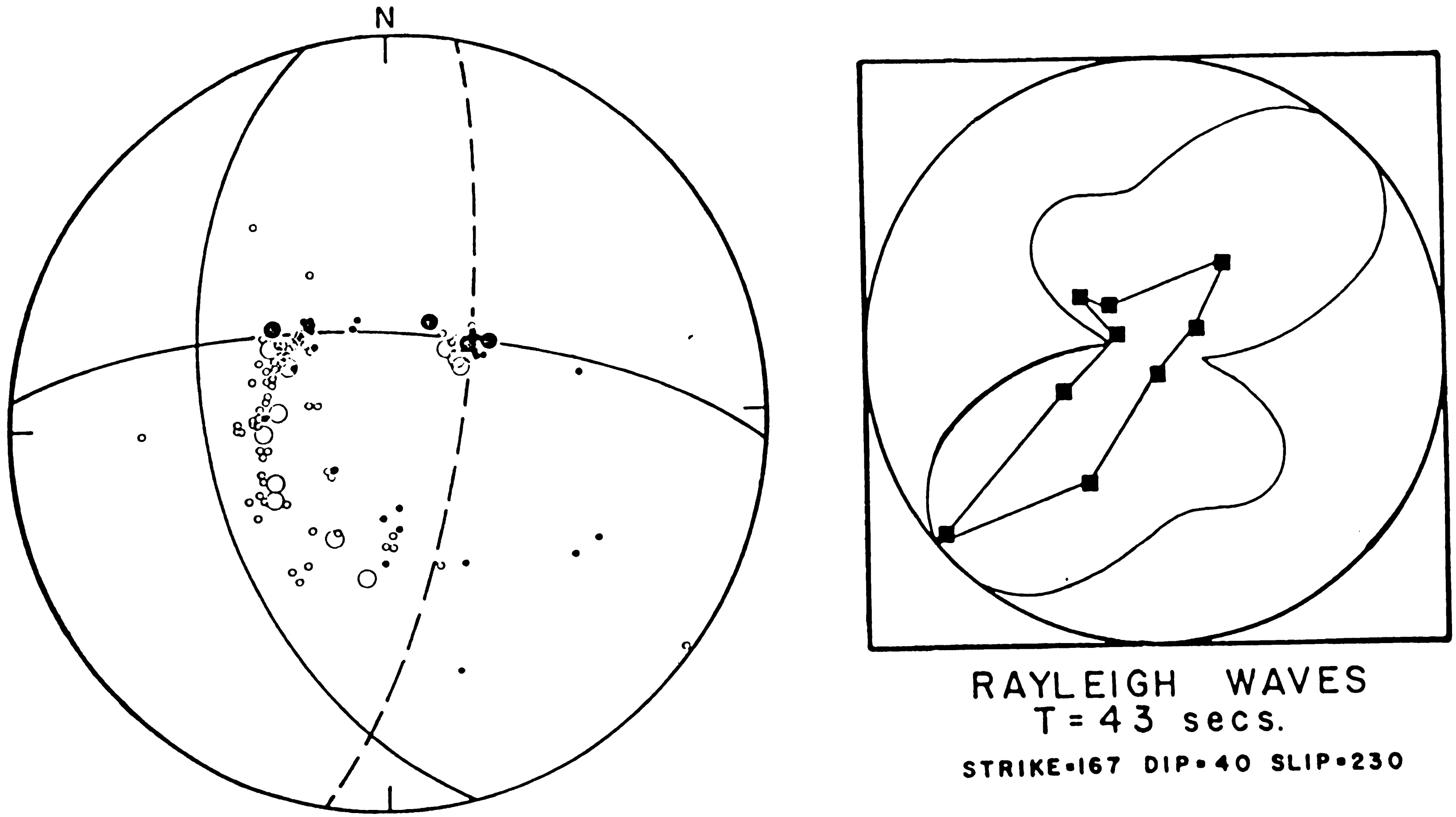

1 FEBRUARY 1980

Figure 3-13

Figure 3-14: P-wave solutions for the May 5, 1963, and August 12, 1975, earthquakes south of the Lena River delta. Dashed lines represent alternative solutions. Conventions as in Figure 3-4.

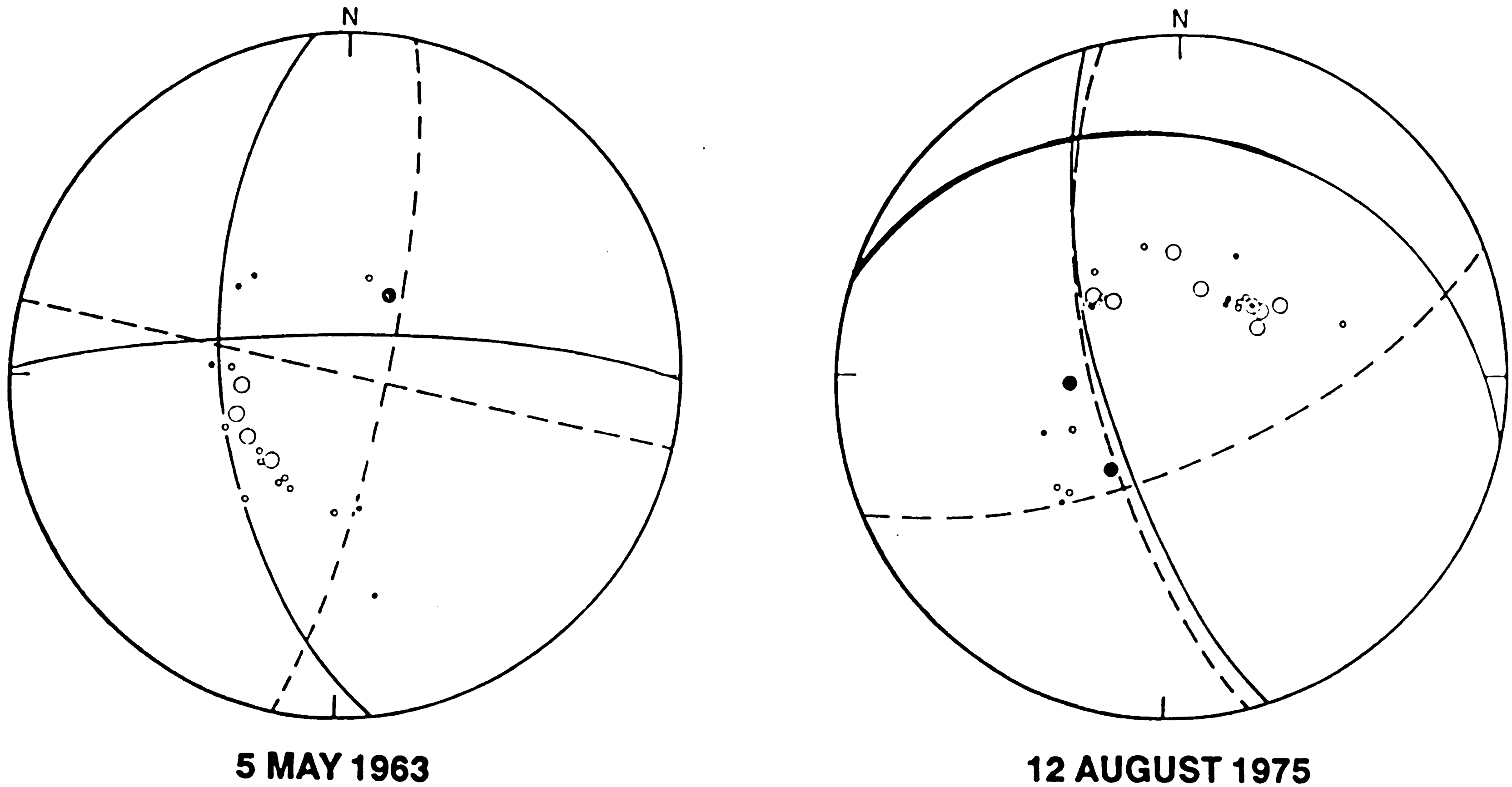

Figure 3-14

or south (Figure 3-14). For each of these earthquakes, either mechanism can be chosen without dramatically affecting the azimuth of the horizontal projection of the slip vector (Table 3-1).

There is a reason to select preferred solutions to events 6 through 8 despite the poor constraint offered by P-wave first motions. For each event, one solution has a north-northwest trending, west-dipping nodal plane. This is, in fact, the preferred solution for the February, 1980, earthquake based upon the distribution of Rayleigh wave energy. The north-northwest orientation is also nearly parallel to the strike of the hinge line of the Siberian platform (335^{o}). Therefore, not only can a preferred solution be offered, but the nodal plane paralleling the hinge line may be chosen as the fault plane for each of these events.

Northern Cherskii Mountains

The seismicity of the northern Cherskii Mountains trends southeast in a 400 km wide band toward the Sea of Okhotsk. As discussed earlier, this distribution may be caused by poor epicentral locations. The larger earthquakes (M_b > 4.5) define a linear trend along the western margin of the Cherskii Mountains which is more likely to represent the position of the North American plate boundary in northeast Siberia. Solutions are presented for four earthquakes (nos. 9-12) within this structurally complex region, which has commonly been regarded as the onshore extension of the Arctic mid-ocean ridge (Grachev et al., 1970; Churkin, 1972; Chapman and Solomon, 1976; Savostin and Karasik, 1981; Grachev, 1982). All of the solutions have compressional mechanisms which are difficult to explain in a rifting regime.

A magnitude 6.2 (M_b) earthquake on April 19, 1962, (no. 9) is the largest of the Cherskii Mountain events chosen for study. Nearly all of the observed and ISS reported first motions are compressions (Figure 3-15). The lack of dilitations and nodal picks therefore prevents any constraint on the nodal plane orientations. Compressions fill the northwest and northeast quandrants of the focal sphere, and would allow only slight, if any, strike-slip component in any solution.

An earthquake on November 22, 1984 was the most recent large ($M_b > 5.0$) event in the northern Cherskii Mountains. A Centroid-Moment Tensor solution by Dziewonski et al. (1985) indicates a thrust mechanism with a shallow-dipping, northeast trending P-axis (Table 3-1). As was noted for Laptev Sea earthquakes (nos. 1, 3, 4), P-wave first-motion distribution is inconsistent with the solution obtained through moment tensor inversion. ISC reported first-motions are more consistent with a nearly pure strike-slip solution (Figure 3-16, Table 3-1) with north-northwest and east-northeast trending nodal planes. Either solution is consistent with fault orientations reported in Zonenshain et al. (1978) and Savostin and Karasik (1981), and with fault azimuths mapped from LANDSAT images (Path 126, Row 13 and Path 128, Row 12). Therefore, either or both (Appendix 3A) of the solutions may be allowed since both are consistent with observed geology. The possible reasons for discrepancies between moment tensor inversions and P-wave first-motions, first discussed by Hinzen (1986), are addressed in Appendix 3A.

A small (M_b 5.0) earthquake on January 21, 1976, has been studied by Savostin and Karasik (1981) and Koz'min (1984), who utilized Soviet local network data and ISC Bulletin reported first motions. I have supplemented these solutions by picking P-wave first motions from WWSSN records. All three solutions are fairly consistent with the P-wave first motion data, and do not vary more than 25^{o} in the azimuth of their slip vectors. The local

Figure 3-15: P-wave solution for the April 19, 1962, event. Conventions as in Figure 3-4.

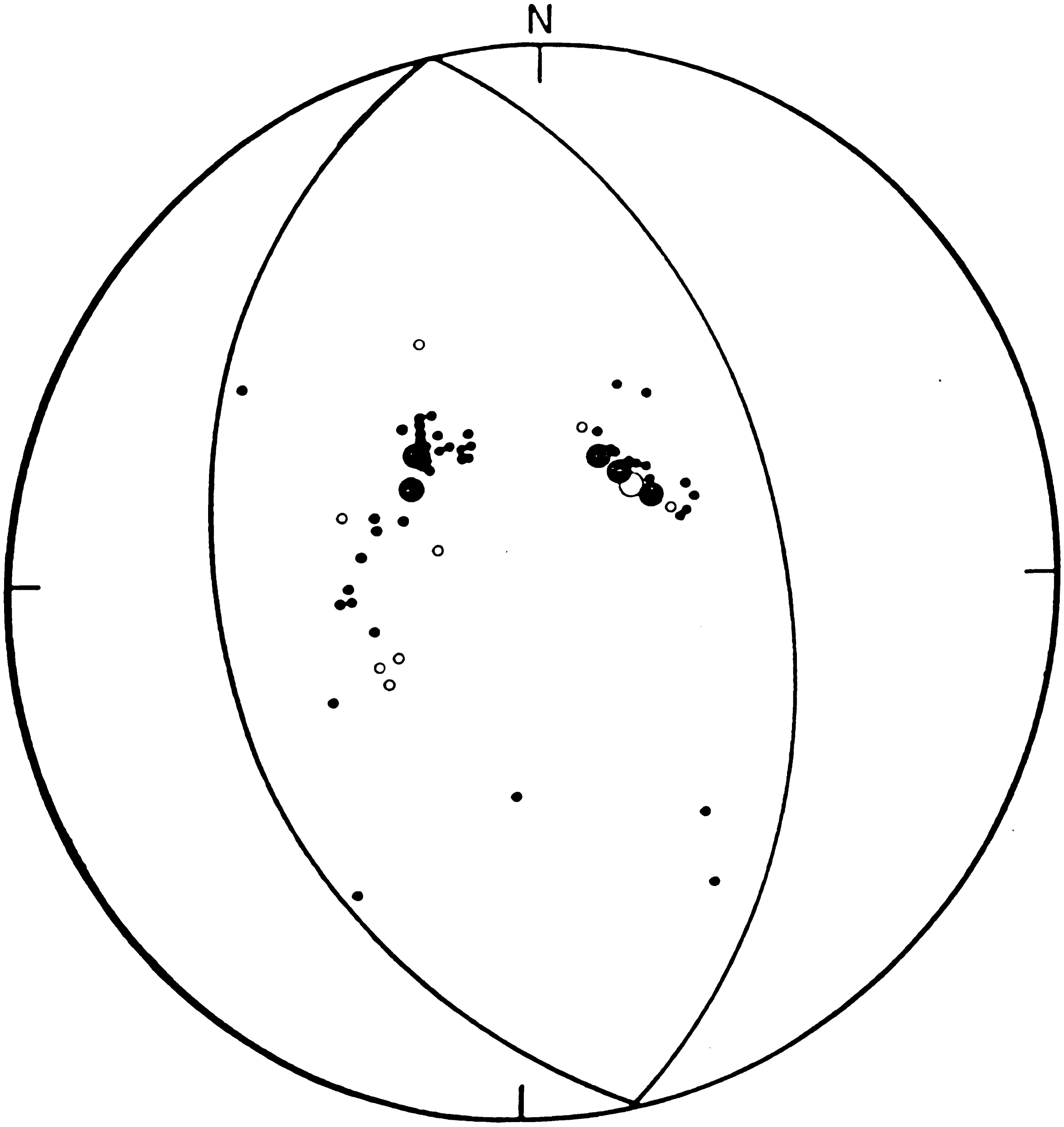

19 APRIL 1962

Figure 3-15

Figure 3-16: Solutions for the November 22, 1984, event. Conventions as in Figure 3-4.
— — — Dziewonski et al., 1985
——— This study

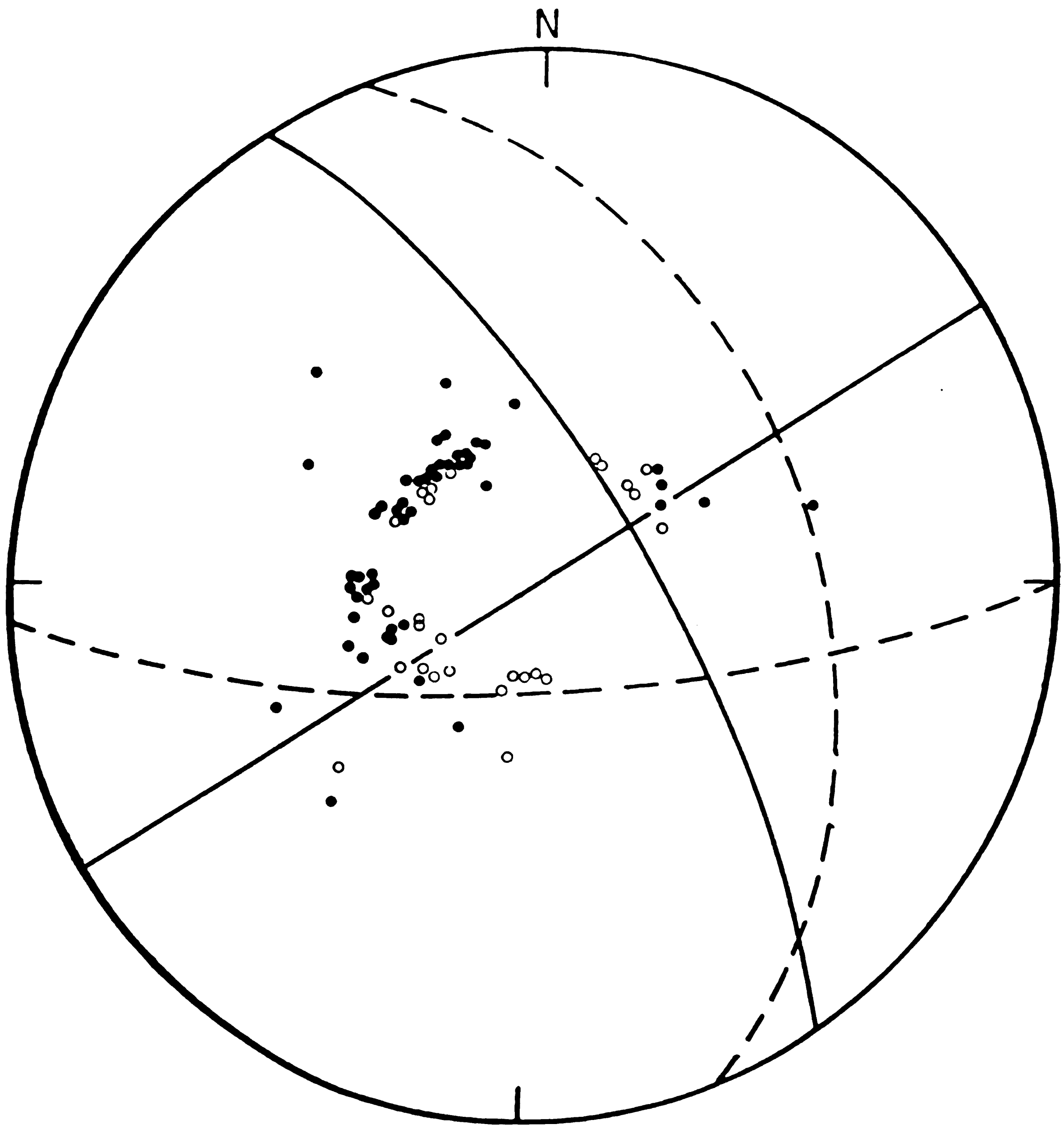

22 NOVEMBER 1984
All Solutions

Figure 3-16

network data of Koz'min (1984) also fit the solution constrained in this study (Figure 3-17). The mechanism indicates thrusting with some strike-slip component. The 090^{o} strike of one of the nodal planes is consistent with the general trend of azimuths (070^{o} to 085^{o}; Table 3-2) of large faults identified on LANDSAT imagery (Path 126, Row 13 and Path 128, Row 12) or reported in the epicentral region (Zonenshain et al., 1978; Savostin and Karasik, 1981), and is presumed to be the strike of the fault plane.

The final event examined in the northern Cherskii Mountains occurred on September 9, 1968. This earthquake has also been examined by Savostin and Karasik (1981) and Koz'min (1984). Both studies, however, determined northwest trending thrust fault mechanisms which do not fit P-wave first motion data which have been read from seismograms (Figure 3-18).

The solution presented has a large strike-slip component along a 241^{o} trending nodal plane, which is presumed to be the fault plane. This plane, again, trends sub-parallel to the azimuth of faults mapped (Table 3-2; Zonenshain et al., 1978; Savostin and Karasik, 1981) in the epicentral region. Body-wave modelling of short-period seismograms (Figure 3-19) was very sensitive to the slip angle of the solution, and best fit at a focal depth of about 5 km.

TECTONIC IMPLICATIONS

The seismicity from the Arctic mid-ocean ridge to the Cherskii Mountains exhibits varying characteristics along its trend. The narrow band of epicenters along the Arctic mid-ocean ridge gives way to broadly distributed seismicity within the Laptev Sea. A small gap marks the transition from extensional mechanisms on the Laptev Sea shelf to compression in the northern Cherskii

Figure 3-17: Solutions for the January 21, 1976, event. Conventions as in Figure 3-4.

— — — Savostin and Karasik, 1981

• • • • • Koz'min, 1984

——— This study

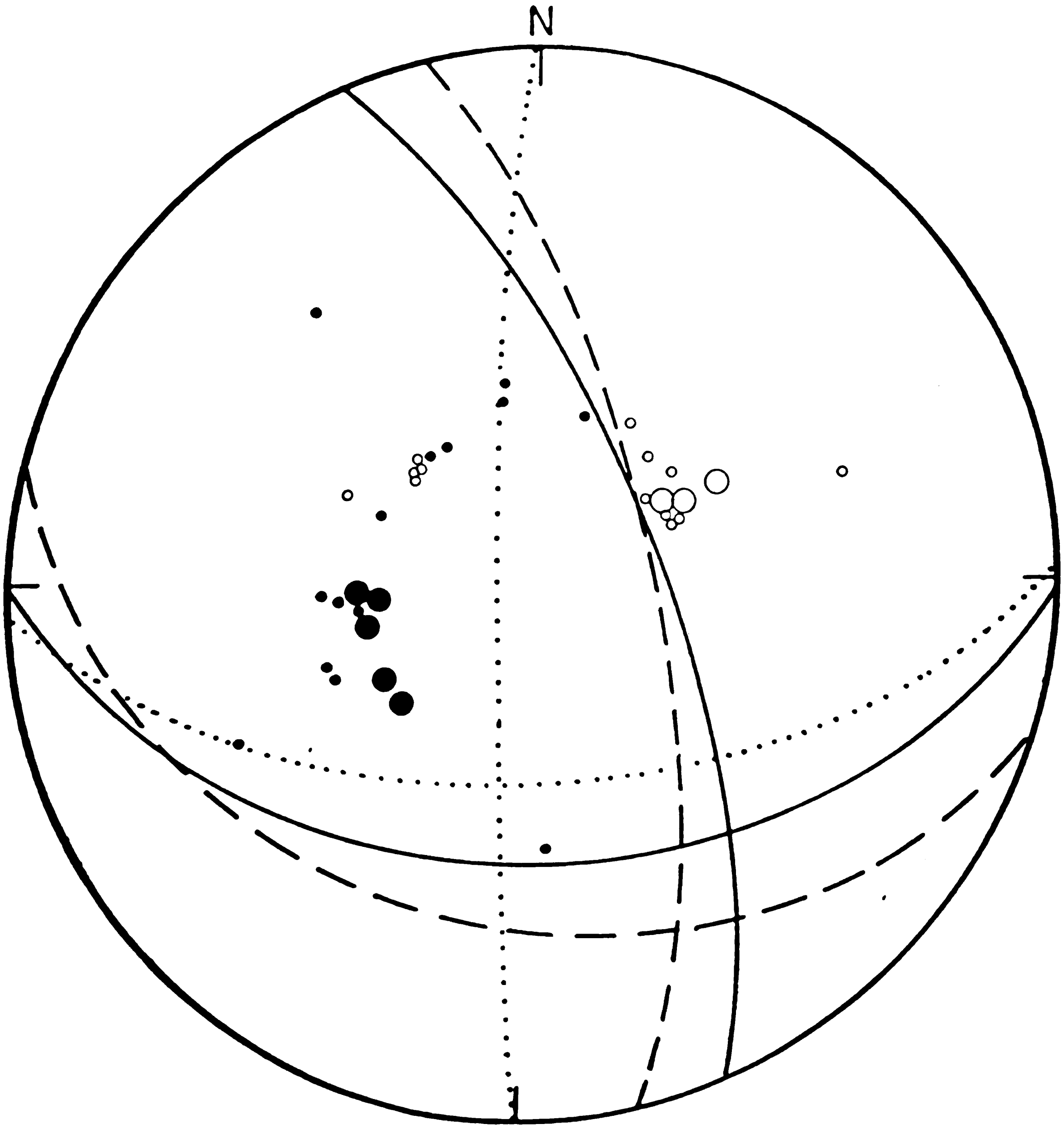

21 JANUARY 1976

Figure 3-17

Table 3-2

FAULT PARAMETERS FROM LITERATURE (DATA FROM ZONENSHAIN, 1978 AND SAVOSTIN AND KARASIK, 1981)

LOCATION		ORIENTATION
67.00 N	136.00 E	65.0
67.41 N	138.50 E	68.0
67.66 N	140.25 E	71.0
67.97 N	141.00 E	78.0
68.34 N	137.50 E	59.0
64.05 N	146.00 E	112.0
64.45 N	144.00 E	112.5
63.32 N	144.00 E	113.0
66.09 N	144.00 E	98.0
65.69 N	146.59 E	128.0
64.81 N	147.00 E	115.0
64.69 N	147.50 E	120.0
64.42 N	148.00 E	125.0
64.00 N	149.25 E	131.0

MAJOR FAULTS IDENTIFIED IN THIS STUDY

IMAGE NUMBER	APPROXIMATE LOCATION		ORIENTATION
P115 R17	61.0 N	152.0 E	79.00
	61.5 N	152.5 E	110.00
P116 R16	62.5 N	151.0 E	136.00
	63.3 N	152.0 E	126.00
P122 R14	61.5 N	146.5 E	107.00
	61.5 N	147.0 E	98.00
	65.5 N	145.0 E	158.00*
P126 R13	67.5 N	142.0 E	85.00
P128 R12	67.7 N	140.0 E	70.00

Figure 3-18: Solutions for the September 9, 1968, event. Conventions as in Figure 3-4.

— — — Savostin and Karasik, 1981

. . . . . . Koz'min, 1984

——— This study

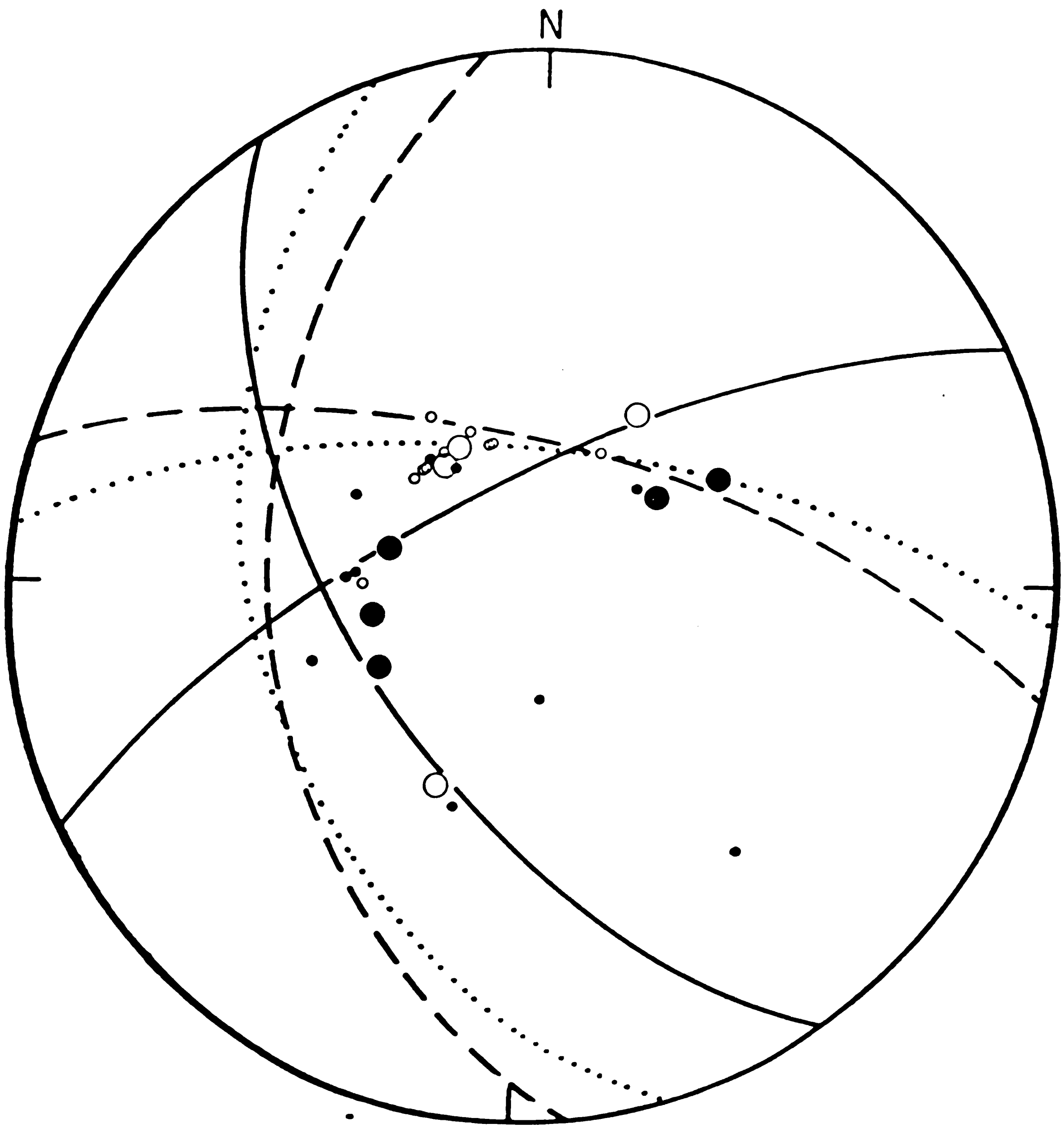

09 SEPTEMBER 1968

Figure 3-18

Figure 3-19: Synthetics for the September 9, 1968, event.

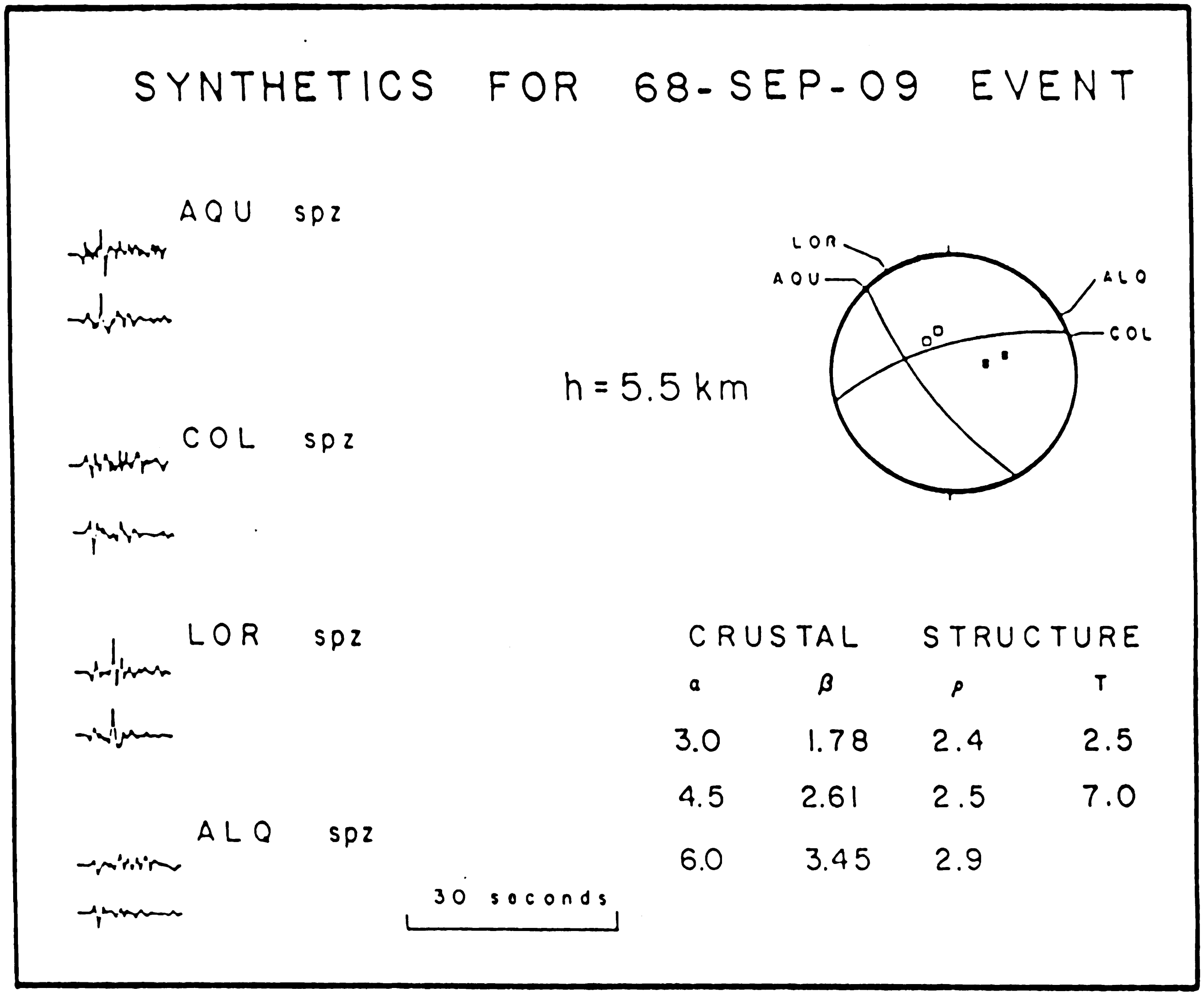
SYNTHETICS FOR 68-SEP-09 EVENT
AQU spz
COL spz
LOR spz
ALQ spz
h = 5.5 km
LOR
AQU
ALQ
COL
CRUSTAL STRUCTURE
α β ρ T
3.0 1.78 2.4 2.5
4.5 2.61 2.5 7.0
6.0 3.45 2.9
30 seconds

Figure 3-19

Mountains. Focal mechanism solutions are consistent with distinguishing three regions of differing seismic character along the plate boundary. These solutions, especially when combined with other geological and geophysical data, are important in understanding the tectonics of each segment of the plate boundary. There is possibly a unique transition of earthquake slip along the boundary due to the proximity of the proposed North America - Eurasia pole of rotation with the plate boundary (e.g., DeMets et al., in press). The discussion of the tectonic implications of such a pole position, in light of the data presented here, are discussed in Chapter 4. Here I discuss only the tectonic implications of each independent region.

Laptev Sea

Focal mechanism solutions for events 1 through 4 indicate that normal faulting associated with the Arctic mid-ocean ridge continues onto the continental slope and shelf of the Laptev Sea. Complex ruptures and/or fault geometries are indicated by the inconsistent solutions obtained through moment tensor inversions and P-wave first motion studies. The discrepancies, which may result from moment tensor solutions that average the entire rupture process as opposed to initial rupture patterns indicated by first motion data (Appendix 3A), may prove useful in more detailed studies of the ocean to continent rift transition. Increased lower crustal and upper mantle temperatures below the rift are indicated by the non-orthogonal nodal planes of two focal mechanism solutions.

Lena River Delta

The combined seismicity in the Laptev Sea and Lena River delta must be used when modelling the transition from oceanic to continental crust. Unfortunately, the three earthquakes on the Lena River delta (nos. 6, 7 and 8) cannot be used without some question as to their true position along the plate boundary. Options to consider include 1) the events are intraplate, not related to the North American interplate boundary seismicity; 2) the events are due to interplate deformation, but are controlled by the structures of the Siberian platform hinge line; 3) the events are true interplate earthquakes representative of a definitive North American boundary; and, 4) the events are interplate earthquakes associated with a more diffuse plate boundary.

Options 1 and 3 seem unlikely. The earthquakes' proximity to other interplate seismicity makes it unreasonable to assume that they are not, at least to some degree, controlled by interplate dynamics. On the other hand, the distribution of the interplate seismicity does not in the least suggest a distinct, simple plate boundary geometry in the Laptev Sea-Lena River delta region.

Option 2 cannot be disregarded regardless of conclusions reached on option 4. Should option 4 hold true, the pre-existing structure of the Siberian platform may still control some of the plate geometry. Therefore, option 2 can only be examined in light of models developed for option 4.

The 4th option seems plausible given the broad distribution of larger (M_b > 4.5) earthquakes in the Laptev Sea-Lena River delta area. The boundary is not likely to be diffuse as in the Indian Ocean usage of Wiens et al. (1985), who distribute the Australian - Indo-Arabian interplate deformation throughout a zone 800 km wide and over 1000 km long. Rather, a more systematic distribution may be modelled such as has been suggested by Engeln et al. (1988) or Lister et al. (1986). Greatly simplified, each of these models incorporates assymetric deformation broadly around a newly evolving boundary. More detailed study of hypocentral distribution and source mechanisms of earthquakes in Laptev Sea and Lena River Delta must be conducted in order to evaluate these models.

South of the Lena River delta region is a small decrease in seismicity between the Arctic mid-ocean ridge and the northern Cherskii Mountains. The relatively few events in this 300 km wide zone are less than M_b 4.5, and are recorded only by local Soviet stations. This apparent "gap" in seismicity may be due to either a large (M_b 6.3) earthquake which reportedly occurred in the region in 1918, which released accumulated stresses, or to the proximity of the zone to the proposed North American - Eurasian pole of rotation (Chapter 4; DeMets et al., in press). If the pole of rotation were in this zone the relative motion would approach zero, thereby limiting the stresses to very small values and decreasing seismic potential. This position for the pole of rotation is also supported by the transition from normal faulting to the north to thrust faulting in the south (Chapter 4).

Northern Cherskii Mountains

The northern Cherskii Mountains are located along the southern boundary of the Moma "rift," a series of depressions extending from approximately 70°N, 138°E, to 63°N, 153°E, which are paralleled by the seismicity. The depressions, bounded by apparent normal faults and cut by "transform" faults (Zonenshain et al., 1978; Savostin and Karasik, 1981), are sites of relative subsidence, high heat flow and limited basaltic volcanism. These geological and geophysical indicators have led numerous investigators (Demenitskaya and Karasik, 1969; Grachev et al., 1970; Zonenshain et al., 1978; Savostin and Karasik, 1981; Grachev, 1982) to consider this region as an extension of the Arctic mid-ocean ridge and thus to interpret the depressions as rift grabens.

In contrast to the above interpretations, however, focal mechanism solutions (nos. 9-12) for the northern Cherskii Mountains all indicate compression approximately perpendicular to the axis of the depressions. These mechanisms could potentially result from two differing hypotheses. The first is that extension is still taking place along the Moma rift system, and that the earthquakes all represent strike-slip motion along continental transform faults. Although possible, it seems unusual that no normal faulting mechanisms would be determined anywhere in the rift. The second hypothesis is that the rift is no longer undergoing extension. In this case, a transition from extension to compression in the recent past could explain both the geologic and geophysical data. Such a scenario is consistent with the results of Rezanov and Kochetkov (1962) who find that recent tectonic movements, based on the elevation of the pre-Pleistocene peneplanation surface, indicate uplift in the Cherskii Mountains and Moma "rift." Furthermore, L. Parfenov (pers. comm., 1986) reports that the Moma "rift" is inactive, and that active faults are strike-slip and thrust. A more detailed discussion of the implications of such a recent transition, and the effect on the North American - Eurasian pole of rotation, is presented in Chapter 4.

ROLE OF PRE-EXISTING STRUCTURE

As discussed earlier, the distribution of larger earthquakes in the Cherskii Mountains can be interpreted as representing a distinct, rather than diffuse, North American plate boundary. However, structures associated with the Moma "rift" may act as pre-existing weaknesses which control the location of and slip along the present-day plate boundary. Additionally, poles of rotation calculated using the strike of transform faults within the Moma "rift" (e.g. Zonenshain et al., 1978; Savostin and Karasik, 1981) actually describe the pole of the past rifting event rather than the present plate configuration. To determine what influence pre-existing structure had on 1) earthquake slip vector azimuths, and correspondingly, 2) previous computations of North American poles of rotation (e.g., Pitman and Talwani, 1972; Minster et al., 1974; Karasik, et al., 1975; Chapman and Solomon, 1976; Chase, 1978; Savostin and Karasik, 1981), I utilized fault data from literature (Zonenshain et al., 1978; Savostin and Karasik, 1981) and from LANDSAT imagery (Table 3-2). This was combined with seven Cherskii Mountain earthquake slip vectors determined in this study (nos. 10, 11 and 12) and in McMullen (1985; earthquakes of May 18, 1971, June 5, 1970, January 13, 1972 and June 19, 1974). The slip associated with earthquakes is assumed to be induced by regional stress acting along faults.

Initial inspection of the relationship between slip vector orientation and fault azimuth suggests a very high correlation (Figure 3-20). It is clear that there exist two clusters of fault orientations (Figure 3-20, Table 3-2). Faults in the southern Cherskii Mountains, south of 66^{o}N, have a mean orientation of 117^{o} (standard deviation = 10.1^{o}) while those the northern Cherskii Mountains, north 67^{o}N, have a mean orientation of 68^{o} (standard deviation = 7.0). Interestingly, the transition between the two groups occurs at the same position (approximately 66^{o}N, 140^{o}E) which was independently found to define a change in earthquake slip vector azimuth (Table 3-1). Thus, azimuthal and spatial agreement between the fault and slip vector data can possibly be interpreted as evidence for structural control on the earthquake slip.

A calculation of the theoretically predicted range of slip, using the method of Angelier (1979), was done using a simplified model of the fault orientations and regional stress (Appendix 3B). The regional stress, assumed to

Figure 3-20: Horizontal slip and fault azimuths in the northern and southern Cherskii Mountains. Stippled bars are earthquake slip vector azimuths, cross-hatching are fault azimuths.

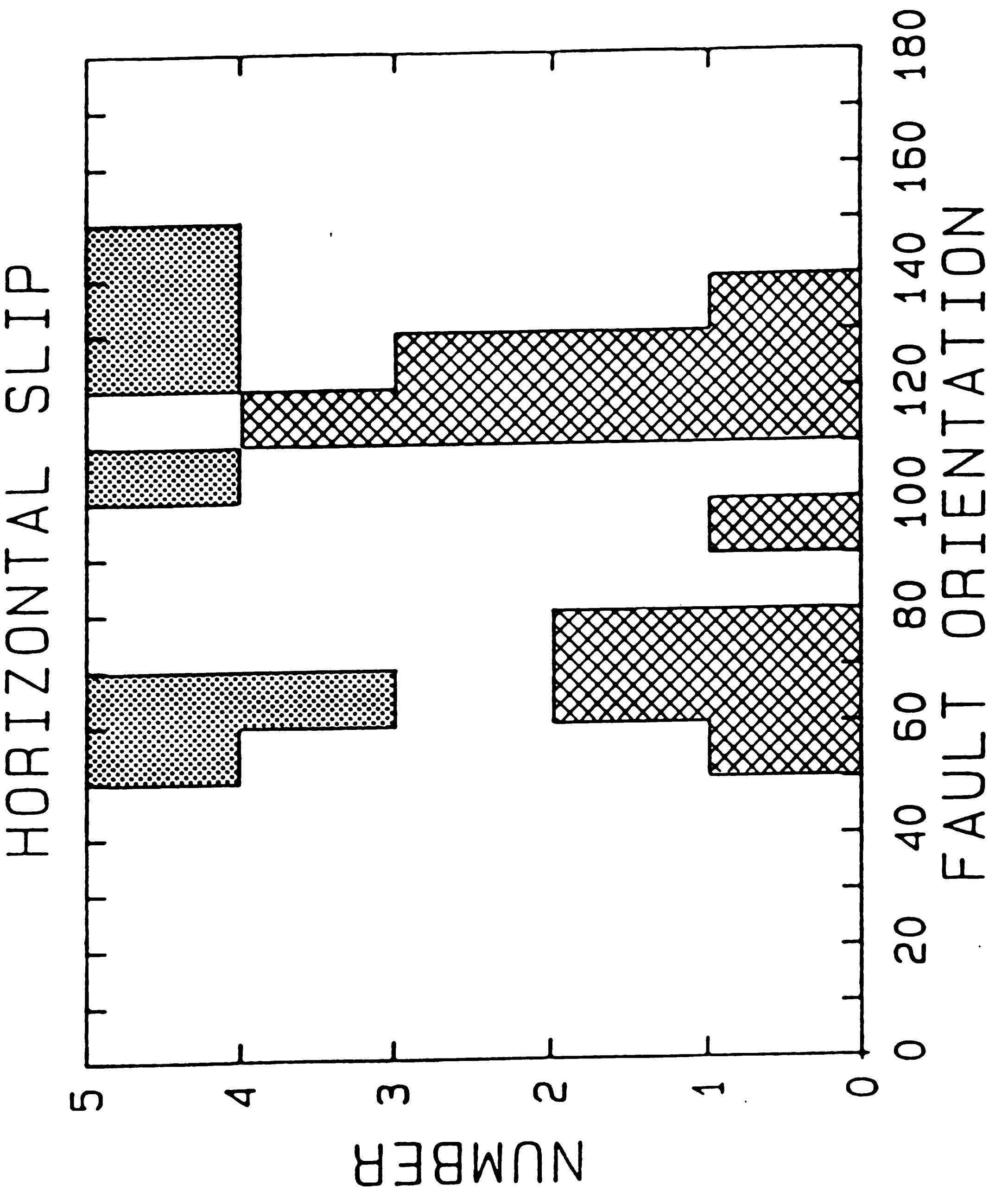
HORIZONTAL SLIP
NUMBER
0
1
2
3
4
5
FAULT ORIENTATION
0
20
40
60
80
100
120
140
160
180

Figure 3-20

be spatially and temporally constant over short periods of geologic time, and the fault azimuths are combined to predict the range of slip direction along the fault plane. The fault dip is not constrained from the fault azimuth, and is therefore allowed to vary from vertical to 42^{o}. This is then compared to the slip vectors of the earthquakes within the region. A more detailed explanation of this application of Angelier's (1979) method is presented in Appendix 3B.

The method was applied to both southern and northern Cherskii fault groups. The results are shown in Figures 3-21 and 3-22. The relation between the predicted range of slip for the northern Cherskii faults and earthquake slip vectors is ambiguous. The three slip vectors scatter inside and outside the predicted range of slip, and no statistically significant conclusion can be drawn. The result of the southern Cherskii data is significant, however, as all four of the earthquake slip vectors fall outside the predicted range of slip on pre-existing faults. From this it can be suggested that earthquakes south of 66^{o}N along the North American plate boundary are occurring on new fractures, and are not controlled by the pre-existing structural fabric. This conclusion is consistent with the results of Chapter 4, which suggest the southern Cherskii Mountain region is a newly developing plate boundary.

An auxiliary result of this was an explanation of why there have generally been two locations, southern and northern, proposed for the North American - Eurasian pole of rotation. As shown in Table 3-3, data used in the determinations of the North America - Eurasia relative motion have been obtained from the Atlantic Ocean basin, the Eurasia basin and in continental Eurasia. Realizing that rifting is no longer active in the Cherskii Mountain system, and therefore that the continental transforms describe past relative

Figure 3-21: Predicted range of slip azimuth for the northern Cherskii Mountains. Shaded area is predicted range of slip as calculated using the method of Angelier (1979). Stars represent the dip and slip azimuth of earthquakes in the northern Cherskii Mountains (events 10, 11 and 12).

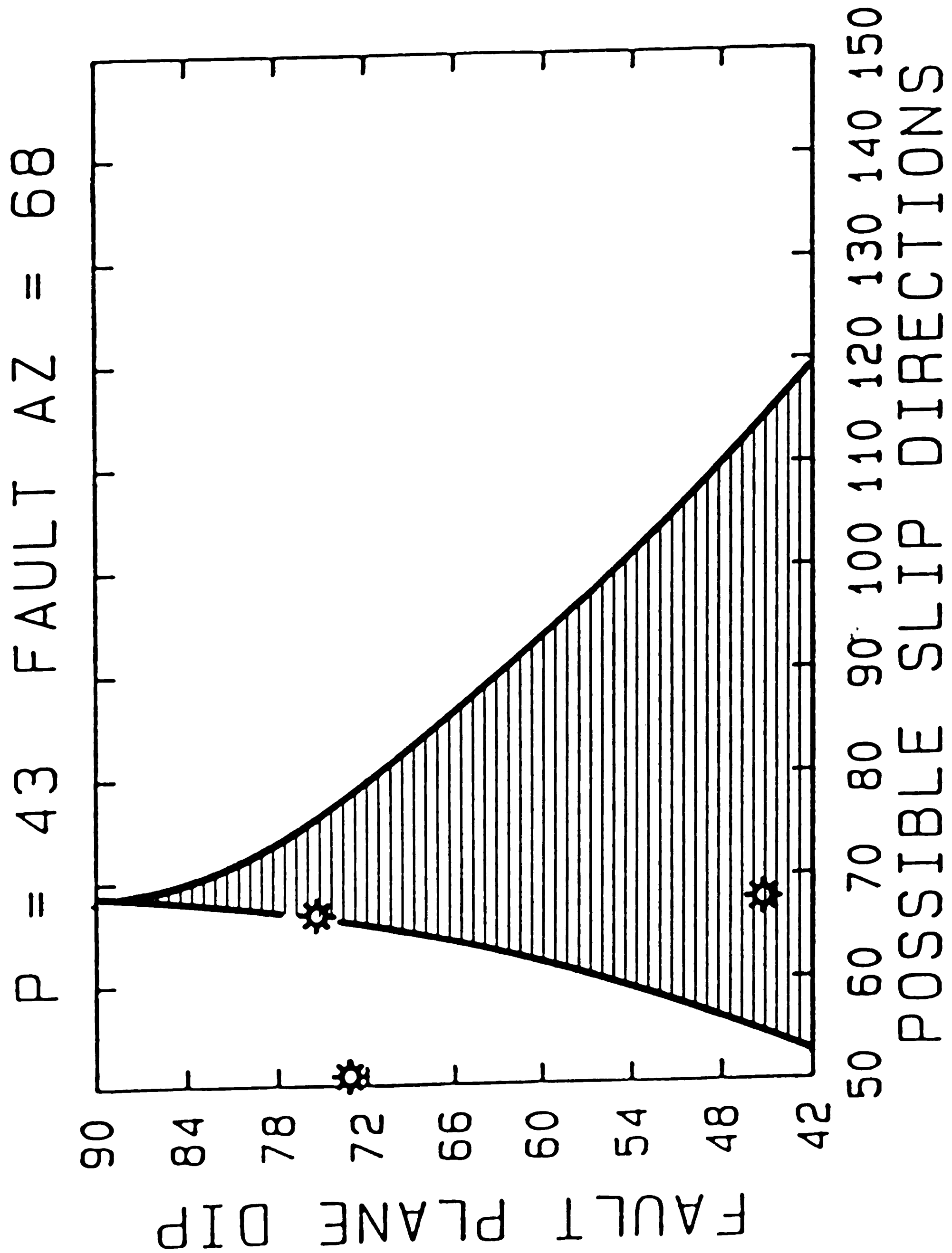
P = 43 FAULT AZ = 68
FAULT PLANE DIP
90
84
78
72
66
60
54
48
42
POSSIBLE SLIP DIRECTIONS
50
60
70
80
90
100
110
120
130
140
150

Figure 3-21

Figure 3-22: Predicted range of slip azimuth for the southern Cherskii Mountains. Shaded area is predicted range of slip as calculated using the method of Angelier (1979). Stars represent the dip and slip azimuth of earthquakes in the southern Cherskii Mountains (data from McMullen (1985)).

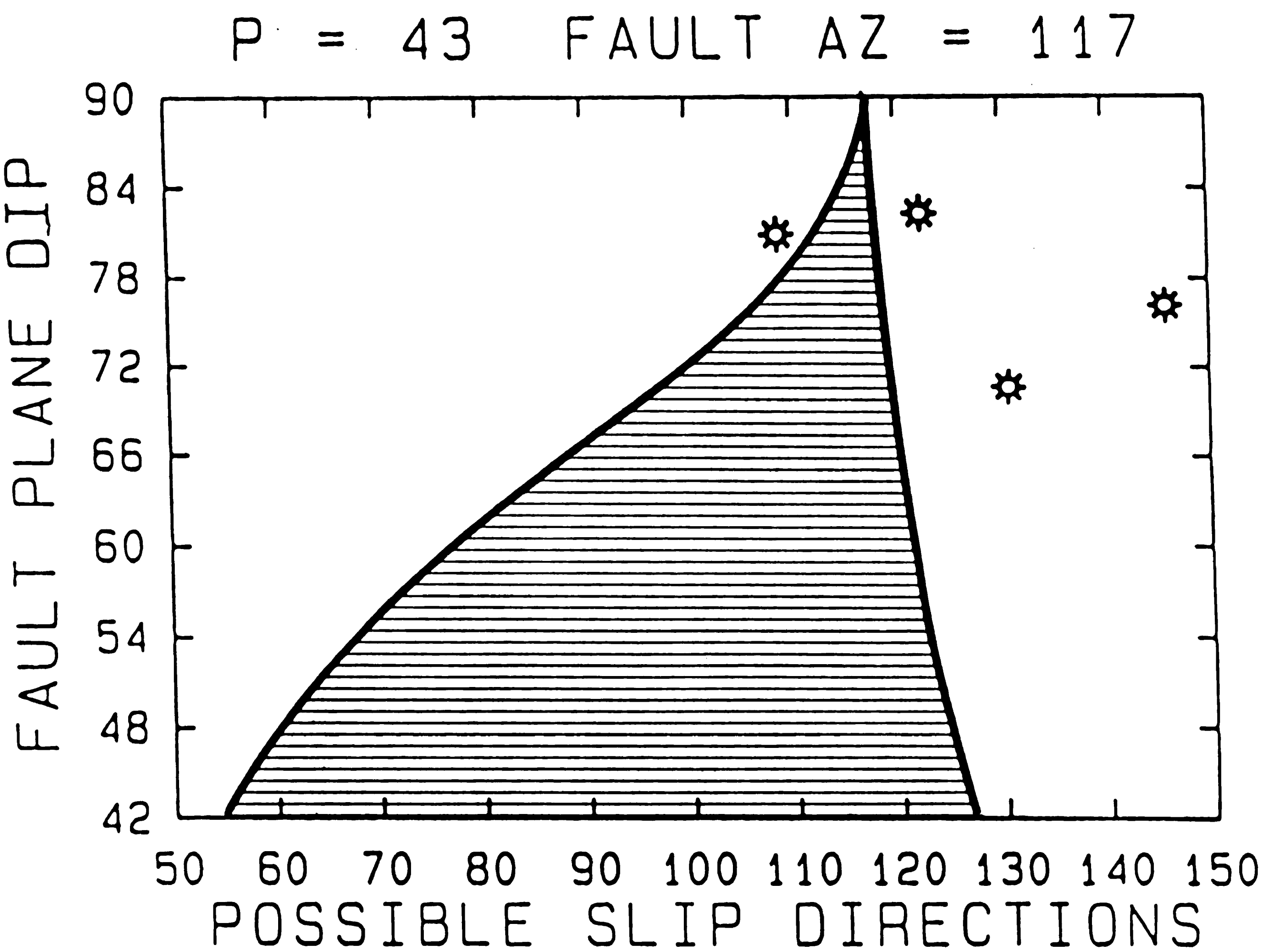
P = 43 FAULT AZ = 117
FAULT PLANE DIP
90
84
78
72
66
60
54
48
42
50 60 70 80 90 100 110 120 130 140 150
POSSIBLE SLIP DIRECTIONS

Figure 3-22

Table 3-3

NORTH AMERICAN - EURASIAN POLE STUDIES

STUDY	POLE	PLATES	METHODS ATL	METHODS ARC	METHODS EUR
	NORTHERLY POLES				
Pitman & Talwani, 72	68.0, 137.0	NA,EU	MAG TFO	MAG	
Minster et al., 74	69.3, 128.0	NA,EU	MAG TFO	MAG	
Cook et al., 86	71.2, 132.1	NA,EU,OK	SV TFO	SV	SV
DeMets et al., in prep.	69.3, 130.6	NA,EU,OK	MAG SV TFO	MAG SV	
Minster & Jordan, 78	65.9, 132.4	NA,EU	MAG SV TFO		
Karasik et al., 75	65.5, 139.5	NA,EU		MAG	
	SOUTHERLY POLES				
Chapman & Solomon, 76	61.8, 130.0	NA,EU	MAG TFO	MAG TFO	SV
Chase, 78	53.7, 137.3	NA,EU	MAG TFO	MAG TFO	SV
Zonenshain, 78	62.2, 143.6	NA,EU,OK			SV TFC
Savostin & Karasik, 81	59.5, 140.3	NA,EU,OK	SV	SV	SV TFC

PLATES: NA = NORTH AMERICA EU = EURASIA OK = OKHOTSK

METHODS: DESCRIBES THE DATA USED IN EACH OF THREE REGIONS:
ATL = ATLANTIC OCEAN
ARC = ARCTIC OCEAN
EUR = EURASIA (NORTHEAST SIBERIA)

THE DATA THEMSELVES INCLUDE:
SV = EARTHQUAKE SLIP VECTORS
MAG = OCEANIC MAGNETIC ANOMALIES
TFO = OCEANIC TRANSFORM STRIKES
TFC = CONTINENTAL TRANSFORM STRIKES

plate motions and not present motion, new conclusions may be drawn about previous pole determinations.

Southern poles calculations such as those by Zonenshain et al. (1978) and Savostin and Karasik (1981) utilized the strike of continental transforms in the Moma rift system. These faults bias the pole southward toward the paleopole which described the rifting event. Chapman and Solomon (1976) and Chase (1978) also calculated southernly positions for the North American - Eurasian pole of rotation. In these cases, the investigators did not include a Sea of Okhotsk plate in their models, but included data from the southern Cherskii Mountains which are ascribed to North American - Sea of Okhotsk relative motion (McMullen, 1985). The inclusion of this data will shift the North American - Eurasian pole toward the position of the North American - Sea of Okhotsk pole. Therefore, North American - Eurasian pole calculations which do not utilize fault strikes from the Cherskii Mountains and which do attribute southern Cherskii Mountain slip vector data to North American - Okhotsk relative motion result in a northern position for the Euler pole. With this in mind, a new North American - Eurasian pole of rotation is determined in Chapter 4.

CONCLUSIONS

Models which consider the depressions of the Cherskii Mountains as the onshore continuation of the Arctic mid-ocean ridge cannot account for compression indicated by earthquake focal mechanisms. Instead, extension along the Arctic mid-ocean ridge terminates in the southernmost Laptev Sea after a broad distribution over the Laptev Sea shelf. A small "gap" in seismicity southeast of Buor Khaya Bay may be indicative of a nearby Euler pole describing the relative motion along the plate boundary. Increased seismicity within the Cherskii Mountains is characterized by compressive mechanisms, inconsistent with the observed geology. Additionally, the slip direction determined from focal mechanisms in the northern Cherskii Mountains is opposite the slip in the southern Cherskii Mountains (McMullen, 1985; Chapman and Solomon, 1976). This is possibly indicative of motion between differing plate pairs (i.e., North America - Eurasia and North America - Okhotsk).

The structural complexity in the Cherskii Mountains may play a role in the location and direction of present-day slip. Simplified models suggest that earthquakes in the northern Cherskii Mountains are not inconsistent with slip along the pre-existing structure, although the earthquakes in the southern Cherskii's appear to be occurring on recent fractures.

Complex structure and/or complex rupture along much of the plate boundary is indicated by inconsistent P-wave solutions and moment tensor inversions in the Laptev Sea and the Cherskii Mountains. Rather than being mutually exclusive, it is suggested that such discrepancies may instead be helpful in understanding the source processes in large continental earthquakes. An apparent slow velocity in the upper mantle below the Arctic mid-ocean ridge, indicated by non-orthoganal focal mechanism nodal planes, further complicates the understanding of the present plate geometry within the Laptev Sea.

APPENDICES

APPENDIX 3A

DISCREPANCIES BETWEEN MOMENT TENSORS AND P-WAVE DATA: POTENTIAL CAUSES AND IMPLICATIONS

Four earthquakes included in this study (nos. 1, 3, 4 and 10; Table 3-1) had either Centroid-Moment Tensor (CMT; Dziewonski et al., 1981) or body-wave inversion (Jemsek et al., 1986) solutions derived from previous studies. For each of these events, there was some degree of misfit between the CMT or body-wave inversion and solutions consistent with P-wave first motions.

Teleseismic P-wave first motion plots often cannot well constrain the nodal planes when either of the planes are shallow dipping. Therefore, these solutions often cannot be considered good solutions to the faulting process without support from other methods (e.g., synthetic seismograms, surface-wave analysis). Similarly, moment tensor analysis also has problems when inverting small, shallow earthquakes. Certain components of the moment tensor (specifically the M_{xz} and M_{yz} terms; see for example Kennett (1983)) become indeterminate when the hypocenter is shallow (<30 km). Better constraint can be obtained by inverting shorter wavelengths, as the minimun usable depth decreases in proportion to the wavelength. However, there exist further trade-offs as these shorter wavelengths are more susceptible to lateral heterogenieties.

The above explanation may sufficiently explain the discrepancy observed between inversion and P-wave first motion solutions. However, interesting observations in this study warrant further speculation on the discrepancy between P-wave first motion solutions and those based on other methods.

Chung and Kanamori (1978) noted that waves of different periods carry separate information, and should therefore not be expected to provide the same results. It is now known that many earthquakes, especially those of great magnitude, have complex rupture histories of long duration and numerous sub-events. These complexities are components of moment tensor and inversion determinations, which account for such processes over the entire rupture duration. P-wave first motion studies, however, are blind to such complex histories, and instead best record the initial rupture process. This initial rupture is undoubtedly an important aspect of understanding the complete source mechanism, albeit potentially more influenced by local dynamics (e.g., over-burden stresses or pre-existing weaknesses). It is more likely, however, that the moment tensor and inversion determinations better reflect the true plate dynamics through the incorporation of an average solution which is not necessarily constrained to be double couple (Hinzen, 1986).

More importantly, it may be possible to predict where discrepancies between first motion solutions and moment tensors or inversions will occur. Hinzen (1986) concluded that differing solutions from the two methods are most likely attributable to changes in fault plane geometry or slip direction after initial rupture. Fewer differences were noted as a function of non-double couple component or earthquake strength. A possible negative correlation between depth and misfit was also suggested. The conclusions of Hinzen (1986) may be further interpreted to indicate a correlation between tectonic setting and misfit between first motion and moment tensor or inversion solutions.

Many shallow earthquakes occur in rift settings of either oceanic or continental affinity. Complex fault geometries (e.g., curved faults) potentially characterize rift settings, and strong inhomogenieties exist in continental crust. It can therefore be expected that shallow earthquakes have more complex rupture processes, and thus greater discrepancies between first motion and inversion solutions may be expected beyond the limitations of the inversion process as discussed above. This is in agreement with Hinzen's (1986) conclusion regarding depth and misfit. An exception to this rule may be found in large strike-slip settings (e.g., mid-oceanic ridge transforms, western California or southern Alaska) which may have fault geometries which are simple in comparison to rifts. Discrepancies may still exist in areas of continental crust (e.g., western California).

Dziewonski and co-workers (e.g., Dziewonski et al., 1983; Dziewonski et al., 1985) have compiled an extensive database of moment tensor solutions for nearly the past decade. An comparison between these moment tensor, or other inversion, determinations and P-wave first motion solutions in well defined tectonic settings is suggested to test the above speculation.

APPENDIX 3B

DETERMINATION OF POSSIBLE RANGE OF FAULT SLIP USING THE METHOD OF ANGELIER (1979)

Angelier (1979) evaluates the validity of approximating the relative motion on a fault as being due to a regional mean stress (defined as a tensor). A number of simplifying assumptions are applied in the method, and some limitations are implied. However, the results of Angelier's (1979) study indicate the approximating model gives satisfactory results.

Angelier (1979) makes the assumptions that 1) the orientation of fault planes does not contain any information regarding the regional stress (i.e., pre-existing zones of weaknesses are present), 2) the magnitude and direction of stress remains constant throughout the rupture time, and 3) the relative sizes of the principal stresses (ϕ) are not explicity known. Assumption 3 limits the method in that only a range of predicted slip, dependent on the value of shear stress, can be resolved. Similar assumptions made in seismological studies of fault orientation and regional stress direction (e.g., Gephart and Forsyth, 1984; Vasseur et al., 1983) demonstrate the interchangability of the method between focal mechanism solutions and field data. More recent structural studies (e.g., Michael, 1984) have simplified the computational aspect of Angelier's (1979) method by further assuming that the tangential traction on individual faults is similar throughout the region. However, for my investigation a graphical method (Angelier, 1979) was utilized to obtain the predicted range of slip, and the assumptions of Michael (1984) do not change the results.

The graphic method defines windows of potential slip through the intersection of great circles (lower hemisphere Schmidt projection) between the pole to the fault plane and the P- and T-axes of the regional stress (Figure 3-23). The value of the range of slip is expressed by

$$\text{COS}\ \delta = \text{TAN}\,\alpha_0 * \text{TAN}\,\alpha_1 \qquad \text{Angelier (1979)}$$

The regional stress directions (P, T and B representing maximum, minimum and null directions) are derived from an intraplate event (December 12, 1975; Figure 3-24) in the nearby New Siberian Islands. Although a somewhat circular proof, these stress orientations are taken as valid due to their consistency with the P-axis orientation of the interplate events (Table 3-1) included in this study. The use of a horizontal orientation of the P-axis even at shallow depths is supported by the results of Engelder and Sbar (1984), who utilize *in situ* measurements and obtain horizontal stresses several times the vertical stress as shallow as 100 m.

In order to obtain the predicted ranges shown on Figures 3-21 and 3-22, great circles were drawn between the P- and T-axes and the pole to the fault plane. The intersection of these circles with the fault plane then defined the range of slip. Since the fault plane dip is not obtainable, in most cases, from LANDSAT imagery, nor was it reported in the literature, slip ranges were determined for fault plane dips ranging from 90° to 42° in 8° increments.

Figure 3-23: Graphical representation of Angelier's (1979) method for determining ranges of slip. P: P-axis azimuth; T: T-axis azimuth; B: null axis; n: pole to the fault plane, f.

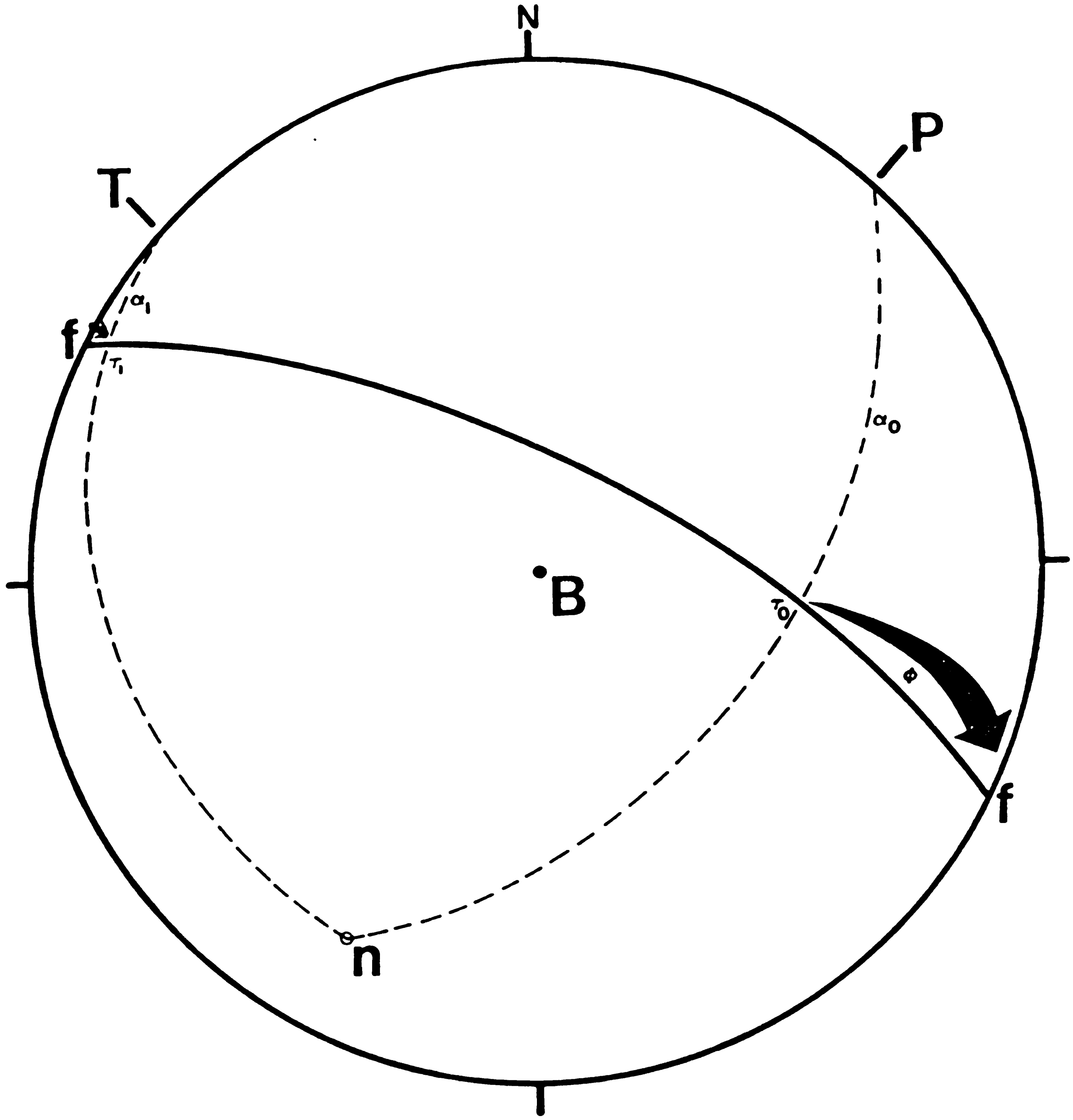

GRAPHICAL METHOD OF ANGELIER (1979)

Figure 3-23

Figure 3-24: P-wave solution and Rayleigh wave radiation pattern of the December 15, 1973 New Siberian Islands intraplate earthquake. The epicenter's location in the New Siberian Islands is shown on the map.

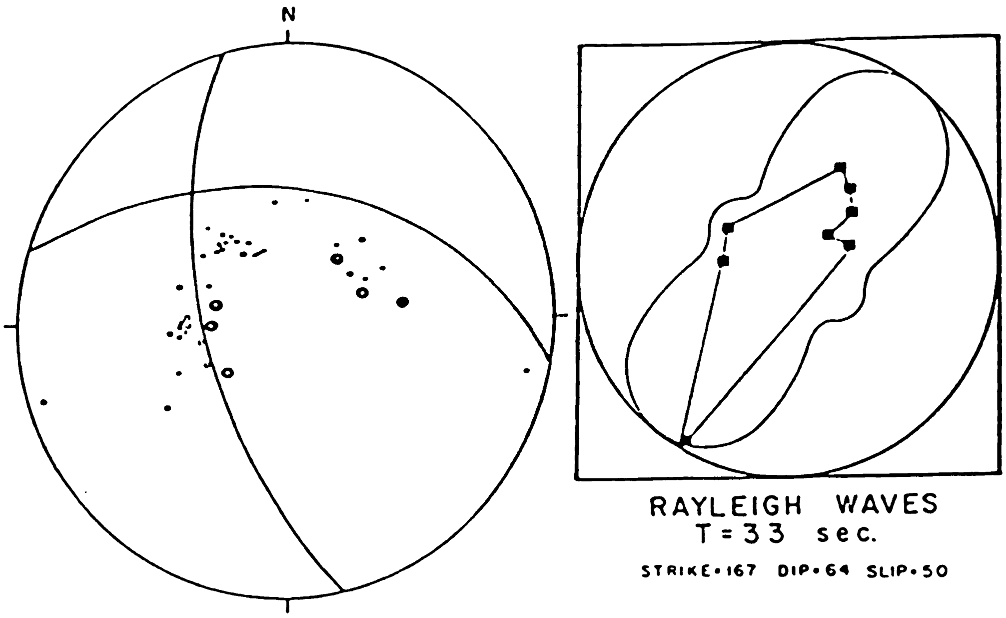

15 DECEMBER 1973

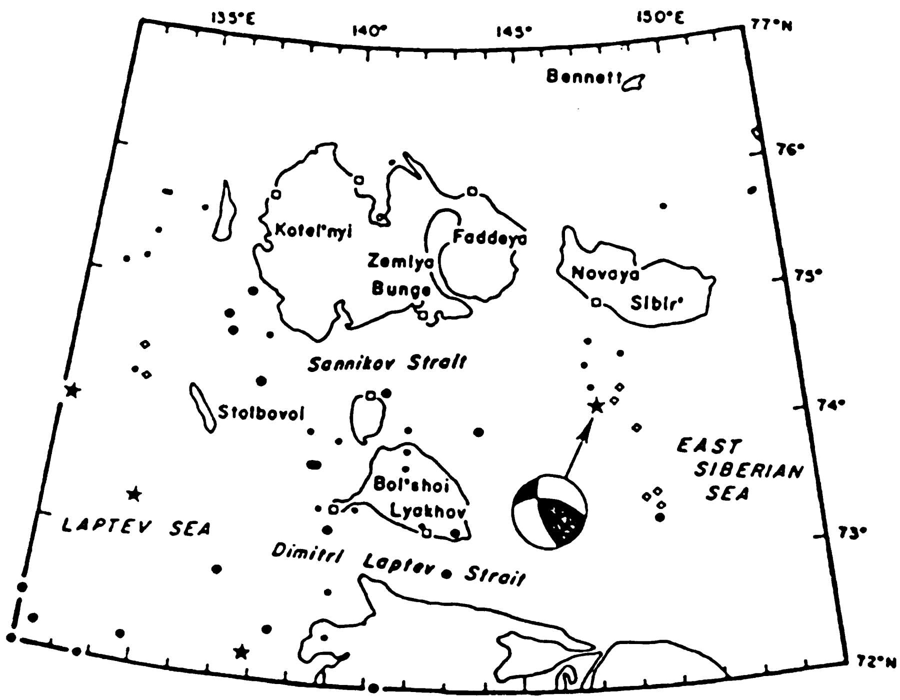

Figure 3-24

LIST OF REFERENCES

LIST OF REFERENCES

Andreev, V. S., 1983. Boguchanskii glubinnyi razlom (in Russian), Vestnik Moskva Universitet, ser. 4, Geologiya, 2, 77-80.

Angelier, J., 1979. Determination of the mean principal stress directions of stresses for a given fault population, Tectonophysics, 56, T17-T26.

Argunov, M.S. and S. I. Gavrikov, 1960. Balagan-Tas, an Early Quaternary volcano, Izv. Acad. Sci. USSR, (8), 72-74.

Chapman, M.E. and S. C. Solomon, 1976. North American - Eurasian plate boundary in northeast Asia. J. Geophys. Res., 81, 921-930.

Chase, C.G., 1978. Plate kinematics: the Americas, East Africa, and the rest of the world. Earth Planet. Sci. Lett., 37, 355-368.

Chung, W.-Y. and H. Kanamori, 1978. Subduction process of a fracture zone and aseismic ridges - the focal mechanism and source characteristics of the New Hebrides earthquake of 1969 January 19 and some related events, Geophys. J. Royal Astr. Soc., 54, 221-240.

Churkin, M. Jr.,1972. Western boundary of the North American continental plate in Asia, Geol. Soc. Amer. Bull., 83, 1027-1036.

Conant, D. A., 1972. Six new focal mechanism solutions for the Arctic and a center of rotation for plate movement, M. A. Thesis, Columbia University, New York, 18 pp.

DeMets, C., Gordon, R.G., Stein, S., Argus, D.F., Engeln, J., Lundgren, P., Quible, D.G., Stein, C., Wiens, D., Weinstein, S.A., and Woods, D.F., in press. Current plate motions. J. Geophys. Res.

Dziewonski, A. M., T.-A. Chou and J. H. Woodhouse, 1981. Determination of earthquake source parameters from waveform data for studies of global and regional seismicity, J. Geophys. Res., 86, 2825-2852.

Dziewonski, A.M., J. E. Franzen and J. H. Woodhouse, 1983. Centroid-moment tensor solutions for April - June, 1983, Phys. Earth Planet. Inter., 33: 243-249.

Dziewonski, A.M., J. E. Franzen and J. H. Woodhouse, 1985. Centroid-moment tensor solutions for October - December, 1984, Phys. Earth Planet. Inter., 39, 147-156.

Engelder, T. and M. L. Sbar, 1984. Near-surface in situ stress: introduction, J. Geophys. Res., 89, 9321-9322.

Engeln, J. F., S. Stein, J. Werner and R. G. Gordon, 1988. Microplate and shear zone models for oceanic spreading center reorganizations, J. Geophys. Res., 93, 2839-2856.

Fujita, K., E. A. Lynch and D. B. Cook, 1987. History of the Soviet seismograph network in northeast Siberia (abstract), EOS, 66, p. 1062.

Fujita, K., D. B. Cook, H. Hasegawa, D. Forsyth and R. Wetmiller, in press. Seismicity and focal mechanisms of the Arctic region and the North American plate boundary in Asia, in, A. Grantz et al. (eds.), The Geology of North America, vol. L, The Arctic Ocean Region; Geol. Soc. Amer., Boulder, CO.

Gephart, J. W. and D. W. Forsyth, 1984. An improved method for determining the regional stress tensor using earthquake focal mechanism data: Application to the San Fernando earthquake sequence, J. Geophys. Res., 89, 9305-9320.

Grachev, A. F., 1973. Momskii materikovii rift (severo-vostok SSSR), in, R. M. Demenitskaya (ed.), Geofizicheskie Metody Razvedki v Arktike, vyp. 8, NIIGA, Leningrad, 56-75.

Grachev, A. F., 1982. Geodynamics of the transitional zone from the Moma rift to the Gakkel Ridge, Amer. Assoc. Pet. Geol Mem. 34, 103-113.

Grachev, A.F., Demenitskaya, R.M. and Karasik, A.M., 1970. The Mid-Arctic ridge and its continental continuation, Geomorphology, 1, 30-32.

Hinzen, K.-G., 1986. Comparison of fault-plane solutions and moment tensors, J. Geophys., 59, 112-118.

Jemsek, J. P., E. A. Bergman, J. L. Nabalek and S. C. Solomon, 1986. Focal depths and mechanisms of large earthquakes on the Arctic mid-ocean ridge system, J. Geophys. Res., 91, 13993-14005.

Kennett, B. L. N., 1983. Seismic Wave Propagation in Stratified Media, Cambridge University Press, London, pp. 342.

Kogan, A.L., 1974. Postanovka seismicheskikh rabot metodom KMPV-GSZ s morskogo l'da na shel'fe Arkticheskikh Morei (opyt rabot v More Laptevykh)(in Russian), Geofiz. Metody Razv. Arktiki, 9, 33-38.

Karasik, A.M., Rozhdestvenskiy, S.S. and Donets, E.G., 1975. The structure of the magnetic anomaly field and the geometry of the spreading of the Mohn Ridge in the Norwegian-Greenland Sea, Izv. Acad. Sci. USSR, Earth Physics, 11, 115-123.

Koz'min, B.M., 1984. Seismicheskie poyasa Yakutii i mekhanismy ochagov ikh zemletryasenii (in Russian), Nauka, Moscow, 126 p.

Lazareva, A. P., and L. A. Misharana, 1965. Stresses in earthquake foci in the Arctic seismic belt, Izvestiya Academy of Sciences of the USSR, Physics of the Solid Earth, 1, 84-87.

Lister, G. S., M. A. Etheridge and P. A. Symonds, 1986. Detachment faulting and the evolution of passive continental margins, Geology, 14, 246-250.

McMullen, C. A., 1985. Seismicity and Tectonics of the Northeastern Sea of Okhotsk. M. S. Thesis, 107 p., Michigan State Univ., E. Lansing.

Michael, A. J., 1984. Determination of stress from slip data: faults and folds, J. Geophys. Res., 89, 11517-11526.

Minster, J.B., Jordan, T.H., Molnar, P. and Haines, E., 1974. Numerical modelling of instantaneous plate tectonics, Geophys. J. Roy. Aston. Soc., 36, 541-576.

Minster, J.B. and Jordan, T.H., 1978. Present-day plate motions, J. Geophys. Res., 83, 5331-5354.

Morgan, W.J., 1968. Rises, trenches, great faults, and crustal blocks, J. Geophys. Res., 73, 1959-1982.

Naymark, A.A., 1976. Neotectonics of the Moma region, northeastern USSR, Doklady Acad. Sci. USSR, Earth Science Sections, 229, 39-42.

Pitman, W.C. III, and Talwani, M., 1972. Sea-floor spreading in the North Atlantic, Geol. Soc. Am. Bull., 83, 619-646.

Prilozhenie k Seismologicheskomu Bulletenu, 1983. Parametri, Amplitudnie and Fazovie Kharakteristiki Pribopov Opornikh Seismicheskikh Stantsii SSSR, 1981 (in Russian), Akademiya Nauk SSSR, Moscow.

Rezanov, I.A. and Kochetkov, V.M., 1962. Recent tectonics and seismic regionalization in the north-eastern region of the USSR, Izv. Acad. Sci. USSR, Geophys. Ser., 1045-1052.

Savostin, L.A. and Karasik, A.M., 1981. Recent plate tectonics of the Arctic basin and of northeastern Asia, Tectonophysics, 74, 111-145.

Savostin, L., Zonenshain, L. and Baranov, B., 1983. Geology and plate tectonics of the Sea of Okhotsk, Am. Geophys. Union, Geodynamics Ser, 11, 189-221.

Seismologicheskii Bulleten', Akademiya Nauk SSSR Institut of Fiziki fo the Earth (in Russian), Obninsk.

Seno, T., 1985. Is northern Honshu a microplate?, Tectonophysics, 115, 177-196.

Stein, S., 1987. Introduction to Seismology, Earthquakes and Earth Structure, September, 1987, draft text, 522 pp.

Solomon, S. C. and B. R. Julian, 1974. Seismic constraints on ocean-ridge mantle structure: anaomalous fault plane solutions from first motions, Geophys. J. Royal Astr. Soc., 38, 265-285.

Sykes, L. R., 1965. The seismicity of the Arctic, Bull. Seismol. Soc. Amer., 55, 501-518.

Sykes, L. R., 1967. Mechanisms of earthquakes and nature of faulting on the mid-oceanic ridges, J. Geophys. Res., 72, 2131-2153.

Vasseur, G., A. Etchecopar and H. Philip, 1983. Stress state inferred from multiple focal mechanisms, Annales Geophysicae, 1, 291-298.

Wiens, D. A., C. DeMets, R. G. Gordon, S. Stein, D. Argus, J. F. Engeln, P. Lundren, D. Quible, C. Stein, S. Weinstein and D. F. Woods, 1985. A diffuse plate boundary model for Indian Ocean tectonics, Geophys. Res. Letters, 12, 429-432.

Zonenshain, L. P., L. M. Natapov, L. A. Savostin and A. P. Stavsky, 1978. Recent plate tectonics of northeastern Asia in connection with the opening of the northern Atlantic and Arctic basins, Oceanology, 18, 846-853.

CHAPTER FOUR

PRESENT-DAY PLATE INTERACTIONS IN NORTHEAST ASIA: NORTH AMERICAN, EURASIAN AND OKHOTSK PLATES

INTRODUCTION

Previous studies have delineated the North America - Eurasia plate boundary along the Arctic Mid-Ocean Ridge from the North Atlantic to the Lena River delta (Figure 4-1; Sykes, 1965; Zonenshain et al., 1978). The seismicity along this segment follows a narrow band, not exceeding 50 km in width (Figure 4-2). As the ridge impinges on the continental shelf of Eurasia, the depth of seismicity increases (Jemsek et al., 1984) and the zone of seismicity increases in width. In the continental part of northeast Asia, between the Sette-Daban and the Cherskii Mountains, the zone of seismicity reaches widths of about 500 km and has been suggested to be a diffuse plate boundary (Chapman and Solomon, 1976). Along the northeastern edge of this zone of seismicity is a series of depressions (Figure 4-1; Moma "rift"), first suggested by Grachev et al. (1970) to be a continental continuation of the Arctic Mid-Ocean Ridge. South of the Sette-Daban Mountains the seismicity appears to decrease. Active seismicity has been noted, however, along Sakhalin Island (Chapman and Solomon, 1976) and along the eastern coast of Kamchatka (Cormier, 1975) north of the Aleutian-Kurile arc-arc junction (here referred to as the northeast Kamchatka seismic zone). These observations led Chapman and Solomon (1976) to postulate that the Sea of Okhotsk was part of the North American plate and most global plate inversions have followed this configuration.

In the past decade, however, a series of moderate ($5 < m_b < 6$) earthquakes occurred along the northern coast of the Sea of Okhotsk (Figure 4-2) in a zone between the southern Cherskii Mountains and the northeast Kamchatka seismic zone. In addition, several well constrained focal

Figure 4-1: Index map of northeast Siberia showing grabens (stippled) as shown by Savostin and Karasik (1981) and Savostin et al. (1983). B-T denotes location of Balagan-Tas volcano. EP denotes the El'ginskii Plateau. Star indicates the position of the Aleutian-Kurile arc-arc junction.

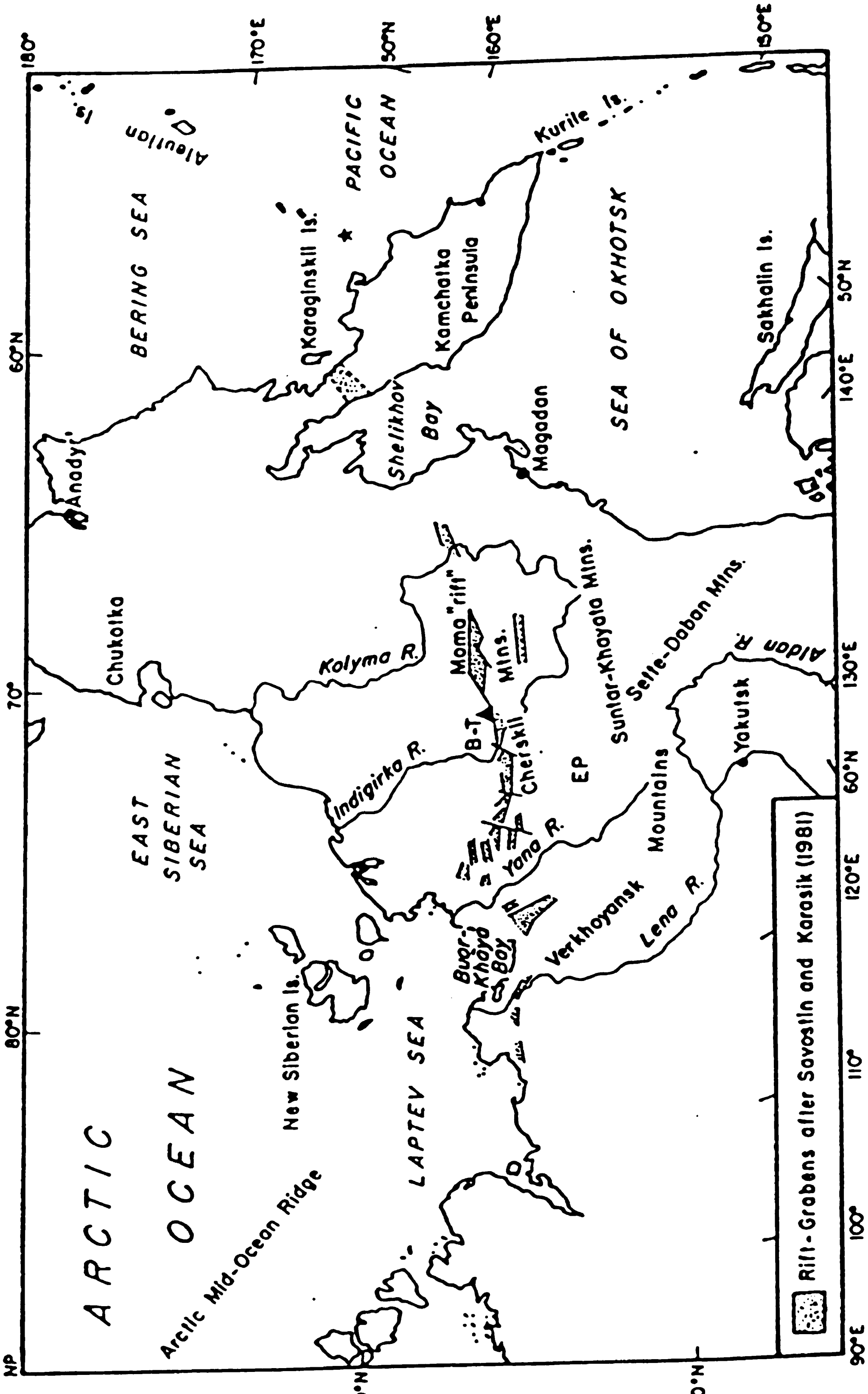
ARCTIC OCEAN
Arctic Mid-Ocean Ridge
New Siberian Is.
LAPTEV SEA
EAST SIBERIAN SEA
BERING SEA
Aleutian Is.
PACIFIC OCEAN
Karaginskii Is.
Kamchatka Peninsula
Kurile Is.
SEA OF OKHOTSK
Sakhalin Is.
Shelikhov Bay
Magadan
Anadyr
Chukotka
Kolyma R.
Indigirka R.
Yana R.
Lena R.
Aldan R.
Yakutsk
Verkhoyansk Mountains
Suntar-Khayata Mtns.
Sette-Daban Mtns.
Moma "rift"
Mtns.
Cherskii
B-T
EP
Buor-Khaya Bay
Rift-Grabens after Savostin and Karasik (1981)
NP
80°N
70°N
90°E
100°
110°
120°E
130°E
140°E
150°E
160°E
170°E
180°
80°N
70°
60°N
60°N
50°N
50°N

Figure 4-1

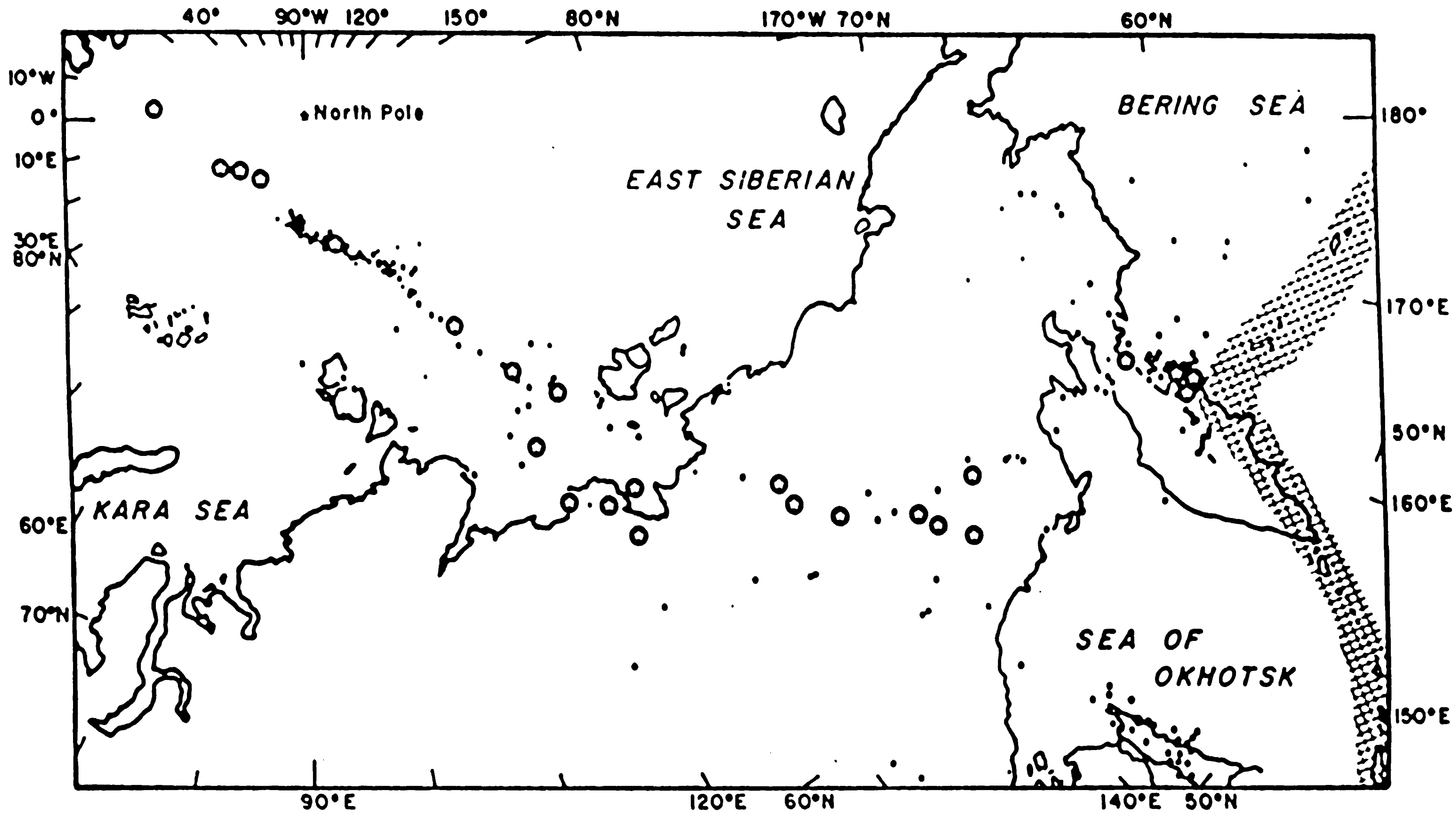

Figure 4-2: Shallow and intermediate (h < 100 km) teleseismic seismicity of northeast Siberia and the adjacent Arctic north of 50°N and east of 90°E. Large dots with stars indicate events used in this study, medium sized dots denote earthquakes with $m_b > 4.0$, and small dots indicate earthquakes with $m_b < 4.0$. The shaded region along the Kurile and Aleutian arc denotes numerous events.

mechanisms in the Cherskii Mountains have been determined that allow the rift hypothesis for the Cherskii Mountains to be tested.

In this chapter, events occurring in northeastern Siberia are examined to determine the present nature of the North American plate boundary in northeast Siberia and whether an independent Okhotsk plate exists. Additionally, preliminary estimates concerning the relative motion of the Okhotsk plate with respect to the North American plate are made.

SEISMICITY AND FOCAL MECHANISMS

In the last 25 years about two dozen events of magnitude 5 or greater have occurred along the continental extension of the Arctic seismic zone. These events are concentrated on the northeastern edge of the zone of diffuse seismicity. The largest, M_S = 6.6, occurred on May 18, 1971, in the southern Cherskii Mountains. Details of the seismicity within the diffuse seismic zone are unclear. Although Soviet workers have tabulated the seismicity of the region since about 1700 (Koz'min and Andreev, 1977) and with a fair degree of macroseismic data since about 1900 (Kochetkov, 1968; Koz'min, 1984), the detection and location capability within northeast Siberia varies greatly in time and space. The apparent concentration of microseismic activity northeast of Magadan shown by Koz'min (1984) has been shown by Fujita et al. (1983) to result from station distribution and detection capability in the region, as does the apparent lack of microseismicity in northern Shelikhov Bay.

Several large events occurred prior to the 1960s when there were few stations in the area. Particularly destructive earthquakes occurred in the 1920s in the northern part of the region, near the Arctic Ocean, and several damaging earthquakes have occurred along the northern shores of the Sea of Okhotsk (Koz'min, 1984).

Prior to the 1970s there were no instrumentally recorded moderate-sized teleseismic events from the Shelikhov Bay and northwestern Kamchatka regions. In the past 15 years, however, six moderate-sized events (Figure 4-2) have been recorded which form a lineation from the southern Cherskii Mountains to Karaginskii Island. These events suggest that the Sea of Okhotsk may not be part of the North American plate.

Based on the North America-Eurasia pole of rotation computed by Chapman and Solomon (1976) the Cherskii Mountains should represent a tensional regime or have right-lateral strike-slip faulting, assuming a northwest striking fault plane. Savostin and Karasik (1981) proposed that these depressions were rift-grabens along a continental extension of the Arctic Mid-Ocean Ridge, based on the presence of down-dropped blocks with high heat flow and basaltic volcanism (Naymark, 1976; Grachev, 1982). Using strikes of "transform faults" offsetting these grabens, Savostin and Karasik (1981) obtained a North America-Eurasia pole of rotation in the southern Sette-Daban Mountains, that is not too dissimilar from the Chapman and Solomon (1976) pole.

Examination of published focal mechanisms by Savostin and Karasik (1981), Chapman and Solomon (1976), and Filson and Frasier (1972) indicate that the sense of motion on the earthquakes is opposite to what was expected; i.e., thrust faulting and left-lateral strike-slip faulting. Therefore, this investigation seeks to verify the accuracy of these mechanisms and uses additional solutions presented in Chapter 3 and McMullen (1985) to increase the data set.

Focal mechanisms from Chapter 3 and McMullen (1985) have been determined using P-wave first motions, Rayleigh wave amplitude radiation patterns, and synthetic seismograms. P-wave first motions were reread from World-Wide Standardized Seismograph Network (WWSSN) records whenever possible. Except for the largest events, first motions could only be read from short-period records. Due to the small size of the events, bulletin-reported first motions from the International Seismological Center (ISC) Bulletin and the Soviet Operational Catalog were needed to supplement the reread first motions. Rayleigh wave radiation patterns (Kanamori, 1970) are obtained for events of M_S 5.5 and greater. Due to the size of the events and station distribution, data for most events are obtained only in two or three quadrants. Finally, synthetic seismograms are computed for several events to confirm or further constrain the mechanisms and obtain focal depths. Short-period P-waves were modelled using the layered-media algorithm of Kroeger and Geller (1983). As noted by Seno and Kroeger (1983), this requires some knowledge of the crustal structure, therefore results of Soviet refraction surveys (e.g., Kogan, 1974) are used where possible. Short-period synthetics prove to be extremely useful in confirming mechanisms. Each earthquake is studied with as many of the above methods as possible. Due to the small magnitudes of the events, however, uncertainties of 10-20 degrees are common and some results should be viewed as preliminary. In all of the cases presented, however, the type of faulting is clear. The methods used to constrain the focal mechanisms are presented in Chapter 3, and detailed explanations of the solutions found in Chapter 3 and McMullen (1985) are not repeated here.

Figure 4-3 shows both new and previously published focal mechanisms determined for the interplate region of northeast Siberia. These indicate a transition from nearly pure normal faulting in the Laptev Sea to thrust and strike-slip mechanisms in the Cherskii Mountains. Along the lower Lena River, some events show a large strike-slip component as well. In Shelikhov Bay and northwestern Kamchatka, mechanisms are poorly constrained but are not inconsistent with thrusting and left-lateral strike-slip motion, while the largest events in the northeast Kamchatka seismic zone show thrusting.

The events west of the Bour Khaya Bay, in the Lena River delta, lie on the hinge line of the Siberian platform along a series of fractures (Andreev, 1983). They appear to be associated with reactivated faulting due to the opening of the Eurasia basin of the Arctic Ocean. The plane parallel to the hinge line is chosen as the fault plane.

In the northern Cherskii Mountains, all events show a thrust faulting component. Although one nodal plane of these solutions (Table 4-1, nr. 30-32) is usually very close to the strike of the "grabens" of Savostin and Karasik (1981) (Figure 4-1), choosing these planes as the fault plane results in major inconsistencies in plate motion calculations. Thus, the east-west striking plane is chosen, which is close to the strike of the faults offsetting the "grabens". A large event which occurred in the northern Cherskii Mountains in 1962 has only been studied using first motions reported in the International Seismological Summary (ISS). The mechanism is poorly constrained but also appears to be a thrust of indeterminate orientation; it is not used in these calculations.

In the southern Cherskii Mountains, all mechanisms yields strike-slip solutions. Due to the size of the events, all of them are relatively well constrained and show northeast-southwest and northwest-southeast striking

Figure 4-3: Focal mechanisms of earthquakes in northeast Siberia and the adjacent Arctic. Compressional quadrants are solid; stippled compressional quadrants denote less certain mechanisms and dashed nodal planes denote that the orientation of the plane is indeterminate. Events used in this study are numbered (see Table 4-1).

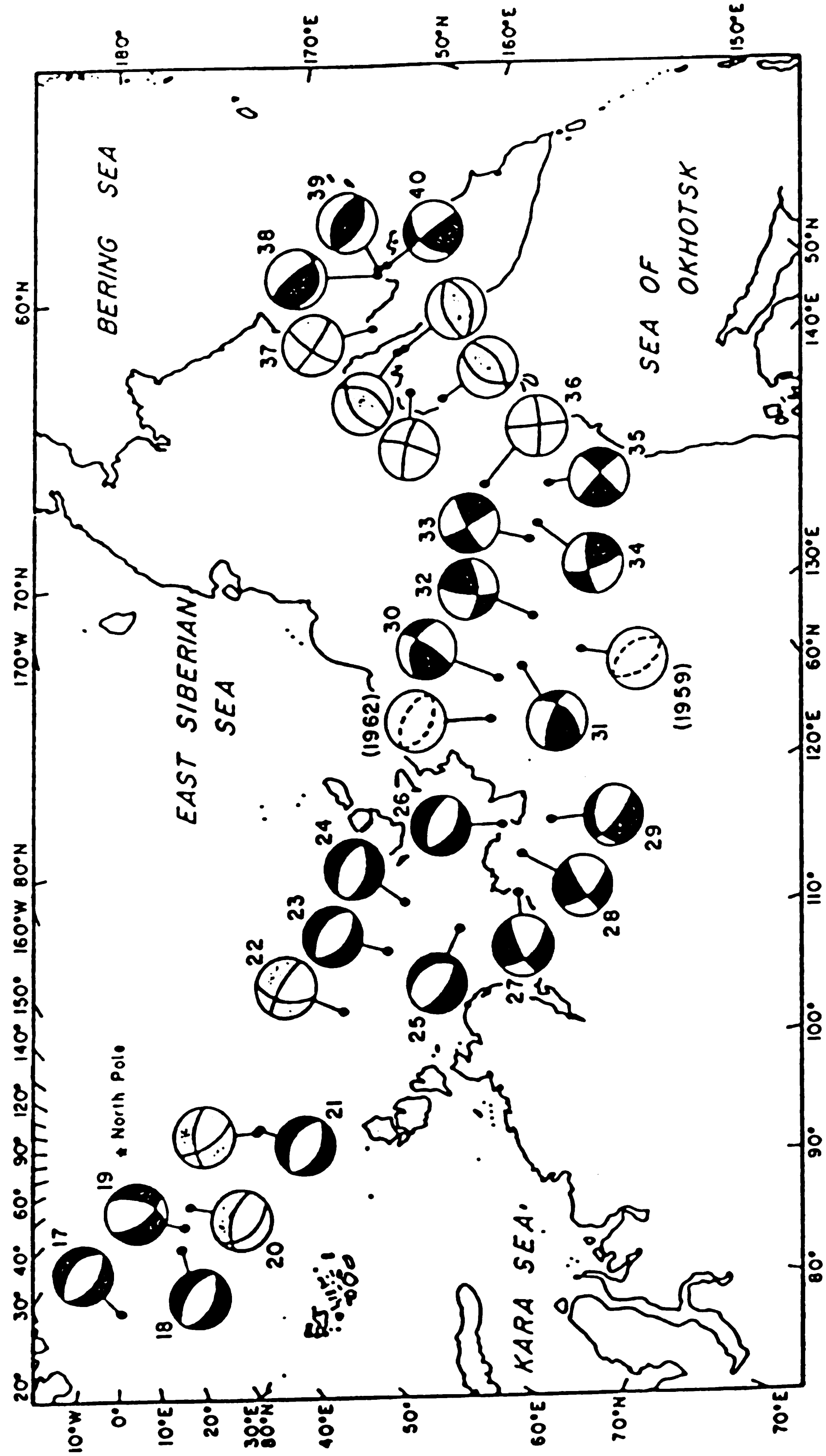
BERING SEA
EAST SIBERIAN SEA
SEA OF OKHOTSK
KARA SEA
North Pole
(1962)
(1959)
17
18
19
20
21
22
23
24
25
26
27
28
29
30
31
32
33
34
35
36
37
38
39
40
60°N
70°N
80°N
50°N
170°W
160°W
180°
170°E
160°E
150°E
140°E
130°E
120°E
110°
100°
90°
80°
70°E
60°E
50°
40°E
30°E
20°
10°E
0°
10°W

Figure 4-3

nodal planes. McMullen's (1985) solutions are essentially identical to those obtained by Chapman and Solomon (1976). The northwest - southeast striking nodal plane is chosen as the fault plane based on aftershocks of the May 18, 1971, event located using a portable array by Koz'min et al. (1975) and on directivity studies by Filson and Frasier (1972).

Across Shelikhov Bay and northwestern Kamchatka, no obvious trends or lineations parallel the nodal planes. Inspection of space shuttle imagery (STS-9), however, shows lineations in northern Kamchatka oriented N155°E and N88°E. Two thrust events (Figure 4-3) have a nodal plane close to the first trend, while an event near Karaginskii Island (Table 4-1, nr. 36) appears to be left-lateral strike slip on a nearly east-west plane. Thus, the east-west lineations may be strike slip features, while the N155°E lineations may be steeply dipping reverse faults. The 1976 sequence on Karaginskii Island is problematic in that quite different mechanisms have been proposed by various workers. The mechanism proposed by Koz'min (1984) has nodal planes close to both lineation strikes in Kamchatka. However, observable lineaments on Karaginskii Island and the aftershock distribution mapped by Fedotov et al. (1980) strike northeast-southwest. It is also possible that this sequence is an intraplate series (McMullen, 1985). Due to these uncertainties, the 1976 sequence is not used in this investigation. South of Karaginskii Island, in the northeast Kamchatka seismic zone, the chosen fault planes are parallel to the seismic zone (and the coastline) which results in convergence between Kamchatka and the Bering Sea.

Table 4-1: Focal mechanisms and slip vectors. Plane 1 is the presumed fault plane. h: focal depth; Q: Quality (Good, Fair, Poor, N denotes not known, - denotes inversion); Az: Azimuth of the horizontal projection of the slip vector; Va: Variance of the strike;
S: Reference - C This study
1 McMullen, 1985
2 Savostin and Karasik, 1981
3 Jemsek et al., 1984
4 Koz'min, 1984
5 Cormier, 1975
6 Veith, 1974
7 Dziewonski et al., 1985
8 Stauder and Mualchin, 1976
9 Minster et al., 1974
10 Chapman and Solomon, 1976

Table 4-1: FOCAL MECHANISMS AND SLIP VECTORS

Nr	Date	Lat N	Long E	h	mb	Plane 1	Plane 2	Az	Va	Q	S
01	Transform	52.5	-35.0	--	---	-------	-------	96	4	-	10
02	Transform	52.5	-33.5	--	---	-------	-------	95	4	-	10
03	1967 02 13	52.82	-34.25	17	5.6	095/88S	005/90V	95	10		10
04	1963 03 28	66.29	-19.86	15	7.3	106/86N	017/78E	107	10		9
05	Transform	66.5	-20.0	--	---	-------	-------	98	10	-	10
06	1969 05 05	66.91	-18.17	33	5.2	112/82N	025/72E	115	10		10
07	Transform	71.0	-08.0	--	---	-------	-------	115	5	-	10
08	1971 03 23	70.97	-06.86	29	5.9	120/74S	026/72E	116	10		10
09	1970 02 22	71.23	-08.21	33	5.1	111/87S	020/74E	110	10	F	2
10	1975 04 16	71.49	-10.36	15	6.0	107/80S	016/81E	106	10	G	2
11	1968 01 03	72.22	001.55	33	5.2	142/58W	030/60E	120	10	P	2
12	1970 10 21	74.62	008.56	33	5.4	133/61W	030/64E	122	10	F	2
13	Transform	79.0	002.5	--	---	-------	-------	128	10	-	10
14	1970 10 26	79.80	002.9	34	5.6	138/76W	017/81N	139	10		10
15	1967 10 18	79.81	002.9	42	5.7			134	10	N	10
16	1967 11 23	80.20	-00.7	16	5.7	128/74W	040/84N	130	10		10
17	1976 09 16	84.30	000.9	01	5.4	038/48E	224/42W	134	5	-	3
18	1973 11 09	86.05	032.8	01	5.4	058/48S	248/43N	157	5	-	3
19	1964 07 31	86.47	040.7	07	5.2	331/53E	089/59S	178	10	F	2
20	1968 06 08	87.00	051.4	32	5.2	248/54N	096/40S	006	10	P	2
21	1975 02 26	84.98	098.5	02	5.3	308/40N	126/50S	036	5	-	3
22	1970 04 23	80.65	122.0	27	5.2	226/50N	332/72E	063	10	P	2
23	1964 08 25	78.15	126.65	05	6.2	171/46W	341/45E	072	10	-	3
24	1969 04 07	76.55	130.86	11	5.4	142/48W	343/42E	072	5	-	3
25	1983 06 10	75.53	122.75	25	5.4	003/33E	156/60W	065	10	-	3
26	1964 07 21	72.10	130.10	12	5.4	170/45W	326/50E	056	5	G	C
27	1980 02 01	73.06	122.59	22	5.4	168/50W	274/71N	005	10	F	C
28	1963 05 20	72.20	126.25	10	5.0	174/60W	270/80N	000	10	F	C
29	1975 08 12	70.76	127.12	16	5.1	164/72W	286/30N	018	10	F	C
30	1984 11 22	68.53	140.88	26	5.4	087/75S	341/45E	066	10	-	7
31	1976 01 21	67.70	140.00	18	5.0	090/45S	338/70E	068	10	F	C
32	1968 09 09	66.17	142.13	06	5.0	238/73N	140/65W	050	10	F	C
33	1971 05 18	63.92	146.10	10	5.9	300/82N	210/88W	122	2	G	1
34	1970 06 05	63.26	146.18	04	5.4	316/70E	218/72W	130	5	G	1
35	1972 01 13	61.94	147.04	33	5.3	100/80S	010/82E	109	15	G	1
36	1974 06 19	63.14	150.92	17	4.9	146/77W	236/90V	146	15	F	4
37	1972 08 03	59.51	163.10	11	5.2	287/72N	197/82W	104	10	F	1
38	1969 11 22	57.70	163.56	51	6.3	032/75E	172/19W	82	8	G	8
39	1970 01 27	57.64	163.60	51	5.0	010/45E	190/45W	100	10	N	6
40	1969 12 23	57.34	163.14	13	5.4	033/82E	293/41N	123	20	F	5

SLIP VECTORS AND POLES OF ROTATION

Slip vectors computed for the newly determined mechanisms are based on the above discussed choice of fault plane (Table 4-1) and are combined with data from the North Atlantic and the Arctic Oceans obtained or cited by previous workers (e.g., Savostin and Karasik, 1981; Chapman and Solomon, 1976). Slip vector uncertainties are assigned based on the quality of the focal mechanism. The horizontal projection of the slip vectors for the Arctic Ocean and northeast Siberia are shown in Figure 4-4. Unnumbered events in Figure 4-3 are not used since either the constraint on the slip vector is weak or the mechanism is poorly constrained.

Poles of rotation are computed using the strikes of the slip vectors using the algorithm of Morgan (1968). Error ellipses are estimated based on a value of $F = 1.25*F_{min}$, where F_{min} is the minimum r.m.s. error obtained in the pole calculation (LePichon et al., 1973). The final data set consists of 5 transform fault strikes from the North Atlantic and 34 slip vectors (Table 4-1).

The data were first divided into five subsets based on geographic regions and combinations of regions. Best fitting results are obtained by dividing the region into two subsets: the North Atlantic and Arctic Oceans to the northern Cherskii Mountains, and the southern Cherskii Mountains to the northeast Kamchatka seismic zone. Inclusion of the southern Cherskii Mountains events in the Arctic data set results in large misfits as does including the Lena River events in the southern Cherskii data set. The northern Cherskii Mountains events can be included in either data set, depending on the choice of fault plane. However, their inclusion with the southern Cherskii events results in inconsistent motions along the plate boundary defined by those events. An uncertainty exists with the northeast Kamchatka seismic zone. A fairly good fit

Figure 4-4: Horizontal projections of slip vectors (solid lines) and poles computed in this study (circled stars). Numbers identify earthquakes with Table 4-1.

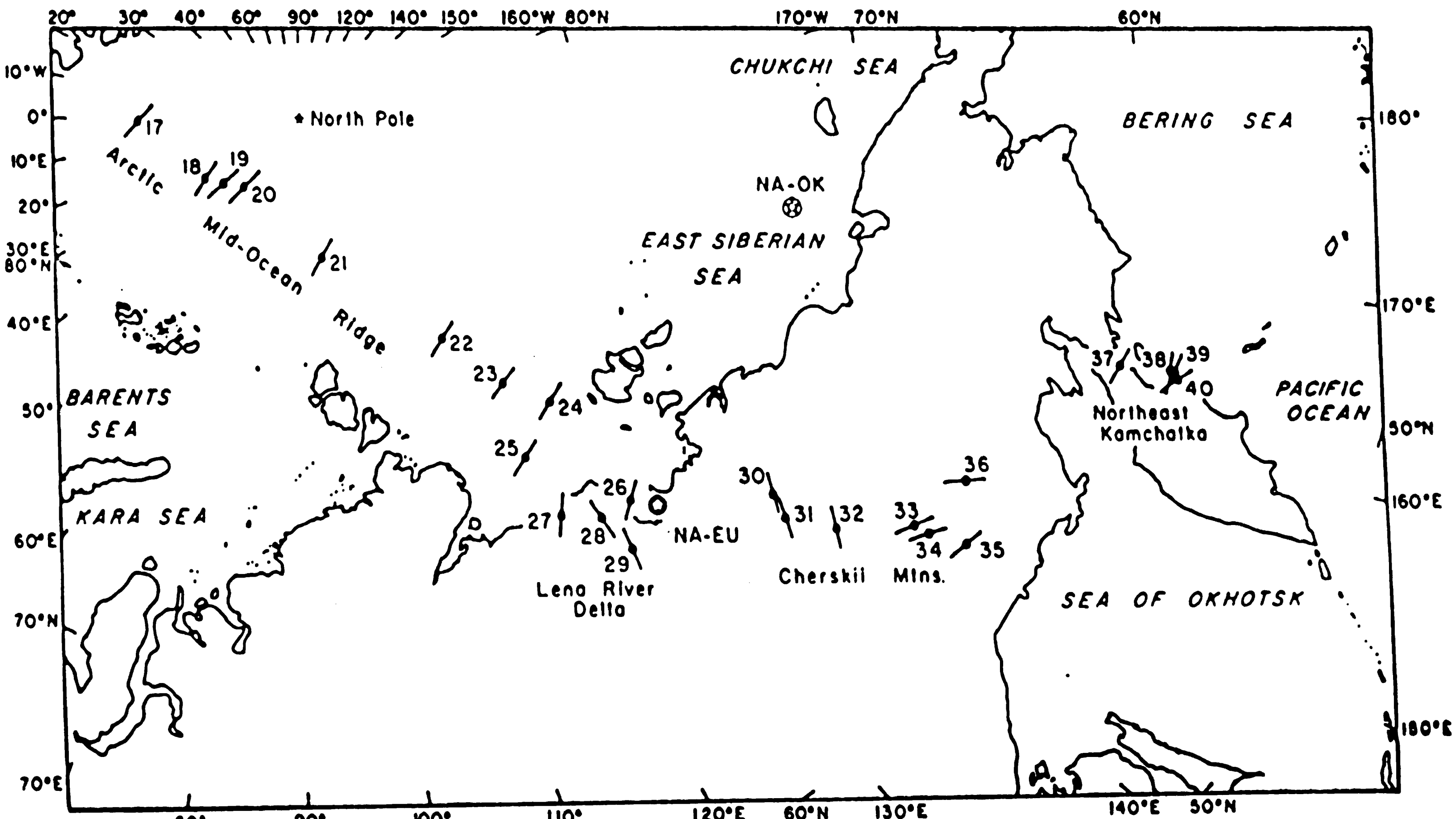
CHUKCHI SEA
BERING SEA
EAST SIBERIAN SEA
PACIFIC OCEAN
SEA OF OKHOTSK
BARENTS SEA
KARA SEA
NA-OK
NA-EU
North Pole
Arctic Mid-Ocean Ridge
Northeast Kamchatka
Cherskii Mtns.
Lena River Delta
17
18
19
20
21
22
23
24
25
26
27
28
29
30
31
32
33
34
35
36
37
38
39
40
20°
30°
40°
60°
90°
120°
140°
150°
160°W 80°N
170°W
70°N
60°N
10°W
0°
10°E
20°
30°E 80°N
40°E
50°
60°E
70°N
70°E
80°
90°
100°
110°
120°E
60°N
130°E
140°E
50°N
180°
170°E
50°N
160°E
180°E

Figure 4-4

for the November, 1969, event is obtained by choosing the N032^{o}E striking nodal plane as the fault plane. This results in a high angle thrust that is admissible based on other data (Cormier, 1975) and is supported by the narrowness of the northeast Kamchatka seismic zone. Use of the low-angle thrust plane yields a much poorer fit and should be accompanied by a wider seismic zone representing the surface projection of the fault plane. The December, 1969, event is less well constrained (Cormier, 1975) and may have a mechanism more similar to the November event. More study of these events and this region is needed.

For the Arctic data set, a pole in the Lena River delta (71.24^{o}N, 132.05^{o}E) is obtained and for the southern Cherskii-Kamchatka data set a pole is obtained off the coast of western Chukotka (72.4^{o}N, 169.8^{o}E; Figure 4-5). The fit for the southern Cherskii pole is poorer with up to 25^{o} variations from the model azimuth. The three Lena River delta events (Table 4-1, nrs. 27-29) are included in the data set although two of them yield large (25^{o}) misfits. Exclusion of these events only moves the pole slightly (71.42^{o}N, 131.53^{o}E). They are therefore retained, as they probably represent tension at the edge of the rift zone.

The region between the November 22, 1984 (northernmost thrust event), and the August 12, 1975 (southernmost normal faulting event), events represents a 500 km-wide sector where no large earthquakes have occurred since the installation of the WWSSN. Because of this, the exact nature of the transition zone is not clear. Large events have been located in, or near, the region, in 1918 and 1927, and Grachev (1982) proposes that it represents an incipient transform fault. More likely, the region is relatively aseismic due to its proximity to the pole of rotation.

Figure 4-5: Schematic plate configuration in northeast Siberian and poles of rotation for North America - Eurasia and North America - Okhotsk. Plate boundaries shown dashed where uncertain. Arrowsheads along plate boundaries denote approximate relative motions. Solid dots show locations of North America - Eurasia poles computed by previous workers, triangles show paleopole positions computed by Savostin et al. (1984), and open circles show Okhotsk - North America poles computed by other workers. Starred poles are those computed in this study with the stippled regions denoting an error ellipsoid.

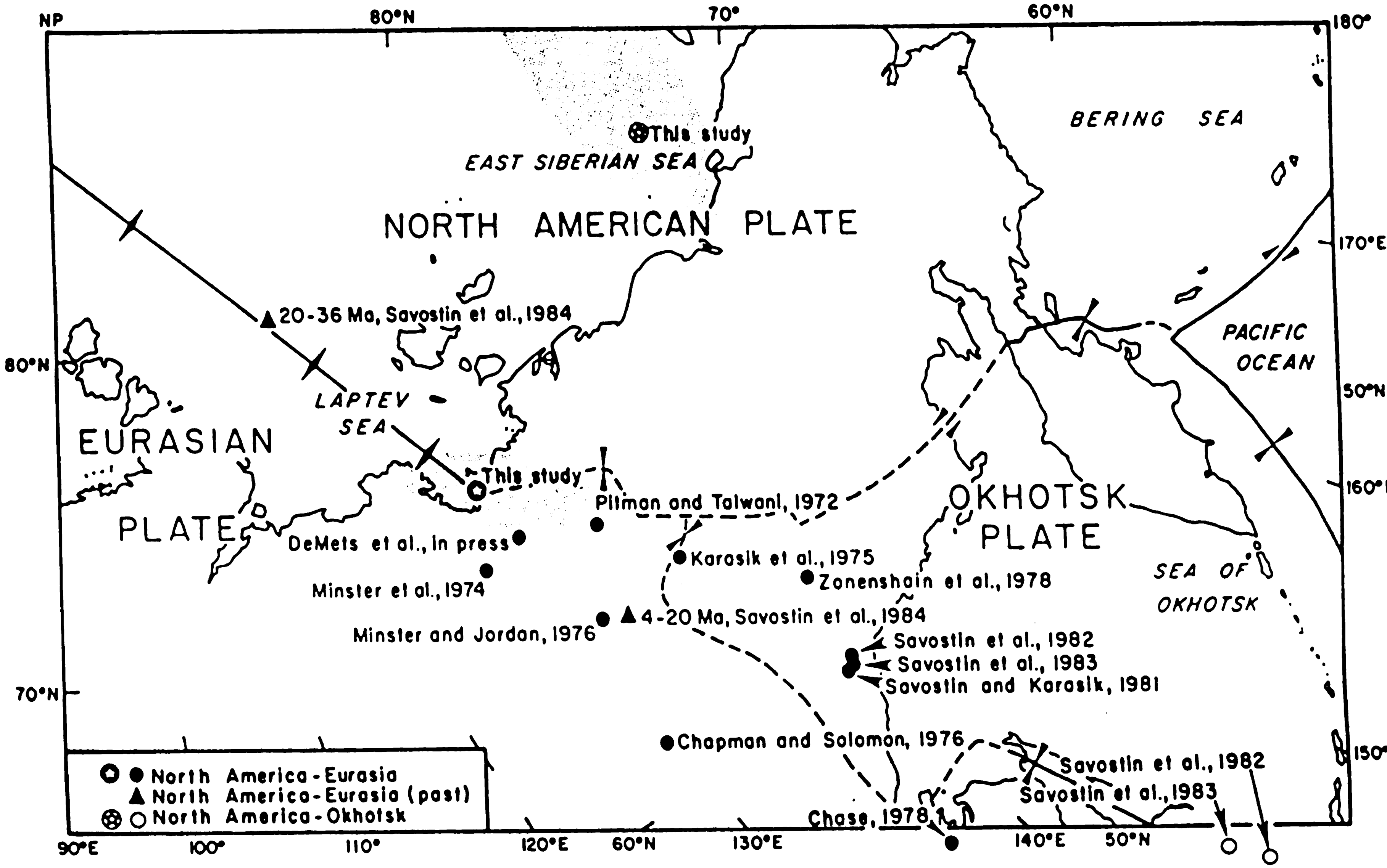
NP
80°N
70°
60°N
180°
170°E
50°N
160°E
150°E
80°N
70°N
90°E
100°
110°
120°E
60°N
130°E
140°E
50°N
BERING SEA
PACIFIC OCEAN
This study
EAST SIBERIAN SEA
NORTH AMERICAN PLATE
20-36 Ma, Savostin et al., 1984
LAPTEV SEA
EURASIAN PLATE
This study
Pitman and Talwani, 1972
OKHOTSK PLATE
DeMets et al., in press
Karasik et al., 1975
Zonenshain et al., 1978
SEA OF OKHOTSK
Minster et al., 1974
Minster and Jordan, 1976
4-20 Ma, Savostin et al., 1984
Savostin et al., 1982
Savostin et al., 1983
Savostin and Karasik, 1981
Chapman and Solomon, 1976
Savostin et al., 1982
Savostin et al., 1983
Chase, 1978
North America-Eurasia
North America-Eurasia (past)
North America-Okhotsk

Figure 4-5

The relative consistency of all the slip vectors between the southern Cherskii Mountains and eastern Kamchatka with respect to a pole off western Chukotka suggests that all of these events reflect motion between common plates. The distinction of this pole from that between North America and Eurasia then indicates that the Suntar-Khayata Mountains and the Sea of Okhotsk lie on a common plate. Following previous workers (Savostin et al., 1982, 1983) this is called the Okhotsk plate, although the boundaries are different. The Okhotsk plate is undergoing counterclockwise rotation with respect to North America.

An important observation is that the Suntar-Khayata Mountains and the southwestern Cherskii Mountains appear to be part of the Okhotsk plate. This means that the triple junction between the Okhotsk, North American, and Eurasian plates probably lies in the central Cherskii Mountains, near the epicenter of the September 9, 1968, event (Table 4-1, nr. 32). The exact location and orientation of the plate boundaries near the triple junction is indeterminate, thus the relative motion between Eurasia and Okhotsk can not be determined. However, an event occurred in 1959 several hundred kilometers west of the 1968 event and has first motions reported in the ISS that are consistent with a thrust mechanism. This suggests a more north-northeast orientation for the Okhotsk-Eurasia boundary near the triple junction.

DISCUSSION

The North America - Eurasia pole of rotation obtained here is considerably further north of most recent determinations (Table 4-2), the notable exception being the pole of DeMets et al. (in press). It is further north of the Chapman and Solomon (1976) pole, which does not explain the

Table 4-2: COMPARISON OF POLES OF ROTATION

Eurasia-North America

68.0°N	137.0°E		Pitman and Talwani, 1972
69.3°N	128.0°E	0.27°/Ma	Minster et al., 1974
65.5°N	139.5°E		Karasik et al., 1975
61.8°N	130.0°E	0.248°/Ma	Chapman and Solomon, 1976
65.85°N	132.44°E	0.231°/Ma	Minster and Jordan, 1976 (global pole)
53.7°N	137.3°E	0.229°/Ma	Chase, 1978
62.2°N	143.6°E		Zonenshain et al., 1978
59.48°N	140.83°E	0.189°/Ma	Savostin and Karasik, 1981
59.6°N	141.4°E	0.21°/Ma	Savostin et al., 1982
59.46°N	141.26°E	0.219°/Ma	Savostin et al., 1983
69.30°N	130.56°E	0.266°/Ma	DeMets et al., in press (best fit pole)
71.24°N	132.05°E		This study

North America-Okhotsk

45.8°N	145.3°E	0.41°/Ma	Savostin et al., 1982
47.09°N	144.85°E	0.478°/Ma	Savostin et al., 1983
72.4°N	169.8°E		This study

compression in the Cherskii Mountains or the slip vectors from the Lena River delta, and was derived using slip vectors from Sakhalin Island which may represent motion between the Okhotsk and Amurian plates (Savostin et al., 1982, 1983). In addition, Chapman and Solomon (1976) noted that their pole does not satisfy the strike-slip mechanisms in the southern Cherskii Mountains. The addition of an Okhotsk plate solves these problems. The pole determined here is also close to the recently determined pole by DeMets et al. (in press) which uses slip-vector, transform orientation, and magnetic lineations from the North Atlantic and Arctic Oceans. A similar pole, located near the Laptev Sea, was obtained earlier by Minster et al. (1974) based only on North Atlantic data.

The Soviet poles (Savostin and Karasik, 1981; Savostin et al., 1982, 1983) also differ from that proposed here and are located in the southern Sette-Daban Mountains. These poles were obtained using strikes of faults offsetting the depressions in the Cherskii Mountains, i.e., considering them to be transform faults. This approach is only valid if the faults are presently active and represent interplate motion. The thrust focal mechanisms in the Cherskii Mountains make untenable the interpretation that they are pure transform earthquakes, and the slip vectors indicate that that the northern and southern segments represent motion between different plate pairs. Thus it may be concluded that the premise is in error. Instead, it is suggested that these faults may represent past plate motions.

This investigation indicates the existence of a separate plate encompassing the Sea of Okhotsk and the Suntar-Khayata Mountains. Although the northeastern boundary of this plate is well defined by the seismic zone discussed above, its full western boundary is not clearly defined. The southern part of its western boundary is well defined by a seismic zone along Sakhalin Island (Chapman and Solomon, 1976). At the northern tip of Sakhalin Island, this seismic zone turns west and continues in a linear band to the Baikal rift zone. This has led to the identification of a separate Amurian block or plate (Savostin et al., 1982, 1983; Ishikawa and Yu, 1984; Tapponier et al., 1982) which includes the Maritime Provinces and western Sakhalin. Between the northern tip of Sakhalin and the Cherskii Mountains, discontinuous segments of seismicity are known in the Sette-Daban Mountains and in the El'ginskii Plateau, which may be occurring on the Okhotsk-Eurasia plate boundary.

It is also interesting to note that the El'ginskii Plateau and the Suntar-Khayata Mountains display considerable diffuse microseismicity (Koz'min, 1984) and that the largest events, studied in this paper, lie along the northern and eastern edge. The western edge of this diffuse zone connects the central Cherskii Mountains and the Sette-Daban Mountains and was the site of large earthquakes in 1951. If the boundaries of this diffuse zone are not a result of the epicentral location process, then it is possible that the relatively aseismic regions represent the North American and Eurasian plates, and that the seismically active zone represents the northern part of the Okhotsk plate being compressed between its larger neighbors. Further study is required before this problem can be clarified.

The rate of relative motion between North America and the Okhotsk plate is not clear. However, the low level of seismicity along Shelikhov Bay and the relative consistency of slip vectors and convergence rates between the Pacific plate and the Sea of Okhotsk, computed assuming that the Sea of Okhotsk is part of the North American plate (Minster and Jordan, 1976; Seno, 1985), suggest that the rate of motion is fairly small. Soviet workers (Savostin et al., 1982, 1983) have estimated a rate of about 1-1.5 cm/yr along the northern Sea of Okhotsk, however, their Okhotsk-North America pole differs significantly from this investigation's and their plate model for the region incorporates different plates and configurations. In addition, the rate data were estimated from a regional inversion using measured offsets on thrust faults on Sakhalin Island. Further analysis will be needed, especially of the Okhotsk-Eurasian interaction, before accurate rate data can be derived since the Okhotsk plate has no easily measureable rate information.

Finally, it is important to address the apparent discord between the observed geology and focal mechanism solutions for the Cherskii Mountains. Soviet workers have mapped a series of grabens extending from Bour Khaya Bay through the Cherskii Mountains (e.g., Moma Depression) and into northwestern Kamchatka (Figure 4-1; Savostin and Karasik, 1981; Grachev, 1982; Savostin et al., 1983). The grabens are filled with Pliocene sediments in the Moma depression and are older (Oligocene) near the Lena River delta and may be Eocene in the Laptev Sea (Zonenshain et al., 1978). These grabens are associated with high heat flow and several volcanic edifices are known from the Moma region. One of them, Balagan-Tas, is reported to have been active in the Early Quaternary (Argunov and Gavrikov, 1960) and perhaps as recently as 1770 (Vlodavetz and Piip, 1959). Thus, a rifting environment in the not too distant past is indicated. The focal mechanisms presented above, in addition to mechanisms determined for some of the same events by Savostin and Karasik (1981) and Koz'min (1984), are clearly thrust faults or events with a thrusting component. In addition, the sense of motion on the fault planes contradict the mapped offsets of the grabens.

One possible explanation of this discrepancy, assuming that North America, Eurasia, and Okhotsk are the only plates in the system, is a change in the pole of rotation in the recent past. Peters and Vink (1985) have proposed that the North America-Eurasia pole of rotation was located near its present position since Oligocene (anomaly 13) time. Alternatively, Savostin et al. (1984) have suggested that the pole of rotation between North America and Eurasia migrated steadily towards northeastern Siberia over at least the last 36 m.y. I propose that the pole was located in continental Eurasia, near Bour Khaya Bay, in the Miocene (anomaly 5 time) and then began, or continued, a migration towards the southeast, opening up the Moma and associated depressions. In the last few million years the migration continued to the Pacific basin, creating a tensional regime throughout northeast Asia and separating the Sea of Okhotsk from the North American plate. Due to the resulting change in plate configuration, to North America-Okhotsk-Eurasia, the pole of rotation changed to its present site in the Lena River delta region; perhaps 0 to 3 Ma.

Most pre-Tertiary structural lineations in Shelikhov Bay and northwestern Kamchatka strike northeast - southwest (Parfenov, 1983). The grabens in this area are only weakly manifested (Savostin et al., 1983) in topography or observable lineaments (Filatova et al., 1980) indicating that they are either very young (Savostin et al., 1982) or were extremely short lived. Lineaments visible on space shuttle photography are consistent with focal mechanism solutions and indicate that the region now consists of east-west strike-slip segments offsetting northwest-southeast striking thrust faults. The variability of the slip vector azimuths in the Cherskii Mountains and the northern Sea of Okhotsk may also reflect the recent change, i.e., that good strike-slip faults have not developed and some pre-existing faults are still being used.

Based on the congruence between one nodal plane for each of the earthquakes of the Cherskii Mountains and the strike of faults offsetting the grabens, I infer that much of the present-day faulting is occurring along reactivated faults from the rifting episode (Cook and Fujita, 1987). In addition, numerous strike-slip and thrust faults from prior episodes of plate accretion (Fujita and Newberry, 1983) strike northwest-southeast (Parfenov, 1983) and some seismic activity is probably occurring along reactivated segments of these faults. In addition, Rezanov and Kochetkov (1962) note that the Pliocene peneplation surface has been uplifted some 1500-2000 m in the Cherskii Mountains, a possible indicator of compression.

CONCLUSIONS

On the basis of newly determined focal mechanisms and trends in seismicity, it is proposed that there exists a separate Okhotsk plate which incorporates the Sea of Okhotsk, Kamchatka Peninsula, and the Suntar-Khayata Mountains of the northeast USSR. Based on slip vectors from these earthquakes, I have calculated a present-day North America-Eurasia pole of rotation in the Lena River delta region and a North America-Okhotsk pole off of western Chukotka.

Structural and geologic data from northeast Siberia suggest the possibility that the North America-Eurasia pole of rotation migrated across northeast Siberia until a tensional regime separated the North American and Okhotsk plates within the past 3 million years. Due to the plate reconfiguration, the North America-Eurasia pole of rotation shifted back to the Lena River delta leaving residual evidence of rifting across the northeast USSR. Present day seismicity, in many places, appears to be occurring on reactivated faults from prior tectonic episodes.

LIST OF REFERENCES

LIST OF REFERENCES

Andreev, V.S., 1983. Boguchanskii glubinnyi razlom (in Russian). Vestnik Moskva Universitet, ser. 4, geologiya, (2): 77-80.

Argunov, M.S. and Gavrikov, S.I., 1960. Balagan-Tas, an Early Quaternary volcano: Izv. Acad. Sci. USSR, (8): 72-74.

Chapman, M.E. and Solomon, S.C., 1976. North American - Eurasian plate boundary in northeast Asia. J. Geophys. Res., 81: 921-930.

Chase, C.G., 1978. Plate kinematics: the Americas, East Africa, and the rest of the world. Earth Planet. Sci. Lett., 37: 355-368.

Cook, D. B. and K. Fujita, 1987. Fault orientations and recent slip as indicators of the Eurasia - North America - Okhotsk plate configuration (abstract). Geol. Soc. Am. Abst. with Prog., 19, 626.

Cormier, V.F., 1975. Tectonics near the junction of the Aleutian and Kuril-Kamchatka arcs and a mechanism for middle Tertiary magmatism in the Kamchatka basin. Geol. Soc. Am. Bull., 86: 443-453.

DeMets, C., Gordon, R.G., Stein, S., Argus, D.F., Engeln, J., Lundgren, P., Quible, D.G., Stein, C., Wiens, D., Weinstein, S.A., and Woods, D.F., in press. Current plate motions. Jour. Geophys. Res.

Dziewonski, A.M., Franzen, J.E. and Woodhouse, J.H., 1985. Centroid-moment tensor solutions for October - December, 1984. Phys. Earth Planet. Inter., 39: 147-156.

Fedotov, S.A., Simbireva, I.G., Feodilaktov, V.D. and Matvienko, Y.D., 1980. Zemletryaseniya Kamchatki (in Russian). In Zemletryaseniya v SSSR v 1976 godu. Nauka, Moscow, 83-87.

Filatova, N.I., Mazhenshteyn, F.A., Kuznetsova, N.A. and Smelovskaya, M.M., 1980. The structure of the junction zone between the Verkhoyansk-Chukchi and Koryak-Kamchatka regions based on data from satellite Meteor-25. Geotectonics, 14: 398-406.

Filson, J. and Frasier, C.W., 1972. The source of a Siberian earthquake (abstract). Eos (Trans. Am. Geophys. Union), 53: 1041.

Fujita, K. and Newberry, J.T., 1983. Accretionary terranes and tectonic evolution of northeast Siberia. In: Accretion tectonics in the Circum-Pacific regions, eds. M. Hashimoto and S. Uyeda. Terra Scientific Publ. Co., Tokyo, 43-57.

Fujita, K., E. A. Lynch and D. B. Cook, 1987. History of the Soviet seismograph network in northeast Siberia (abstract). Eos (Trans. Am. Geophys. Union), 68: 355.

Grachev, A.F., 1982. Geodynamics of the transitional zone from the Moma rift to the Gakkel Ridge. Am. Assoc. Pet. Geol. Mem. 34: 103-113.

Grachev, A.F., Demenitskaya, R.M. and Karasik, A.M., 1970. The Mid-Arctic ridge and its continental continuation. Geomorphology, 1: 30-32.

Ishikawa, Y. and Yu, L.-W., 1984. Higashi Ajia no tekutonikkusu (abstract)(in Japanese): Seismol. Soc. Japan, Progr. and abstr. (2): 42.

Jemsek, J.P., Bergman, E.A., Nabelek, J.L. and Solomon, S.C., 1984. Focal depths and mechanisms of large earthquakes on the Mid-Arctic ridge system (abstract). Eos (Trans. Am. Geophys. Union), 65: 273.

Kanamori, H., 1970. Synthesis of long-period surface waves and its application to earthquake source studies - Kurile Islands earthquake of October 13, 1963. J. Geophys. Res., 75: 5011-5027.

Karasik, A.M., Rozhdestvenskiy, S.S. and Donets, E.G., 1975. The structure of the magnetic anomaly field and the geometry of the spreading of the Mohn Ridge in the Norwegian-Greenland Sea. Izv. Acad. Sci. USSR, Earth Physics, 11: 115-123.

Kochetkov, V.M., 1968. Yakutskaya zona (in Russian). In: Seismicheskoe raionirovanie SSSR, ed. S.V. Medvedev. Nauka, Moscow, 372-389.

Kogan, A.L., 1974. Postanovka seismicheskikh rabot metodom KMPV-GSZ s morskogo l'da na shel'fe Arkticheskikh Morei (opyt rabot v More Laptevykh)(in Russian). Geofiz. Metody Razv. Arktiki, 9: 33-38.

Koz'min, B.M., 1984. Seismicheskie poyasa Yakutii i mekhanismy ochagov ikh zemletryasenii (in Russian). Nauka, Moscow, 126 p.

Koz'min, B.M. and Andreev, T.A., 1977. Yakutiya i Severo-vostok (in Russian). In: Novyi katalog sil'nykh zemletryasenii na territorii SSSR, eds. N.V. Kondorskaya and N.V. Shebalin. Nauka, Moscow, 339-357.

Koz'min, B.M., Emel'yanov, N.P., Emel'yanova, A.A., Zhelinskaya, E.A., Garionov, A.G. and Li, B.F., 1975. Sil'nye zemletryasniya Yakutii (in Russian). In Zemletryaseniya v SSSR v 1971 godu. Nauka, Moscow, 133-141.

Kroeger, G.C. and Geller, R.J., 1983. An efficient method for computing synthetic reflection seismograms for plane layered media (abstract). Eos (Trans. Am. Geophys. Union), 64: 772.

LePichon, X., Francheteau, J. and Bonnin, J., 1973. Plate Tectonics. Elsevier, Amsterdam, 300 p.

McMullen, C. A., 1985. Seismicity and Tectonics of the Northeastern Sea of Okhotsk. M. S. Thesis, 107 p., Michigan State Univ., E. Lansing.

Minster, J.B., Jordan, T.H., Molnar, P. and Haines, E., 1974. Numerical modelling of instantaneous plate tectonics. Geophys. J. Roy. Aston. Soc., 36: 541-576.

Minster, J.B. and Jordan, T.H., 1976. Present-day plate motions. J. Geophys. Res., 83: 5331-5354.

Morgan, W.J., 1968. Rises, trenches, great faults, and crustal blocks. J. Geophys. Res., 73: 1959-1982.

Naymark, A.A., 1976. Neotectonics of the Moma region, northeastern USSR. Doklady Acad. Sci. USSR, Earth Science Sections, 229: 39-42.

Parfenov, L.M., 1983. Kontinental'nye okrainy, ostrovnye dugi v Mezozoidakh Severo-Vostoka azii i kinematika Mezozoiskoi skladchatosti. stat'ya 1. Mezozoidy Verkhoyano-Chukotskoi oblasti (in Russian). Tikhookeanskaya Geologiya, (3):3-22.

Peters, M.F. and Vink, G.E., 1985. Plate reconstruction poles determined by a least squares algorithm (abstract). Eos (Trans. Amer. Geophys. Union), 66: 1061.

Pitman, W.C., III Talwani, M., 1972. Sea-floor spreading in the North Atlantic. Geol. Soc. Am. Bull., 83: 619-646.

Rezanov, I.A. and Kochetkov, V.M., 1962. Recent tectonics and seismic regionalization in the north-eastern region of the USSR. Izv. Acad. Sci. USSR, Geophys. Ser. 6: 1045-1052.

Savostin, L.A. and Karasik, A.M., 1981. Recent plate tectonics of the Arctic basin and of northeastern Asia. Tectonophysics, 74: 111-145.

Savostin, L.A., Verzhbitskaya, A.I. and Baranov, B.V., 1982. Holocene plate tectonics of the Sea of Okhotsk region. Doklady Acad. Sci. USSR, Earth Sci. Sect., 266: 62-65.

Savostin, L., Zonenshain, L. and Baranov, B., 1983. Geology and plate tectonics of the Sea of Okhotsk. Am. Geophys. Union, Geodynamics Ser, 11: 189-221.

Savostin, L.A., Karasik, A.M. and Zonenshain, L.P., 1984. Istoriya raskrytiya Evraziiskogo basseina Arktiki (in Russian). Doklady Akad. Nauk SSSR, 275(5): 1156-1161.

Seno, T., 1985. Is northern Honshu a microplate? Tectonophysics, 115: 177-196.

Seno, T. and Kroeger, G.C., 1983. A reexamination of earthquakes previously thought to have occurred within the slab between the trench axis and double seismic zone, northern Honshu arc. J. Phys. Earth, 31: 195-216.

Stauder, W. and Mualchin, L., 1976. Fault motion in the larger earthquakes of the Kurile-Kamchatka arc and of the Kurile-Hokkaido corner. J. Geophys. Res., 81: 297-308.

Sykes, L.R., 1965. The seismicity of the Arctic. Bull. Seismol. Soc. Am., 55: 519-536.

Vlodavetz, V.I. and Piip, B.I., 1959. Kamchatka and continental areas of Asia. Catalog of the Active Volcanoes of the World Including Solfatara Fields, part 8, 104 p.

Tapponier, P., Peltzer, G., LeDain, A.Y., and Armijo, R., 1982. Propagating extrusion tectonics in Asia: New insights from simple experiments with plasticine. Geology, v. 10, p. 611-616.

Veith, K.F., 1974. The relationship of island arc seismicity to plate tectonics. Ph.D. Thesis, Southern Methodist University, Dallas, Texas.

Zonenshain, L.P., Natapov, L.M., Savostin, L.A. and Stavskii, A.P., 1978. Recent plate tectonics of northeastern Asia in connection with the opening of the North Atlantic and the Arctic Ocean basins. Oceanology, 18: 550-555.